Biophysical and pharmacological characterisation of recombinant and native rat P2X7 receptors

Thesis submitted for the degree of Doctor of Philosophy

Sarah Crawford Lappin

Department of Anaesthetics, Pain Medicine and Intensive Care
Imperial College London

2009

Author's declaration

I declare that the work presented in this dissertation was carried out in accordance with the regulations of Imperial College London. The work is original, except where indicated by specific reference in the text, and no part of the dissertation has been submitted for any other academic award. Any views expressed in the dissertation are those of the author.

Signed:..... Date:.....

Abstract

P2X7 receptors exhibit a mainly non-neuronal localisation on immune and glial cells and primarily function as non-selective cation channels. After prolonged or repeated exposure to agonist, functional and cellular changes occur: the formation of a large diameter pore, cell lysis and the release of mature, biologically active interleukin-1β (IL-1β) a potent inflammatory cytokine. It is this repertoire of functions, along with its localisation that underlies the hypothesis for its involvement in pain processing.

The biophysics and pharmacology of rat P2X7 receptors were investigated using stable cell lines. Increases in the current amplitude were shown to be dependent upon the agonist concentration and current deactivation was agonist application number and voltage dependent. These results increased our understanding of the receptor, but have also had implications for the design of protocols to investigate antagonist potency and efficacy. GSK31418A was identified as a potent, reversible and voltage-independent antagonist of rat and human P2X7 receptors. GSK314181A was >10000 fold selective over P2X4 receptors and >1000 fold selective over P2X2/3 receptors. GSK314181A produced a significant reversal of FCA-induced hypersensitivity when profiled *in vivo*, providing further validation of the role of P2X7 receptors in inflammatory pain.

Although the influence of glia cells on neuronal activity in the CNS is now well documented, the role of peripheral glia, Schwann cells and satellite cells of sensory ganglia, is less well established. Non-neuronal cells in DRG cultures were shown to express P2X7 receptors by pharmacological, biophysical and immunofluorescence techniques. Native P2X7 receptors expressed on these cells were shown to have many of the properties of recombinant P2X7 receptors, in regards to the response to agonist activation and pharmacology.

Finally, I have shown that Lamotrigine is an effective inhibitor of recombinant rat and human P2X7 receptors and native P2X7 receptors expressed in DRG. The potent inhibition of human P2X7 by Lamotrigine was replicated with the chemical analogue and neuroprotective agent Sipatrigine. However, little effect was recorded for a P2X7 antagonist in two models of epileptiform activity studies.

Acknowledgments

I would like to thank my supervisors, Istvan Nagy, Valerie Morisset and Martin Gunthorpe for all their help and support. Istvan, for all his advice and for helping me navigate a path through the Imperial College system that was so unfamiliar.
Valerie, who initially pushed for me to be granted this opportunity, and then provided me with continuous encouragement throughout the last 4+ years. Finally Martin who has spent many an hour reading drafts of this thesis and always gave thoughtful comments and suggestions. But above all provided me with the time away from my 'real job' to undertake this PhD and the work that has gone into it. For that I am very grateful.

The many lab mates, past and present, but particularly Jon S, Nicolle and Catherine have made the lab a great place to work, provided reassurance, and generally put up with me. In addition thanks to Martyn Evans who taught me the joys of immunocytochemistry.

More recently, thanks to the girls at Lenthall road who were so supportive both emotionally and over my weekend use of the dining room table! Jo must have a special mention as someone who went through this a couple of years before me and provided no end of encouragement and friendship. And to Carl, a huge thank you for too many things to mention.

Finally, mum and dad for making me someone that does not give up even when I would really like to!

Table of Contents

List of Figures and Tables

Chapter 1: Introduction

1.1 Purines and Purinergic receptors

Purines are heterocyclic aromatic organic compounds, consisting of a pyrimidine ring fused to an imidazole ring. It is a term used to define any compound that contain this basic structure (Figure 1.1), often termed purine bases. The combination of a purine base attached to a pentose sugar, or ribose, forms a molecule known as a nucleoside. In Figure 1.1, adenine is attached to a ribose, forming the molecule, Adenosine. With the addition of three phosphate groups attached at the 5' carbon atom of the pentose sugar, the molecule becomes adenosine 5′-triphosphate (ATP).

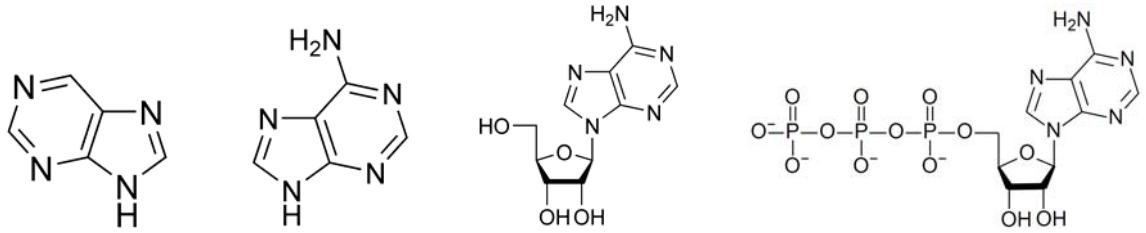

Purine Adenine Adenosine Adenosine Triphosphate (ATP)

Figure 1.1:Chemical Structures of key purines

Puringergic transmission was first proposed in 1972 (Burnstock 1972), following the identification of ATP as the neurotransmitter in non-adrenergic and non-cholinergic nerves supplying the gut and urinary bladder (Burnstock et al. 1970). Purinergic receptors is a term that encompasses receptors that use purines as a ligand (Burnstock 1972). This form of neurotransmission was then dissected based on the main ligands for activation of puringeric receptors, and resulted in the separation into those that responded to the nucleoside, adenosine (P1) and those that were activated by ATP (P2) (Burnstock 1978). P1 receptors have since been further subdivided based on molecular, biochemical and pharmacological evidence into four subtypes labelled A_1, A_{2A}, A_{2B}, and A_3, and all of

which couple to G proteins and mediate their actions via adenylate cyclase (AC). The P2 receptor family were divided into ionotropic P2X and metabotropic P2Y receptors on the basis of pharmacology (Gordon 1986) and molecular biology (Ralevic and Burnstock 1998). There are now 7 subtypes of ionotropic P2X receptors, names P2X1-P2X7, and 8 subtypes of metabotropic P2Y (P2Y1, P2Y2, P2Y4, P2Y6, P2Y11-14) receptors known to exist (Koles et al. 2005; Abbracchio et al. 2006). The activation of neuronal P2Y receptors regulate both outwardly and inwardly recitfying K^+ channels, voltage-activated Ca^{2+} channels and trigger IP3-mediated release of Ca^{2+} from endoplasmic reticulum Ca^{2+} stores (Illes and Alexandre 2004). See **Table 1.1** for overview of P2Y receptors.

Table 1.1: Characteristics of P2Y Receptors and examples of their modification of ion channel function (Modified from Abbracchio et al. 2006; Burnstock 2008)

P2YR	Agonist (human)[a]	Main Distribution	Main Function	Primary G-Protein coupling/2nd messenger	Ca^{2+} channel	K_M	GIRK
P2Y1	ADP	Platelets, epithelial, endothelial, CNS, immune and glial cells	Smooth muscle relaxation, mitogenic actions, platelet aggregation, bone resorption	$G_{q/11}$; PLCβ activation	Inhibition	Inhibition	activation
P2Y2	ATP=UTP	Epithelial, endothelial, immune and glial cells, osteoblasts	Vasodilatation and vasoconstriction; mitogenic actions; epithelial cell Cl^- secretion; bone remodelling	$G_{q/11}$; PLCβ activation	Inhibition	Inhibition	activation
P2Y4	UTP	Epithelial, endothelial cells; intestine, pituitary, CNS	Regulates epithelial Cl^- transport; vasodilatation; mitogenic actions	$G_{q/11}$; PLCβ activation	Inhibition	Inhibition	no effect
P2Y6	UDP	Epithelial cells, placenta, T cells, thymus, spleen, kidney, activated microglia	NaCl secretion in colonic epithelium; role in epithelial proliferation	$G_{q/11}$; PLCβ activation	Inhibition	Inhibition	no effect
P2Y11	ATP	Spleen, intestine, brain, granulocytes	Role in maturation & migration of dendritic cells; granulocytic differentiation	$G_{q/11}$; PLCβ activation G_s; inhibition of AC	nd	nd	nd
P2Y12	ADP	Platelets, glial cells, spinal cord	Platelet aggregation; role in dense granule secretion	$G_{i/o}$; inhibition of AC	Inhibition	no effect	activation
P2Y13	ADP	Spleen, brain, lymph nodes, bone marrow, liver, pancreas, heart.	Function largely unknown, but present in both the immune system and brain	$G_{i/o}$; inhibition of AC	Inhibition	nd	nd
P2Y14	UTP-Glucose	Placenta, adipose tissue, stomach, intestine, brain, spleen, lung, heart, immune cells, bone marrow, astroctyes	Chemoattractant receptor in bone marrow hematopoietic stem cells; dendritic cell activation	$G_{i/o}$; inhibition of AC	nd	nd	nd

[a], Main agonist at human receptor.

AC, adenylate cyclase; K_M, M-current K^+ channel; GIRK, G protein-activated inwardly rectifying K^+ channels

nd, Not Determined.

1.1.1 P2X receptors

P2X receptors are membrane bound ion channels that are activated by the binding of extracellular ATP, resulting in the opening of a non-selective cation channel (Jahr and Jessell 1983; Krishtal et al. 1983). The P2X subunit proteins are 384 (P2X4) to 595 (P2X7) amino acids long, and have two hydrophobic regions which span the plasma membrane (Brake et al. 1994; Valera et al. 1994; North 1996). Separating these 2 transmembrane domains is the majority of the polypeptide on the extracellular side of the membrane, and the NH2 and COOH termini are cytoplasmic (See Figure 1.2 for a schematic representation of P2X receptor). The transmembrane regions are thought to form the ion conduction pore and undergo conformational changes during receptor activation (Silberberg et al. 2005). Transmembrane region 2 is thought to play a role in ion permeation and channel gating (Migita et al. 2001), and is involved in the assembly of subunits into oligomeric complexes (Samways et al. 2006). All the evidence to date indicates that the subunits of P2X receptors form trimeric receptor complexes (Nicke et al. 1998; Aschrafi et al. 2004).

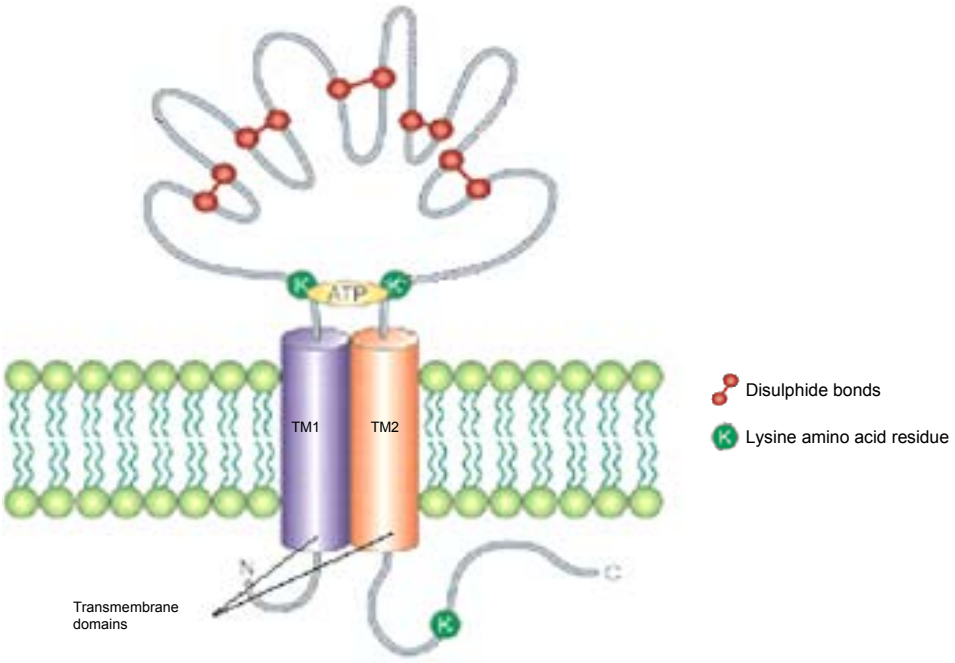

Figure 1.2: Schematic representation of P2X receptor subunit topology.

Within the large extracellular domain of P2X receptors a number of key residues have been identified. Firstly, the loop is known to contain 10 conserved cysteine residues (Cys117-Cys165, Cys126-Cys149, Cys132-Cys159, Cys217-Cys227, and Cys261-Cys270) which participate in disulphide bond formation and may help define the tertiary structure (Ennion and Evans 2002). The disulphide bonds between Cys261-Cys270 and Cys117-Cys165 also have a role in receptor trafficking (Ennion and Evans 2002). Secondly, there are consensus sequences for N-linked glycosylation (Asn-X-Ser/Thr) in all of the P2X receptor subunits in the extracellular loop. Some glycosylation is essential for trafficking to the cell surface (Newbolt et al. 1998; Torres et al. 1998a; Rettinger et al. 2000), and particular sites can also affect ATP potency (Asn210 in P2X1 receptors (Rettinger et al. 2000).

The ATP binding site on P2X receptors is located in the extracellular domain, and there have been many studies detailing some of the residues involved in ATP binding to P2X receptors (reviewed in Roberts et al. 2006). As ATP is a charged molecule with negative charge on the phosphate groups, the conserved charged residues across the P2X receptor family were investigated for their interaction with ATP using alanine-scanning-based mutagenesis. This determined a number of residues and regions that play a role in mediating the action of ATP as measured by a significant reduction in the potency of ATP in these mutants. For the P2X1 receptor the positively charged Lysine (Lys) at position 68 and 309 are thought to bind the phosphate tail of ATP (See Figure 1.2 for schematic representation of the location of these residues), with possible involvement of the Arg292. Studies using mutagenesis and analysis of receptor polymorphisms supports a role of these charged amino acids in the binding of ATP to P2X7 receptors also (Jiang et al. 2000b; Worthington et al. 2002), with the Arg307 shown to regulate ATP potency (Gu et al. 2004). Based on the P2X1 receptor, the binding of the adenine ring of ATP is through interactions with 2 motifs; the Phe and Thr at positions 185 and 186 respectively; and Asn290, Phe291, and Arg292 (Ennion et al. 2000; Roberts and Evans 2004; Vial et al. 2004a).

Intracellularly, the amino acid sequence and length of the C-terminal domain vary across the P2X receptor family. However there is a conserved protein kinase C site in the NH_2-terminal domain, mutations of which led to a range of effects including a change in the kinetics of the response to agonist of P2X2 receptors (Boue-Grabot et al. 2000), and non-functional P2X3 receptors (Paukert et al. 2001). A number of different residues have been identified in the intracellular C-terminus that are involved in regulating desensitisation or channel gating, in P2X2 receptors (Simon et al. 1997; Smith et al. 1999). Whereas the fast desensitisation of P2X1 and P2X3 was shown regulated within the two transmembrane domains (Werner et al. 1996) from chimeric studies.

The seven P2X receptors identified and cloned to date, named P2X1-P2X7 (Koles et al. 2005), are 36–48% identical to one another at the amino acid level and, with the possible exception of P2X6, all form functional homomeric channels. The P2X6 was cloned from superior cervical ganglion cDNA (Collo et al. 1996), but its expression has only been recorded in a small proportion of transfected cells (Collo et al. 1997), possibly indicating that the protein is not sufficiently glycosylated in heterologous expression systems to form functional channels. There is also evidence for heteromultimeric assemblies of P2X subunits, including P2X1/P2X2 (Brown et al. 2002), P2X1/P2X4 (Nicke et al. 2005), P2X1/P2X5 (Torres et al. 1998b), P2X2/P2X3 (Radford et al. 1997), P2X2/P2X6 (King et al. 2000), and P2X4/P2X6 (Le et al. 1998), and although until recently P2X7 receptors were thought to be homomeric only (Torres et al. 1999), there is now evidence for heteromultimerisation of P2X7 with P2X4 receptors (Guo et al. 2007). An overview of the P2X receptor homomers and heteromers is detailed in **Table 1.2**.

Table 1.2: Summary of distribution and general properties of P2X receptors

	Main Distribution	ATP EC_{50} (μM)[a]	αβme-ATP sensitive	Antagonists[b]	Desensitisation	Effect of Ca^{2+} ions[c]	Main Function	
Homomers								
P2X1	Smooth muscle, platelets, spinal dorsal horn	1	yes	NF449	Fast	No effect	Smooth muscle contraction, platelet aggregation	Hechler et al, 2003; Ruggieri, 2006
P2X2	Smooth muscle, CNS, retina, autonomic and sensory ganglia	10	no	NF023	Slow	Inhibition	Modulation of synaptic function & sensory transmission	Ren at al, 2003; Jarvis, 2003
P2X3	Sensory neurons,	1	yes	TNP-ATP	Fast	No effect	Sensory neurotransmission	Jarvis, 2003
P2X4	CNS, testis, colon	7	no	TNP-ATP	Medium	-	Transmitter release, modulates chronic pain	Tsuda et al, 2003
P2X5	Gut, bladder, thymus, skin	0.5	no	PPADS	Slow	Inhibition	Cell proliferation and differentiation	Greig et al, 2003
P2X6	CNS, motor neurons, spinal cord	0.5	yes	-	Slow	-	Not Known	
P2X7	Immune and glial cells	>100	no	BBG	Slow	Inhibition	Pro-inflammatory cytokine release, cell proliferation, apoptosis	Ferrari et al, 1997; Zheng et al, 1991
Heteromers[d]								
P2X1/2[e]	Sensory nerves, spinal dorsal horn	0.6	yes	-	Mixed	-	Not Known	
P2X1/4[f]	Brain	-	yes	Suramin	Slow	-	Not Known	
P2X1/5[g]	Ventral horn of spinal cord	5	yes	TNP-ATP	Mixed	No effect	Not Known	
P2X2/3[h]	CNS, Sensory neurones	1	yes	TNP-ATP	Slow	Inhibition	Sensory neurotransmission	Jarvis, 2003
P2X2/6[i]	Respiratory centres in brainstem	32	no	Suramin	Slow	-	Synaptic transmission	Ren at al, 2003
P2X4/6[j]	Brain	6	yes	PPADS	Slow	-	Synaptic transmission	Le et al, 1998
P2X4/7[k]	Immune cells and Microglia	-	-	-	Slow	-	Not Known	

[a]North & Surprenant 2000; Li et al, 2008
[b]Most potent commercially available antagonist
[c]Effect on ATP activated currents
[d]Overlapping distribution
[e]Brown et al, 2002
[f]Nicke et al, 2005
[g]Torres et al, 1999
[h]Radford et al, 1997
[i]King et al, 2000
[j]Le et al, 1998
[K]Guo et al, 2007

- data not available

PPADS pyridoxalphosphate- 6-azophenyl-28,48-disulfonate
NF449 4,4',4'',4'''-(carbonylbis(imino-5,1,3-benzenetriylbis(carbonylimino)))tetrakis-benzene-1,3-disulfonic acid
TNP-ATP 2',3'-O-(2,4,6-Trinitrophenyl) adenosine 5'-triphosphate
NF023 8,8'-[carbonylbis(imino-3,1-phenylenecarbonylimino)]bis -1,3,5-naphthalene-trisulphonic acid
BBG Brilliant Blue G

1.1.1.1 P2X1

The P2X1 receptor was cloned from rat vas deferens in 1994 (Valera et al. 1994; Valera et al. 1995). They are highly expressed in smooth muscle and activation in response to nerve stimulation results in smooth muscle contraction in vas deferens (Mulryan et al. 2000) and bladder (Vial and Evans 2000; Ruggieri, Sr. 2006). P2X1 receptors are also expressed by platelets where they are involved in thrombosis (Hechler et al. 2003), and in the central nervous system (CNS), P2X1 subunits are expressed in the cerebral cortex, striatum, hippocampus and cerebellum (Kidd et al. 1995). The use of P2X1 knockout mice enabled the identification of functional P2X1 receptors in neurones of the superior cervical ganglion (Calvert and Evans 2004), and the medial nucleus of the trapezoid body (MNTB) (Watano et al. 2004) providing evidence for a functional role for P2X1 subunit containing receptors in the CNS. The response to agonist activation of P2X1 receptors results in rapidly activating currents which desensitise during the application, with slow (>15mins) recovery from desensitisation. The main features of P2X1 pharmacology are a high sensitivity to alpha-beta-methylene adenosine 5′-triphosphate (αβme-ATP) as well as ATP (Valera et al. 1994; Evans et al. 1995), although the most potent agonist is 2',3'-(benzoyl-4-benzoyl)-ATP (BzATP) (Bianchi et al. 1999). P2X1 currents are inhibited by the pan-P2X antagonists, PPADS and Suramin, but more potently by the suramin analogue, NF449, which is also selective (Rettinger et al. 2005) and so has use in the identification of P2X1 currents.

1.1.1.2 P2X2

The P2X2 receptor was initially cloned from pheochromocytoma PC12 cells (Brake et al. 1994). P2X2 receptors have a wide distribution throughout the peripheral nervous system and CNS, and are also found in smooth muscle in the bladder and intestine (North 2002). P2X2 receptors are involved in sensory neurotransmission and in the modulation of synaptic function (Sawynok et al. 1993; Jo and Schlichter 1999; Ren et al. 2003). A role for P2X2 receptors in mediating pain-related behaviour and mechanosensory transduction

in the urinary bladder were confirmed using P2X2 gene deleted mice (Cockayne et al. 2005). Pharmacologically, the P2X2 receptor is activated by ATP but not by αβmeATP, and is sensitive to suramin, PPADS and TNP-ATP (King et al. 1997). P2X2 receptors are the only homomeric P2X receptor that shows an increased current response to ATP following acidification of the extracellular solution. This occurs by reducing the time spent in the closed state and so potentially increasing the agonist affinity (Ding and Sachs 1999), and is a property of these receptors that can be useful in confirming their function.

1.1.1.3 P2X3

The P2X3 receptor cDNAs were isolated from rat DRG (Chen et al. 1995).
P2X3 are found predominantly in sensory neurons, where they mediate sensory neurotransmission (Burnstock 2001). Clarification of the role of P2X3 receptors was found with the production of the P2X3 knockout mouse which had a reduced pain threshold in an inflammatory pain model, and reduced urinary bladder reflexes in response to bladder distension (Cockayne et al. 2000; Cockayne et al. 2005). The development of the selective P2X3/P2X2/3 receptor antagonist, A-317491, confirmed a key role in pain of these receptors when it was shown to reverse hypersensitivity induced in a number of pain models (McGaraughty et al. 2003). P2X3 receptors respond to αβmeATP and ATP to a similar degree. Receptor activation produces currents that are either sustained for several seconds (in low agonist concentrations) or show prominent desensitisation that is only recoverable following a 15 min washout phase, a profile similar to that recorded following P2X1 activation. NF023, a suramin analogue, is around 40 times more potent an antagonist at P2X3 receptors (Soto et al. 1999), and the Abbott compound, A-317491, shows even greater selectivity over P2X and P2Y receptors (Jarvis et al. 2002), and so is a particularly useful antagonist for distinguishing P2X3 currents from P2X1.

1.1.1.4 P2X2/3

The P2X2/P2X3 heteromer is activated by αβmeATP as well as ATP and the currents produced have the same kinetic profile as P2X2 currents, with fast activation and little desensitisation within the agonist activation. They are blocked by the non-selective P2X antagonists, Suramin, PPADS, but also by NF023 and TNP-ATP, and are potentiated by low pH, indicating a hybrid pharmacological profile incorporating elements from both P2X2 and P2X3 receptors. There have been numerous studies detailing the importance of P2X2/3 (along with P2X3) receptors in pain (Jarvis 2003 for review). P2X2/3 heteromeric receptors are highly expressed on primary afferent neurones (Lewis et al. 1995) and may also be important in bladder reflexes, mimicking the profile of that of P2X3 receptors (Cockayne et al. 2000; McGaraughty et al. 2003; Cockayne et al. 2005)

1.1.1.5 P2X4

The P2X4 receptor was cloned by a number of different groups at the same time, among the first were Buell and colleague who used superior cervical ganglion (Buell et al. 1996) and Bo et al, who isolated P2X4 from brain tissue (Bo et al. 1995). They are the most ubiquitously expressed of all the P2X receptors, found on immune cells and throughout the peripheral and central nervous systems (North 2002). P2X4 receptors are involved in promoting an inflammatory response through upregulation of expression on activated microglia (Tsuda et al. 2003). This also leads to the enhancement of pain behaviours after nerve injury (Tsuda et al. 2003), and formalin-induced inflammation (Guo et al. 2005). There is also evidence for a role of P2X4 receptors in long term potentiation (LTP) in the hippocampus, confirmed using P2X4 knockout mice (Sim et al. 2006), and indicating a role for these receptors in synaptic strengthening. Homomeric P2X4 receptors are activated by ATP and the resultant current is rapidly activating and shows little desensitisation throughout the application. There is much species variability in the pharmacology of P2X4 receptors with αβmeATP and Adenosine-5'-tetraphosphate (AP4) acting as partial agonists at mouse and human orthologues (Jones et al. 2000). Ivermectin

potentiates currents at P2X4 receptors, but has no effect at homomeric P2X2, P2X3, or P2X2/3 heteromers (Khakh et al. 1999b).

1.1.1.6 P2X5

P2X5 receptors were cloned from rat heart (Garcia-Guzman et al. 1996), and are expressed in skeletal muscle, skin, gut, bladder, and thymus (North 2002), where they may play a regulatory role in cell proliferation and differentiation (Greig et al. 2003). P2X5 currents resemble those recorded through P2X2 receptors, in that they show little desensitisation and are blocked by the generic P2X antagonists. However rat P2X5 currents are of a considerably smaller amplitude compared with current observed following activation of other P2X receptors expressed under similar conditions (Collo et al. 1996; Garcia-Guzman et al. 1996), and despite equivalent protein expression as observed using Western blotting (Bo et al. 2003).

1.2 P2X7 receptor

1.2.1 The structure of the P2X7 receptor

The presumed endogenous form of the P2X7 receptor was first described as the receptor that mediated the permeabilising action of ATP on mast cells (Dahlquist and Diamant 1974) and large conductance in macrophages (Buisman et al. 1988), and was initially known as the P2Z receptor (Gordon 1986). The full length cDNAs were first cloned from rat brain in 1996 (Surprenant et al. 1996), followed by human monocytes (Rassendren et al. 1997) and mouse microglia (Chessell et al. 1998b). The human P2X7 receptor gene was localized by in situ hybridization to chromosome 12q24, within 130 kb of the gene for the homologous P2X4 receptor (Buell et al. 1998b). The P2X7 subunit protein is 595 amino acid long, the longest of the P2X family, and is the least similar, sharing only 35–40% homology with the other six members (Surprenant et al. 1996). The P2X7 subunit is

unique structurally as it has an extended C-terminal domain, (239 amino acids) 27-129 amino acids longer than any other P2X subunit. Several apparent protein-protein interaction motifs, potentially important to macrophage signalling have been identified (Denlinger et al. 2001). A lipopolysaccharide (LPS)-binding site has also been identified close to the carboxy terminus of the receptor (Denlinger et al. 2001), whereby the receptor could translate inflammatory signals to signal transduction events. The region between residues 551 and 581 has been identified as essential for trafficking (Wiley et al. 2003), and cell surface expression of the P2X7 receptor (Smart et al. 2003). The ATP binding site is suggested to be located within an antiparallel six-stranded beta-pleated sheet (Freist et al. 1998), nearby a cysteine-rich region of the extracellular domain of the receptor, with residues K193 and K311 having particularly importance (Worthington et al. 2002; Gu et al. 2004).

1.2.2 Pharmacology

As mentioned above, the pharmacology of P2X receptors overlaps considerably when considering most of the tool compounds available, and hence causes difficulties when trying to identify and isolate receptors subtypes. There are also considerable differences between the potency of antagonists at the P2X7 receptor orthologues See Table 1.3 (Chessell et al. 1998a; North and Surprenant 2000; Hibell et al. 2001b). This has been detailed throughout the literature and can cause complication when comparing between studies.

1.2.2.1 Agonists

P2X7 receptors response to agonist activation differs from that of other P2X receptors in a number of ways. Firstly, activation of P2X7 receptors requires a concentration of ATP greater than 100 μM, much higher than for other P2X receptors, and the ATP analogue BzATP is a more potent agonist at these receptors (Surprenant et al. 1996; Rassendren et al. 1997; Chessell et al. 1998b). Other agonists are less effective than ATP including

2MeSATP, ATPγS, ADP, or ineffective such as βγmeATP, UTP, and adenosine (North and Surprenant 2000). The need to use concentrations of ATP around 1 mM to activate P2X7 receptors means that the ATP solutions used are often acidic and will contain other nucleotides (North and Surprenant 2000) which may activate other receptors that are present, therefore BzATP is often used instead. The endogenous agonist for P2X7 receptors is the free acid form of ATP (ATP^{4-}), which was first put forward following the assumption that the inhibition of P2X7 by divalent cations represented an alteration in the concentration of ATP (Dahlquist and Diamant 1974), or through a direct blockade of permeation (Surprenant et al. 1996). However, the primary mechanism is likely to be via modulation of the agonist binding site, resulting in a reduction in the agonist affinity for the P2X7 receptor (Virginio et al. 1997), and possibly through a direct effect on the P2X7 receptor itself (Jiang 2008; Liu et al. 2008b). Two histidine residues, H130 and H210, have been implicated in the inhibitory actions of Mg^{2+} ions, suggesting that this cation acts at a defined allosteric site involving these two residues (Acuna-Castillo et al. 2007).

The potency of agonists varies across species, with greater potency recorded for agonists at rat and human P2X7 receptors compared to mouse receptors (Surprenant et al. 1996; Rassendren et al. 1997; Chessell et al. 1998b), and this theme of pharmacological species variability is found across ligands for P2X7 receptor modulation. Site-directed mutagenesis studies revealed the Asn at residue 284 are responsible for higher ATP sensitivity in the rat P2X7 receptor, where as differences in the potency of BzATP between rat and mouse receptors was found to be dependent upon residues Lys127 and Asn284 (Young et al. 2007), indicating that the variability in the potency of agonists at different P2X7 receptors orthologues can be altered by changes in single amino acids.

1.2.2.2 Antagonists

The generic P2X antagonists, Suramin, PPADS, oxidised-ATP and TNP-ATP all block P2X7 receptors but at lower potency than their effects at the other subtypes (Surprenant

et al. 1996; Evans et al. 1996; Chessell et al. 1998a; Chessell et al. 1998b; North and Surprenant 2000). There are a number of more selective antagonists including KN-62 (1-[N, O-bis(5-isoquinolinesulphonyl)-N-methyl-L-tyrosyl]-4-phenylpiperazine), Brilliant Blue G (Jiang et al. 2000a) and Calmidazolium (Virginio et al. 1997). KN-62, is an antagonist of Ca^{2+}/calmodulin-dependent protein kinase II (CaMKII), but it also potently antagonises human P2X7 receptors, with IC_{50} values of around 12 nM (Gargett and Wiley 1997). Brilliant Blue G is also a potent antagonist of P2X7 receptors, exhibiting a higher potency at rat (IC_{50}=10nM) than human receptors (IC_{50}= 200 nM). It does have activity at other P2X receptors, but with inhibitory concentrations around 2 to >30μM at these subtypes, it can be considered selective at P2X7 receptors at lower concentrations (Jiang et al. 2000a). Calmidazolium, an inhibitor of cyclic nucleotide-gated receptor, inhibits the ionic channel of rat P2X7 receptors by up to 90% (IC_{50} = 15 nM), but interestingly, with no effect on the large diameter pore form (Virginio et al. 1997).

Although many of these antagonists are potent inhibitors of P2X7 function and so useful in *in vitro* studies, they often differentiate between the species orthologues, with many exhibiting a much greater potency at the human P2X7 orthologues and limited rodent P2X7 activity (North and Surprenant 2000). Examples of this are seen with the commonly used tool compounds such as PPADS, Suramin (see Table 1.3) and the more potent suramin analogue, NF279, which show 5 to10 fold greater potency at human P2X7 receptors than at rat (Klapperstuck et al. 2000b) and as mentioned above, KN-62 only inhibits human receptors and is ineffective at other P2X7 orthologues (Humphreys et al. 1998). However this problem has extended to some of the newer tool P2X7 antagonists produced through drug discovery research, like AZ116453743 which shows a similar potency reduction at the rat receptor (> 500-fold less effective at inhibiting rat P2X7 currents (Stokes et al. 2006)) and the Triazole-based compounds (Carroll et al. 2007). Conversely, BBG and Calmidazolium are examples of compounds that show greater potency to inhibit rat P2X7 receptors compared to human P2X7 (Virginio et al. 1997;

Jiang et al. 2000a). The inter-species differences in activities of these compounds is surprising given there is 80% similarity between the amino acid sequences of the human and rat P2X7 receptors (Rassendren et al. 1997). However, this is also a facet of the P2X4 receptor pharmacology, where marked differences in sensitivity to suramin and PPADS have been recorded between orthologues despite their 89% homology (Garcia-Guzman et al. 1997).

Table 1.3: Summary of Antagonist Pharmacology of P2X receptors (IC_{50} values in μM)

	WC Patch-clamp		Ca^{2+} Uptake	YOPRO/EthBr	IL-1β release					
	hP2X7[a]	rP2X7[b]	rP2X7	rP2X7	hP2X7 (THP-1)	P2X1	P2X2	P2X3	P2X4	P2X5
PPADS[c]	1	45	8	1.3	3.5	1	1	1	>300	3
Suramin[d]	70	78		16		1	10	3	>300	4
KN-62[e]	0.015	>3	>100	>100	0.075				>100	
BBG[f]	0.2	0.01	8.1	0.6		>5	1.4	>10	>10	
Calmidazolium[g]	0.1	0.013	-	>10						
A-740003[h]			0.018	0.138	0.156	>100	>100	>100	>100	
AZ11645373[i]	0.007	>10		>10	0.092	>10	>10	>10	>10	>10

[a] Activated by 300 μM BzATP
[b] Activated by 30 μM BzATP
[c] (Surprenant et al. 1996; Chessell et al. 1998a; North and Surprenant 2000; Donnelly-Roberts et al. 2008)
[d] (Surprenant et al. 1996; Chessell et al. 1998a; North and Surprenant 2000)
[e] (Chessell et al. 1998a; Donnelly-Roberts et al. 2004; Donnelly-Roberts et al. 2008)
[f] (Jiang et al. 2000a; Honore et al. 2006; Donnelly-Roberts et al. 2008)
[g] (Virginio et al. 1997; Chessell et al. 1998a)
[h] (Honore et al. 2006)
[i] (Stokes et al. 2006)

P2X7 function is also voltage-independently inhibited by many different ions, including Ca^{2+}, Mg^{2+} (Surprenant et al. 1996), Zn^{2+}, Cu^{2+} and protons (H^{+}) (Virginio et al. 1997; Michel et al. 1999). The inhibition of P2X7 function by divalent cations was thought to be mediated via the chelation of the effective agonist, ATP^{4-}, thereby reducing the relative concentrations of ATP (North 2002). However, there may also be a direct effect on the P2X7 receptor itself, that could account for the inhibition (Jiang 2008; Liu et al. 2008b). The inhibition produced with zinc and copper ion application is potent; with IC_{50} values 11.2μM and 0.5μM respectively at rat P2X7 activated by 30 μM BzATP (Virginio et al. 1997), and has been shown to be via a direct interaction with residues in the extracellular domain of the P2X7 receptor, specifically involving His62 and Asp197 residues (Liu et al. 2008b). These effects allow the P2X7 receptor to be distinguished from other family members as these ions have been shown to potentiate P2X2 and P2X4 responses to agonist (North and Surprenant 2000). They also provided direct evidence against the previous view of divalent cation interaction with ATP^{4-} (Liu et al. 2008b).

The studies detailed in the literature using these antagonists are often quite difficult to compare, even between the same species. This is due to many of the antagonists effects being agonist concentration dependent. Also agonist potency can variable following multiple applications and is dependent upon the divalent cation concentrations of the bathing solution (Hibell et al. 2001b). Preincubation times for antagonists may also affect potency, as is the case for PPADS, and incubation times often vary from study to study (Chessell et al. 1998a).

1.2.3 Expression/localisation

P2X7 receptors are expressed on cells of haematopoietic lineage including mast cells, lymphocytes, erythrocytes, fibroblasts, and macrophages (Surprenant et al. 1996), and schwann cells (Colomar and Amedee 2001). Within the central nervous system, functional P2X7 receptors are localized on microglia (Collo et al. 1997) and astrocytes

(John et al. 2001; Panenka et al. 2001). The existence of functional P2X7 receptors on peripheral or central neurons remains controversial owing to the poor specificity of both antibodies and ligands targeting the rat P2X7 receptor (Anderson and Nedergaard, 2006) and is detailed below.

1.2.3.1 Neuronal P2X7 Receptors

The existence of functional P2X7 receptors on peripheral or central neurons is still subject to some debate. P2X7 receptor expression on neurones was first identified in a number of layers of rat retina (Brandle et al. 1998b). P2X7 mRNA has been identified in several different CNS areas including the cortex, (Papp et al. 2004), brainstem and spinal cord (Deuchars et al. 2001), and in peripheral neurons, such as cultured sympathetic (Allgaier et al. 2004), and dorsal root ganglion (Kobayashi et al. 2005) neurons. P2X7 receptor immunoreactivity has been reported to selectively target excitatory nerve terminals of the spinal cord (Deuchars et al. 2001; Atkinson et al. 2004; Wang et al. 2004b), and has also been reported in a number of brain regions including, medulla oblongata, cerebellum, striatum, thalamus, amygdala (Deuchars et al. 2001; Atkinson et al. 2004; Hervas et al. 2005) and hippocampus (Armstrong et al. 2002; Sperlagh et al. 2002; Kang et al. 2004). (See Sperlagh et al. 2006 for review). Further evidence for neuronal localisation was obtained following co-localization studies revealing co-expression of P2X7 receptor immunoreactivity with vesicular glutamate transporters, VGLUT1 and VGLUT2, GABA transporter, vGAT, and vesicular acetylcholine transporter, vAChT, immunoreactivity in many areas of the brain and spinal cord (Atkinson et al. 2004).

However the pattern of immunostaining in neurones detailed in these studies has been inconsistent and more recent work has suggested that the most commonly used antibodies may not be as specific as first thought (Sim et al. 2004; Kukley et al. 2004). P2X7 immunoreactivity was present in hippocampal sections taken from two different P2X7

knockout mice, but was absent in non-brain tissue, such as submandibular gland, and microglia (Sim et al. 2004). This has been postulated to be either due to a failure to eliminate brain P2X7 expression in the knockout mice; deemed unlikely due to two different knockout mice strains; or the existence of a 'P2X7-like' protein in neurones that these antibodies recognise (Sim et al. 2004). Interestingly, the epitopes recognised by the antibodies are identical to the genuine P2X7 receptor but differ in the sequence that has been disrupted by genetic manipulation in the Pfizer knockout mouse (Sanchez-Nogueiro et al. 2005).

Functionally, P2X7 activation following BzATP application, increased the firing rate of glutamatergic neurones in spinal cord (Deuchars et al. 2001), possibly through presynaptic glutamate release, increased evoked EPSC amplitude in brainstem slices (Ireland et al. 2004), and enhanced the release of GABA in hippocampus (Sperlagh et al. 2002), an effect that is attenuated in hippocampus from P2X7 knock-out mice (Papp et al. 2004). Conversely a long-lasting inhibition of neurotransmission was observed following P2X7 receptor activation in mossy fibre–CA3 synapses (Armstrong et al. 2002). A role for P2X7 receptors postsynaptically has also been shown in the paraventricular nucleus, where their activation leads to an increase in synaptic strength through AMPA receptor insertion (Gordon et al. 2005). Although pharmacological characterisation of BzATP- or ATP-activated currents were reported in some of these experiments (Armstrong et al. 2002; Sperlagh et al. 2002), caution should be used when interpreting data, as the inhibition of synaptic transmission recorded in hippocampal slices (Armstrong et al. 2002), has been mimicked in slices from P2X7 knock-out mice (Kukley et al. 2004), and there is evidence that some of the effects detailed above may be mediated through neuronal adenosine A1 receptors (Ireland et al. 2004; Kukley et al. 2004). Finally astrocytic glutamate and GABA release can often not be discounted as a source of these neurotransmitters. It has been shown that cultured astrocytes can release Glutamate and GABA following the activation of P2X7 receptors (Wang et al. 2002; Duan et al. 2003).

Therefore it is as yet unclear as to whether P2X7 receptors are expressed on neurones. It is clear that P2X7 receptor activation can modulate synaptic transmission, regardless of their location.

1.2.4 Response to agonist activation

The low affinity of ATP for P2X7 receptors, the lowest of all the P2X receptors, infers a potential pathological role for P2X7 receptors when large amounts of ATP are released. *In vitro*, P2X7 receptors have been shown to have an almost unique response to ATP. During a brief activation, P2X7 receptors behave as (1) a classical non-selective cation channel. However, after a prolonged or repeated exposure to agonist, functional and cellular changes occur: (2) formation of a large diameter pore and cell lysis and (3) the release of mature, biologically active interleukin-1β (IL-1β), a potent inflammatory cytokine. Each of these responses to activation will be discussed below.
However there are also a number of other cellular processes that occur, including the activation of caspases (Perregaux and Gabel 1994), cytokine release (Ferrari et al. 1997a) and apoptosis (Zanovello et al. 1990; Zheng et al. 1991).

1.2.4.1 Channel opening

The main action following brief activation of the P2X7 receptor is the opening of a cation channel that allows the bidirectional flux of Na^+, Ca^{2+} and K^+ ions (Surprenant et al. 1996). The channel activates rapidly and currents show little desensitisation during applications lasting for many seconds. However, the current response to multiple agonist activations is not static. The time course of closure of the channel following agonist activation, deactivation, slows with each subsequent agonist application. It is related to the agonist potency and is thought to be due to a slow dissociation of agonist from the receptor rather than being an intrinsic property of the ion channel (Hibell et al. 2001a). Interestingly, it is much less evident when ATP is the agonist and the slowest channel

closure times were recorded for the rat P2X7 receptor (Hibell et al. 2001a) indicating species variability. The peak current amplitude is also not stable, and often steady increases are recorded with each addition of agonist. The extent of these changes is species dependent (Michel et al. 1999; Hibell et al. 2000; Hibell et al. 2001a).

1.2.4.2 Pore formation

Changes to the agonist response occur with prolonged or high concentration agonist applications, producing perhaps the most interesting phenomenon related to P2X7 function; that of the formation of a "pore" that allows the passage of large diameter molecules into, or out of, the cell (Surprenant et al. 1996), and often resulting in cell lysis. The large diameter pore that forms in macrophages, microglial cells and mast cells is typically permeable to molecules of molecular mass up to 900 Da (Steinberg et al. 1987; Tatham and Lindau 1990), but in lymphocytes this is reduced to around 300 Da (Wiley et al. 1993). This formation of a large diameter pore in the membrane is often measured using plate-based fluorescence readers as an increase in the permeation of extracellular dyes, such as YO-PRO-1 (YOPRO) and Ethidium Bromide (EthBr), that fluoresce once bound to nucleic acids within the cell. There has been much discussion with regards to the nature of the pore form of the P2X7 receptor and two main theories have been put forward in the last 8 years. These two will be outlined and discussed separately and are exemplified in the schematic in Figure 1.3.

"Dilation theory"

It was initially hypothesised that the channel of the receptor undergoes a progressive dilation, resulting in an increase in the size of the transmembrane pathway and hence allows the permeation of larger molecules (Virginio et al. 1999a; Virginio et al. 1999b; Figure 1.3). The fact that the pore may form when P2X7 receptors are expressed in many different expression systems; HEK293 (Surprenant et al. 1996; Rassendren et al. 1997), mouse microglial cell line (Chessell et al. 1998b), granulocytic cells (HL-60 and

neutrophil-like cells) (Suh et al. 2001), rat peritoneal mast cells (Tatham and Lindau 1990) and human THP-1 cells (Donnelly-Roberts et al. 2004) inferred that it was likely to be mediated through P2X7 receptors themselves. There is also considerable overlap in the pharmacology of the channel and pore forms, with MAP kinases (Faria et al. 2005), Brilliant blue G (Jiang et al. 2000a), and many of the newer tool molecules such as A-740003 (Honore et al. 2006), and AZ11645373 (Stokes et al. 2006) blocking both forms of the P2X7 receptor. The formation of large diameter pores has also been associated with the expression of the P2X2 and P2X4 subtypes (Khakh et al. 1999a; Virginio et al. 1999b). It is more difficult to induce pore formation in cells expressing these other P2X receptors and so difference between their structures was investigated. The most obvious difference between the P2X subtypes is the elongated C-terminal domain of P2X7 receptor and so this became the focal point for manipulation. Truncation of the C-terminus of P2X7 receptors by deletion of residues 419 to 595 resulted in a functional cation channel, but a much reduced uptake of YOPRO (Surprenant et al. 1996), and no ethidium bromide uptake into cells (Smart et al. 2003). Conversely, an augmentation in pore-forming ability was conferred to human P2X7 receptor by the substitution of C-term region with corresponding region of rat receptor, an orthologue that undergoes pore formation more readily than the human. These data again provided evidence that it is the P2X7 receptor itself, and specifically residues located in the C-terminal domain, that participate in pore formation (Rassendren et al. 1997).

"Separate pore hypothesis"

The main alternative theory for P2X7-induced pore formation centres around the hypothesis that P2X7 activation initiates the formation of a separate pore-forming protein in the membrane, and was discussed once it emerged that in some expression systems, particularly xenopus oocytes, the activation of P2X7 only produced the opening of a non-selective cation channel and not a large pore (Petrou et al. 1997; Watano et al. 2002; Ramirez and Kunze 2002). Also pharmacological differences were identified when the

P2X7 ionic channel was shown to be blocked by Calmidazolium and a monoclonal antibody, with no effect on YOPRO uptake (Virginio et al. 1997; Chessell et al. 2001). The discovery that maitotoxin, a potent cytolytic agent, activated a non-selective cation channel and a large diameter pore, allowing the uptake of ethidium bromide and YOPRO, strengthened the separate pore hypothesis (Schilling et al. 1999a; Schilling et al. 1999b; Lundy et al. 2004). Maitotoxin does not bind or interact with P2X7 receptors and yet produced similar effects on the membranes of cells over a similar time scale to that seen following P2X7 activation, and raises the possibility that Maitotoxin and P2X7 receptors activate a common cytolytic pore. More recent work has shown P2X7-induced pore formation to be dependent upon a cascade of events involving the release of second messengers (Coutinho-Silva and Persechini 1997; Faria et al. 2005), and in particular p38 MAP Kinase (Donnelly-Roberts et al. 2004), but also caspase pathways (Donnelly-Roberts et al. 2004).

The formation of the pore has been measured electrophysiologically as a progressive increase in the permeability of a large cation N-Methyl-D-Glucamine (NMDG) (Virginio et al. 1999a), and using plate based fluorescence readers as an increase in the permeation of extracellular dyes (YOPRO and Ethidium Bromide) that bind to nucleic acids once they enter cells. These two mechanisms are widely used and the uptake of both NMDG and dyes was considered to be occurring via the same route. However, Jiang and colleagues cast doubt on this with work that indicated a common pathway for NMDG and Na^+ ion permeation, where as the influx of dyes such as YOPRO, may be occurring via another route (Jiang et al. 2005). It has also been shown that other stimulants can result in YOPRO/Ethidium Bromide uptake into cells, including maitotoxin application, but that these channels are not permeable to NMDG (Martinez-Francois et al. 2002; Lundy et al. 2004). The biphasic currents recorded following prolonged agonist applications to P2X7 receptors were suggested to be indicative of dilation of the P2X7 receptor channel and has been shown to be influenced by the C-terminal (Yan et al. 2008). Therefore these data

suggest that the NMDG-permeable pore is part of the P2X7 receptors, whereas the YOPRO entry pathway is via a molecular mechanism distinct from the P2X7 receptor, but is switched on as a consequence of P2X receptor activation (Jiang et al. 2005; Yan et al. 2008).

Recent work has focused on the involvement of pannexin-type hemichannels in the formation of the pore, particularly centring on pannexin-1 (Pelegrin and Surprenant 2006; Locovei et al. 2007). Pannexins are mammalian proteins that are similar, in general structure, to the non-mammalian innexins that form gap junctions in invertebrates (Panchin et al. 2000). There are 3 Pannexins (Panx1, Panx2, Panx3) that have been identified (Panchin 2005; Barbe et al. 2006). The expression of Panx1 cDNA in single oocytes resulted in hemichannel-like membrane currents, and in paired oocytes expressing Panx1, junctional coupling was observed (Barbe et al. 2006). Panx1 mRNA was found in a variety of different cell types, including human and mouse monocytes, macrophages, astrocyte cells and non-immune cell lines such as HEK and HeLa cells and it was co-immunoprecipitated with the P2X7 protein following co-expression in HEK293 cells (Pelegrin and Surprenant 2006). Functional evidence that Panx1 is the molecular correlate of the P2X7-activated pore form was obtained using small interference RNA (siRNA), a Panx1-mimetic inhibitory peptide, or over-expression techniques, to show a modification of dye uptake, but not receptor activation or its resulting ionic current (Pelegrin and Surprenant 2006).

Figure 1.3: Schematic representation of the 2 theories of what underlies the large diameter pore following P2X7 receptor activation.

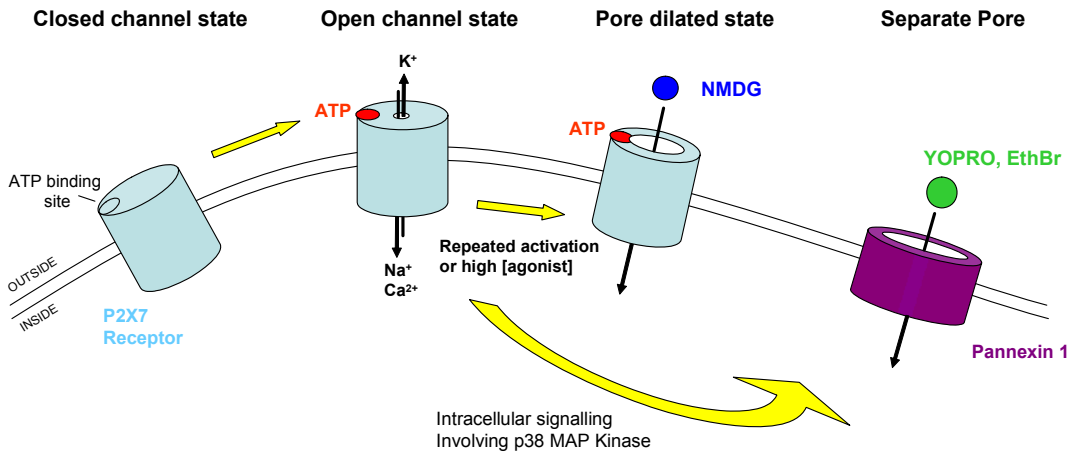

1.2.4.3 IL-1β production and release

Uniquely, the activation of the P2X7 receptor also results in the release of mature, biologically active IL-1β (Perregaux and Gabel 1994; Solle et al. 2001; Ferrari et al. 2006). IL-1β is a pro-inflammatory cytokine that is part of the Interleukin-1 family (Discussed in **1.3.9 Cytokines)**. It is synthesised by cells as an inactive precursor molecule, pro-IL-1β, and following cleavage by a cysteine protease, caspase-1 (previously known as Interleukin-1 converting enzyme, ICE), (Kostura et al. 1989; Thornberry et al. 1992), the 17 kDa mature, active form is produced.

The process of the production and release of IL-1β is tightly controlled. Many different inflammatory mediators such as viruses, endotoxins (e.g. lipopolysaccharide (LPS)), Tumour necrosis factor α (TNF-α) or phorbol esters (e.g. PMA) prime cells through inducing the synthesis of pro-IL-1β, which is normally absent from cells under normal conditions (Martinon and Tschopp 2004), and possibly increasing the expression of pro-

caspase-1 (Le Feuvre et al. 2002b). If halted at this stage more than 95% of the pro-IL-1β will remain unprocessed in the cytoplasm of cells, and so a second stimulus is also required to, indirectly, produce IL-1β. The second stimulus has been shown to be the binding of ATP to the P2X7 receptor, resulting in the opening of the non-selective cationic channel. The movement of Na^+ and Ca^{2+} ions into cells is accompanied by a K^+ ions efflux, and it is this reduction of intracellular K^+ ions that activates the caspase-1 enzyme (Perregaux and Gabel 1994; Kahlenberg and Dubyak 2004). Caspase-1 is constitutively expressed in many cells as a 45-kDa inactive precursor (pro-caspase-1), which requires cleavage before being active (Wilson et al. 1994).

The release of IL-1β is a tightly controlled process that is not dependent upon cytolysis and does not require P2X7-mediated pore formation (Chessell et al., 2001). Although pore formation itself is not required, the activation of Panx1 is required for the cleavage of caspase-1 and the subsequent release of IL-1β, indicating a downstream signalling link between Panx1 and the processing and release of IL-1β *in vitro* (Pelegrin and Surprenant 2006; Pelegrin and Surprenant 2007). IL-1β release can also be prevented by the inhibition of the caspase-1 enzyme (Watanabe et al. 1998), and the inhibition of the ATP-binding cassette-1 (ABC-1), suggesting a role of anion flux in the release of IL-1β (Hamon et al. 1997).

The main routes for IL-1β release are proposed to be by secretion via endosomes (Andrei et al. 1999), secretion via microvesicle shedding (Mackenzie et al. 2001), or the exportation by transporters, such as ABC transporters (Hamon et al. 1997); Figure 1.4.

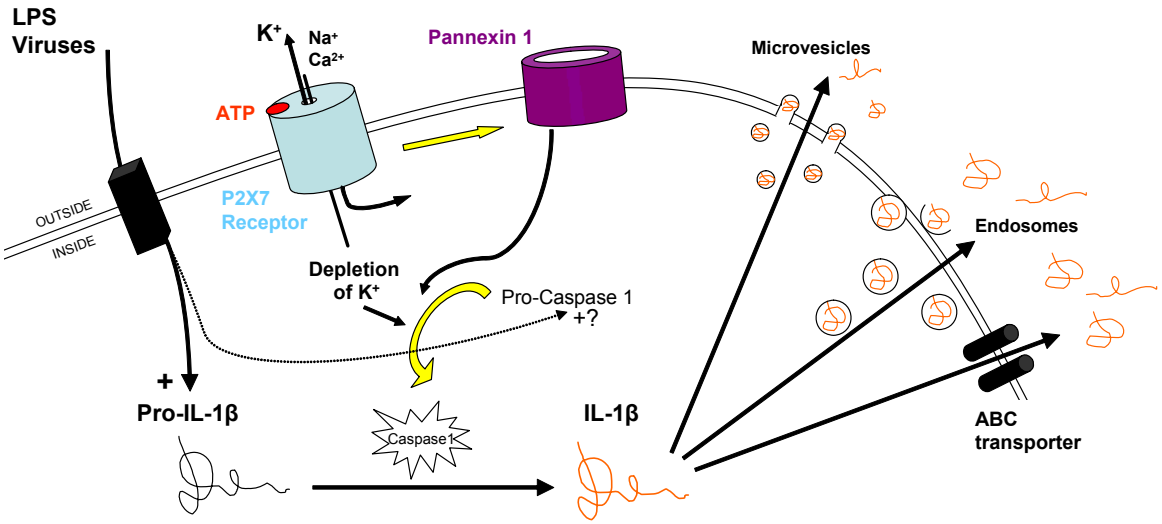

Figure 1.4: Schematic depicting proposed mechanisms of ATP stimulated IL-1β processing and release.

Once mature IL-1β is released it has downstream effects on other cells including the induction of nitric oxide synthase (iNOS), cyclooxygenase 2 (COX-2) (Samad et al. 2001), the production of superoxide products (Parvathenani et al. 2003) TNF- α (Woolf et al. 1997), all of which have well described roles in the generation or maintenance of pain. (This is discussed in section **1.4.6 Role of P2X receptors in pain**)

1.2.4.4 Membrane disruption

P2X7 receptor activation is also associated with membrane blebbing (Virginio et al. 1999a), and cytoskeletal and cellular changes, which occur within 2-30 seconds of receptor activation. These events are reversible, although a prolonged activation will eventually lead to cell death by necrotic and apoptotic mechanisms (Ferrari et al. 1999). Membrane blebs start with the appearance of numerous small vesicles which can be shed

from the cell, or develop into large hemispherical protrusions of the plasma membrane (Mackenzie et al. 2001). These membrane blebs or microvesicles, are characterised by phosphatidylserine translocation (Mackenzie et al. 2001) and actin/β-tubulin rearrangements (Pfeiffer et al. 2004). Although the functional consequences of membrane blebbing following P2X7 activation is unknown, in other systems it is associated with mitosis, apoptosis and secretion (Hagmann et al. 1999). P2X7-mediated membrane blebbing involves epithelial membrane protein interaction with the C-terminus of the P2X7 receptor (Wilson et al, 2002).

Studies *in vitro* show that concentrations in the range of 0.5-5 mM ATP are required to fully activate P2X7 and induce IL-1β release. This is similar to cytosolic concentrations of ATP, but is high for function in the extracellular compartment. Therefore doubts were raised about the physiological relevance of this mechanism as it is unlikely that high (0.5-5 mM) concentrations of ATP would be in the vicinity of target cells for an extended time. However, although prolonged activation of the P2X7 receptor will produce cell death, continuous exposure to ATP is not a requirement. In susceptible cells, once P2X7 receptor activation has occurred, some cells will recover their integrity and function normally, only to die sometime later (Hogquist et al. 1991). This suggests that once activated, the P2X7 receptor sets in motion an irreversible intracellular cascade of events leading to cell death (Di Virgilio 1995).

1.3 Pain

The current definition of pain is “An unpleasant sensory and emotional experience associated with actual or potential tissue damage, or described in terms of such damage”, as put forward by an International Association for the Study of Pain (IASP) Subcommittee on Classification in 1986 (Lindblom et al. 1986) and now used as an official definition by the IASP. Acute pain is an essential component of the body’s

normal defence mechanism, alerting the body to danger and protecting it from further damage. However the development of abnormal sensitivity in the somatosensory system, results in pain of a more chronic nature. Pain is classed as chronic when the symptoms outlast the normal time required for healing following tissue damage, or when it is associated with a pathological condition that does not heal. Chronic pain affects millions of people worldwide, and is regarded by the World Health Organisation (WHO) as a major reason for health related absence from work. In addition, chronic pain can lead to depression, anxiety and insomnia which have detrimental effects on the patients' quality of life (Gureje et al. 1998; Ashburn and Staats 1999).

1.3.1 Treatment of Pain

Inflammatory pain is produced following an insult to tissues resulting in the release of inflammatory mediators from damaged cells, activation of the arachidonic acid pathway and the recruitment of immune cells, which may release further mediators including cytokines and growth factors. Non-steroidal anti-Inflammatory drugs (NSAIDs) such as Aspirin and Ibuprofen are the most commonly prescribed drugs for inflammatory pain. These compounds inhibit arachidonic acid metabolism and prostaglandin production through inhibition of cyclo-oxygenase (COX) (Vane 1971; Kawai 1998), thereby eliminating the direct hyperalgesic effects of these compounds but also their sensitising effect . However NSAIDs have limited efficacy in severe pain, due in part to the many different inflammatory mediators capable of sensitising neurones, and also to side effects from prostaglandin inhibition in other tissues. Adverse effects include gastrointestinal bleeding (Goodwin 1987), renal failure (Lifschitz 1983) and cardiovascular effects (Waksman et al. 2007). Paracetamol, not conventionally classed as an NSAID, is one of the most popular analgesic and anti-pyretic drugs, but the mechanism by which it achieves its effects is still debated. Although its analgesic and antipyretic effects are similar to those of aspirin, it does not have significant anti-inflammatory activity. Therefore it is has been reasoned that although it may have effects on COX enzymes,

they are different from that seen with NSAIDs. There is evidence for alternative mechanisms of action including inhibition of the nitric oxide pathway, increase in descending inhibitory serotonergic pathways and cannabinoid receptor agonism (Reviewed in Anderson 2008).

The other main type of chronic pain is classed as neuropathic pain. Neuropathic pain is defined as "Pain initiated or caused by a primary lesion or dysfunction in the peripheral or central nervous system" by IASP. It is found in a number of conditions including post-herpetic neuralgia (PHN), diabetic neuropathy, HIV-related neuropathies and trigeminal neuralgia. Neuropathic pain often responds poorly to commonly used analgesics and to standard doses of opioid analgesics (Tremont-Lukats et al. 2000), and so antiepileptic drugs, such as Carbamazepine, Lamotrigine, Gabapentin and Pregabalin, or tricyclic antidepressants, e.g. amitripytline, and selective mono-amine re-uptake inhibitors such as Duloxetine, are often used to treat a wide range of neuropathic pain disorders (Zaremba et al. 2006; Mico et al. 2006). Although there are treatments available, the efficacy of these drugs in this condition is poor and can be limited by poor tolerability. When this is combined with a low responder rate, as often seen, the result is a large patient group with unmet need, therefore highlighting the requirement for novel effective analgesics in this area.

1.3.2 Nociceptive processing

The ability to sense pain has two main purposes; 1) it allows the organism to detect potential injury and triggers an appropriate protective response and 2) it alerts the organism to previously injured tissue with an aim to prevent further injury. Nociceptive information is transmitted from the periphery via primary afferents into the dorsal horn of the spinal cord. From here nociceptive information moves up to supraspinal sites mainly through the spinothalamic pathway, but also via the spinoreticular, spinomesencephalic, spinoparabrachial, and spinohypothalamic pathways (Bernard et al. 1996; Willis and

Westlund 1997; Gauriau and Bernard 2004). Non-nociceptive sensory information is transmitted in the dorsal column. See Figure 1.5 for a schematic representation.

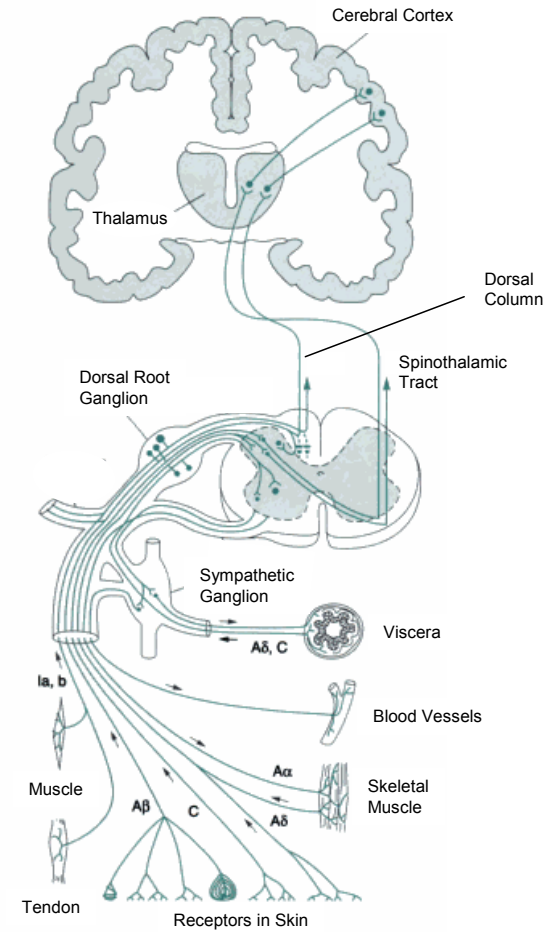

Figure 1.5: Schematic showing the main pathway for sensory information from the periphery to the cortex. (Modified from Clinical Anesthesiology (Morgan et al. 2005)).

1.3.3 Primary afferents

Somatosensory fibres innervate the skin, muscle, joints and viscera and detect information regarding the surrounding environment and the condition of the tissue. Fibres that innervate regions of the head and body arise from cell bodies in the trigeminal and dorsal root ganglia (DRG) respectively.

Primary afferent fibres transmit sensory information from the periphery to the spinal cord. Unlike other types of receptors in the skin, nociceptors can respond to multiple stimulus modalities, including temperature, mechanical and chemical stimuli (Bessou and Perl 1969; Beck et al. 1974; Van and Gybels 1981). They are categorised based on their myelination, the modality of stimulation that evokes a response and the characteristics of the response. Aβ-fibres are large, myelinated fibres that respond predominantly to light touch and have a fast conduction velocity. Aδ-fibres are lightly myelinated fibres with a medium axon diameter and a slower conduction velocity (Table 1.4). Aδ-delta fibres carry responses to strong noxious stimuli that are potentially or actually damaging tissues and represent approximately 10% of all primary afferents. Activation of Aδ-fibres leads to a well localised, sharp and acute pain sensation (Dubner 1978; Handwerker and Kobal 1993). C-fibre make up the majority of fibres within the DRG (70%), and these have the smallest diameter axons, and are non-myelinated, and hence have slow conduction velocities (Table 1.4; Millan 1999). C-fibre activation produces a more diffuse, poorly localised pain sensation (Dubner 1978; Handwerker and Kobal 1993).

Table 1.4: Characteristics of Primary Afferent Fibres

Fibre Type	Fibre diameter (μm)	Myelination	Conduction Velocity (m/s)	% Primary Afferents	Sensation following fibre activation
Aβ	>10	thick	30-100	20	non-noxious light touch
Aδ	2-6	thin	12-30	10	noxious, sharp, prickling pain
C	0.4-1.2	none	0.05-2	70	noxious, diffuse, persistent, and poorly localised pain

1.3.4 The spinal cord

Primary afferent fibres enter the spinal cord and immediately ascend or descend one or two segments in Lissauer's tract before terminating in the grey matter. The areas of termination were segregated into 10 laminae based on density and type of cell bodies and myelination (Rexed, 1952, see Fig 1.2) (Willis and Coggeshall 1991). The first six lamina, which make up the dorsal horn, represent the principal site of modulation of pain by ascending and descending pathways. The different nociceptive primary afferent fibres terminate in specific laminae within the spinal cord. The termination of Aβ-fibres is the most widespread, with most synapsing in laminae III, IV and V. Aδ-fibre afferents predominantly synapse onto lamina I neurones, and to a lesser extent into laminae II, V and X. C-fibres terminate in lamina I, II and V (Millan 1999), (Willis and Coggeshall 1991). All of these primary afferent fibres synapse onto second order neurones which have their cell bodies in the dorsal horn.

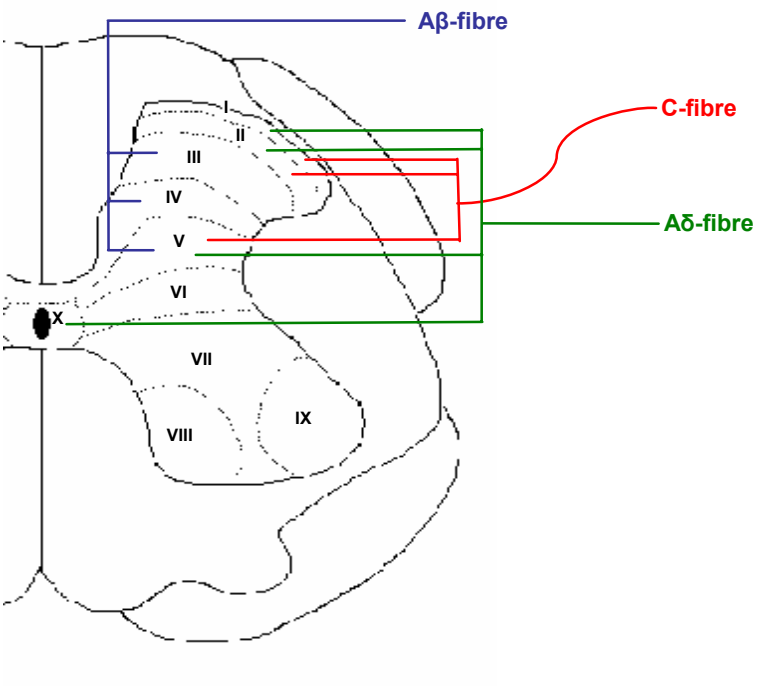

Figure 1.6: Diagram of Rexed's laminae of the spinal cord indicating the main laminae for the termination of fibres

1.3.5 Peripheral Sensitisation

Peripheral sensitisation is a reduction in threshold and an increase in responsiveness of the peripheral nociceptors. It occurs when primary afferents become directly activated following tissue injury or inflammation. Sensory and sympathetic neurones, blood vessels and immune cells can all release mediators of inflammation in response to tissue injury. Bradykinin and prostaglandins are released from injured tissues, along with serotonin from activated platelets. The walls of blood vessels undergo an increase in permeability, inducing the release of nitric oxide by plasma extravasation. These chemical and inflammatory mediators along with others such as adenosine, ATP and protons can act directly on primary afferent neurones, causing pain or sensitisation (Kress and Reeh 1996). There is also indirect sensitisation of neurones through the release of cytokines

such as IL-1β and TNF-α (Bianchi et al. 1998). IL-1β is produced by a variety of non-neuronal cells (including macrophages, mast cells, fibroblasts and synoviocytes) during inflammation (Bianchi et al. 1998). Once released, IL-1β has the potential to cause sensitisation of afferents by a variety of different mechanisms including; stimulating the release of PGE_2 from inflammatory cells (Dayer et al. 1986), the induction of Nerve Growth Factor (NGF) (Yoshida and Gage 1992) and the upregulation of substance P levels in neurones (Jonakait et al. 1990). The resulting increase in activation of primary afferent neurones leads to neurogenic inflammation through the release of pro-inflammatory neurotransmitters such as calcitonin-gene related peptide (CGRP) and substance P (Lynn 1996). The sensitisation induced by these peptides can lead to a change in the excitability of sensory nerves, and nearby postganglionic sympathetic fibres. In areas of primary hyperalgesia, primary afferents innervating inflamed tissues have a reduced threshold for activation, an increase in the response to a given stimuli and an increase in spontaneous firing. The overall effect of this leads to an increase in the input into the spinal cord, a greater release of glutamate and substance P from central afferent terminals and results in hyperexcitability of dorsal horn neurones (Woolf 1983; Woolf and Thompson 1991).

1.3.6 Central Sensitisation

Central sensitisation manifests itself by (1) a reduction in the threshold for activation of dorsal horn neurones; (2) an increases in the responsiveness of dorsal horn neurones; (3) an expansion of the receptive field (Woolf 1991). This occurs following prolonged nociceptive fibre input as a result of tissue damage or peripheral inflammation. This results in a state of hypersensitivity where low-intensity stimuli, which are innocuous under normal conditions, are able to initiate pain sensations. This mechanism has a protective purpose by sparing injured body parts from further injury while healing occurs (Woolf and Walters 1991).

1.4 Glia

Until very recently, spinal central sensitisation as detailed above, was thought to be predominantly the result of a cascade of neuronal events in the spinal cord (Woolf and Salter 2000). However there is now compelling evidence that spinal cord glial and immuno-competent cells and their cross-talk with neurones play a key role in the induction and maintenance of central sensitisation (Watkins et al. 1997; Colburn et al. 1999; Colburn and DeLeo 1999; Milligan et al. 2003).

Non-neuronal cells were first identified in the mid-19th century by Rudolph Virchow, a German anatomist, and were called 'glia', the Greek for 'glue'. It is now know that the term glial cells encompasses 3 cell types, called microglia, astrocytes and Oligodendrocytes, and that these cells make up around 70% of the total cell populations in the CNS.

1.4.1 Oligodendrocytes

Oligodendrocytes are the myelinating cells of the central nervous system. However unlike the peripheral nervous system, where one schwann cell myelinates one axon, a single oligodendroglial cell synthesises myelin sheaths for multiple neurones (Peters 1964) allowing fast nerve conduction.

1.4.2 Microglia

Microglia are known as the resident macrophages of the CNS and account for 5-10% of the total glial cell population (Kreutzberg 1996; Stoll and Jander 1999). Quiescent microglia have small cell bodies and short processes, but they are not passive cells, rather they actively sense their environment with their ramified processes (Nimmerjahn et al. 2005; Hanisch and Kettenmann 2007). Following even minor pathological changes in the CNS, such as in response to infectious diseases, inflammation, trauma, ischemia, brain tumours and neurodegeneration, microglia become activated. Microglial activation

manifests itself in a number of ways, including a change in morphology from ramified to amoeboid shape (Eriksson et al. 1993), an increase in the expression of markers such as MHC II and CD 11b (Hayes et al. 1987; Eriksson et al. 1993), and proliferation (Tsuda et al. 2005). Once activated, microglia perform a variety of functions in tissue repair and neural regeneration, as well as phagocytosis and the release of proinflammatory cytokines such as TNF-α, IL-1β and interleukin-6 (IL-6) (Hanisch and Kettenmann 2007; for review)

1.4.3 Astroctyes

Astrocytes are the most numerous of all glial cells in the CNS and are star-shaped cells with a central cell body, approximately 15–17 μm in diameter, and long processes extending in all directions. These processes make contact with neuronal synapses and the vasculature, allowing bi-directional communication between these two tissues, and the connections with the endothelial cells of the capillaries form the basis of the blood-brain barrier (Abbott et al. 2006). Connections are also formed between astrocytes through gap junctions, thereby forming networks of coupled astrocytes (Blomstrand et al. 1999; Guthrie et al. 1999). Astrocytes also have important roles at synapses, and one astrocyte may make contact with over 100,000 synapses (Bushong et al. 2002). They enwrap nerve terminals (Peters et al. 1964), which positions them perfectly to influence synaptic transmission. This led to the concept of the Tripartite synapse (Araque et al. 1999). At the synapse of pre- and post-synaptic neurones they are responsible for the clearance of transmitters such as glutamate and GABA from synaptic clefts, but also have the ability to release gliotransmitters (Araque et al. 1999). Astrocytes are activated by several substances including excitatory amino acids (Kettenmann and Schachner 1985), nitric oxide (Mollace et al. 1998), substance P (Wienrich and Kettenmann 1989), prostaglandins (Bezzi et al. 1998) and ATP (Neary et al. 1988). They can also be activated by invading organisms, such as bacteria and viruses (Meller et al. 1994; Milligan et al. 2001), which do not directly activate neurones. The gliotransmitters they

release include proinflammatory cytokines such as IL-1β, IL-18 and TNF-α, excitatory amino acids and growth factors, all of which are neuroactive (Wienrich and Kettenmann 1989; Mollace et al. 1998; John et al. 2001; Haydon 2001). Therefore they are ideally placed to influence synaptic transmission and play a role in neuronal activity.

1.4.4 Glial activation in Pain models

Initially the literature around glial activation was focused around the observation that peripheral nerve damage led to CNS glial activation (Sjostrand 1971; Hall et al. 1989; Hajos et al. 1990) without making any link back to pain. It was in 1991 that Garrison and colleagues first made a link between nerve damage-induced pain and nerve damaged-induced glial activation. Using the astrocyte-specific marker Glial-Fibrillary Acidic Protein (GFAP) they demonstrated astrocyte activation in a neuropathic pain model, and then the reversal of the activation following the administration of an analgesic compounds (Garrison et al. 1991).

Since then the activation/proliferation of spinal cord glia and immune cells have been identified in a wide range of preclinical models of chronic pain, such as inflammation (Sweitzer et al. 1999; Raghavendra et al. 2004a), nerve injury (Colburn et al. 1999) and bone cancer (Schwei et al. 1999; Zhang et al. 2005a). It has also been shown that inhibition of glial activation can block or prevent pain. Fluorocitrate is a general glial inhibitor, blocking the activity of both astrocytes and microglia. It takes advantage of the fact that glia, and not neurones, take up extracellular citrate for metabolism in the Krebs cycle (Fonnum et al. 1997). Low doses must be used in order to only target glia as higher dose result in irreversible and toxic effects on glial cells and so affects neuronal cell function also (Paulsen et al. 1987). Fluorocitrate has been shown to be an effective blocker of pain states induced in a range of models including sciatic inflammatory neuropathy (Milligan et al. 2003), intrathecal delivery of viral components (Milligan et al. 2000; Milligan et al. 2001) and subcutaneous formalin (Watkins et al. 1997).

More specifically, Minocycline, a semi-synthetic tetracycline derivative, also inhibits microglial function (Tikka et al. 2001). The administration of Minocycline pre-emptively blocked the production and release of pro-inflammatory cytokines in neuropathic pain models (Raghavendra et al. 2003), and could block the induction of hypersensitivity (Raghavendra et al. 2003; Ledeboer et al. 2005). However, minocycline has little, or no effect on hypersensitivity once it is established (Raghavendra et al. 2003; Ledeboer et al. 2005), indicating a necessity for microglial activation in the development of such pain states, but little role in their maintenance. These data have led to the proposal that early microglial activation leads in turn to activation of astrocytes, and that astrocyte activation serves to maintain the hypersensitivity and consequently the pain. It is also important to note that the involvement of glia in pain processing seems to be limited to hypersensitivity, and has no effect on basal, acute pain processing.

Interestingly, an upregulation of markers of glial activation is recorded following chronic morphine treatment (Song and Zhao 2001), and the tolerance associated with morphine was attenuated following dual dosing with Fluorocitrate. This lead to speculation that glial activation may account in some way for the tolerance seen with prolonged opioid use, highlighting another possible mechanism by which glial cells influence chronic pain.

1.4.5 Cytokines

Cytokines are soluble proteins that are released by a variety of cells such as fibroblasts, synoviocytes and mast cells (Watkins et al. 1995). They are classically associated with cell proliferation, differentiation and changes in gene expression (Janeway et al. 2001), but in addition, they are essential in fighting infection and responding to injury. Cytokines are chemical messengers that regulate the balance between cell mediated and antibody mediated immune responses, and produce either a proinflammatory or an anti-inflammatory response. Inflammatory cytokines include TNFα, IL-1, IL-6 and IL-8 are often released in a cascade, where an initial release of TNF is followed first by IL-1 and

then by IL-6. Less than 10 IL-1 receptors are estimated to need occupation to induce a physiological response, highlighting the exceptionally powerful ability of these proinflammatory cytokines (Gallis et al. 1989).

1.4.6 Role of P2X receptors in pain

Following inflammation or nerve injury, release of ATP by neuronal and non-neuronal cells is greatly increased in the periphery as well as in the CNS (Chizh and Illes 2001; for review). In spinal dorsal horn, ATP can increase the release of glutamate, GABA and glycine via the activation of presynaptic P2X2, P2X3 and P2X2/3 receptors (Sawynok et al. 1993; Gu and MacDermott 1997; Rhee et al. 2000). There have been numerous studies detailing the importance of P2X2/3 and P2X3 receptors in pain (Jarvis 2003, for review). P2X3 receptors are highly expressed on primary afferent neurones and preferentially on nociceptive C-fibers (Lewis et al. 1995; Chen et al. 1995), were as P2X2 receptors are mainly expressed on medium to large diameter fibres, with overlap of these two subtypes on small diameter neurones (Petruska et al. 2000). The expression of P2X3 receptors has been shown to increase following a peripheral nerve injury (Novakovic et al. 1999). More recently, the novel dual P2X2/3 and P2X3 antagonist, A-317491, has been shown to reduce hypersensitivity associated with inflammatory and neuropathic insult in animals (Jarvis et al. 2002; McGaraughty et al. 2003; McGaraughty and Jarvis 2005), providing useful *in vivo* data confirming a key role of these receptors in pain processing.

ATP also activates non-neuronal cells such as astrocytes, microglia and macrophages, and once activated, these cells release cytokines and other pro-inflammatory mediators (Interleukin-6, interleukin-1β, tumour necrosis factor α, prostaglandins, and excitatory amino acids) which are known to induce or increase hyperexcitability of spinal neurones (Watkins and Maier 2002). P2X4 receptors are expressed on a wide variety of cells types, including both neurons (Buell et al. 1996) and microglia (Tsuda et al. 2003). There is increasing evidence for their involvement in mediating neuropathic and inflammatory

pain. P2X4 expression levels change in spinal microglia following nerve injury (Tsuda et al. 2003) and formalin-induced inflammation (Guo et al. 2005), and intrathecal administration of P2X4 antisense oligoucleotide was able to suppress the tactile allodynia caused by a peripheral nerve injury (Tsuda et al. 2003). The activation of P2X4 receptors on microglia results in the release of cytokines that can enhance synaptic transmission (Tsuda et al. 2003), therefore preventing P2X4 receptor function may represent a novel therapeutic approach for treating pain hypersensitivity.

There is also increasing evidence for a substantial role of P2X7 receptors in pain pathology. The repertoire of responses to agonist activation, along with their localisation on non-neuronal cells makes them ideally placed to influence nociceptive functioning.

1.4.6.1 P2X7 receptors and Pain processing

There is substantial evidence to indicate a role for P2X7 receptors as a key mediator of the inflammatory response (Ferrari et al. 2006) and so as a potential therapeutic target with which combat chronic inflammatory pain (Romagnoli et al. 2008). The proposed role for P2X7 receptors in inflammatory and neuropathic pain centres on the maturation and release of IL-1β following receptor activation (Ferrari et al. 2006).

The role of IL-1β in pain is well defined *in vivo*, where blockade of IL-1 receptors with an IL-1 receptor antagonist (IL-1ra), reduced thermal hyperalgesia and mechanical allodynia in a mouse neuropathic pain model (Sommer et al. 1999). The release of IL-1β initiates a signalling cascade leading to the up-regulation of various other inflammatory mediators such as COX-2, IL-6, TNFα, nitric oxide synthase (iNOS) (Woolf et al. 1997; Samad et al. 2001), and the production of superoxide products (Parvathenani et al. 2003), all of which have a role in pain (Lister et al. 2007). IL-1β may be of further importance as its release, after P2X7 activation, caused an increase in the expression levels of P2X7 receptors in astrocytes (Narcisse et al. 2005). This is also mimicked in satellite cells in nerve and DRG sections from patients suffering with persistent neuropathic pain

(Chessell et al. 2005). The increase in P2X7 receptor expression seen under these conditions may well result in a larger cationic current into cells following activation, influencing neuronal processing via a greater release of inflammatory cytokines; and the release and uptake of neurotransmitters such as glutamate (Colburn et al. 1997; Haydon 2001).

The production of P2X7 gene deleted mice showed a reduction or a removal of the release of IL-1β following ATP/BzATP stimulation of LPS primed blood samples or plated cells from P2X7 knockout mice compared to control animals (Solle et al. 2001; Labasi et al. 2002; Chessell et al. 2005). There is also an overall reduction in the release of inflammatory mediators following Freunds Complete Adjuvant (FCA) treatment in these animals (Chessell et al. 2005). Behaviourally, P2X7 knockout mice showed reduced pain sensitivity following both a partial nerve injury and FCA treatment (Chessell et al. 2005), indicating a role for P2X7 in mediating the hypersensitivity associated with inflammatory and neuropathic pain. Importantly, no changes in nociceptive responses were recorded for these P2X7 knockout mice (Chessell et al. 2005). Following on from this the effect of antagonists of P2X7 receptors were profiled. The possibility of P2X7 antagonists being anti-hyperalgesic was first introduced when oxidised ATP was used in a model of arthritis and reversed the deficit in paw withdrawal threshold recorded following the adjuvant injection (Dell'Antonio et al. 2002b). More recently a number of small molecule selective P2X7 antagonists have been shown to be efficacious in models of inflammatory and neuropathic pain, providing more evidence for the key role of this receptor in mediating pain (Lappin et al. 2005; Honore et al. 2006; Carroll et al. 2007; Nelson et al. 2008).

1.5 Satellite Cells in DRG

The cell bodies of primary afferent fibres that innervate the skin and viscera congregate in the dorsal root ganglia (DRG) found just before the dorsal root of the spinal cord. The DRG consists of these sensory neurone cell bodies, glial derived satellite cells, dendritic cells, macrophages, and endothelial cells (Olsson 1990). In the DRG, each neuronal cell body is encapsulated by a layer of satellite cells, usually consisting of several satellite cells, that forms a distinct morphological unit (Pannese 1981).

Satellite cells are glial-like and so possess many of the regulatory and immune-like functions recorded in glial cells. They have been shown to be important controllers of the contents of the ganglia extracellular space, exhibiting mechanisms for neurotransmitter uptake (Keast and Stephensen 2000) or breakdown (Braun et al. 2004) and can therefore exert a tight control over the neuronal microenvironment. Specifically, they are involved in the uptake of glutamate and aspartate and also provide the precursor to glutamate production, glutamine, to DRG neurones (Duce and Keen 1983; Kai-Kai and Howe 1991). They are also known to release proinflammatory cytokines and growth factors (Ramer et al. 1998; Ramer et al. 1999; Zhou et al. 1999).

Like glial cells in the CNS, satellite glial cells are stimulated following peripheral nerve injury or inflammation, exhibiting cell proliferation (Pannese 1981; Lu and Richardson 1991) and upregulation of GFAP labelling (Woodham et al. 1989). Whether this increase in GFAP is due to cell proliferation, hypertrophy or an increase in synthesis is not yet known and would be useful to know to determine the reasons for this change. As mentioned above, they also release cytokines that are pro-inflammatory, although it is not clear whether there is an enhancement of release under conditions of injury (Ramer et al. 1998; Ramer et al. 1999; Zhou et al. 1999). Satellite glial cells are often electrically-coupled to each other, in most cases between the cells that envelope a particular neuron (Hanani et al. 2002). However the number of gap junctions is expanded following nerve

injury (Hanani et al. 2002), a change that is seen in glia in the spinal cord and is correlated with hyperalgesia (Spataro et al. 2004). Thus these satellite cells are well positioned both anatomically and physiologically, to regulate neuronal activity in the DRG.

1.5.1 Role of P2X receptors on Satellite Cells

P2X receptors have been shown to be present on satellite cells from peripheral ganglia, specifically, P2X3, P2X2/3 (Kumagai and Saino 2001) in superior cervical ganglia (SCG), and P2X2 (Vulchanova et al. 1997) and P2X7 receptors (Zhang et al. 2005b) in DRG. However the exact roles of these receptors in the functioning of satellite cells in physiology and pathophysiology is unclear. Functionally, there is evidence for somatic release of ATP from DRG neurones and that this plays an important role in bi-directional communication between satellite cells and neurones in DRG (Zhang et al. 2007). The activation of P2X7 receptors on satellite cells can also lead to the release of TNF-α, which can in turn increase the excitability of neurones (Zhang et al. 2007). This suggests that neuronal somata have a significant role in inter-cell signalling and satellite cells can influence neuronal activity. The increased expression of P2X7 receptors on satellite cells from neuropathic pain patients and following IL-1β release (Chessell et al. 2005; Narcisse et al. 2005), mentioned earlier, provides further indirect evidence for a specific role of P2X7 receptors expressed in these cells. As well as the effects of satellite cells on neuronal functioning through release of mediators of inflammation, it has been proposed that the electrical coupling of satellite cells may influence sensitisation associated with pain (Spataro et al. 2004). In chronic pain, an augmentation of coupling among satellite cells has been recorded (Dublin and Hanani 2007), and there is evidence that ATP release via P2X7 receptor activation may amplify Ca^{2+} signalling between spinal cord astrocytes (Suadicani et al. 2006).

In summary, there is evidence for changes in satellite cells functioning and coupling following nerve injury or inflammation, and also evidence for upregulation of P2X7 receptors on these cells, although much of it indirect and further work is needed (Dublin and Hanani 2007).

1.6 Epilepsy

Epilepsy affects about 1% of the world's population and describes a group of neurological disorders characterized by the periodic occurrence of spontaneous seizures. Although there are a good range of anti-epileptic agents available, about 30% of epileptic patients do not respond to these therapies and are defined as pharmaco-resistant.

1.6.1 The neurophysiology of epilepsy

EEG recordings from epilepsy patients have identified two broad categories of paroxysmal neuronal discharge: inter-ictal and ictal epileptiform discharge. Inter-ictal discharges are brief (<1s) bursts of synchronous neuronal activity occurring between seizures. Ictal discharges occur during seizures and often last several seconds to minutes (Prince 1978).

Broadly speaking, epilepsy is thought to arise from an imbalance between excitatory and inhibitory synaptic transmission, which results in excessive excitation and leads to synchronous discharges of large neuronal populations. Recent experimental and clinical evidence supports a crucial role of inflammation in epilepsy (Vezzani and Granata 2005) and in particular in the mechanisms underlying the generation of seizures (ictogenesis) and the development of seizure-generating neural network from a normal one (epileptogenesis) (Pitkanen and Sutula 2002). There is also evidence for a marked reactive gliosis in epileptogenic tissue, and alterations in the functioning of specific glial membrane channels, receptors and transporters (Steinhauser and Seifert 2002). Until the bidirectional communications between neurones and glial cells are completely

understood, it is not clear whether the glial changes are an accompanying facet of the disease or have a role in the production of epilepsy.

1.6.2 P2X7 receptors and epilepsy

The proposed role for P2X7 receptors in epileptogenesis is based on their properties and localisation. Firstly, even though the localisation of P2X7 receptors is still under some debate, their activation has been shown to increases neurotransmitter release from presynaptic excitatory nerve terminals in the hippocampus (Deuchars et al. 2001; Sperlagh et al. 2002). Secondly P2X7 receptors are expressed on astrocytes (Ballerini et al. 1996; Kukley et al. 2001) and activation of P2X7 receptors results in the release of Glutamate and GABA (Wang et al. 2002; Duan et al. 2003). Data from hippocampal slices shows that glutamate release from astrocytes activates neuronal NMDA receptors, and can lead to neuronal network synchronisation (Angulo et al. 2004; Fellin et al. 2004). Thirdly, there is growing evidence for the role of cytokine, in particular IL-1β, in epileptogenesis. Seizures have been shown to stimulate the release of this cytokine (Vezzani and Baram 2007; for review). Inflammatory cytokines, including IL-1β, have been shown to be over-expressed during epileptogenesis in astrocytes, but not in microglia, suggesting a predominant role of astrocytes in sustaining chronic inflammation before the onset of spontaneous seizures (Ravizza et al. 2008). They have also been shown to be pro-convulsant in a large variety of seizure models (Vezzani et al. 1999). Finally, there may be a change in the responsiveness of P2X7 receptors in epilepsy. There are conflicting reports from *in vivo* models of epilepsy, showing an upregulation of P2X7 receptor expression in some rat models (Vianna et al. 2002; Rappold et al. 2006), but also a decrease in P2X7 receptor immunoreactivity in seizure sensitive gerbil hippocampus (Kang et al. 2004).

1.7 Aims of this thesis

In this thesis, I have used electrophysiological and immunocytochemical techniques to investigate P2X7 receptors stably expressed in cell lines and native P2X7 receptors expressed in non-neuronal cells from DRG cultures.

The main aims were;

- To assess some of the defining characteristics of this receptor, focusing on the response to agonist activation. What differences, if any, are there in the functioning of the receptor when it is expressed in a recombinant system compared to in native cells?
- To investigate the pharmacology of P2X7 receptors and assess the activity of a novel compound at recombinant and native P2X7 receptors. Using potency and selectivity data for this compound in order to support the conclusion that P2X7 antagonists may provide a novel mechanism to target inflammatory pain.
- To investigate P2X responses recorded in non-neuronal cells in DRG cultures and confirm P2X7 receptor expression in these cells through receptor biophysics, pharmacological assessment and immunocytochemical techniques.
- To identify the specific cell type of non-neuronal cells that expresses the P2X7 receptor using immunocytochemistry.
- To investigate the activity of the anticonvulsant Lamotrigine at P2X7 receptors, and whether P2X7 inhibition could account for some of Lamotrigine's efficacy by assessing the effect of a selective P2X7 antagonists in *in vitro* models of epileptiform activity.

Chapter 2: General Materials and Methods

2.1 Methods for Cell Lines

Experiments were performed using HEK293 cells stably transfected with rat P2X7, human P2X7, rat P2X4 or human P2X4 receptors; or CHO-K1 cells stably transfected with human P2X2/3 receptors.

2.1.1 Production and maintenance of stable cell lines

All cell lines were available from GSK cell line storage system. HEK293 cells were stably transfected with rat or human P2X7 or P2X4 cDNA, contained on plasmids with Geneticin resistance genes on them. CHO-K1 cells were stably transfected with human P2X2 and human P2X3 cDNA, contained on plasmids with Geneticin and Hygromycin resistance genes on them.

2.1.2 Recombinant Cell culture

2.1.2.1 Materials and Solutions

HEK293 cells stably expressing rat or human P2X7 receptors were maintained in a 1:1 mixture of Dulbecco's modified Eagle's medium (DMEM) and Hams F12 containing 10% foetal bovine serum and supplemented with 0.6 mg/ml geneticin sulphate (G418). HEK293 cells stably expressing rat or human P2X4 receptors were maintained in Dulbecco's modified Eagle's medium nutrient mix supplemented with FBS (10%) and 0.6 mg/ml G418. CHO-K1 cells stably expressing human P2X2 and human P2X2/3 receptors were maintained in Dulbecco's modified Eagle's medium nutrient mix supplemented with FBS (10%), 0.6 mg/ml G418, and 0.4mg/ml hygromycin. All cells were grown as monolayer cultures at 37°C in a humidified atmosphere containing 95% air and 5% CO_2.

2.1.2.2 Cell Passage

Cells were passaged when they were between 70-90% confluent with a 1:10 dilution, approximately every 3-4 days. For all cell lines the solutions were used cold, straight from the fridge (~4ºC). The media was removed from the flask with care taken not to

dislodge the cells. The cells that were adhered to the flask were washed twice with phosphate buffered saline without calcium or magnesium ions (5mls) and then 2mls of accutase was added to enzymatically digest the cell linkages, allowed to cover the cells. For P2X7 cell lines the flask was left in the cell culture hood while the accutase was incubated for 5 -10 minutes. For all other cells lines, it was placed into the incubator at 37°C for 5-10 minutes. The flask was then agitated to aid the removal of cells stuck to the flask. 8 ml of media was added and used to wash the bottom of the flask, ensuring the removal of any other cells still stuck to the flask. The 10mls of cells suspension was placed in a 50ml falcon tube and centrifuged at 200g for 5 mins in order to pellet the cells. The excess media was then removed and the cell pellet resuspended in 1 ml of fresh growth media using a P1000 Gilson pipette to ensure the cells were dispersed and then a further 9 mls of media was added. For a 1:10 dilution, 1ml of the cell suspension was added to a T75 cell culture flask (Nunclon) containing 20 mls of media.

2.1.2.3 Preparation of cells for electrophysiology

Cells were passaged and plated out onto glass coverslips (13 mm; Chance Propper Ltd, West Midlands, U.K.) 2-48 hours prior to electrophysiological recordings. These coverslips were autoclaved and then pre-coated with a 2 μg/ml solution of poly-D-lysine before being washed in double distilled water and then individually placed into 35mm diameter petri dishes. They were then stored at 4 ºC until needed. 40,000 cells in 2mls of media was used for each coverslip, and in order to obtain the correct volume of cells required for electrophysiological recording, 1 ml of the cell suspension was analysed in the CEDEX cell counter (Innovatis; Bielefeld, Germany) and a viable cell count for the sample was obtained. Once the cells had stuck down to the coverslips, the cells could be used for electrophysiological recordings. They were broken into smaller sections using a diamond tipped pen and then transferred to the recording chamber.

2.2 Methods for Native cells

2.2.1 Coverslip preparation

Glass coverslips were coated with 100 µg/ml poly-L-lysine in sterile water. The solution was washed off with sterile water and left at 37^{o}C. On the morning of the preparation, the coverslips were coated with 5 µg/ml Laminin in PBS (50 µl of 1 mg/ml laminin in 10 ml PBS) and left at room temperature. The laminin was removed just before DRG cells were plated onto the coverslips.

2.2.2 Dorsal Root Ganglia Dissociation and culturing

Sprague-Dawley rat pups (7-10 days old) were decapitated in accordance with UK home office guidelines. A laminectomy was performed and the dorsal root ganglion neurons (DRGs) were isolated and collected into 5ml Hanks Buffered Salt Solution (HBSS). The meninges and roots were removed and the DRGs were incubated in trypsin (5mls) for 20 minutes at 37°C. Dulbeccos Modified Eagle's Medium (DMEM, + 10% FCS; 5mls) was added to inactivate the enzyme, and then the cells in 10mls of medium were centrifuged at 100g for 3 min. The supernatant was removed and replaced with a 0.1% collagenase solution (1ml of 0.5% stock plus 4ml HBSS) which was incubated with the ganglia for 50 min at 37°C. After incubation, 5mls of the DMEM and 10% FCS mixture was added and then the solution was centrifuged for 3 min at 100g. The supernatant was removed, replaced with 2ml DMEM (+ 10% FCS) and then cells were triturated up to 20 times with a long fire polished Pasteur pipette to mechanically dissociate the ganglia. The solution was made up to 10mls with an additional 8ml DMEM (+ 10% FCS), and then plated onto a 100 mm tissue culture dish for 1 hour at 37^{o}C to allow the removal of the excess of non-neuronal cells and large diameter DRGs which stick to the bottom of the dish. The media containing unattached neurones and some non-neuronal cells was then collected and centrifuged at 200g for 5 minutes. The supernatant was removed and the cells resuspended in 2ml serum-free DMEM (supplemented with 50 ng/ml NGF, N2 supplements and 0.05% BSA). Cells were counted with a haemacytometer and plated at the required density for electrophysiological experiments, of 100,000 cells in 0.5ml onto poly-L-lysine and laminin coated coverslips. The cells were then incubated for 1 hour at 37^{o}C to allow the cells to attach to the coverslip after which time the culture dish was

flooded with 2 ml of medium. This method has been modified from Lindsay et al (Lindsay 1988).

2.3 Electrophysiology

2.3.1 The Equipment and Set up

2.3.1.1 Microscope

The microscope, a Nikon ECLIPSE TE2000-S (Nikon UK Limited, Surrey, UK), was isolated from vibration by placing it on an air table (Technical Manufacturing Corporation, MA 01960, USA). Phase contrast optics was used to identify healthy cells. Fragments of coverslips with cells attached were visualised initially with a 10X objective and the electrode was positioned above an appropriate cell using a coarse manual manipulator (LBM-7 manual manipulator, Scientifica Ltd, East Sussex, UK). Cells were approached using the 20X objective using a fine manipulator (PatchStar Micromanipulator, Scientifica Ltd, East Sussex, UK).

2.3.1.2 Chambers and perfusion systems

All experiments used an open diamond bath perfusion chamber (RC-26G, Warner Instruments Corp.) in which a vacuum grease (Dow Corning) sealed coverslip (22 x 40 mm coverslip, Chance Proper Ltd) formed the floor. This was electrically isolated from the microscope using a plastic stage adapter (PH-1, Warner Instruments Corp). Both the ground wire and pipette electrode were AgCl, made by soaking silver wire in household bleach for a few hours and then rinsing in distilled water. Extracellular solution was fed by gravity from a 50ml syringe (Becton Dickinson) to the recording chamber and was aspirated from the chamber by a vacuum system into a container below the anti-vibration table. Different solutions were applied to cells under investigation using a Warner Fast-step drug delivery system (SF-77B, Warner Instruments Corp, Figure 2.1). 25ml syringes were connected via 3-way taps to tubing that led into to perfusion manifolds (ML series, Warner Instruments Corp), and finally into single-walled 3-barrel glass tubing (3SG700, Warner Instruments Corp). This allowed solutions to be exchanged within 20ms.

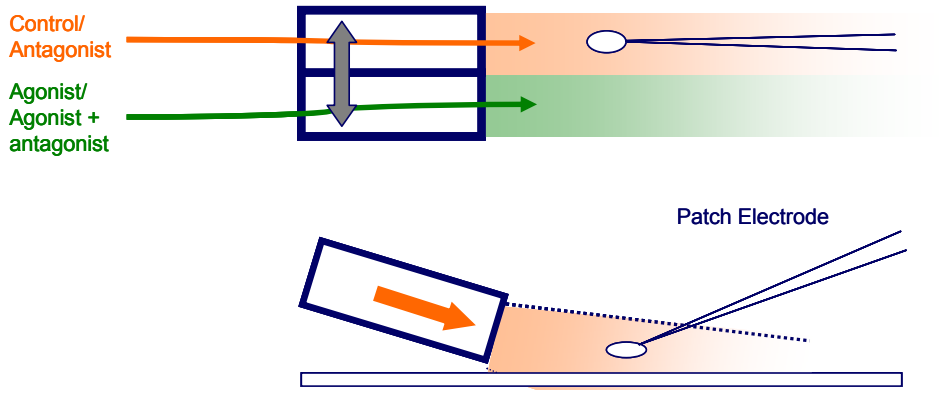

Figure 2.1: Schematic representation of drug delivery system

2.3.1.3 Patch-clamp

Positive pressure was applied to recording pipettes before they were placed into the bath solution close to an appropriate cell. Any current offset from zero was negated by manually adjusting the pipette offset control. A voltage step of 5 mV was used to monitor the resistance between the pipette and bath electrodes. The pipette was then moved onto the cell using the micromanipulator and contact with the cell was indicated by an increase in the resistance. The positive pressure was then released and gentle suction applied resulting in the formation of a giga-ohm seal between the cell and the pipette. Fast capacitance transients were neutralised and the voltage was stepped down to -60mV. On the application of further suction, the membrane under the electrode was ruptured and the whole-cell configuration was obtained. The capacitance transients were neutralised and the series resistance compensated up to 80% (compensated lag time = 10μs). All experiments were performed at 21°C and once whole cell recording had been established, cells were lifted up from the coverslips to speed solution exchange.

2.3.1.4 Electronics

The voltage protocol was generated by pClamp9 Clampex Software, originating from the computer in digital form and was converted to an analogue signal following input into the Analogue-Digital board (A-D board, Axon Instruments Palo Alto, Calif., USA). The

analogue data was then amplified by the amplifier Axopatch200B (Axon Instruments) before being applied to the cell. Currents across the membrane recorded in response to changes in voltage or ligand application were amplified by the Axopatch200B before being digitised by the A-D board and recorded by the computer for subsequent analysis.

2.3.1.5 Amplification and Filtering

Data was low pass filtered between 2 and 5 kHz and sampled at 2-5x the filter corner frequency using pClamp9 Clampex acquisition programs. Analysis appropriate for the voltage protocol is detailed below.

2.3.2 Solutions

All solutions were made up in double distilled Millipore water. The pH was adjusted using a Titan pH meter (Sentron, The Netherlands) and the osmolarity determined by vapour pressure using Vapro Vapor Pressure Osmometer (Vapro 5520, Wescor Inc.).

2.3.2.1 Extracellular Solutions

RAT AND HUMAN P2X7 - (mM) 135 NaCl, 2 KCl, 0.5 $MgCl_2$, 1 $CaCl_2$, 10 HEPES, 12 *D*-Glucose, pH 7.3 with NaOH, osmolarity 290-300 mOsm

DRG NON-NEURONAL CELLS – (mM) 147 NaCl, 2 KCl, 0.3 $CaCl_2$, 10 HEPES, 12 *D*-Glucose, pH 7.3 with NaOH, osmolarity 300-310 mOsm.

RAT AND HUMAN P2X4 – (mM) 145 NaCl, 2 KCl, 1 $MgCl_2$, 2 $CaCl_2$, 10 HEPES, 10 *D*-Glucose, pH 7.3, osmolarity 300 mOsm.

HUMAN P2X2/3 – (mM) 135 NaCl, 2 KCl, 1 $MgCl_2$, 2 $CaCl_2$, 12 HEPES, 10 *D*-Glucose, pH 7.3, osmolarity 305 mOsm.

2.3.2.2 Intracellular Solutions

RAT AND HUMAN P2X7 – (mM) 150 NaCl, 10 HEPES, 10 BAPTA, pH 7.3 with NaOH, osmolarity 320 mOsm.

DRG NON-NEURONAL CELLS – (mM) 150 NaCl, 10 HEPES, 10 BAPTA, pH 7.3 with NaOH, osmolarity 320 mOsm.

RAT AND HUMAN P2X4 – (mM) 145 Cs aspartate, 11 EGTA, 5 HEPES, 2 NaCl, pH 7.3, osmolarity 310 mOsm.

HUMAN P2X2/3 – (mM) 150 CsCl, 2 EGTA, 10 HEPES, pH 7.3, osmolarity 312 mOsm.

2.3.3 Electrodes

Glass microelectrodes were pulled from thick wall borosilicate glass capillaries with an inner filament (inner diameter: 0.69mm; outer diameter: 1.2mm; 120F-10; Clark Electromedical Instruments, UK) using a horizontal micropipette puller (Flaming-brown P-97, Sutter Instruments Co., USA). Electrodes were back-filled with an intracellular solution and had resistances ranging from 1-5 MΩ. Electrodes were fitted into a universal electrode holder (HL-U, Axon Instruments, USA), so that the pipette solution was in contact with a silver chloride coated silver wire. The holder was attached to a unity gain headstage and connected to the amplifier. A silver-silver chloride reference electrode was submerged in the recording chamber and connected to the headstage.

2.3.4 Recording Protocols and Data Analysis

All data were captured using pClamp9 software (Axon Instruments Ltd) and analysed off-line using the Clampfit (Axon Instruments) programme.

2.3.4.1 Standard agonist activation protocol for P2X4 and P2X7 receptors

Cells were exposed to a 2s application of agonist every 2 minutes using the Warner drug delivery system (Figure 2.1).

2.3.4.2 Standard agonist activation protocol for P2X2/3 receptors

Cells were exposed to αβme-ATP in a dual 1.5s application with 3.5s between pulses and this was repeated every 3.5 minutes until a stable baseline of peak current was established (see Chapter 4, Figure 4.7Ai). To uncover the P2X3 current component, the current from the second agonist application was subtracted from the first, resulting in the removal of the P2X2/3 current component, leaving a purely P2X3 mediated current.

2.3.4.3 Agonist Concentration-response Curves

Data for agonist concentration–response curves were obtained by an individual cell being exposed to 2 concentrations, 1 test concentration and 1 standard concentration. Responses were normalised to the standard concentration for each cell. In order to measure the peak current amplitude in response to agonist activation, cursors were first placed over the baseline region, defined as a 1 second time before the application of the agonist. A second set of cursors were placed across the application area and the data was measured relative to this baseline or 'leak' current level. Data were then placed into Excel spreadsheet and Origin (Oirgin Software) and curves were constructed. This was done using raw data fitted using the following logistic equation:

$$\mathbf{Y = \frac{A_1 - A_2}{1 + (x/x_0)^p} + A_2}$$

Where x is the concentration of the drug, X_0 is the EC_{50} or IC_{50}, p is the power and A_1 and A_2 are the minimum and maximum values respectively.

2.3.4.4 Antagonist Concentration-response Curves

Data for antagonist concentration–response curves were obtained by an individual cell being exposed to 1 or 2 concentrations of antagonist once a stable baseline response to agonist had been obtained where possible. Antagonists were preincubated for 2 minutes and co-applied with the agonist. Concentration response curves were constructed as detailed above.

2.3.4.5 Kinetics of Agonist Response

Deactivation rates for inward currents were measured as the time taken for each response to decay from 95% to 50% of its maximum and the slope was calculated using exponential fitting (Clampfit). Data were compared using the students T test, with $P < 0.05$ being taken as a measure of statistical significance. All data are expressed as means ± S.E.M; *n* refers to the number of cells studied.

2.3.4.6 Baseline adjustment

In some cases multiple agonist applications led to unstable peak current responses, with some currents consecutively increasing and others decreasing. These cells had the baseline gradient adjusted to enable the effects of the compounds to be more accurately analysed. To calculate the gradient the following equation was used:

Gradient = [(First response (pA) - Last response (pA)) / (Last agonist application number – First agonist application number)]

The original recorded peak current amplitudes were then converted to new, adjusted peak current amplitudes by the following equation:

Adjusted peak current amplitude = Original peak current amplitude + (Gradient * Agonist application number)

2.4 Hippocampal Slice Recordings

2.4.1 Tissue preparation

Male Lister-Hooded rats (150-250 g) were anaesthetised with halothane and subsequently cervically dislocated and decapitated in accordance with UK Home Office guidelines. The brain was removed and placed in ice cold (~4ºC) artificial cerebrospinal fluid (aCSF). The whole brain was placed on filter paper to remove excess fluid and then fixed to a polypropylene slate using cyanoacetate. An agar block was placed at the caudal end of the brain and stuck down using cyanoacetate. The polypropylene slate was then placed

in a chamber containing ice cold aCSF. The brain was then sectioned to produce 400 µm thick horizontal sections using a Leica VT1000S automatic slicer (Leica Microsystems, Milton Keynes, UK). The slices were transferred to a petri dish containing room temperature (~21ºC) aCSF continuously bubbled with 95% O_2, 5% CO_2. The hippocampus was cut away from the rest of the slice and transfered to a recording chamber where they were placed on a nylon mesh at the interface of a warmed (32–34°C), perfusing (1–2 ml min^{-1}) artificial cerebrospinal fluid (aCSF) and an oxygen-enriched (95% O_2, 5% CO_2), humidified atmosphere. The slices were allowed to equilibrate for at least 1 hour prior to the start of the experiment. The standard perfusion medium (aCSF) comprised (mM): NaCl, 124; KCl, 3; $NaHCO_3$, 26; NaH_2PO_4, 1.25; $CaCl_2$, 2; $MgSO_4$, 1; D-glucose, 10; and was bubbled with 95% O_2, 5% CO_2. The aCSF was made up from a 10X stock solution.

2.4.2 Set-up for Extracellular recordings

The interface recording chamber was based on a design by Spencer et al, 1976 (Spencer et al. 1976), and consists of an outer water bath fitted with a lid, and an inner recording chamber. The distilled water in the outer chamber is heated to 32 ± 1 ºC by a metal plate fitted to the bottom of the chamber, which is connected to a constant power source. The water is bubbled with 95% O_2, 5% CO_2 creating a humidified atmosphere over the recording chamber. The aCSF was pumped (1-3 ml/min), via a peristaltic pump, to a gravity feed which then flowed into the main recording chamber, under a nylon mesh, and was then removed by suction through a syringe needle. The level of the flow was adjusted to bathe the bottom of the slice, but not submerge it. The slices were illuminated in the recording chamber by a fibre optic system connected to a light source. Electrodes were mounted on micromanipulators and the slice was visualised using a dissecting microscope (World Precision Instruments, UK) mounted above the recording chamber. The setup was mounted on a stainless steel anti-vibration table (Scientifica, UK) and enclosed in a Faraday cage (Scientifica, UK) which was grounded through the amplifier (Axoclamp-2B, Axon Instruments, CA, USA) in order to isolate the system from ambient noise.

2.4.3 Electrodes.

Glass microelectrodes (1-5 MΩ) were filled with standard aCSF before being connected to the headstage. The recording electrodes used for extracellular recording are detailed in section 2.3.3.

2.4.4 Extracellular Recording

Following a 1 h equilibration period, the perfusing solution was changed to induce epileptiform activity. Extracellular field potential recordings were obtained from the CA3 region of *stratum pyramidale* and measured as the potential difference between the recording microelectrode and the bath reference electrode. Epileptiform activity was induced by modification of the perfusing solution by (a) the combined addition of the $GABA_A$ and $GABA_B$ receptor antagonists gabazine (10 μM) and CGP55845 (10 μM), or (b) removal of extracellular magnesium. Once a stable baseline period of bursting was established, the compound of interest (compound A or Lamotrigine) was added to the bathing medium.

2.4.5 Amplification and Filtering

The recordings that were made using the ME1 channel on the AxoClamp-2B were amplifier 10 times by an internal gain. Signals were further amplifier and filtered using a Brownlee precision Instruments amplifier giving a further 100 times amplification (total gain = 1000) and a band width of 0.1 Hz to 5 KHz. The signal was passed through a Humbug (Digitimer, UK) noise subtraction device which removed signals occurring at 50Hz, conventionally known as ambient noise. The resultant signal was digitised using a Digidata 1322A interface (Axon Instruments).

2.4.6 Data storage

All data were captured using pClamp8 software (Axon Instruments Ltd) and digitized records were stored on the hard disk of a PC for off-line analysis using Clampfit software.

2.4.7 Data Analysis

The epileptiform bursting induced via manipulations of the aCSF was analysed by measuring the frequency of bursting and burst duration. Once the epileptiform activity was stable, a baseline period of activity was measured before the application of drugs of interest. The final 4 minutes of each application; Control, drug addition 1, drug addition 2, etc. were used to measure the frequency of bursting. To evaluate the effects on the duration of individual bursts, the last 6 bursts were analysed prior to the change in the solution and measurements of the duration of the burst were taken from the start of the event to the end of the afterhyperpolarisation (Figure 2.2).

The analysed data was then transferred into Microsoft Excel and Microcal Origin software packages for further analysis and generation of graphs. Data are presented as means ± standard error of the mean (SEM) and statistical significance was assessed using paired or unpaired Student's *t*-tests performed on raw data with $P<0.05$ being taken as indicating statistical significance. *n* values refer to the number of times a particular experiment was performed, each in a different slice prepared from a different rat. Where concentration-response relationships have been determined, the data were fitted as detailed above (**2.3.4.3 Agonist Concentration-response Curves)**

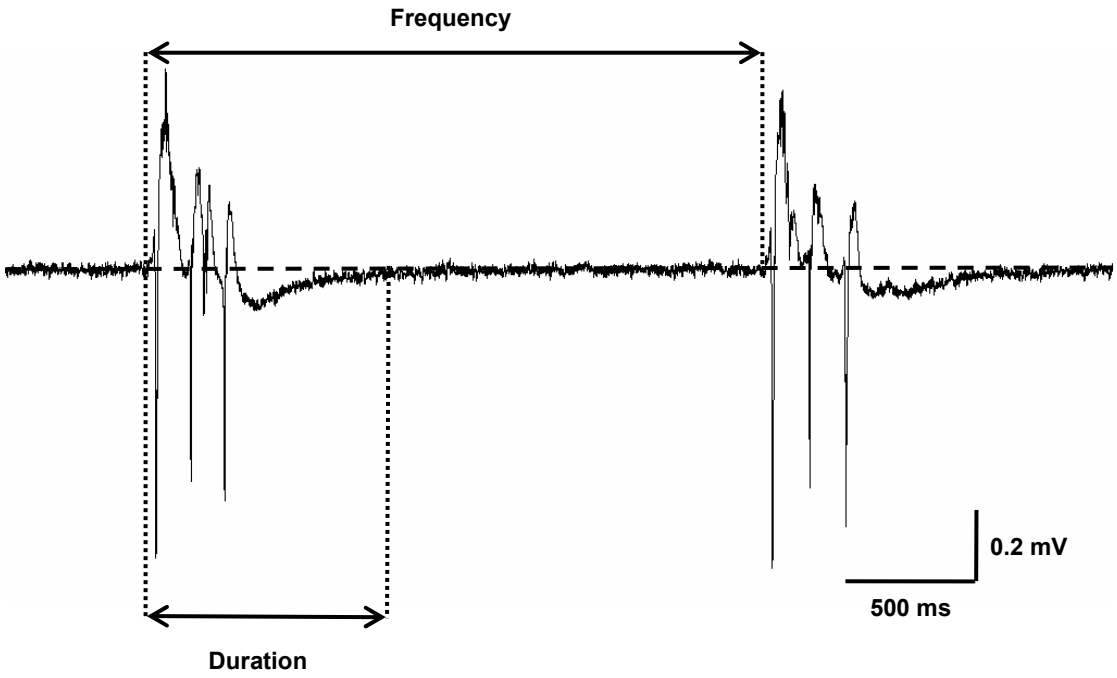

Figure 2.2: Example recording showing parameters used for analysis

2.5. Drugs

All drugs were stored frozen (at -20°C) in aliquots and were dissolved in deionised water, or dimethyl sulphoxide (DMSO). Drugs were added to the extracellular solution/perfusing medium up to desired concentration. For hippocampal slice preparations, drugs were perfused for at least 30 minutes to allow sufficient time for full equilibration with the slices. The final DMSO concentration was never greater than 0.3%.

Adenosine Triphosphate (ATP), 2',3-*O*-(4-benzoyl)benzoyl-ATP (BzATP), α,β-methylene ATP (αβmeATP), TNP-ATP, PPADS and Coomassie brilliant blue G, were obtained from Sigma.

CGP55845A and Bicuculline methiodide (referred to as Bicuculline) were obtained from Tocris-Cookson Ltd (Bristol, UK). Bicuculline was dissolved in distilled water to 10mM and CGP55845 was dissolved in 100% DMSO to form a stock solution before being diluted into the perfusing medium.

GSK314181A, Compound A, Compound X, Lamotrigine (Lamictal) and Sipatrigine were synthesised in the medicinal chemistry laboratories in Harlow, Essex, and was made up to 10 mM in 100% dimethyl sulphoxide (DMSO) or distilled water.

2.6 Immunocytochemistry

2.6.1 Preparation of Cells

HEK293 or CHO cells stably expressing P2X7, P2X4 or P2X2/3 receptors were cultured and plated onto glass coverslips as described above (section.2.1.2). DRGs were removed, cultured and plated onto glass coverslips as described above.

Glass coverslips were placed into individual 5 mm petri dishes. Each coverslip was washed twice with 2mls of phosphate buffered saline (PBS) for 5 minutes before being fixed with paraformaldehyde (4% in PBS) for 20 minutes on ice. Following this coverslips were rinsed in PBS and permeabilised with 0.05% Tween 20, added for 10 minutes at room temperature. Then coverslips were washed 3 times with 2 mls of blocking solution containing 10% donkey serum, and left overnight.

2.6.2 Immunocytochemistry

Coverslips were washed twice in PBS standard blocking solution containing normal donkey serum (NDS, 2%). This solution was then removed and the appropriate primary antibody raised against specific tissue antigens (human P2X7, β3-tubulin, S100β or glutamine synthetase) diluted as appropriate in blocking solution was applied to the coverslip, flooding the petri dish and covering all the cells. Petri dishes were then placed in a humid box (sealed, damp filter paper lined tray) and left in an incubator at 37^{o}C for 30 mins. Following the primary phase, coverslips were rinsed in PBS 3 times, for 5 minutes per rinse. The labelled secondary antibody against the relevant immunoglobulin of the animal species in which the primary antibody was raised in, was diluted as appropriate with PBS and applied to the cells. The coverslips were then placed in the incubator at 37oC for 30 minutes. Following the secondary phase, slides were washed in

PBS 3 times, 5 minutes per wash. In some cases the solution used for the middle wash step also contained To-Pro-3 (1:1000 of 1 mM), or Sytox Green (1:5000-10,000) to label the cell nuclei, and was applied for 10 mins. Glass coverslips were inverted into mounting medium (ProLong Gold antifade reagent, Invitrogen), on microscope slides (Super Frost Slides; Agar Scientific) and left to dry in the dark. Incubations using primary anti-sera in the absence of secondary anti-sera and vice versa were also performed, as negative controls.

2.6.2.1 P2X7 selectivity immunocytochemistry

The human P2X7 monoclonal mouse antibody (GSK antibody) was diluted 1:1000, 1:500 and 1:250 in PBS (2% NDS) solution. The secondary antibody used was Donkey anti-mouse Alexa 488 (Molecular probes, UK) diluted at 1:200 with PBS.

2.6.2.2 P2X7 DRG immunocytochemistry

The human P2X7 monoclonal mouse antibody (GSK antibody) was diluted 1:1000, 1:500, 1:250 in blocking solution. The secondary antibody used was Donkey anti-mouse Alexa 488 (Molecular probes, UK) diluted at 1:200 with PBS.

The anti-β3-tubulin antibody was used at dilutions of 0.5 μg/ml, 1 μg/ml and 3 μg/ml. The anti-S100β antibody was used at dilutions 1:100, 1:200, and 1:400, and the anti-glutamine synthetase antibody was used at dilution 1:2000. The secondary antibody used was Donkey anti-rabbit Alexa 647 (Molecular probes, UK) diluted at 1:200 with PBS.

2.6.3 Microscope analysis

All slides were observed under a Leica Confocal microscope using filters appropriate for Alexa Fluor 488 illumination (excitation 450-490 nm; emission 515-565 nm) and Alexa Fluor 647 illumination (excitation 650 nm; emission 665 nm). Digital images were generated using Leica Confocal Software (Leica Microsystems, GmbH, Heidleberg).

2.6.4 Reagents

Rabbit polyclonal antibody to β3-tubulin, rabbit monoclonal antibody to S100 beta and rabbit polyclonal antibody to Glutamine Synthetase were purchased from Abcam, MA, USA.

To-Pro3 Iodide, Sytox Green, Alexa Fluor Donkey anti-mouse 488, Alexa Fluor 647 Donkey anti-rabbit, Prolong Gold antifade reagent were all purchased from Invitrogen, Paisley, UK.

Normal Donkey Serum 10mls freeze dried powder was purchased from Stratech Scientific Limited, Suffolk, UK

Chapter 3: Biophysics and Pharmacology of the rat P2X7 receptor stably expressed in HEK293 cells

3.1. Introduction

The P2X7 receptor was initially cloned from a cDNA library from rat brain in 1996 (Surprenant et al. 1996), followed by isolation of human P2X7 cDNA from monocytes (Rassendren et al. 1997) and finally the mouse receptor was cloned from microglia (Chessell et al. 1998b). Stable cell lines expressing rat, human or mouse P2X7 receptors were then produced following initial transient transfections (Surprenant et al. 1996; Chessell et al. 1998a; Chessell et al. 1998b), allowing the investigation of the biophysical properties and pharmacology of these receptors in isolation.

There has been much work reported previously on the biophysical properties of rat P2X7 receptors (rP2X7) when they are stably expressed in a recombinant system (Surprenant et al. 1996; Virginio et al. 1997; Bianchi et al. 1999; Hibell et al. 2000; Hibell et al. 2001a). However there is not a consensus as to the kinetics of P2X7 receptor activation. Activation of P2X7 receptors have been described as biphasic with fast and slowly activating components (Klapperstuck et al. 2001), partially inactivating (Virginio et al. 1997), or as being kinetically even more complex (Chessell et al. 2001). Similarly, current deactivation was observed to follow a mono-exponential time course (Klapperstuck et al. 2000a), or to occur with a delay of up to several minutes (Surprenant et al. 1996; Chessell et al. 2001). Repeated long term agonist stimulations of rP2X7 receptors have been found to elicit either successively increasing currents (Surprenant et al. 1996) or decreasing currents (Hibell et al. 2000). These contrary results may be due to differences in host cell type (native cells such as lymphocytes compared to recombinantly expressed receptors), but could also be interpreted to result from activation-dependent changes to the P2X7 receptor conformation, or activation of other channels downstream of the P2X7 receptor. The experimental conditions employed can play a role in these differences. For example, agonists concentrations, divalent cation concentration, agonist addition and inter-agonist addition times and the consequences of receptor activation can

all causes difficulties when comparing data from different sources. Therefore the aim of the experiments detailed here was to characterise rat P2X7 receptors stably expressed in HEK293 cells, focusing on the changes that occur following multiple agonist additions. This was with a view to determining a stable set of experimental conditions that can be employed to allow accurate pharmacology assessments to be performed (see Chapter 4) and enable comparison studies with native receptors (see Chapter 5).

3.2 Methods Summary

Methods are described in Chapter 2 (Materials and Methods).

3.3 Results

3.3.1 Characterisation of rat P2X7 receptors stably expressed in HEK293 cells

3.3.1.1 Agonist evoked currents

Whole cell patch clamp recordings were made from single cells stably expressing rat P2X7 receptors. All cells studied responded to BzATP, were as an application of BzATP (30 μM) to untransfected HEK293 cells produced no currents (Fig3.1A). Activation of rat P2X7 receptors by a 2s application of BzATP (30 μM) produced a rapidly activating inward current, with a rise time (10-90%) of 207 ± 13 ms (n=17). The current showed little desensitisation throughout the 2s application and deactivated on removal of the agonist (Fig 3.1B and 3.1C). To confirm that the channel was acting as a non-selective cation channel, cells were voltage clamped at -60mV before a voltage ramp from -80mV to +40 mV was injected. A small current, termed non-specific leak current, was produced in control solution (standard extracellular solution), and a linear increase in the current amplitude was produced by the application of BzATP (Figure 3.1D). Mean data showed BzATP activated currents that were almost linear and reversed at 0.2 ± 0.4 mV (n=4), as expected for a non-selective cation channel (Figure 3.1E).

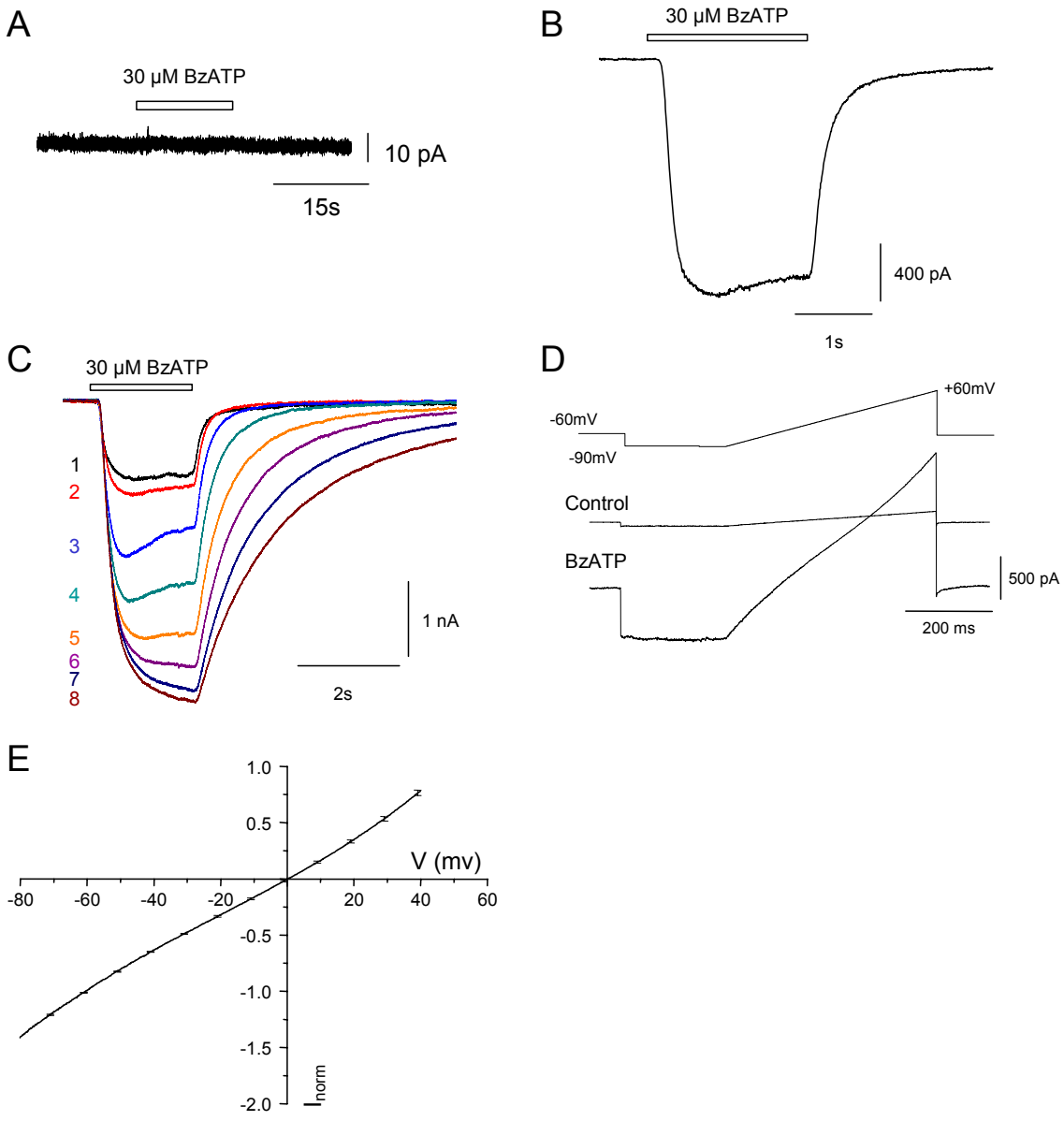

Figure 3.1: Effect of BzATP on recombinant P2X7 receptors
A. Representative trace recorded from 'wild-type' HEK293 cells. No currents are activated following a 15s addition of BzATP (30 µM).
B. Representative trace recorded from HEK293 cells stably expressing rat P2X7 receptors in response to an application of 30 µM BzATP. Rise time (10-90%) is 207 ± 13 ms (n=17). Deactivation time (95-50%) is 117 ± 7 ms (n=14).
C. Overlayed representation of currents in response to multiple applications of BzATP (30 µM), note current growth and slowing of deactivation.
D. Voltage ramps (-80 mV to +60 mV, 500 ms) applied in the presence of BzATP (30 µM) resulted in linear currents that reversed at 0.2±0.4 mV (n=4).
E. Pooled, leak-subtracted data from voltage ramps applied in the presence of 30 µM BzATP. Current responses recorded at each holding potential were normalised to the current recorded at −60 mV. BzATP-activated whole cell currents have a reversal potential close to 0 mV (0.2 ± 0.4 mV (n=4).

To study the concentration-response relationship of agonist activation of rat P2X7 receptors, each cell was normalised to a test concentration of agonist; 300 μM BzATP or 3 mM ATP; and only exposed to one additional concentration of agonist, in order to minimise the activation-dependent changes in the receptor (discussed later). Concentration response curves were generated for BzATP (Figure 3.2A) and ATP (Figure 3.2B) and resulted in EC_{50} values of 33 ± 4 μM (Hill slope = 1.7 ± 0.4, n = 3-5) and EC_{50} values of 670 ± 50 μM (Hill slope = 2.2 ± 0.3, n= 4-7), respectively, demonstrating the greater potency of BzATP, than the natural ligand ATP, at rat P2X7 receptors.

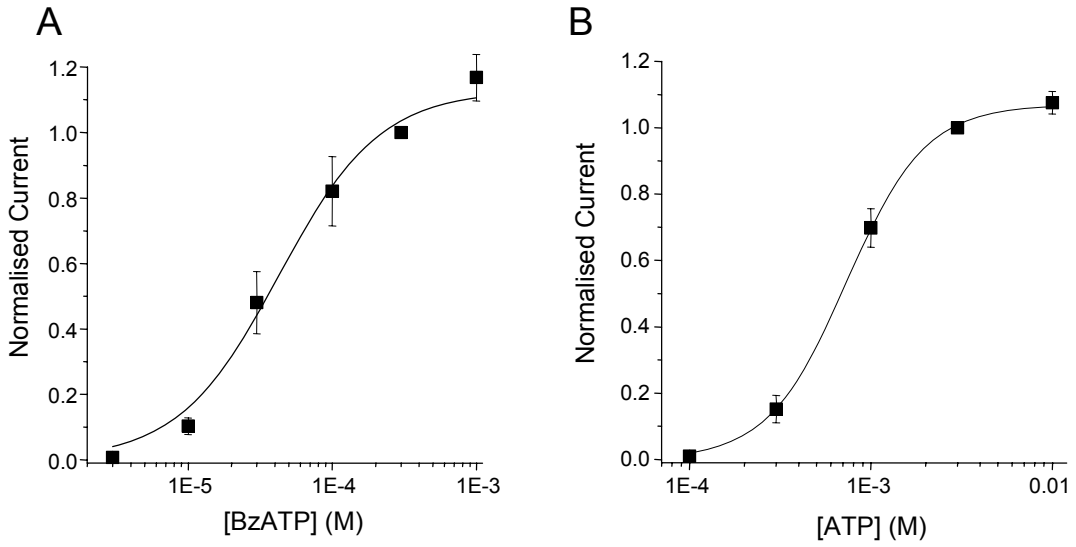

Figure 3.2: Concentration-response curves for ATP and BzATP on recombinant rat P2X7 receptors
A. The graph illustrates the mean concentration response curve to BzATP for rat P2X7 currents. Each cell was normalised to 300 μM BzATP application and was exposed to one other concentration of BzATP after a 2 minute interval. EC_{50} = 33±4μM (n = 3-5), Hill slope = 1.7±0.4. B. The graph illustrates the mean concentration response curve to ATP for rat P2X7 currents. Each cell was normalised to 3 mM ATP application and was exposed to one other concentration of ATP after a 2 minute interval. EC_{50} = 670 ± 50 μM (n= 4-7) Hill slope = 2.2 ± 0.3.

3.3.1.2 Concentration- and time-dependence of current amplitude increase

The increase in the peak current following each application of agonist is an interesting phenomenon associated with P2X7 receptors. In Figure 3.1C a single cell has been exposed to BzATP (30 μM) for 2 seconds every 2 minutes and the traces have been overlayed to illustrate the increasing current amplitude produced for the same concentration of agonist. To further quantify this effect, multiple applications of BzATP were applied to 12 separate cells and the resulting peak current amplitude values were plotted (Figure 3.3A). The first application of BzATP activated currents that had peak current amplitudes ranging from 803pA to 2110pA (giving a mean of 1247 ± 116 pA (n=12), and the final current amplitudes (7^{th} application) produced a wide range of values from 2032pA to 7633pA (Figure 3.3A). Peak current amplitudes were normalised to the first response and the mean data plotted against time in Figure 3.3B, illustrating a gradual increase in the current amplitude that peaked at 335 ± 49% of control (ranging from -2122pA to -7627pA) at the 6^{th} application. There is no further significant increase in the mean current following the 6th application of BzATP, a trend that is also visible from the individual current amplitude plot (Figure 3.3A). Due to the large variability in the final current amplitudes, the correlation between initial current density (current amplitude/whole cell capacitance) and the percentage increase observed after 6 BzATP applications was investigated. No correlation was found (Linear regression line, R=0.11), indicating the lack of relevance of the current density to the changes in current amplitude.

To establish if the current amplitude increase was agonist concentration dependent, further experiments were performed across a range of BzATP concentrations (3-1000 μM). Cells were exposed to 6 applications of a concentration of agonist, and the percentage change in the peak current amplitude from the first response was plotted (Figure 3.3D). 6 applications of agonist were chosen because the current amplitude in response to 30 μM BzATP peaked at this application number. The increase in current amplitude diminished as the concentration of BzATP increased, with no significant increase produced by multiple applications of 1 mM BzATP (127 ± 23%, n=5). However the largest increases in current amplitude was produced by 10 μM BzATP (336 ± 110%, n=5, p=0.003), rather than the lowest concentration tested, 3 μM BzATP. The current

amplitude change in response to 3 μM BzATP was variable across the cells recorded, ranging from 64% to 177% of control, and resulted in a mean non-significant increase in current amplitude of 129 ± 13%, (n= 9), Figure 3.3D.

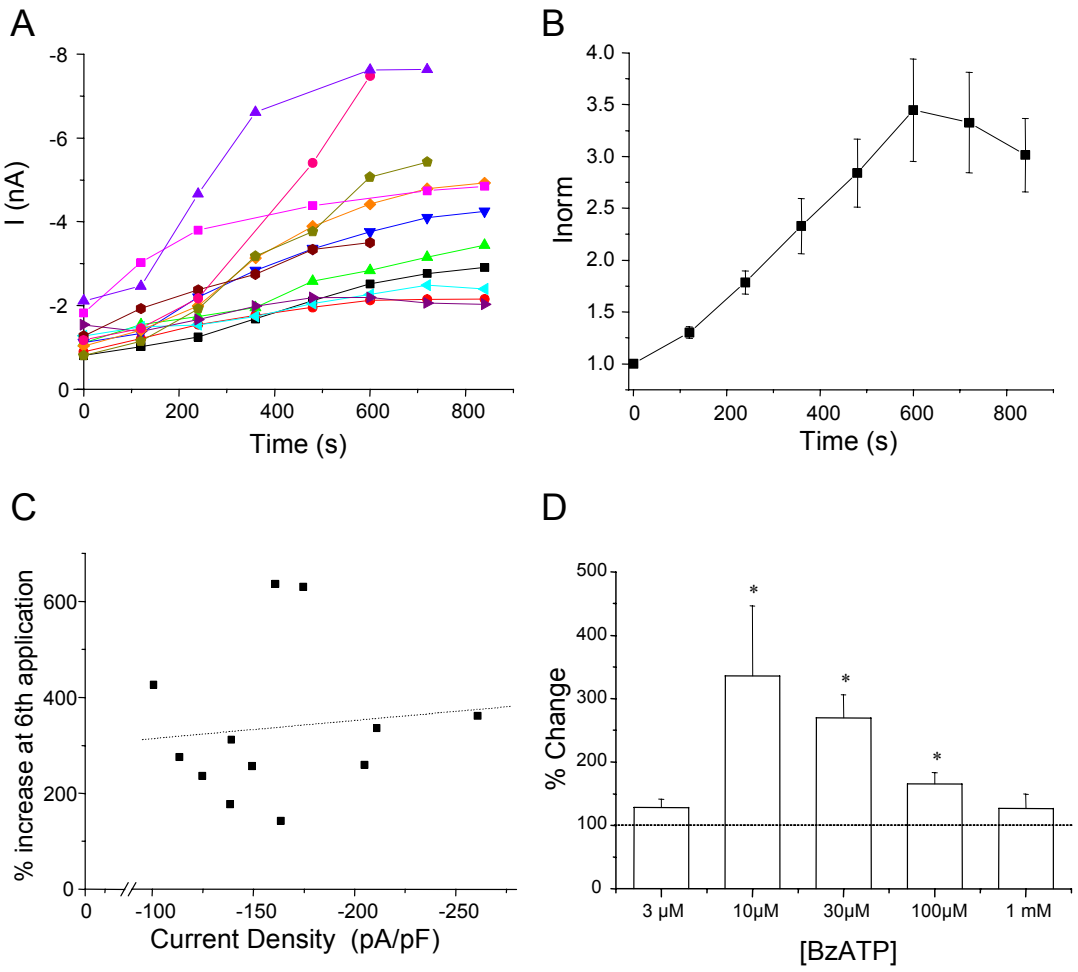

Figure 3.3: Concentration- and time-dependence of current amplitude increase
A. Graph illustrating the increase in the peak current response to 30 µM BzATP recorded following multiple applications of BzATP every 2 min to 12 different cells expressing rat P2X7.
B. Graph showing the normalised mean data for the peak current recorded in response to multiple applications of BzATP (30 µM) over 14 minute period, n=9-12. Note the plateau of the response after the sixth application.
C. Graph showing the lack of correlation between the current density of the initial response to BzATP (30 µM) and the increase in the current amplitude after 6 applications, R=0.11.
D. Graph illustrating the percentage change in the current amplitude after 6 applications, 2 min apart, of different concentrations of BzATP on rat P2X7 receptors. The peak current on the 6th application is expressed as a percentage of the initial application. (n=3-7; * = $p<0.05$).

3.3.1.3 Changes in the potency of BzATP at rat P2X7 receptors

Divalent Cations

The effect of the divalent cations, Ca^{2+} and Mg^{2+} ions on BzATP-activated currents through rat P2X7 receptors was investigated using the 'antagonist' protocol detailed in the methods. As Ca^{2+} and Mg^{2+} ions are present in the standard extracellular solution, the concentrations were reduced or increased in the same concentration of agonist, once a stable response to BzATP was obtained (Figure 3.4A). The BzATP activated current increased to a plateau of 2.9 nA (data shown once plateau was recorded), and the removal of Mg^{2+} ions from the agonist solution resulted in a further increase in peak current amplitude to 3.6nA, 116 ± 3% (n=3) increase, which reversed back to pre-zero Mg^{2+} level (100 ± 3% of control) on the reintroduction of Mg^{2+} ions into the agonist solution (Figure 3.4A). Therefore the BzATP-activated current can be potentiated with the removal of Mg^{2+} ions after it has reached an assumed maximum. The concentration-response relationship for Ca^{2+} and Mg^{2+} ion modulation/inhibition of BzATP evoked current was then established. The peak current amplitude of the response was normalised to currents in the presence of control Ca^{2+} or Mg^{2+} ion concentrations, and concentration response curves for Ca^{2+} and Mg^{2+} ions (0mM to 5 mM) were plotted and yielded IC_{50} values of 1 ± 0.1 mM (n= 3-4, Hill slope n = 1.9 ± 0.3) for Mg^{2+} ions, and 2 ± 0.1 mM (n= 4-5, Hill slope n = 2.7 ± 0.4) for Ca^{2+} ions (Figure 3.4B).

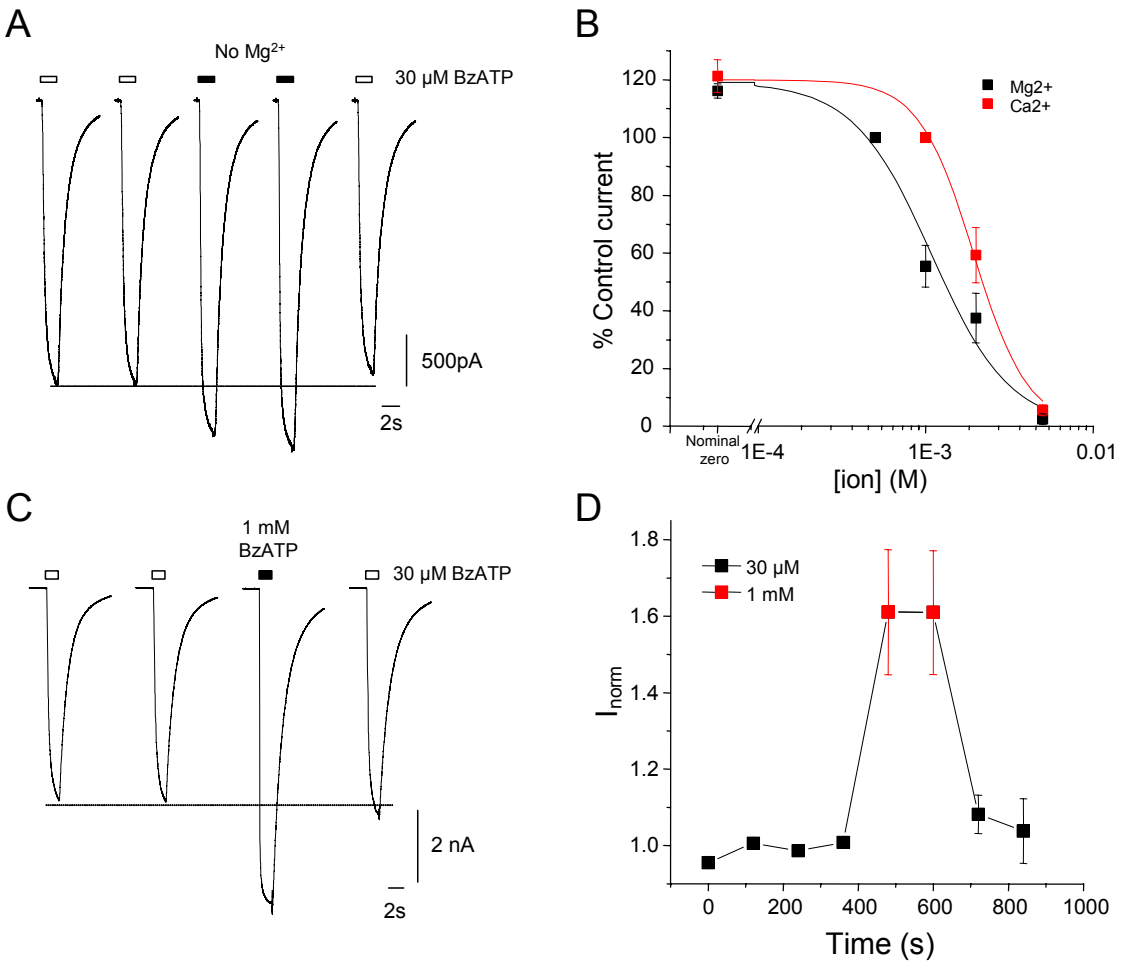

Figure 3.4: Change in BzATP potency – divalent cations
A. Representative trace showing multiple applications of 30 µM BzATP to rat P2X7 cell. Clear bars are agonist with normal (0.5 mM $MgCl_2$ and 1 mM $CaCl_2$) solutions and dark bars are 30 µM BzATP with 1 mM $CaCl_2$, but no added $MgCl_2$.
B. Concentration response curve for Ca^{2+} and Mg^{2+} ions at rP2X7 activated by 30 µM BzATP. Responses are expressed as a percentage of the control current which is the normal extracellular solution containing 0.5 mM $MgCl_2$ and 1 mM $CaCl_2$. IC_{50} = 1 ± 0.1 mM for Mg^{2+} ions, n= 3-4, Hill slope n = 1.9 ± 0.3, and IC_{50} = 2 ± 0.1 mM for Ca^{2+} ions, n= 4-5, Hill slope n = 2.7 ± 0.4.
C. Representative trace showing current in response to a 30 µM (clear bars) or 1 mM (black bar) BzATP application to rat P2X7 cell.
D. Graph illustrating the peak current recorded in response to 30 µM BzATP. Once a maximal current was recorded the cell was exposed to 1 mM BzATP resulting in 161 ± 16% (n=4) increase in the current amplitude that returned to pre-1mM levels on return to 30 µM BzATP.

Agonist potency

The increase in the current amplitude produced by multiple applications of the same concentration of agonist may represent an increase in the potency of the agonist at the receptor (Hibell et al. 2000; Michel et al. 2000). Therefore, with each application of agonist and subsequent activation of P2X7 receptors, the current growth may reflect an increase in receptor occupancy leading to an increase in open channel probability. In order to investigate whether the changes in current amplitude in the absence of divalent cations represents a change in the potency of the agonist at the P2X7 receptor the effect of a high concentration of BzATP was assessed once the response to 30 μM BzATP had increased to a plateau. On average current amplitudes elicited by BzATP application reached a plateau after 6 applications (Figure 3.3B), but was variable across cells. The application of 1 mM BzATP following this resulted in a larger current amplitude (Figure 3.4C), 161 ± 16% (n=4) of the control response, and reversed to pre-addition levels on return to 30 μM BzATP (Figure 3.4D).

3.3.1.4 Deactivation kinetics

Unlike many channels, the rate of deactivation of BzATP-activated current, defined as the time taken for current to return to baseline following removal of the agonist, varies dramatically over time. To add further complication, it is also a species dependent effect, with successive BzATP applications causing the deactivation rate to slow at the rat P2X7 receptor (Surprenant et al. 1996), to a lesser extent with the human receptor (Rassendren et al. 1997) and no obvious changes are seen for the mouse orthologues (Chessell et al. 1997).

The effect of multiple applications of BzATP to the deactivation of rat P2X7 receptors is shown in Figure 3.5A, where responses have been normalized to the pre-deactivation point and overlayed to illustrate the slowing of the deactivation and the changing kinetics after the first response. The rate of deactivation slows with each subsequent application of agonist to a point where the closure of the channel is so slow it results in cell lysis (possibly due to excessive calcium ion influx).

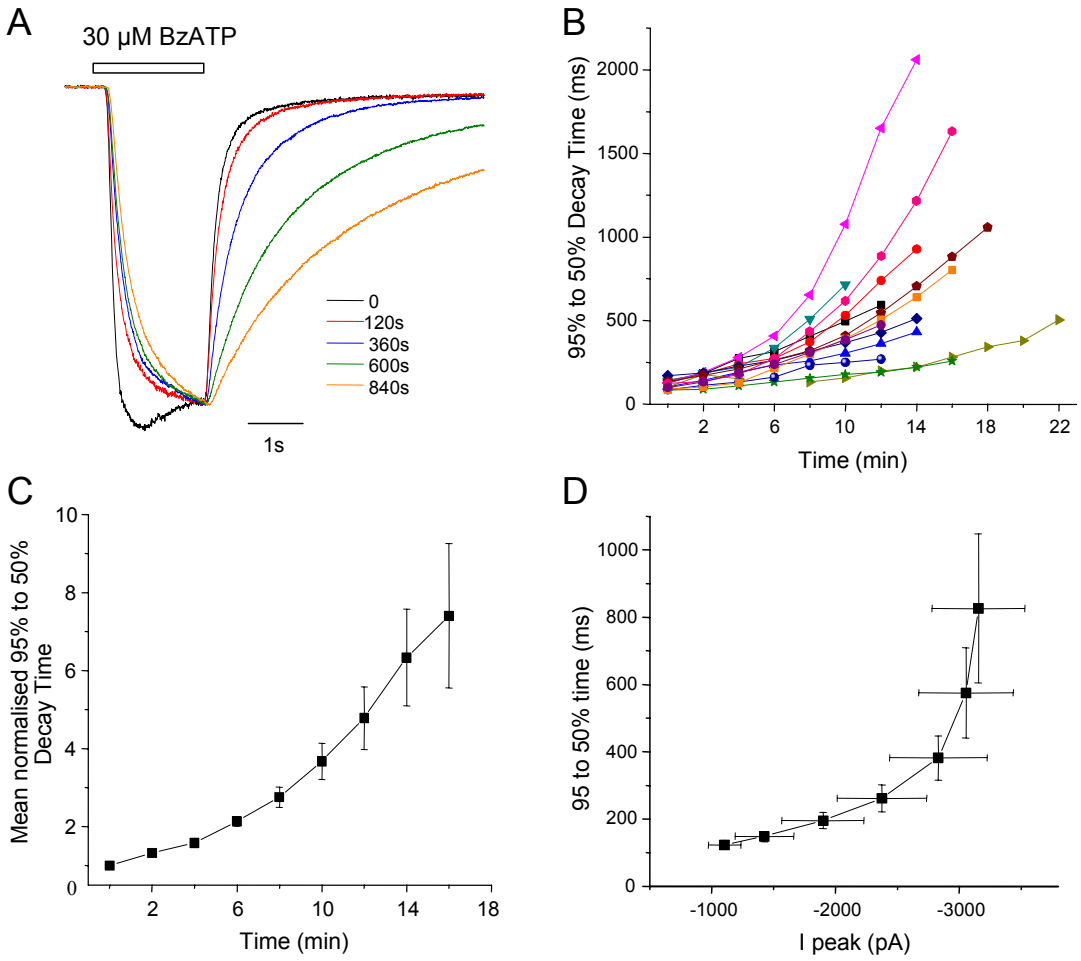

Figure 3.5: Slowing of deactivation of BzATP-activated rP2X7 currents
A. Representative recording from HEK293 cells stably expressing rP2X7 receptors in response to a series of applications of BzATP. Currents are normalized to the pre-deactivation point and overlayed to illustrate the slowing of the deactivation and the changing kinetics after the first response
B. Graph illustrating the 95-50% decay time for individual cells in response to 2s applications of BzATP 30 µM every 2 minutes (n=14).
C. Graph showing the mean normalised data for the effects of BzATP applications on the 95-50% decay time (n=5-13). Data are normalised to the 95-50% decay time of the first application.
D. Graph showing the mean data for the 95-50% decay time (n=7-14) in comparison to the mean peak current amplitude. Note the continuing increase in deactivation rate as the peak current plateaus.

To quantify P2X7 receptor deactivation, the time for the current to return to 50% of its maximum was determined (95-50%) and was 117 ± 7 ms (n=14) following the application BzATP to previously unstimulated (naïve) P2X7 receptors. The rate of slowing of deactivation is dependent upon the individual cell and varies greatly, with the deactivation time ranging from 222ms to 2060ms after 8 BzATP applications (Figure 3.5B). The mean data for the deactivation time is shown in Figure 3.5C, and although there is variability in the absolute values, the trend for a continual increase in the time for deactivation is consistent across all cells (also see Figure 3.5B). As the deactivation rate slows (to the point of constant activation – data not shown), the peak current will continue to increase until a maximum level is reached for that cell. The slowing of the increase in the peak current can be seen in Figure 3.5D where the 95-50% decay times are plotted against this value.

The slowing of deactivation time is also voltage-dependent, where the P2X7 channel deactivates more slowly at +60 mV compared to the deactivation rates at -60 mV. Cells were voltage clamped at -60mV for the first 3 and last applications of BzATP and for the 4th application the voltage command was changed to +60mV. Traces were then normalised and inverted, in the case of the -60mV traces (Figure 3.6A). The deactivation times (95-505%) were measured in all cases and plotted for each application number, against the same data recorded for cells voltage clamped at -60mV only (Figure 3.6). The BzATP-activated current at +60mV had a deactivation time of 2462 ± 1020 ms (n=6), significantly longer than the corresponding application at -60mV of 465 ± 85 ms (n=22; p=0.001).

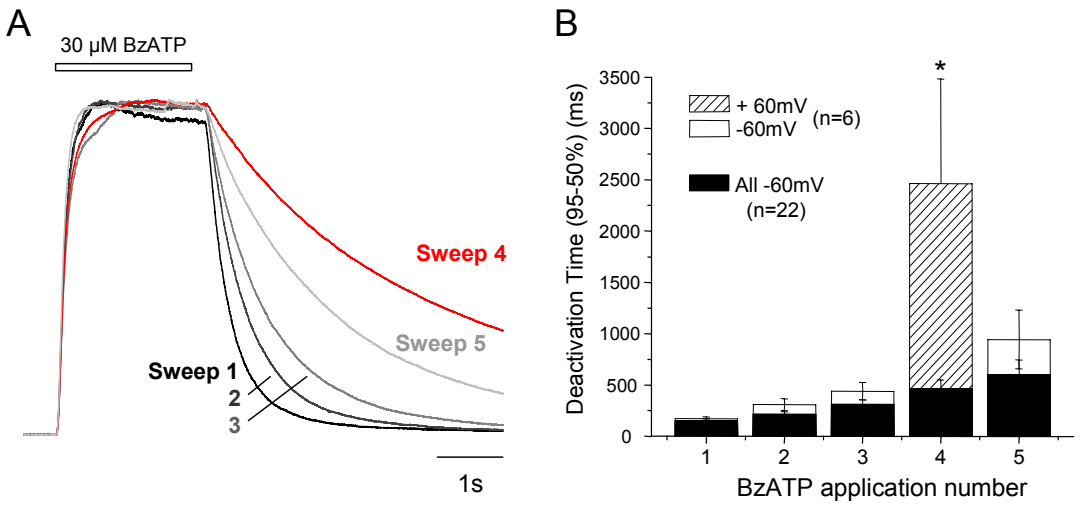

Figure 3.6: Slowing of deactivation of BzATP-activated rP2X7 currents
A. Deactivation is voltage dependent. Representative recording of consecutive response to BzATP (30 µM), normalised to the peak current within each responses. The cell was voltage clamped at -60mV for sweep 1-3 and sweep 5, and at +60 mV for sweep 4. Note the slowing of deactivation at +60 mV compared to the decay at -60 mV.
B. Graph illustrating the mean deactivation time of P2X7 receptors following BzATP (30 µM) activation. Cells were voltage clamped at -60mV (Black bars) for 5 successive BzATP applications, or voltage clamped to +60mV for the 4th application (white and shaded bars). Deactivation time (95-50%) was significantly slowed when cells were voltage-clamped at +60mV (465 ± 85 ms (n=22) compared to 2462 ± 1020 ms (n=6), p= 0.001) 530% of -60mV.

The deactivation of P2X7 was also investigated by fitting the rate of decay with an exponential function using Origin software. The deactivation following agonist activation of previously unstimulated cells is biexponential, and the tau (τ) values that are produced from curve fitting can be separated into a slow and fast τ values based on their kinetics. The mean slow τ value is 2206 ± 278 ms, and the faster τ is 188 ± 10ms. As the BzATP application number increases, the relative influence of the two components alters (see Figure 3.7A). The rate of these two components also changes; the fast component slows (118ms to 567ms) and the slow component has a trend towards slowing, possibly indicating multiple closed states of the P2X7 receptor that unbind ATP as different rates.

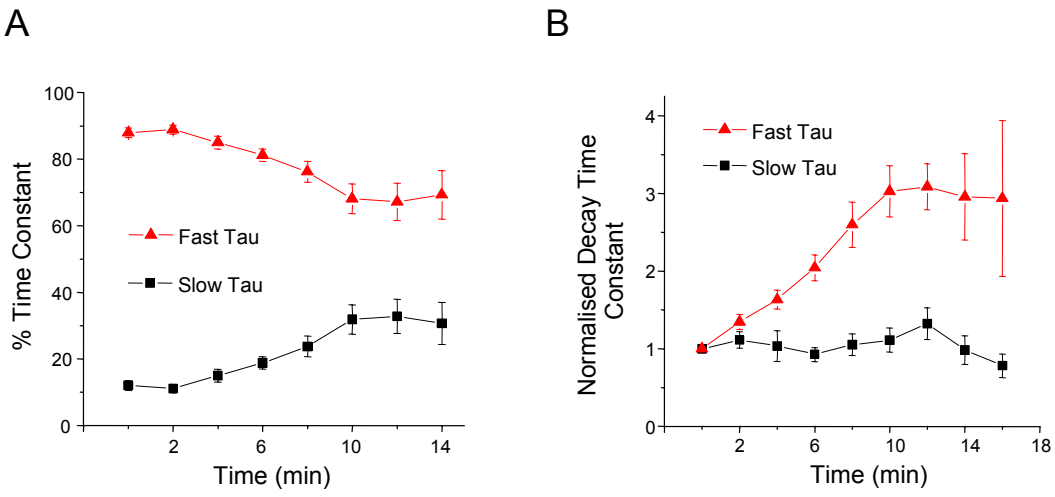

Figure 3.7: Deactivation of rat P2X7 current is biexponential
A. Graph showing the mean normalised time constant for the decay of the current after the application of BzATP (30 µM; n=3-14). Decay is biexponential and data are normalised to the decay time constants of the first application. The fast Tau value exhibits a slowing with each subsequent application of agonist.
B. Graph showing the changing role of the 2 components of the decay with multiple applications of BzATP.

Although it has been shown that the deactivation time of the P2X7 receptor slows with each subsequent application of the agonist BzATP, it is not clear whether the change in the deactivation time is dependent upon repeated agonist activation or simply dependent upon time. To address this, the standard experimental protocol for recording P2X7 currents has been used; exposing the cell to agonist for 2s every 2 minutes. However, between the first response at time zero and the 5th response, 8 minutes later, the cell was not exposed to BzATP. Previously, the 95-50% decay time of the first response to BzATP (30 µM) is 117 ± 7 ms (n=14). The 95-50% decay time of the fifth response, after 8 minutes is 336 ± 36 ms (n=14), which is 287 % longer and significantly ($p<0.0001$) different from the first exposure (Figure 3.8A and 3.8Ai). When the second BzATP (30 µM) application was 8 minutes after the first application, the current decayed with a 95-50% time of 155 ± 28 ms (n=4). This was 128% longer than the first exposure (121 ± 17

ms (n=4), (p=0.8 from 117 ± 7 ms control data), but significantly slower than the 95-50% decay time of the first application (p=0.08). However it was significantly different from the previous value at this time point of 336 ± 36 ms (n=14) (p=0.002) (Figure 3.8B and 3.8Bi). Therefore the slowing of deactivation with agonist addition is application dependent and not time dependent. It is a progressive change with each application of agonist and does not continue significantly in time interval between agonist additions.

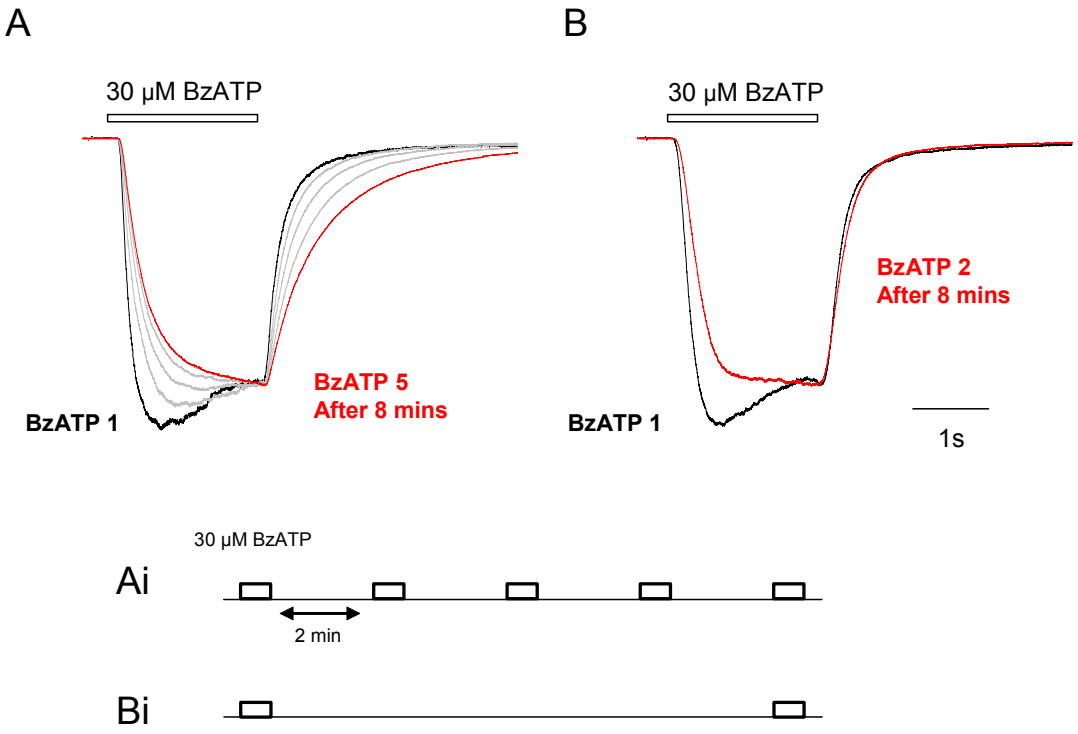

Figure 3.8: Slowing of rat P2X7 receptor deactivation requires repeated receptor activation
A. Representative recording of responses to a 2s application of BzATP (30 µM), normalised to the current prior to agonist removal within each responses. BzATP 1 is agonist addition at time zero and each further agonist addition is at an interval of 2 minutes.
B. Representative recording of responses to a 2s application of BzATP (30 µM), normalised to the current prior to agonist removal within each responses. BzATP 1 is agonist addition at time zero and BzATP 2 is the response to agonist after an interval of 8 minutes. The cell was not exposed to agonist between these 2 responses.
Note the change in deactivation rate seen in (A) after 8 minutes and the lack of change in the rate in (B).
Ai and Bi. Schematic representation of agonist application protocol for each experiment.

3.4 Discussion

The rat P2X7 receptor stably expressed in HEK293 cells that has been characterised here exhibits a number of characteristics expected for rat P2X7, with rapid activation (10-90% rise time 207 ± 13 ms (n=17)), little or no desensitisation during the agonist application and a slow deactivation on removal of the agonist. The changes in the functioning of P2X7 receptors following multiple agonist applications were investigated. Increases in the current amplitude were shown to be dependent upon the agonist concentration. Current deactivation was shown to be dependent upon the agonist application number and on the voltage, and the slowing of deactivation was shown to require repeated receptor activation, rather than be dependent upon the time post agonist addition.

3.4.1 Agonist evoked rat P2X7 receptor currents

The EC_{50} values (EC_{50} = 33 ± 4 μM BzATP; and EC_{50} = 670 ± 50 μM ATP) produced from the concentration-response curve fitting show BzATP to be a much more potent agonist at rP2X7 receptors than ATP. The actual values are very similar, although slightly higher, than those reported previously (6.5-58 μM; Surprenant et al. 1996; Hibell et al. 2000; Jiang et al. 2005 for BzATP and 115 -407 μM for ATP). This is likely to be due to differences in the agonist application protocol used to construct the curves as changes to the current amplitude is dependent upon the application time and intervals between agonist additions (discussed later). The Hill slope of the concentration-response curve for BzATP and ATP activated rP2X7 currents were 1.7 and 2.2 respectively. These values are similar to those reported by Hibell and colleagues (Hill slope = 2.2 and 2.3 for BzATP and ATP respectively; Hibell et al. 2000) and fit with the proposed trimeric assembly of P2X receptors (Nicke et al. 1998), where one would expect a Hill slope of around 2-3 when measured from an agonist concentration-response curve.

3.4.2 Changes in the potency of BzATP at rat P2X7 receptors

The increase in the current amplitude produced by multiple applications of the same concentration of agonist is an interesting property of rat P2X7 receptors stably expressed in HEK293 cells (Figure 3.3). The extent of the increase in the current amplitude was cell

dependent. From the lack of correlation between the current density (in response to the first agonist application) and the percentage change over 6 agonist applications, we can conclude that it is not influenced by the number of P2X7 channels present in the cell (Figure 3.3C). The increase in current amplitude over multiple agonist applications was found to be concentration dependent, inline with previously reported data for this cell line (Hibell et al. 2000), where more applications were needed in order to elicit significant changes in the peak current amplitude at lower agonist concentrations. For example, significant changes were recorded at the 5^{th} application with 3 μM BzATP, but not until the 14^{th} application of 1 μM BzATP (Hibell et al. 2000). In the experiments reported here, the lack of change with the 3 μM concentration may be due to limiting the recording to 6 applications. Differences between these two studies may be due to the extracellular solution composition which differs from the ones used here in the absence of Mg^{2+} ion and a reduction in the Ca^{2+} ions to 0.5 mM. A plateau in the current increase seen at 30 μM BzATP was replicated at 10 μM BzATP and also for 1 mM ATP in other studies (Hibell et al. 2000).

Current growth is an increase in the net movement of ions across the membrane, either via an increase in the open channel probability or through an increase in the available permeation pathway, and can occur through a number of mechanisms. Initially it was thought to be associated with dilation of the P2X7 channel (Chessell et al. 1997; Chessell et al. 1998b). However, it is unlikely to be via the YOPRO permeation pathway, as the addition of supramaximal concentrations of agonist to rP2X7 receptors produced no current growth, but robust YOPRO uptake (Hibell et al. 2000). Although the NMDG permeation pathway is likely to be distinct from the one allowing YOPRO uptake, there is evidence that this may only form under non-physiological conditions such as in the presence of low extracellular Na^{+} concentrations (Jiang et al. 2005), and so it is improbable that it is occurring under the recording conditions employed here. Secondly, there is also evidence for a change in the phosphorylation status of the P2X7 receptor following agonist activation. In HEK cells this is through a complex of the P2X7 protein with a receptor protein tyrosine phosphatase (RPTPβ) that is activated following the binding of ATP with the receptor, and could indicate a direct effect on the channel

conformation (Kim et al. 2001a). This is also true for other P2X receptors, with basal phosphorylation of P2X1 receptors (Vial et al. 2004b), and phosphorylation of T18 in the P2X2 receptor detected with an anti-phosphothreonine antibody (Boue-Grabot et al. 2000). Dephosphorylation of P2X7 receptors at Tyr343 has been shown following exposure to supramaximal concentrations of agonist (Kim et al. 2001a), and so such processes could underlie the change in current amplitude. Further work would be needed to be done to explore these possibilities further and assess the impact of preventing phosphorylation on the current amplitude.

Finally, it was demonstrated that the potency of agonist for the P2X7 receptor increases following repeated or prolonged agonist application, in rP2X7-HEK cells (Hibell et al. 2000), native P2X7 in NTW8 cells (Chessell et al. 1997) and hP2X7-HEK cells (Michel et al. 1999). Therefore the current growth may represent a progressive increase in the potency of agonists at the receptor. If this is correct, then once maximum current amplitude is reached for a given agonist concentration, no further increases in current should be able to be produced. Theoretically, this should be neither via the enhancement of agonist concentration directly (greater concentration), or indirectly by increasing the effective agonist concentration through the removal of Mg^{2+} or Ca^{2+} ions. However, in both cases the current amplitude could be increased after a proposed maximum (plateau of the current) was reached (Figure 3.4). Therefore, although there are changes in the potency of the BzATP at P2X7 receptors, this does not represent a complete shift in the concentration-response curve such that further increases in current are not possible.

3.4.3 Inhibition of BzATP by divalents

The inhibition of P2X7 receptor function by Ca^{2+} and Mg^{2+} ions was confirmed here and produced IC_{50} values of 2 mM, and 1 mM respectively (Figure 3.4B). Although the values for Ca^{2+} and Mg^{2+} ions are more potent than those previously reported (Ca2+ 3.2 ± 0.4mM; Mg2+ 0.5 ± 0.04mM; Virginio et al. 1997), the rank order is the same and differences are likely to be due to differences in the protocols used to construct these curves, such as a higher divalent ion concentration in the standard extracellular solution and up to 6 applications of ions per cell used in the Virginio et al, study. The inhibition of

P2X7 function by divalent cations was initially thought to be mediated via a reduction in the concentration of ATP (Dahlquist and Diamant 1974), or through a direct blockade of permeation (Surprenant et al. 1996). However, the primary mechanism is likely to be via modulation of the agonist binding site, resulting in a reduction in the agonist affinity for the P2X7 receptor (Virginio et al. 1997), and possibly through a direct effect on the P2X7 receptor itself (Jiang 2008; Liu et al. 2008b). Two histidine residues, H130 and H210, have been implicated in the inhibitory actions of Mg^{2+} ions, suggesting that this cation acts at a defined allosteric site involving these two residues (Acuna-Castillo et al. 2007).

3.4.4 Deactivation kinetics of rP2X7 receptors

Deactivation is dependent upon the time of agonist removal from cells, as well as agonist unbinding and channel closure. In this study, as in others (Surprenant et al. 1996; Hibell et al. 2001a), the deactivation of rP2X7 receptors in response to BzATP applications slowed following each activation of the receptors (Figure 3.5). The slowing of the deactivation time of rP2X7 receptors occurs through an application-dependent mechanism rather than a time-dependent mechanism (Figure 3.8), and could arise from either changes in agonist dissociation or changes in the channel closing rates. The deactivation of P2X7 receptors has been shown to be related to the agonist potency (Hibell et al. 2001a), and so suggest it reflects agonist dissociation from the P2X7 receptor rather being an intrinsic property of the ion channel. As mentioned above, the potency of agonists has been shown to increase after repeated agonist applications and deactivation, and hence channel closure time, increased after repeated agonist applications. The deactivation time following agonist removal from rP2X7 receptors was fit with 2 exponential functions, possibly indicating multiple closed states of the P2X7 receptor. Data from hP2X7 receptors expressed in Xenopus oocytes indicated that these receptors possess at least two types of activation sites, which differ in ATP sensitivity and can influence activation and deactivation kinetics (Klapperstuck et al. 2001). Changes to the relative importance of these two states have been suggested here by the differing degree to which they contribute to overall deactivation (Figure 3.7).

Deactivation also possesses some voltage-dependence, with much slower closure times produced when cells are voltage clamped at +60mV rather than -60mV (Figure 3.6). This may be due to the slower agonist unbinding from the receptor at +60mV, or slower channel closure times, prolonging net current movement. Mechanistically this may be due to an influence of the electric field of the membrane on the unbinding of agonist or channel closure. The agonist binding site is situated on the extracellular portion of the receptor and although does not reside in the transmembrane sections, a number of charged residues have been identified that are important in agonist binding (See Introduction, Chapter 1). It is possible that the channel may undergo a conformational change following agonist gating that allows the binding site to move within the electric field of the membrane. Similar effects have been reported for other ligand-gated channels such as the nicotinic acetylcholine receptor (Auerbach et al. 1996) and $GABA_A$ receptors (Mellor and Randall 1998). Further work could be done to investigate the voltage-dependence of deactivation over a range of voltages and also assess the effect, if any, of different agonist application times.

The influence that agonist addition times and solution constituents can have on rat P2X7 receptor function highlights some of the dangers when comparing literature data that may utilise a number of different protocols or techniques. The investigations into the deactivation and current growth have been important for increasing our understanding of the receptor, but have also had implications for the design of protocols used to investigate antagonist potency and efficacy. The work here has shown the importance of completing subsequent studies using a standard set of protocols, and has defined such a set of conditions for pharmacological assessment of rat P2X7 receptors in the next chapter and in the investigation of native P2X7 receptors in Chapter 5.

Chapter 4: P2X7 receptor antagonists

4.1. Introduction

P2X7 receptors have been proposed as a pharmacological target for the therapy of a number of disease states, including Alzheimer's disease (Parvathenani et al. 2003), epilepsy (Rappold et al. 2006), multiple sclerosis (Yiangou et al. 2006) and the focus of the work here inflammatory and neuropathic pain (Donnelly-Roberts and Jarvis 2007). Underlying much of the aetiology of these diseases is inflammation and there is considerable evidence for a role of P2X7 receptors in regulating inflammatory processes (Ferrari et al. 2006). This is reviewed in the Introduction, Chapter 1.

In order to further evaluate P2X7 receptors as a possible target for novel analgesics, tool compounds must be made available. The current tools include a number of ligands first identified some years ago, which are limited in their use by pan-P2X pharmacology, or species specificity (See Introduction, Chapter 1, section 1.2.2.2). More recently a number of new P2X7 antagonists have been described including compounds across a range of chemical series, (Donnelly-Roberts and Jarvis 2007; Romagnoli et al. 2008) some of which display an improved potency, selectivity and less species dependence (Honore et al. 2006; Nelson et al. 2008).

Here a novel P2X7 antagonist, GSK314181A (Alcaraz et al. 2000) from the AstraZeneca patent, WO2000061569A1, has been profiled using whole-cell patch-clamp techniques to define it's potency at P2X7 receptors and investigate its possible mechanisms of action and selectivity profile at other P2X receptors.

4.2 Methods Summary

4.2.1. Electrophysiological studies

Experiments were performed using whole-cell patch-clamp electrophysiology to study P2X7 and P2X4 receptors stably expressed in HEK293 cells, and P2X2/3 heteromeric

receptors stably expressed in CHO cells. Cells were voltage-clamped at -60mV unless otherwise stated. For intracellular application of GSK314181A, pipettes were back filled using the standard intracellular solution containing GSK314181A.

4.3 Results

4.3.1 P2X7 Antagonists

PPADS and Brilliant Blue G were used as tool compounds for pharmacological characterisation of HEK cells stably expressing rP2X7 receptors. PPADS, a non-selective P2X antagonist (30μM), inhibited 30μM BzATP-activated rat P2X7 currents by 97±1 % (n=3) and was slowly reversible over a 12 minute period (78% of control; Figure 4.1A). BBG is a commonly used antagonist of P2X7 as is one of the more potent tools. Figure 4.1B illustrates the potency and reversibility of BBG as 10 nM inhibits currents by 41 ± 6% (n=4) and the current is fully reversed back to baseline within 2 minutes. To enable an estimate of the IC_{50} concentration for inhibition of the BzATP-activation of rat P2X7 by BBG to be made, additional experiments were conducted in the 1 nM to 100 nM concentration range, allowing the production of a concentration-response curve that had an IC_{50} value of 11 ± 1 nM, (Hill slope 1.4, n=3-4; Figure 4.1C) for the inhibitory activity of BBG at rP2X7.

Zn^{2+} ions are known inhibitors of P2X7 currents and are a useful tool with which to distinguish P2X7 mediated currents as they potentiate P2X2 and P2X4 currents (see Introduction, section 1.2.2.2). The concentration-response relationship for Zn^{2+} ion inhibition of BzATP evoked currents was established. Zn^{2+} (10 μM) inhibited BzATP-activated rat P2X7 currents by 86 ± 2 % (n=5), reaching a peak inhibition after 2 minutes preincubation and was fully reversible within 2 minutes (see Figure 4.1D). Additional concentrations were tested from 100nM to 100 μM allowing the production of a concentration-response curve, which yielded an IC_{50} value of 1.9 ± 0.2 μM, (Hill slope 1.2, n=3-6) (Figure 4.1E).

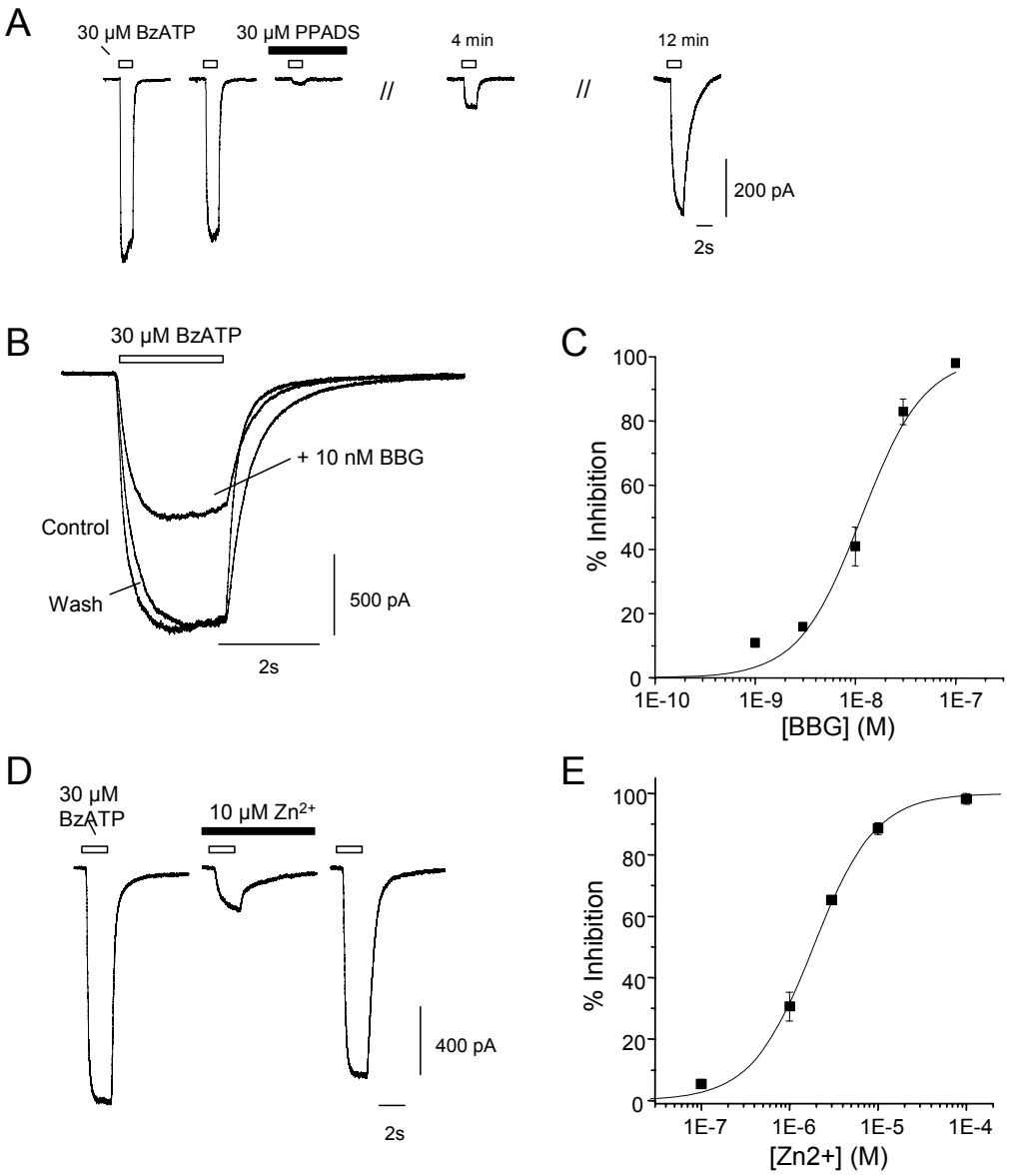

Figure 4.1: Pharmacological characterisation of rP2X7
A. Example recording showing P2X antagonist PPADS (30 µM) inhibiting 30 µM BzATP-activated rP2X7 current by 97 ± 1%, n=3. The recovery from inhibition is slow, with 17% recovery within 4 min and 78% after 12 min.
B. Example recording showing Brilliant Blue G (BBG, 10nM) inhibiting 30 µM BzATP-activated rP2X7 current by 41 ± 6% and the recovery to pre-addition levels in 2 min.
C. Concentration response curve for BBG at rP2X7 activated by 30 µM BzATP, IC_{50} = 11 ± 1 nM, Hill slope n = 1.4 (n=3-4).
D. Zn^{2+} (10µM) inhibits 30 µM BzATP-activated rP2X7 currents by 89 ± 2% (n=5). Inhibition in the presence of Zn^{2+} peaked within 2 minutes and was fully reversible.
E. Concentration response curve for Zn^{2+} inhibition of rP2X7 currents, produces an IC_{50} = 1.9 ± 0.2 µM (Hill slope = 1.2, n=3-6).

4.3.2 GSK314181A is a potent antagonist of rat P2X7 receptors

GSK314181A (Figure 4.2A) has been identified from the Astrazeneca patent WO2000061569A1 (Alcaraz et al. 2003; Romagnoli et al. 2005), as an inhibitor of P2X7 currents ($pIC_{50} > 4.5$). GSK314181A (100 nM) inhibited BzATP-activated rat P2X7 currents by 93 ± 1.3 % (n=4), reaching a peak inhibition after 2 minutes preincubation and was fully reversible within 4 minutes (see Figure 4.2B). Additional concentrations were tested from 10nM to 1 μM allowing the production of a concentration-response curve, which yielded an IC_{50} value of 1 ± 0.2 nM, (Hill slope 0.7, n=3-7) (Figure 4.2C). All concentrations of GSK314181A produced a maximum inhibition of BzATP-activated currents within 4 minutes of preincubation (2 agonist additions) and currents were fully reversible within 4 minutes of washout of GSK314181A (Figure 4.2B). The inhibition of BzATP-activated currents by GSK314181A was not affected by holding cells at a positive potential. The inhibition produced by 100nM GSK314181A at +60mV (89 ± 1 % inhibition, n=4, Figure 4.2D) was not significantly different to that recorded at a holding potential of -60mV (93 ± 1 % inhibition, n=4, p=0.07).

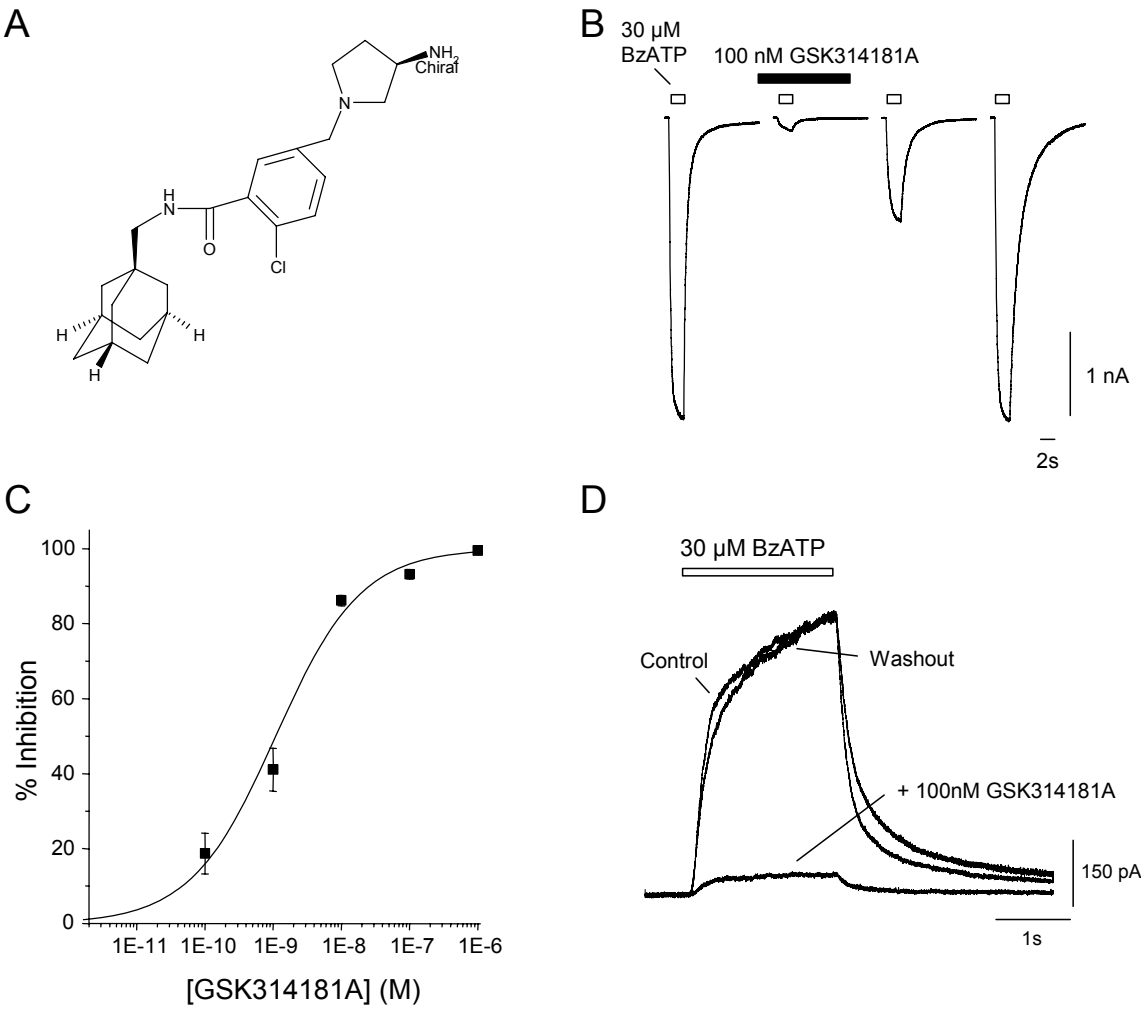

Figure 4.2: GSK314181A is a potent inhibitor of rat P2X7 receptors
A. Molecular Structure of GSK314181A (Romagnoli et al, 2005; WO2000061569A1).
B. GSK314181A 100 nM inhibits 30 µM BzATP-activated rP2X7 current by 93 ± 1 %, n=4. Inhibition with GSK314181A peaked within 4 minutes on average and currents recovered to baseline levels within 4 min.
C. Concentration response curve for GSK314181A inhibition at rP2X7 receptors, IC50= 1 ± 0.2 nM, Hill slope n= 0.7 (n=3-7).
D. The inhibition of BzATP-activated currents by GSK314181A was not voltage-dependent. GSK314181A 100 nM inhibits 30 µM BzATP-activated rP2X7 current by 95%. Recovery to baseline levels is within 4 min. The inhibition produced by 100nM GSK314181A at +60mV (89 ± 1 % inhibition, n=4, Figure 4.2D) was not significantly different to that recorded at a holding potential of -60mV (93 ± 1 % inhibition, n=4, p=0.07).

In addition, we examined whether GSK314181A was capable of blocking BzATP-activated rP2X7 current when applied intracellularly (Figure 4.3A). A high concentration of GSK31418A (1 μM) was included in the standard whole-cell recording solution. In all recordings a robust BzATP-activated current was observed following the first application of BzATP (361 ± 102 pA, n=4). Subsequent applications of BzATP resulted in the normal increase in the current amplitude and no abnormal changes in the kinetics of the responses were observed. In all 4 cells a subsequent extracellular application of 1 μM GSK31418A produced its signature inhibition of currents to 5 ± 2 % of control, n=4, which was reversible on washout of the drug (Figure 4.3A and 4.3B).

Finally the ability of GSK31418A to inhibit BzATP-activated currents without preincubation was tested. rP2X7 receptors were activated by BzATP (30 μM) and after currents had peaked the solution was changed to one also containing 1 μM GSK31418A, resulting in a full inhibition of the current (94 ± 1 % block) inhibited by co-application of GSK31418A (1 μM). This inhibition was fully reversible on removal of the antagonist, and was not significantly different from that produced with GSK314181A preincubated for 2 minutes (p=0.1; Figure 4.3C).

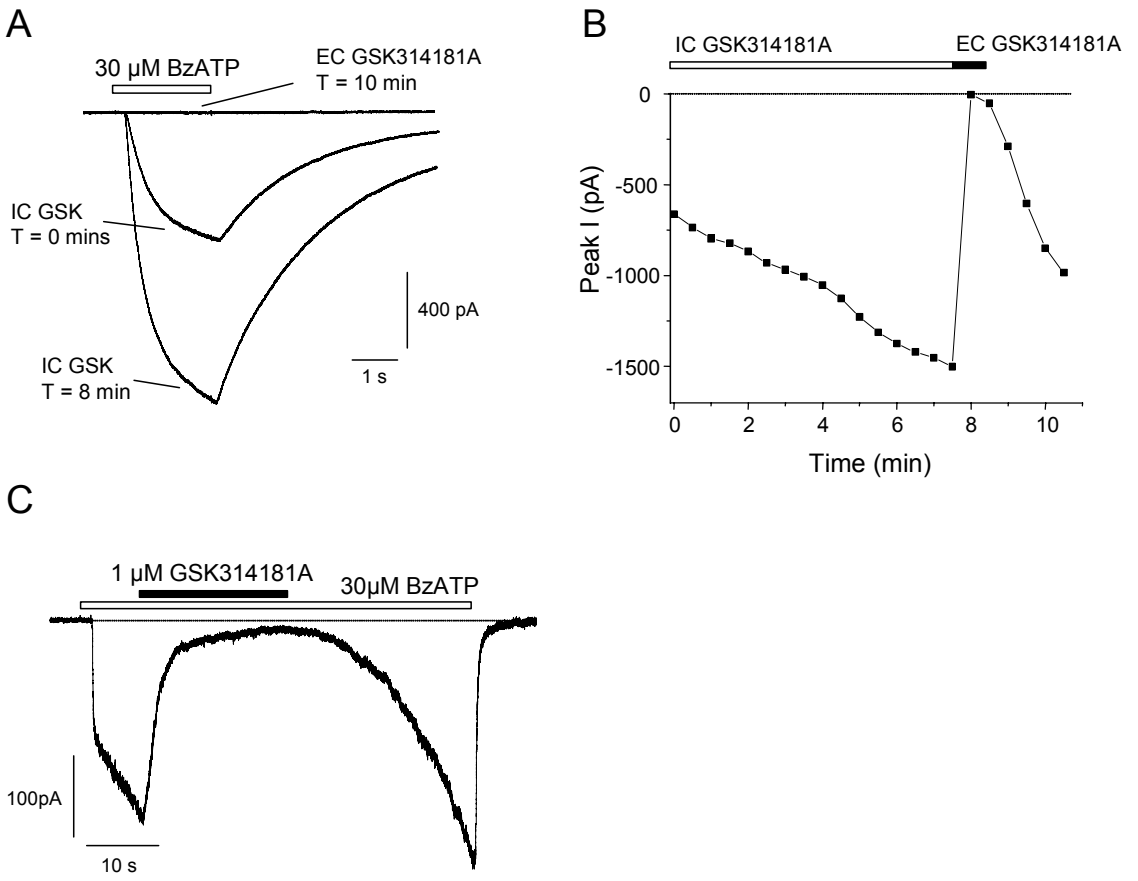

Figure 4.3: GSK314181A inhibits rat P2X7 receptors at +60mV and does not require intracellular access to the ion channel.

A. Example recording showing the first current response to BzATP (30 µM) recorded with 1 µM GSK314181A within the recording electrode and then after 8 minutes. The other trace shows the inhibition of the response to 30 µM BzATP in the presence of extracellular application of GSK314181A (1 µM).

B. Graph showing the peak current amplitude in response to BzATP applications from the recording in (A). The clear bar indicated the presence of GSK314181A (1 µM) in the intracellular pipette solution and the black bar shows the addition of this drug extracellularly. A partial reversal of the inhibited current can be viewed following removal of GSK314181A.

C. Example trace showing BzATP-activated current inhibited by co-application of GSK31418A (1 µM) by 94 ± 1% (n=5). This inhibition was fully reversible on removal of the antagonist.

4.3.3 GSK314181A is an antagonist of human P2X7 receptors

GSK314181A (10nM) inhibited BzATP-activated human P2X7 currents by 88 ± 2 % (n=3), reaching a peak inhibition after 10 minutes preincubation. GSK314181A inhibition of human P2X7 receptors took on average 7 ± 2 minutes to reach peak, and there was very little reversal of the inhibition recorded up to 20 minutes washout (Figure 4.4A). Additional concentrations were tested from 1nM to 1 μM allowing the production of a concentration-response curve, which yielded an IC_{50} value of 5 ± 0.7 nM, (Hill slope 1.5, n=3-4) (Figure 4.4B).

Although BzATP is an analogue of ATP, it was thought prudent to confirm that GSK314181A could inhibit human P2X7 receptors activated by the endogenous ligand, ATP. GSK314181A (100nM) inhibited ATP-activated human P2X7 currents by 89 ± 2 % (n=3), reaching a peak inhibition after 8 minutes preincubation. The currents did not reverse on washout of the drug (Figure 4.4C). Therefore a range of concentrations of GSK314181A were applied to 5 mM ATP-activated currents, allowing the production of a concentration-response curve which yielded an IC_{50} value of 16 ± 3 nM, (Hill slope n= 0.9, n=3-4).

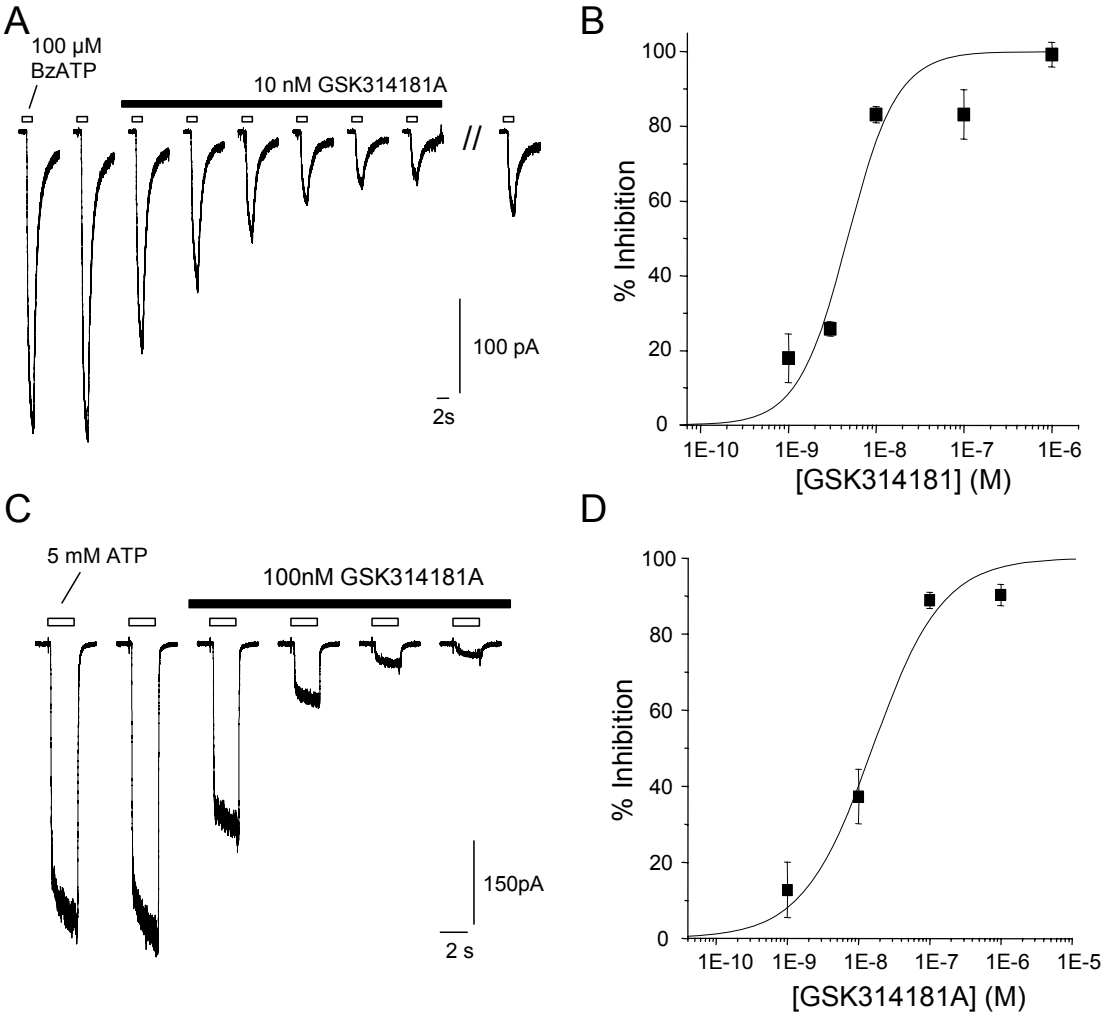

Figure 4.4: GSK314181A is a potent inhibitor of human P2X7 receptors
A. Example trace showing the effect of GSK314181A (10 nM) on 100 µM BzATP-activated currents. hP2X7 currents were inhibited by 83 ± 2 %, n=3. The effect of inhibition of GSK314181A peaked after 10 minutes on average. Little recovery of the current was seen.
B. Concentration response curve for GSK314181A inhibition at human P2X7 receptors, activated by BzATP (100µM) IC_{50}= 5 ± 0.7 nM, Hill slope = 1.5.
C. Example trace showing the effect of GSK314181A (100 nM) on 5 mM ATP-activated currents. hP2X7 currents were inhibited by 89 ± 2 %, n=3. The effect of inhibition of GSK314181A peaked after 8 minutes on average. Little recovery of the current was seen.
D. Concentration response curve for GSK314181A inhibition at human P2X7 receptors, activated by ATP (5mM) IC_{50}= 16 ± 3 nM, Hill slope = 0.9.

4.3.4 GSK314181A reverses FCA-induced hypersensitivity in rats

This work was completed by Nick Clayton and Lisa Winyard (Lappin et al. 2005). See the Appendix A for information on the methods for this study.

One of the most commonly used pain models for assessing the efficacy of tool compounds to reduce inflammatory pain is the Freunds Complete Adjuvant model (FCA). GSK314181A has been shown to be a potent antagonist at rat P2X7 receptors and so is an ideal tool compound with which to try to address the role P2X7 plays in pain processing *in vivo*. Naïve rats distributed their weight equally between the two hindpaws (left: 83.8 ± 1.7 g, right: 88.1 ± 1.9 g, *n*= 35). Following an intraplantar injection of FCA (100 µl of 1 mg/ml) into the left hindpaw there was a significant reduction in the weight bearing on the ipsilateral hindpaw resulting in an 69.5 ± 5.7g difference in weight bearing between the pre-FCA and pre-dose. GSK314181A produced a significant reversal of FCA-induced hypersensitivity at 1.5 hours post dose, 30mg/kg s.c (86.3 ± 17.2%) and the positive control, Celebrex (COX-2 Inhibitor, Celecoxib, (10mg/kg)) significantly reversed FCA-induced hypersensitivity at 1.5 hours, 3 hours and 6 hours post-dose (Figure 4.5). The effect of Celebrex peaked at 3 hours post-dose with an almost complete reversal of the deficit in weight bearing of 95.6 ± 19.4%. The mean data for the difference in weight bearing post FCA injection is shown in Figure 4.5B.
The blood and brains of the rats that had received the dose of 30 mg/kg GSK314181A were taken 3 hours post dose for pharmacokinetic analysis. This yielded mean blood and brain concentrations of GSK314181A of 5.5 µM and 2.5µM, respectively, with a brain: blood ratio of 0.45:1.

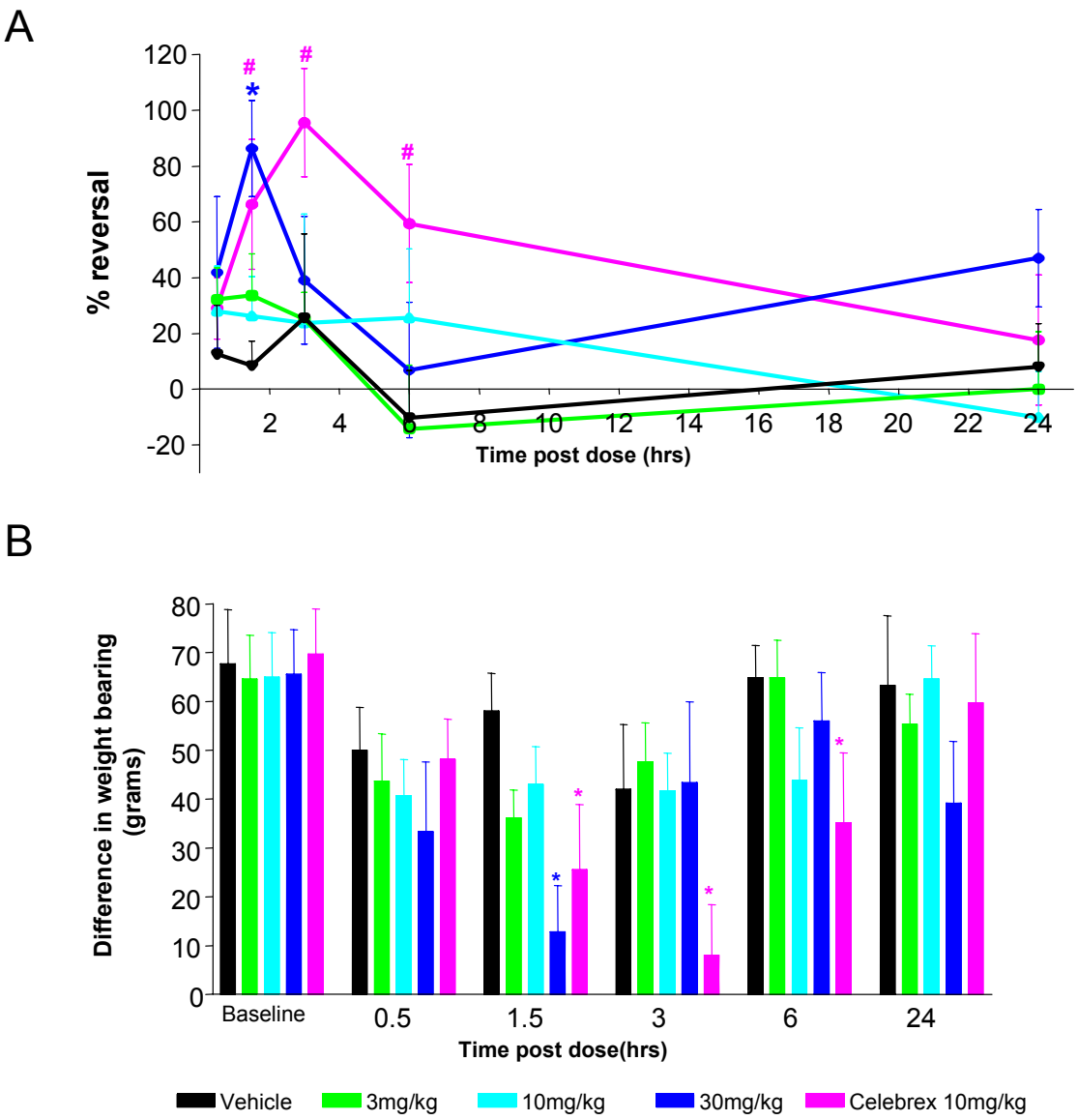

Figure 4.5: GSK314181A reverses FCA-induced hypersensitivity
A. GSK314181A produced a significant reversal of FCA-induced hypersensitivity at 1.5 hours post dose, 30mg/kg s.c ($p<0.05$ *) (86.3 ± 17.2%) Celebrex (10mg/kg) as a positive control significantly reversed FCA-induced hypersensitivity ($p<0.05$ #).
B. Mean data for the difference in weight bearing (g) post FCA injection. GSK314181A gave equal efficacy to that seen with the COX-2 inhibitor, Celebrex.

The reversal of the FCA-induced hypersensitivity by the P2X7 antagonist GSK314181A were encouraging and provided some evidence for a pivotal role of P2X7 activation in pain processing. However due to the relatively high (total) concentrations of GSK314181A found in the bloods and brains of these animals selectivity studies with GSK314181A were required to allow more definite conclusions to be drawn from this work.

4.3.5 Selectivity of GSK314181A

As GSK314181A had been confirmed as a potent antagonist of P2X7 its selectivity for P2X7 over the other P2X receptor subtypes was investigated. As detailed in the Introduction (Chapter 1, section 1.1.1.5.), P2X4 receptors are located on the same chromosome as P2X7 and share the most homology out of all P2X receptor subtypes (North 2002). Recombinant cell lines of stably transfected human and rat P2X4 receptors were used for these selectivity studies and were established and maintained as described in the methods. P2X4 receptors were activated with 10 μM ATP, approximately an EC_{80} concentration at rat and human P2X4 receptors (Jones et al. 2000). PPADS (100μM) inhibited ATP-activated human P2X4 currents by 82 ± 1% (n=3; Figure 4.6A). GSK314181A (10 μM) inhibited ATP-activated rat and human P2X4 currents by 27 ± 3 % (n=7) and 16 ± 3 % (n=6), respectively (Figure 4.6C). As can be seen from Figure 4.6B, the inhibition peaked rapidly, within 4 minutes, following incubation and was fully reversible within 4 minutes (see Figure 4.6B). Additional concentrations of GSK314181A were tested at rat P2X4 receptors, from 1 μM to 300 μM, allowing the production of a concentration-response curve, which produced an IC_{50} value of 26 ± 3 μM, (Hill slope 0.9, n=3-7; Figure 4.6D).

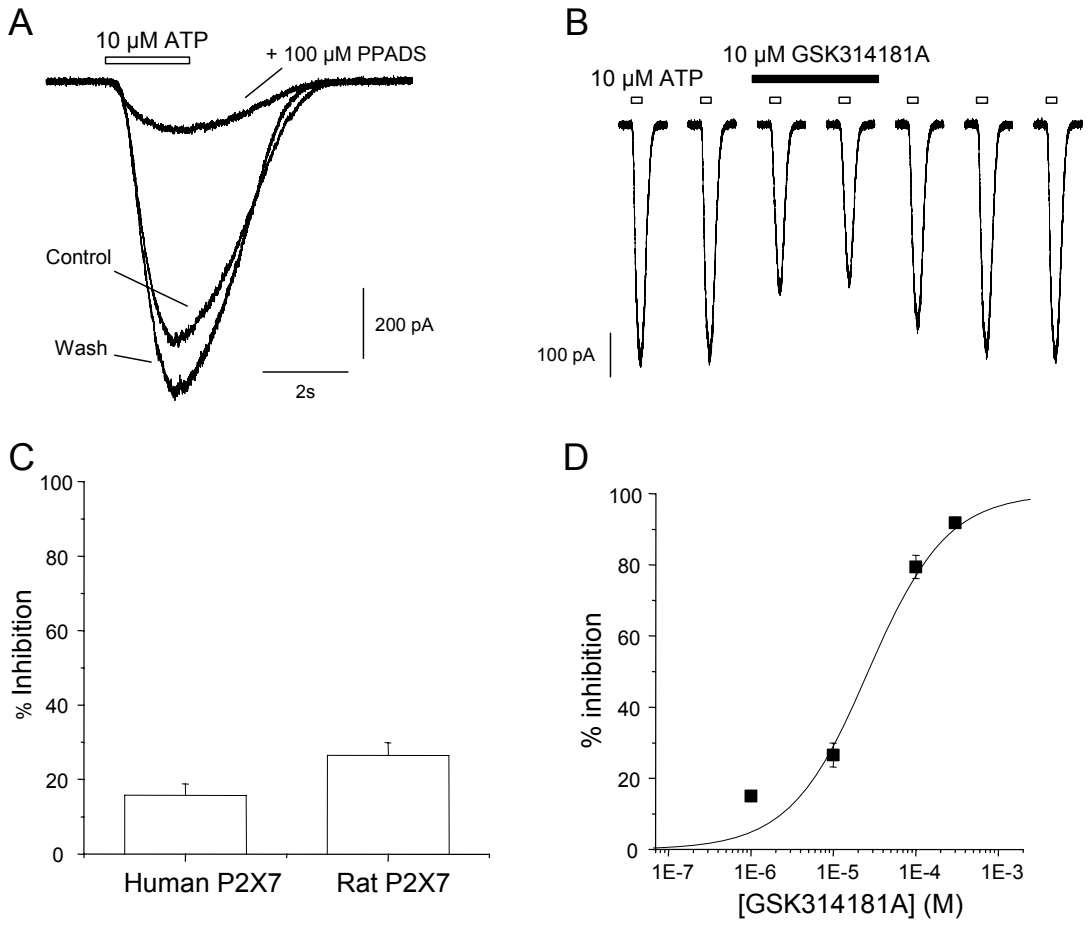

Figure 4.6: Effect of GSK314181A on P2X4 receptors

A. Recording showing PPADS (100 µM) inhibits a 10 µM ATP-activated hP2X4 current by 82 ± 1% (n=3), and reversal of the inhibition after 8 min (wash).

B. Example recording showing GSK314181A (10 µM) inhibits 10 µM ATP-activated rat P2X4 current by 27 ± 3% (n=7). Recovery to baseline levels is within 4 min.

C. Mean data for the inhibition of human P2X4 receptors (15 ± 4 %, n=5) and rat P2X4 receptors (27 ± 3 %, n=7) by 10 µM GSK314181A. IC_{50} value > 10 µM

D. Concentration response curve for GSK314181A inhibition at rat P2X4 receptors, activated by ATP (10µM) IC_{50}= 26 ± 3 µM, Hill slope n= 0.9, n=3-7.

The activity of GSK314181A at P2X2/3 and P2X3 receptors was also investigated using recombinant cell lines stably expressing human P2X2 and P2X3 receptors. αβme-ATP, (7.5μM) is the most potent agonist at hP2X2/3 receptors and also activates hP2X3 receptors, but crucially not hP2X2 at this concentration. The protocol is detailed in Chapter 2, Materials and Methods, and also an example trace is shown in Figure 4.7i. The subtraction step and resulting uncovering of the P2X3 current component is shown in Figure 4.7ii. TNP-ATP (1nM) was used as a positive control antagonist of these currents and inhibited P2X3 current by 78 ± 8%, n=3 and P2X2/3 currents by 32 ± 3%, n=3 (Figure 4.7B). GSK314181A (10 μM) was preincubated and co-applied and inhibited P2X3 and P2X2/3 currents by 60 ± 9 %, n=6 and 61 ± 3 %, n=8, respectively (Figure 4.7C and 4.7D). Due to the previously reported high positive correlation between ligand binding at heteromeric P2X2/3 and homomeric P2X3 receptors (Jarvis et al. 2004), a range of concentrations of GSK314181A (1-100 μM) were tested at P2X2/3 receptors activated by αβ-meATP only, and when data were plotted an IC_{50} value of 4.6 ± 0.8 μM was obtained (Hill slope n= 0.7, n= 4-8; Figure 4.7E).

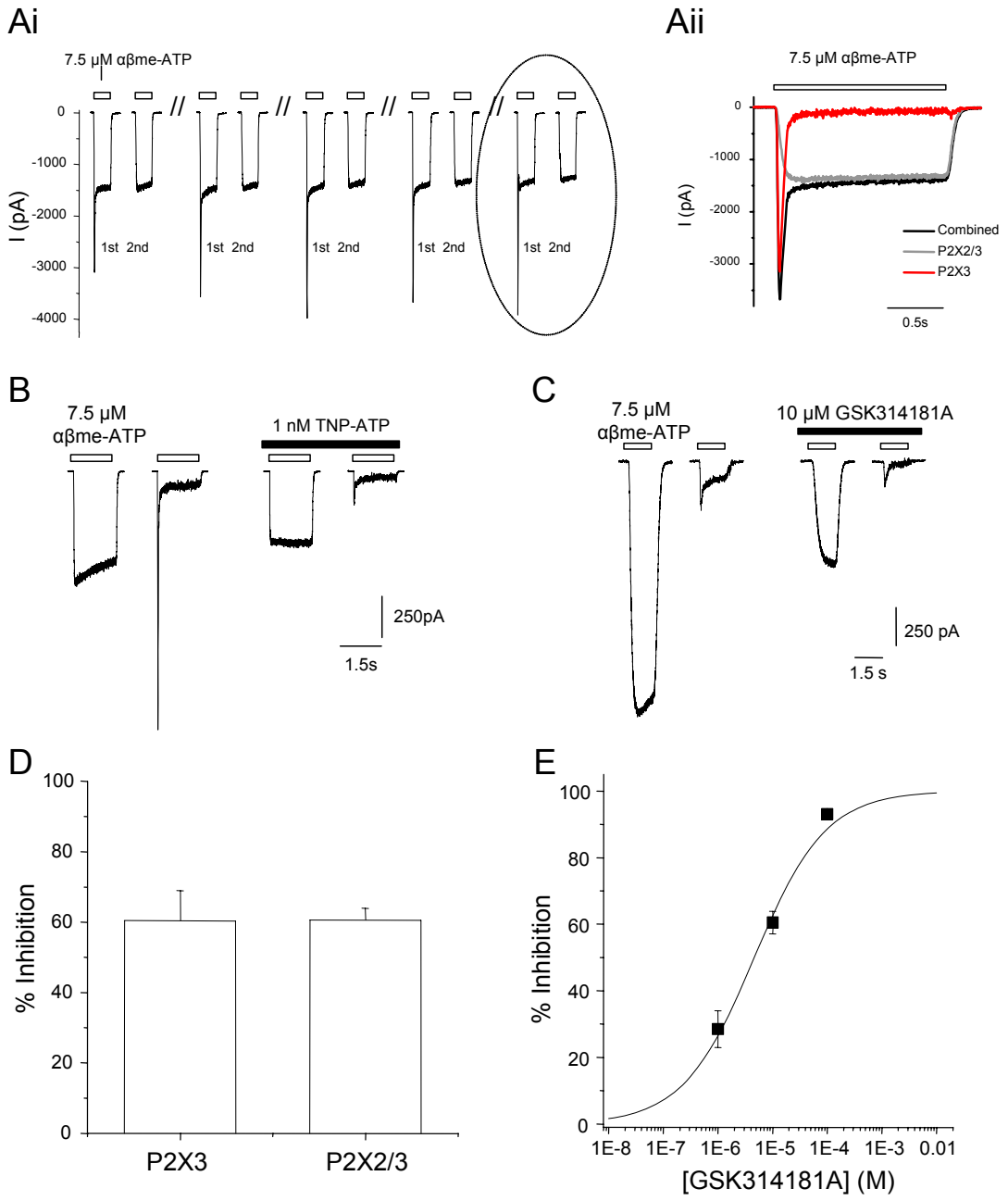

Figure 4.7: Effect of GSK314181A on P2X3 and P2X2/3 receptors
Ai. Example recording showing αβ-meATP activated hP2X2/3 currents using the dual activation protocol. Aii Traces from the final example from Ai. The second trace (grey) has been subtracted from the first trace (black) to dissect out the P2X3 mediated current which is overlayed in red. B. Example recording showing TNP-ATP (1 nM) inhibits a 7.5 μM αβ-meATP-activated hP2X2/3 and hP2X3 current by 78 ± 8% and 32 ± 3% respectively. C. Example recording showing GSK314181A 10 μM) inhibits a 7.5 μM αβ-meATP-activated hP2X2/3 and hP2X3 current by 60 ± 9% and 61 ± 3% respectively.
D. Mean data for the inhibition of human P2X2/3 and hP2X3 receptors by GSK314181A (10μM).
E. Concentration response curve for GSK314181A inhibition at human P2X2/3 receptors, activated by αβ-meATP (7.5μM) IC_{50}= 4.6 ± 0.8 μM, Hill slope n= 0.7 (n=4-8).

4.4 Discussion

In this study we demonstrated that GSK31418A is a potent antagonist of rat and human P2X7 receptors stably expressed in HEK293 cells. GSK314181A blocked BzATP-activated and ATP-activated rat and human P2X7 currents in a reversible, voltage-independent manner and was >10000 fold selective over the closely related P2X4 receptors and >1000 fold selective over P2X2/3 receptors. When profiled *in vivo*, a subcutaneous administration of GSK314181A produced a significant reversal of FCA-induced hypersensitivity at the highest dose tested.

4.4.1 Pharmacological characterisation of rP2X7 cell line

The rat P2X7-HEK293 stable cell line has been used previously but pharmacological validation was needed before novel compounds were assessed using it. PPADS and Brilliant blue G (BBG) are non-specific P2X antagonists. The almost complete inhibition of rat P2X7 receptors with PPADS (30μM) shown here demonstrates a higher potency for this compound compared to previously reported values (IC_{50} value of 45 μM) (Surprenant et al. 1996). However PPADS potency is incubation-time dependent with previously reported IC_{50} values for its inhibition of human P2X7 receptors ranging from 62mM (Rassendren et al. 1997) to 1μM, (Chessell et al. 1998a). Indeed in the Chessell et al, study they demonstrated its dependence on incubation time as little antagonism was apparent when the agonist and antagonist were co-applied, without any prior pre-incubation. It was a particularly difficult tool antagonist to use due to slow wash-out periods (Chessell et al. 1998a), and so no further characterisation work was done using this compound.

The inhibition produced by BBG peaked within 4 minutes of preincubation for all concentrations tested and was concentration dependent, producing an IC_{50} value of 11 ± 1 nM, inline with previously reported data for this cell line (IC50=10nM; Jiang et al. 2000a). However the inhibition of currents in the presence of BBG reported here was rapidly reversible and when the experiment was continued could show complete recovery back to baseline levels. This is at odds with reported data in Jiang et al, where slow reversals of block were recorded with incomplete reversals after a 16- to 20-min wash (Jiang et al. 2000a). The protocols used are almost identical and so unlikely to underlie

the differences seen here. It may be partly due to the run-up recorded following multiple agonist applications to rat P2X7 receptors in this cell line (see Results Chapter 3; Figure 3.1C). The increasing baseline currents observed during multiple application of agonist may contaminate true reversal of inhibition where experiments were performed with cells showing increasing current amplitude responses.

The inhibition of P2X7 receptor function by Zn^{2+} ions was confirmed here and produced and IC_{50} values of 1.9 μM (Figure 4.1E). This is around 6 fold higher than the value reported by Virginio and colleagues (IC50 =11.2 μM; Virginio et al. 1997), but is likely to be explained by differences in the protocols used to construct these curves, and a higher divalent ion concentration in the standard extracellular solution used in these studies.

4.4.2 A novel antagonist of rP2X7 receptors

The data presented here demonstrate that GSK314181A is a potent antagonist of rat and human P2X7 receptors, with IC_{50} values of 1 and 5 nM, respectively (Figure 4.2C and 4.4B). Therefore GSK314181A represents one of the most potent compounds reported to date, and shows little species difference often associated with P2X7 antagonists. Subsequent to the work described in this chapter, GSK314181A has also been shown to be efficacious against the other measures of receptor activation. Ca^{2+} uptake experiments showed similar potency values for GSK314181A to inhibit rat and human P2X7 receptor activation (IC_{50} values of 29nM at rat P2X7and 18nM at human P2X7 (Broom et al. 2008). Pore formation can be measured by assessing the uptake of the fluorescent dyes YO-PRO or ethidium bromide (Hibell et al. 2000). GSK314181A was also able to inhibit pore formation, although the potency was 50-200 times less than that recorded using electrophysiology (IC_{50} values of 980nM at rat P2X7 (Broom et al. 2008). IC_{50} value of 288nM at rat P2X7 (Fonfria et al. 2005) and there was much greater species variability (16-70 time less potent at rat P2X7 than human in these assays (Broom et al. 2008) and (Fonfria et al. 2005). This is of particular importance and interest as considerable species differences in P2X7 receptor pharmacology have been previously reported. It is well known that agonist potency is greater at rat and human P2X7 receptors than at mouse receptors (Rassendren et al. 1997; Chessell et al. 1998b). With regards to antagonists,

many of the previously identified compounds differentiate between the species orthologues, and often exhibiting a much greater potency at the human P2X7 orthologues and limited rodent P2X7 activity (North and Surprenant 2000). This reduction or absence of rodent P2X7 activity can be a serious problem when considering performing the preclinical experiments required to progress compounds into the clinic. Examples of this are seen with the commonly used tool compounds such as PPADS and Suramin which show 5 to10 fold greater potency at human P2X7 receptors than at rat (Rassendren et al. 1997; Chessell et al. 1998a; Chessell et al. 1998b), KN-62, a more P2X7 specific antagonist, only inhibits human receptors and is ineffective at other P2X7 orthologues (Gargett and Wiley 1997; Humphreys et al. 1998). However this problem has extended to newer compounds like AZ116453743 which shows a similar potency reduction at the rat receptors (> 500-fold less effective at inhibiting rat P2X7 currents (Stokes et al. 2006) and for the Triazole-based compounds reported by Carroll and colleagues (Carroll et al. 2007). The obvious exceptions to this are BBG and Calmidazolium where the reverse is true, and greater potency is seen in their ability to inhibit rat P2X7 receptors compared to human P2X7 (Virginio et al. 1997; Jiang et al. 2000a).

When comparing the effect of GSK314181A at rat and human P2X7 receptors the potency of the inhibition produced is very similar, however the rate of onset of block and the recovery from block of BzATP-activated currents were much slower at the human P2X7 receptor than for the rat (Figure 4.2B, 4.4A). The human P2X7 is 80% identical to the rat receptors (Rassendren et al. 1997) and 48 amino acid differences have been identified on the proposed extracellular part of the receptor. These amino acid changes are likely to account for the disparity in the time it takes for GSK314181A to produce its inhibitory effects and will be related to the strength of binding of GSK314181A to the protein. However as the binding site for GSK314181A remains unknown it is difficult to hypothesise which amino acid changes, in particular, are critical. Further work would be needed using site-directed mutagenesis techniques to pinpoint important residues that may underlie this differential interaction between the two orthologues.

The mechanism by which GSK314181A interacts to inhibit P2X7 receptors can be an important factor in determining its potency and efficacy. GSK314181A did not need to be preincubated in order to inhibit BzATP-activated rat P2X7 currents, and inhibition was not significantly different from that produced with GSK314181A preincubated for 2 minutes ($p=0.1$). Therefore it is possible that GSK314181A interacts with the agonist binding site or with a site that is uncovered following agonist binding and hence conformation change. Further site-directed mutagenesis work would be required to gain binding site information and detailed pharmacological analysis is required to ascertain whether GSK314181A has a competitive or non-competitive mechanism of action. These studies can only be done by looking at shifts in the agonist concentration-response curves which are not possible here due to current run-up in the presence of multiple agonist additions. Intracellular application of GSK314181A produced no inhibition of BzATP-activated currents in rat P2X7 expressing cells, strongly suggesting an extracellular binding site of the molecule and no requirement for intracellular access to produce inhibition. The voltage-dependence of inhibition was also assessed, and equal inhibition was recorded at a holding voltage of -60mV or +60mV (Figure 4.2D), indicating a voltage-independence to the activity of GSK314181A. From this we can infer that GSK314181A would have equal effectiveness to antagonise P2X7 receptors whether the cell expressing P2X7 receptors is depolarised or at resting membrane potentials, which may be particularly important if the site of action has a neuronal basis. The neuronal expression of P2X7 receptors is still subject to debate. P2X7 receptors have been localised to presynaptic terminals (Deuchars et al. 2001; Sperlagh et al. 2002; Ishii et al. 2003) and P2X7 activation, with BzATP, enhanced the release of glutamate and GABA (Deuchars et al. 2001; Sperlagh et al. 2002), and increased evoked EPSC amplitude (Armstrong et al. 2002; Ireland et al. 2004). P2X7 receptors may also have a role in increasing synaptic strength postsynaptically through AMPA receptor insertion (Gordon et al. 2005). However, some caution should be used when interpreting data from such studies as the enhancement of synaptic transmission has been mimicked in slices from P2X7 knock-out mice (Kukley et al. 2004), and there is evidence that some of these effects may be mediated through neuronal adenosine A1 receptors (Kukley et al. 2001; Ireland et al. 2004; Kukley et al. 2004). Finally one should not discount glutamate release

from murine cortical astrocyte cultures following the activation of P2X7 receptors as a non-neuronal source of this neurotransmitter (Duan et al. 2003).

When considering the ability of GSK314181A to inhibit P2X7 receptors in vivo, we deemed it necessary to confirm that the compound would inhibit P2X7 currents following ATP activation. BzATP is the most widely used agonist for activating P2X7 receptors due to its greater potency (North and Surprenant 2000). However it is an analogue of ATP and not the endogenous ligand for the receptor. GSK31418A was as efficacious and only slightly less potent at inhibiting ATP-activated P2X7 currents as those activated by BzATP (Figure 4.4), and also demonstrated the same kinetics of block, indicating no potential issues for its use *in vivo*.

4.4.3 *In Vivo* activity of GSK314181A

Subcutaneous administration of the P2X7 receptor agonist GSK314181A inhibited the FCA-induced decrease in weight bearing, a measure of inflammatory hypersensitivity. GSK314181A was effective at a dose of 30mg/kg at 1.5 hours post dose (86.3 ± 17.2% reversal). The FCA model is a well known and described model used to measure inflammatory hypersensitivity, where the hypersensitivity peaks at about 24–72 h after FCA injection (De Alba et al. 2006). These results are consistent with results seen in previous studies showing efficacy for P2X7 antagonists in inflammatory models of pain. Honore at al, demonstrated a significant reversal in both the carrageenan and FCA induced inflammatory pain models with A-740003, 30 minutes after dosing (ED_{50} = 54 mg/kg and ED_{50} = 38 mg/kg respectively). Since the publication of the data reported here (Lappin et al. 2005), further work with this compound, renamed AACBA, confirms our data and reported efficacy of GSK314181A in the carrageenan model of inflammatory pain, and also shows a positive effect on the oedema associated with injection to the hindpaw (Broom et al. 2008).

These antinociceptive effects of GSK314181A in the FCA model are consistent with the proposed role of P2X7 receptors in inflammatory pain. There is substantial evidence to indicate a role for P2X7 receptors in mediating inflammation (Ferrari et al. 2006) and so

as a potential therapeutic target with which combat chronic inflammatory pain (Romagnoli et al. 2008). Gene knock-out studies showing that P2X7 null mice have reduced pain sensitivity following both complete Freund's adjuvant-induced inflammation and partial injury of the sciatic nerve (Chessell et al. 2005) adding confidence for a small molecule antagonist strategy. The rationale for the proposed efficacy of P2X7 receptor antagonists centres around the activation of microglial and astrocytic P2X7 receptors, causing the release of proinflammatory cytokines such as IL-1β, TNF-α and IL-18 (Lister et al. 2007). The maturation and release of IL-1β following P2X7 receptor activation (Perregaux and Gabel 1994; Solle et al. 2001; Ferrari et al. 2006), may be of particular importance not only as a key mediator in the inflammatory cascade, but also because it causes an increase in P2X7 receptor expression levels and function in astrocytes after a 24 hour exposure (Narcisse et al. 2005). This corresponds well to the efficacy produced with GSK314181A in the FCA model investigated here. Animals were assessed 24 hours following the FCA administration, and previous studies document the upregulation of cytokines, including TNF-α, IL-1β, IL-6 and NGF in the inflamed paw 3 hours to 14 days following the FCA injection (Woolf et al. 1997; Raghavendra et al. 2004b). Although not documented in this study, GSK314181A has been shown to inhibit IL-1β release from rat microglia (IC_{50}= 2.1μM) and human THP-1 cells (IC_{50}= 151 nM) (Fonfria et al. 2005) and this prevention of the release of active IL-1β is a likely mechanism by which GSK314181A is producing its antihyperalgesic actions.

Another mechanism by which GSK31418A may be producing its effects is by the prevention of the formation of the P2X7 activated pore. The P2X7 pore is activated following high concentration or prolonged application of ATP, as might be found in a pathological situation (Surprenant et al. 1996). In astrocytes, pore activation may result in the release of neurotransmitters including Glutamate (Duan et al. 2003), possibly contributing to an increase in synaptic strength. Although this was not investigated here, a subsequent study demonstrated that GSK314181A can inhibit YO-PRO and Ethidium bromide uptake, used as measures of pore formation, at IC_{50} values well within the exposures of the compound (IC_{50} values of 980nM at Rat P2X7 (Broom et al. 2008));

IC_{50} value of 288nM at rat P2X7, see Table 4.1 for summary), and previously reported data confirm a high correlation between the potency of compounds at the many ways to record P2X7 receptor activation (YO-PRO, IL-1β release) (Honore et al. 2006; Nelson et al. 2008). Although there have been 2 main mechanisms put forward for pore formation (detailed in Chapter 1, section 1.2.4.2), the data proposing Pannexin-1 as the P2X7-activated pore protein has gained the most credence (Pelegrin and Surprenant 2006; Locovei et al. 2007). There is also evidence that pannexin-1 is required for the activation of caspase-1, the enzyme responsible for the cleavage of pro-IL-1β to its active form (Pelegrin and Surprenant 2006). Therefore the convergence of the activation of the P2X7 pore form and the release of IL-1β provides further rationale for an antinociceptive role of P2X7 receptor antagonists.

4.4.4 Selectivity of GSK314181A

Due to such high circulating concentrations of GSK314181A, the selectivity of the compound at closely related receptors and those that may be important in pain processing must be established. It is clear that although P2X7 receptors play an important role in chronic pain probably through the inflammation associated with the condition (Donnelly-Roberts and Jarvis 2007), other P2X receptors are also likely to contribute. Evidence for a role in pain has been hypothesised for P2X2/3, P2X3 and P2X4 receptors (see Chapter 1; section 1.4.6), and so to enable the interpretation of the animal pain data the selectivity of GSK314181A over these receptors in particular was required.

P2X4 receptors, like P2X7 receptors have been implicated in pain modulation through neuro-glial cell interactions (Tsuda et al. 2003; Zhang et al. 2008). They are the most ubiquitously expressed of all the P2X receptors, found throughout the peripheral and central nervous systems and also on immune cells (North 2002) and it is their overlapping localisation with P2X7, and similar functional effects, that has meant it has been difficult to dissect out their role. The IC_{50} concentration for inhibition of rat P2X4 receptors by GSK314181A was 26 μM, and although around 26000-fold less potent than its activity at rat P2X7 receptors (See Table 1 for summary of potency data), any activity of GSK314181A at other channels known to be involved in pain must be considered. The

recent reports of functional heteromeric P2X4/P2X7 receptors are of further interest as the potency of GSK314181A has not been defined at these heteromeric channels. Often heteromeric channels have pharmacological properties conferred to them from each of the subunit type they possess forming a true mixture of the two channel types. An obvious example of this is seen with P2X2/3 heteromeric channels, where the sensitivity to αβme-ATP and inhibition by TNP-ATP is conferred to the heteromer by P2X3 subunits and the potentiation of currents by low pH and little or no desensitisation to agonist is from the P2X2 subunit (North and Surprenant 2000). Therefore it is difficult to predict whether GSK314181A would inhibit heteromeric P2X4/7 receptors to the same degree as it is effective at P2X7 homomeric receptors. This is unlikely to be able to be elucidated until novel receptor-selective tool P2X4 antagonists are developed.

Table 4.1: Comparison of the potency of GSK314181A at P2X receptors

	P2X7				P2X4		P2X2/3	
	Ca^{2+} uptake	YO-PRO/Ethidium	IL-1β release	WC-PC	WC-PC		WC-PC	
	IC_{50} (nM)	IC_{50} (nM)	IC_{50} (nM)	IC_{50} (nM)	IC_{50} (μM)	x fold *cf* P2X7	IC_{50} (μM)	x fold *cf* P2X7
Rat	29	980 (Fonfria 2005)	2100	1	26	26000	nt	nt
Human	18 (Broom 2008)	288 (Broom 2008)	151 (Fonfria 2005)	5	>10	>2000	5	1000

YOPRO/Ethidium - YOPRO or Ethidium Bromide uptake assay
WC-PC - Whole-Cell patch-clamp; nt - Not tested

GSK314181A was tested at hP2X3 homomeric and hP2X2/3 heteromeric channels and 10 μM was shown to inhibit both subtypes by 60%. The IC_{50} value of 5 μM at hP2X2/3 receptors represents a 1000 fold less potent effect at P2X2/3 receptors compared to the potency at hP2X7 receptors (See Table 4.1 for summary of potency data).

As mentioned above, it is important to consider the concentration of GSK3141781A in the blood and brain of the animals in the model of inflammatory pain when analysing the

efficacy produced by GSK314181A. Although the blood and brain concentrations of 5.5 μM and 2.5μM respectively, are a measure of the concentration present systemically in the blood and in whole brain, but do not give us an actual concentration of the drug at the receptor. This may vary from the reported values due to enzymatic breakdown, uptake into cells or tissues or a reduced access to the site of action. Interestingly, the potency of GSK314181A to inhibit IL-1β release from rat microglia (IC_{50}= 2.1μM) (Fonfria et al. 2005), was a lot lower than reported potency data for other measures of P2X7 receptor activation (IC_{50}= 1nM whole-cell patch-clamp; IC_{50} = 980nM for ethidium bromide inhibition). There are many differences between the assay formats used to measure potency, such as agonist concentration and incubation times, but the higher temperature needed to record IL-1β release was one difference highlighted in (Fonfria et al. 2005). The IL-1β release assay is run at the higher temperature of 37ºC, and this can reduce the potency of GSK314181A. This is illustrated when the ethidium bromide uptake assay is run at this higher temperature a reduction in the IC_{50} to 3.6μM is recorded. Temperature dependent activity of P2X7 receptors have been recorded previously (Chessell et al. 1997; Wiley et al. 1998) and for antagonists such as KN62 and OxATP (Hibell et al. 2001b). This should be considered when trying to correlate the *in vitro* potency of antagonists relative to their exposures *in vivo*. It is also important to note that the values quoted here are 'total' blood and brain concentrations, and although well above the inhibitory effect of GSK314181A at rat P2X7 receptors (1nM), they do not take into account what proportion of GSK314181A is bound by plasma proteins, something that can severely limit the biological efficacy of drugs. GSK314181A has been profiled in a human serum albumin binding assay using High Performance Liquid Chromatography (HPLC) and was found to be 94.5% protein bound. There is often a good correlation of plasma protein binding levels between species and so this data has been extrapolated and applied in the study detailed here. This provides an estimate of the circulating "free" concentrations of GSK314181A in the blood and brain samples of 275nM and 125nM respectively. In Figure 4.8 below, the concentration-response curves for P2X7 (rat and human), P2X4 and P2X2/3 are overlayed with the proposed window of circulating GSK314181A concentration (grey bar), illustrating that although GSK314181A inhibits both P2X4 and P2X2/3 receptors, due to the 'free' concentrations in the blood and brain,

their inhibition may have little role in the reversal of hypersensitivity produced in this inflammatory pain model.

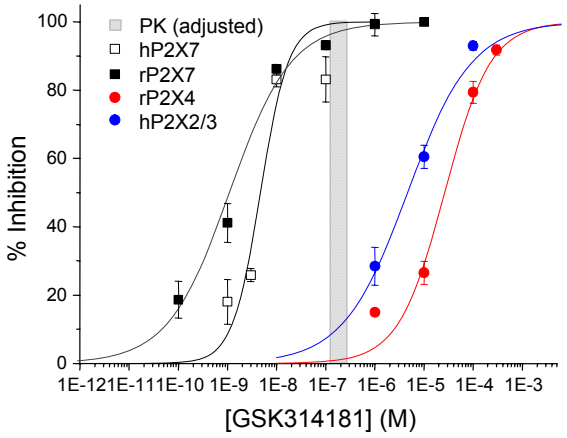

Figure 4.8: Effect of GSK314181A on P2X receptors
Concentration response curve for GSK314181A inhibition at P2X7, P2X4 and P2X2/3 receptors. Grey bar illustrates range of concentrations of GSK314181A found in the blood and brains of rats from the FCA inflammatory pain study, adjusted for protein plasma binding.

Taken together, the present data demonstrate that the acute *in vivo* blockade of P2X7 receptors significantly reduces nociception in animal models of persistent neuropathic and inflammatory pain. Although there is growing appreciation for the role of P2X7 modulation of proinflammatory IL-1β processing (Ferrari et al. 2006), the analgesic activity of A-740003 and other recently described selective P2X7 receptor antagonists (Nelson et al. 2008) suggests a specific role for P2X7 in neuronal-glial cells interactions associated with ongoing pain (Zhang et al. 2007).

Chapter 5: Identification and Characterisation of native P2X7 receptors

5.1. Introduction

Although there is evidence for P2X7 receptor expression on DRG non-neuronal cells (Chessell et al. 2005; Kobayashi et al. 2005; Zhang et al. 2005b), and some functional pharmacological characterisation, the kinetic response to agonist activation was not investigated. Recombinantly expressed P2X7 receptors are widely used to define the biophysics and kinetics of the response to agonist activation of these receptors, and the assumption is made that these properties are also found when the receptors are expressed in native cells. The P2X7 receptor has some interesting properties, such as a non-static response to agonist activation recorded as changes in current amplitude and deactivation rates, as detailed in Chapter 3, which may have important consequences for the physiological and pathophysiological functioning of the receptor. Therefore it is interesting to determine whether these effects are inherent to the receptor function or if they are a property of the expression systems for recombinantly expressed P2X7 receptors.

The dorsal root ganglia (DRG) contain the cell bodies of the fibres that innervate the skin and viscera. Primary cultures of the cells from these ganglia are often used in research because of the ease of which cells can be harvested and prepared, and their importance in the transmission of sensory signal. They are proposed to express the same channels and receptors that are found at the nerve terminals, and so represent an easy way to investigate the function of these native channels or receptors. There is also evidence for a contribution to pain states, as changes in the electrical activity and morphology of DRG neurones have been observed following peripheral insult. For example, changes in sodium channel expression in nerve injury (Rizzo et al. 1995; Cummins and Waxman 1997) and an increase in TRPV1 expression in DRG following a peripheral inflammatory insult (Amaya et al. 2003).

Although the focus of previous studies has been on the neuronal component of DRG, the ganglia itself contains a mixture of non-neuronal cells, including Schwann cells,

fibroblasts, macrophages and endothelial cells, as well as satellite cells (Olsson 1990; Nascimento et al. 2008). More recent evidence has shown that the satellite glial cells that surround neurones in these ganglia may have many important roles in cell communication and can influence neuronal activity through the uptake or release of neurotransmitters, cytokines and growth factors (Hanani 2005 for review; Zhang et al. 2007). As P2X7 receptors may be present on these cells, and have been shown to have a role in the processes detailed above in astrocytes (Ballerini et al. 1996; Duan et al. 2003), it was interesting to compare the functioning of this receptor in native cells, define the cell types they are expressed on, and also hypothesise as to the role these receptors have in normal and pathophysiology.

5.2 Methods Summary

5.2.1 Whole Cell patch Clamp

Experiments were performed using whole-cell patch-clamp electrophysiology to study P2X7 receptors on the non-neuronal cells from acutely dissociated dorsal root ganglia neurones (DRG). The non-neuronal cells from which whole-cell recordings were made were phase-bright, spindle shaped cells (Wilkinson et al. 1999).

5.2.2 Dorsal Root Ganglia dissociation and culturing

Dissociated DRG cells were prepared as detailed in the Material and Methods section (Chapter 2).

5.2.3 Immunocytochemistry (ICC)

ICC was performed as detailed in the Material and Methods section (Chapter 2). Rat DRG cells as prepared for whole-cell patch-clamp electrophysiology were fixed 1-3 days post-plating and ICC was performed within 2 weeks.

5.3 Results

5.3.1 The response of DRG non-neuronal cells to agonist

5.3.1.1 Agonist efficacy

Applications of ATP (100 μM) and BzATP (100 μM) to non-neuronal cells in these cultures produced large non-desensitising inward currents that resembled those recorded from recombinant P2X7 receptors expressed in HEK293 cells (Figure 5.1A). The mean peak current amplitude in response to BzATP (100 μM) was 538 ± 103 pA and the peak current response of the same cell to the same concentration of ATP was 247 ± 64 pA, significantly smaller than the BzATP response (46% of BzATP-activated current peak amplitude, n=8, p=0.001; Figure 5.1B).

5.3.1.2 Current-Voltage Relationship

To investigate the current-voltage relationship of these ATP and BzATP-gated currents, cells were voltage-clamped at -60mV before a voltage ramp protocol from -90 mV to +60mV was applied. A small current, termed non-specific leak current, was produced in control solution (standard extracellular solution), and a linear increase in the current amplitude was produced by the application of BzATP and ATP (Figure 5.1C). Pooled data showed BATP and ATP activated currents that were almost linear and reversed at -5 ± 0.2 mV (n=3) and -5 ± 1 mV (n=9) respectively, as expected for a non-selective cation channel (Figure 5.1D).

5.3.1.3 Agonist Potency

The concentration-response relationship of BzATP on these cells was carried out as previously described. A concentration response curve was generated for BzATP and results in sigmoidal curve with an EC_{50} value of 10 ± 1 μM (n = 3-9, Hill slope = 1.0 ± 0.1; Figure 5.1E). The same was done for ATP producing an EC_{50} value of 534 ± 65 μM (n= 4-6, Hill slope = 1.6; Figure 5.1F).

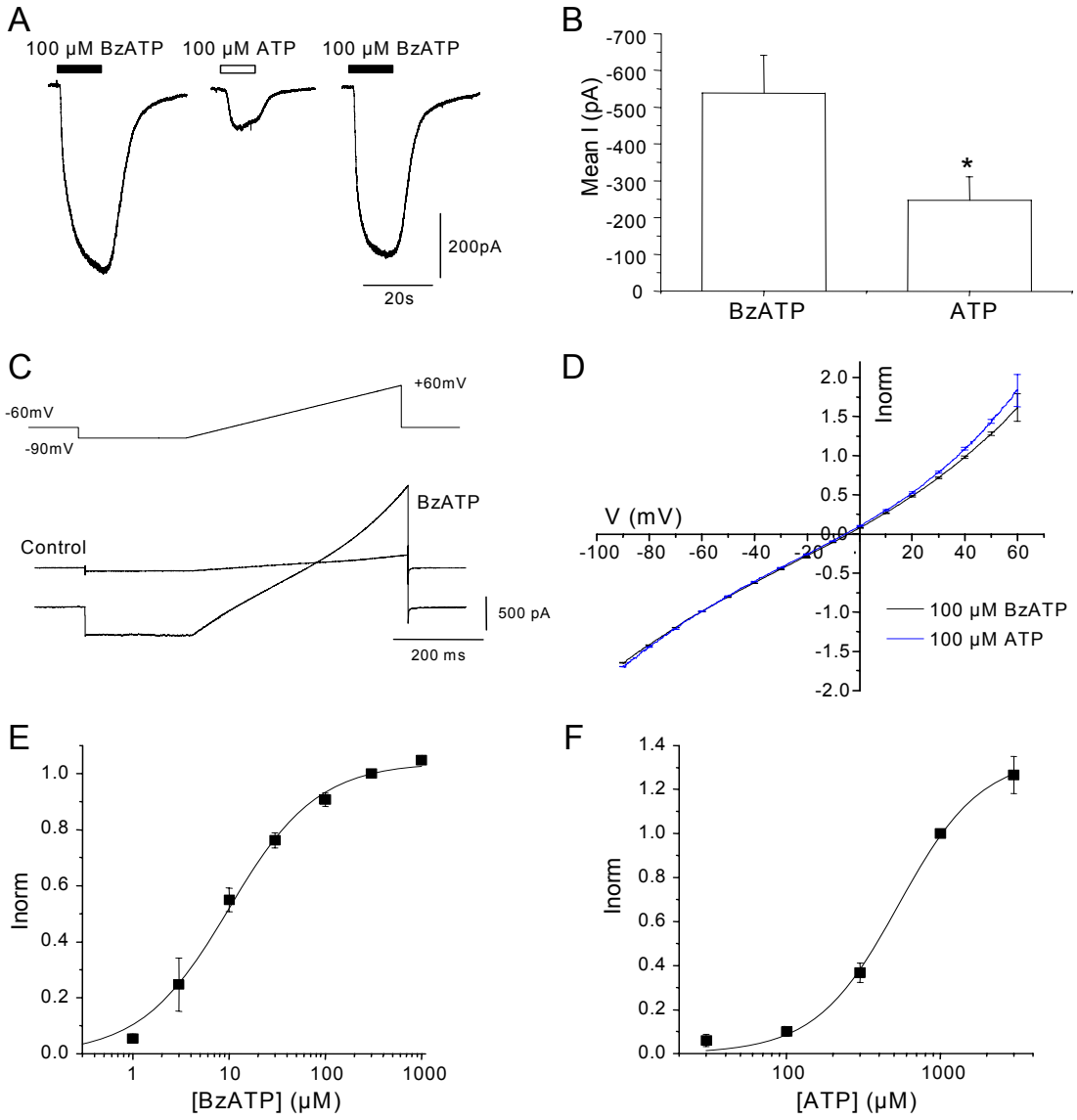

Figure 5.1: Response to agonist in DRG non-neuronal cells
A. Representative currents recorded in response to 10-12 s applications of BzATP (100 µM) and ATP (100 µM).
B. Graph plotting pooled data from experiments in (A) after mean peak current amplitudes were calculated. BzATP (100 µM) mean peak current was significantly larger than the current in response to ATP (100 µM).
C. Representative current trace in control solution and following the addition of 100 µM BzATP during the voltage ramp. The voltage was ramped from -90mV to +60mV over 500ms, every second.
D. Graph plotting pooled data Voltage ramps (-90 mV to +60 mV, 500 ms) applied in the presence of BzATP (30 µM) resulted in linear currents.
E. The graph illustrates the mean concentration response curve to BzATP, EC_{50} value of 10 ± 1 µM (n = 3-9). Data was normalised to 300 µM BzATP application.
F. The graph illustrates the mean concentration response curve to ATP, EC_{50} value of 534 ± 65 µM (n= 4-6). Data was normalised to 1mM ATP application.

5.3.1.4 Multiple applications of Agonist

One of the characteristics of rat P2X7 receptors when they are expressed in HEK293 cells is the changing response to multiple applications of the same concentration of agonist. Here, the first application of BzATP (100 μM) gave peak current amplitudes ranging from 155pA to 806pA, and produced a mean current amplitude of 294 ± 78 pA (n=10). Following further applications of agonist, the peak current amplitude was relatively stable, and was 112 ± 13% of control at the 6th application (n=6; ranging from 90% to 173% of control; see Figure 5.2A).

5.3.1.5 Deactivation

BzATP-activated current deactivation was calculated, as done previously for the recombinant rP2X7 receptor, as the time for the current to return 50% of its maximum (95-50%) and was 211 ± 34 ms (n=8). The rate of slowing of deactivation was found to be dependent upon the individual cell, with the decay time ranging from 221ms to 662ms after 6 BzATP (100μM) applications. When data was pooled and mean values were calculated, the average decay time at the 6th application of BzATP was 400 ± 66ms, (n=7), and was significantly different from the deactivation time of the first application (p=0.02). When comparing this to the data for the rat P2X7-HEK293 cells (see section 3.3.1.4 Deactivation kinetics**)** the values are significantly different for the first application of BzATP (211 ± 34 ms rDRG; 117 ± 7ms rP2X7-HEK, p=0.002). However by the 6th application, no significant difference in the decay times was recorded (400 ± 66ms rDRG; 459 ± 64ms rP2X7-HEK, p=0.7, Figure 5.2B).

The deactivation rate changes are also voltage-dependent. Figure 5.2C shows a representative recording of consecutive response to BzATP (100 μM), normalised to the peak current within each responses. The cell was voltage-clamped at -60mV for the first and third applications of BzATP (sweep 1 and 3) and between these two, was clamped at +60 mV for the second application of agonist (sweep 2). The deactivation rate was significantly slower at +60 mV compared to the rates at -60 mV ($p<0.05$).

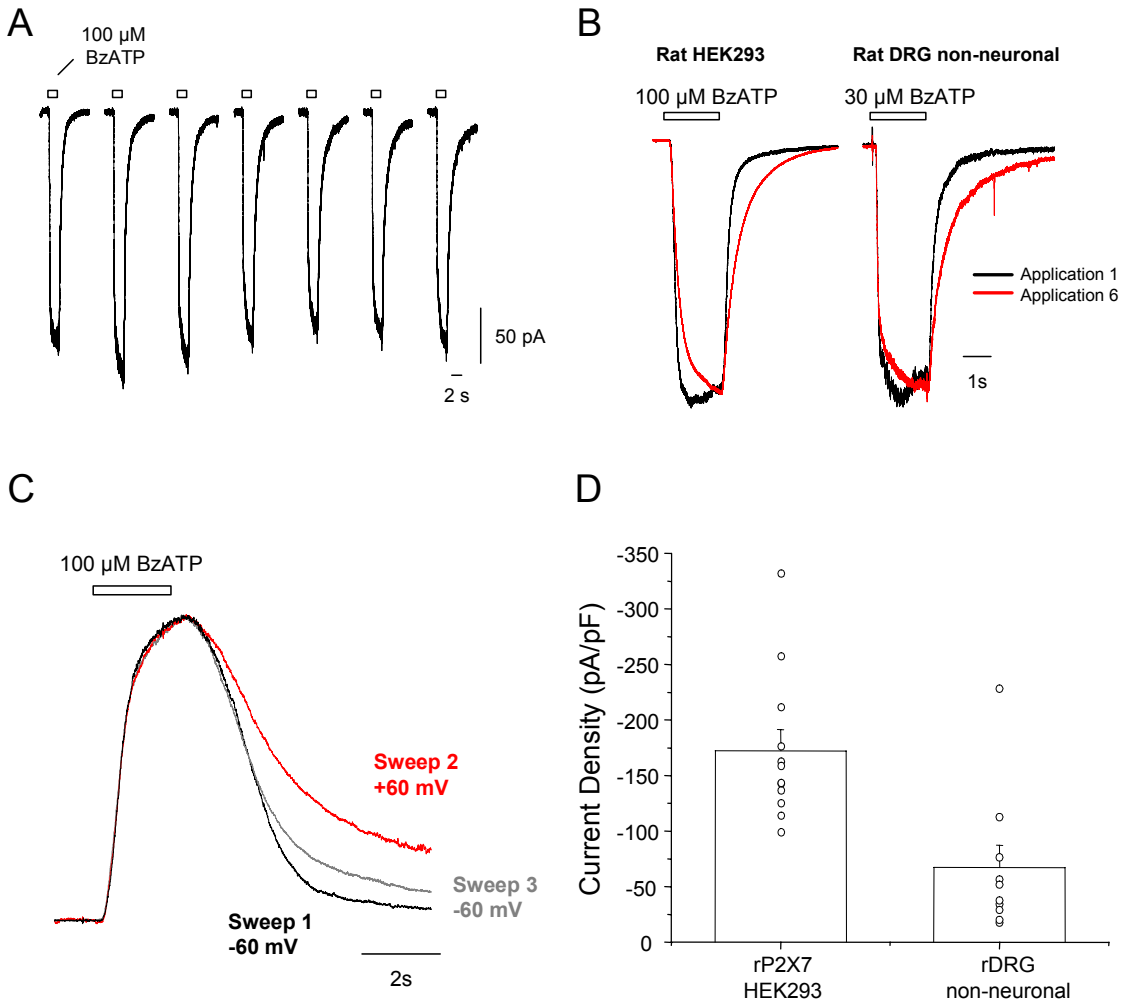

Figure 5.2: Current response of DRG non-neuronal cells to multiple applications of agonist
A. Representative currents recorded in response to 2 s application of BzATP (100 µM). The time between agonist application is 2 minutes. Note the small changes in the peak current amplitude reached following each agonist addition.
B. Representative traces of the first and sixth applications of BzATP overlayed for rat DRG non-neuronal cells and Rat P2X7-HEK293 cells. Currents have been normalised to the peak current. Note the change in the deactivation rate for both cell types.
C. Representative trace showing consecutive responses to BzATP (100 µM), normalised to the peak current within each responses. The cell was voltage clamped at -60mV for sweep 1 and 3 and at +60 mV for sweep 2. Note the slowing of deactivation at +60 mV.
D. Bar graph to illustrate the current density in rat P2X7 expressing HEK293 cells (rP2X7) and rDRG non-neuronal cells (rDRG) in response to the first application of BzATP.

5.3.1.6 Current Density

The current density can be used to give an indication as to the number of functional receptors expressed at the cell membrane. This was measured for DRG non-neuronal cells in response to the first application of BzATP and gave a value of 67 ± 20 pA/pF (n=10). When compared to the data that was recorded from HEK cells stably expressing rat P2X7 receptors, the current density for the recombinant cells was significantly larger (172 ± 19 pA/pF, n=12; p=0.001) possibly indicating a greater number of channels expressed in the recombinant cells compared to the native cells.

5.3.2 Pharmacological evaluation of DRG non-neuronal cells

A novel P2X7 antagonist, GSK314181A, was discussed and its potency defined at rat P2X7 receptors expressed in HEK293 cells in Chapter 4. GSK314181A (100 nM) inhibited BzATP (100 μM)-activated currents by 91 ± 2 % (n=3) and was fully reversible within 6 minutes (Figure 5.3A). Additional concentrations were tested from 10 nM to 1 μM allowing the production of a concentration-response curve, which yielded an IC_{50} value of 23 ± 2 nM, (Hill slope 2 ± 0.3, n=3-4) (Figure 5.3B). This is a 20 fold decrease in the potency of GSK314181A in comparison to the IC_{50} value (1 ± 0.2 nM, Hill slope 0.7, n=3-7), recorded for recombinantly expressed rat P2X7 receptors (Figure 5.3B).

Zn^{2+} ions have been shown to inhibit rat P2X7 receptors stably expressed in HEK293 cells with an IC_{50} value of 1.9 μM (Chapter 4, Figure 4.1). BzATP-activated currents in DRG non-neuronal cells were rapidly and reversibly inhibited by Zn^{2+} ions (10 μM) by 77 ± 7% (n=4; Figure 5.4A). Concentrations from 1 μM to 100 μM were added and plotted yielding an IC_{50} value of 1.4 ± 0.2 μM, (Hill slope 0.8 ± 0.1, n=3-5) (Figure 5.4B).

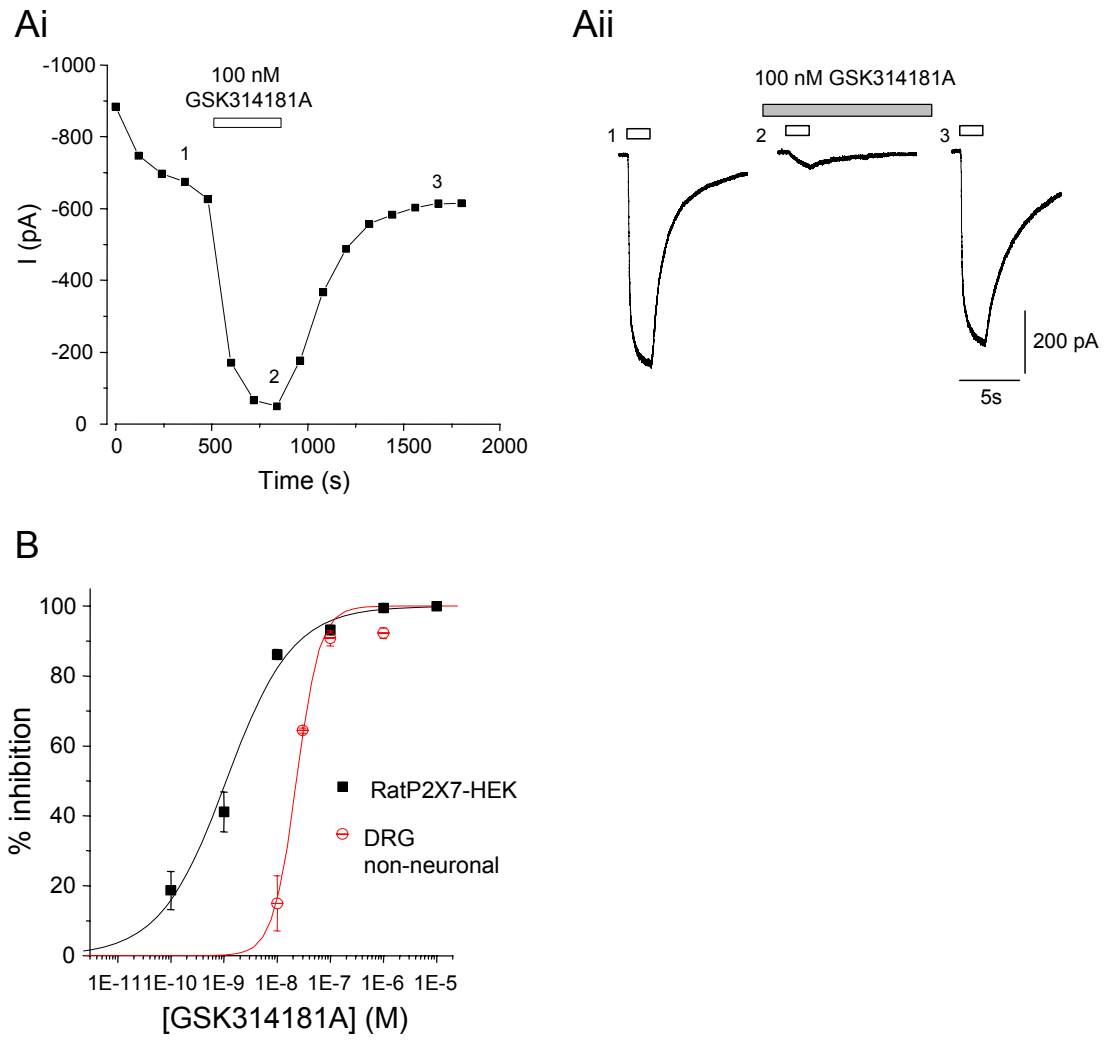

Figure 5.3: GSK314181A inhibits BzATP-activated currents in DRG non-neuronal cells
A. Ai: Graph plotting the time-course data for the effect of GSK314181A (100nM) on BzATP-activated currents. Black squares denote the peak current in response to a BzATP (100 μM) application. The white bar indicates where GSK314181A was applied. In Aii, example traces from Ai are shown.
B. Concentration response curve for GSK31418A at DRG non-neuronal cells in red, compared to the data produced for GSK314181A at rP2X7 stably expressed in HEK293 cells (see Figure 4.2C).

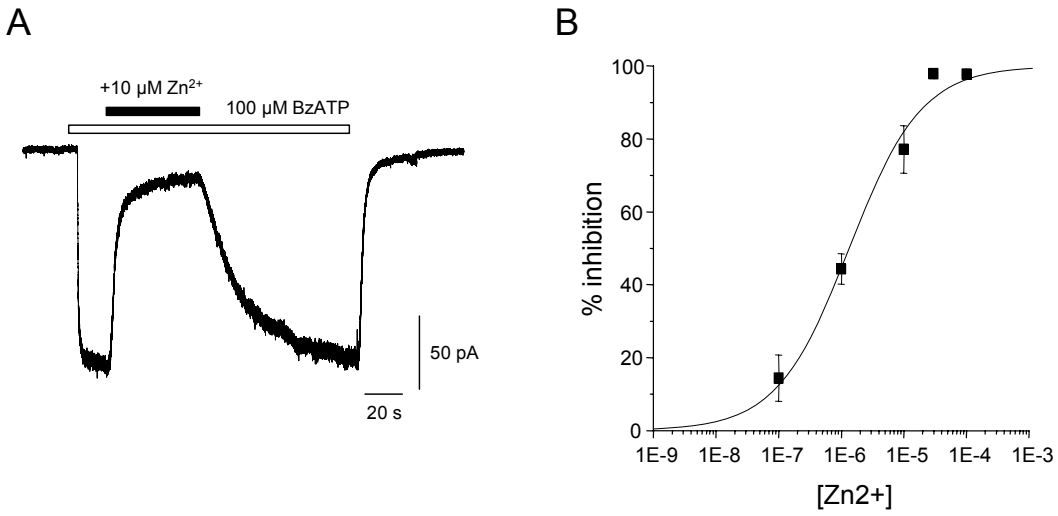

Figure 5.4: Zn^{2+} ions inhibit BzATP-activated currents in DRG non-neuronal cells
A. Representative recording showing the inhibition of the current produced in response to BzATP (100 μM; White bar) with the addition of Zn^{2+} ions (10 μM) into the bathing solution (black bar). This was reversible on return to BzATP alone.
B. Graph plotting pooled data from experiments in (A) after mean peak current amplitudes were calculated.

5.3.3 P2X7 expression in DRG non-neuronal cells

The data above shows that the non-neuronal cells in the DRG cultures have functional P2X7 receptors. The cell types expressing these functional P2X7 receptors were then investigated using immunocytochemistry techniques.

5.3.3.1 Characterisation of a P2X7 monoclonal antibody (MoAb; Buell et al. 1998a)

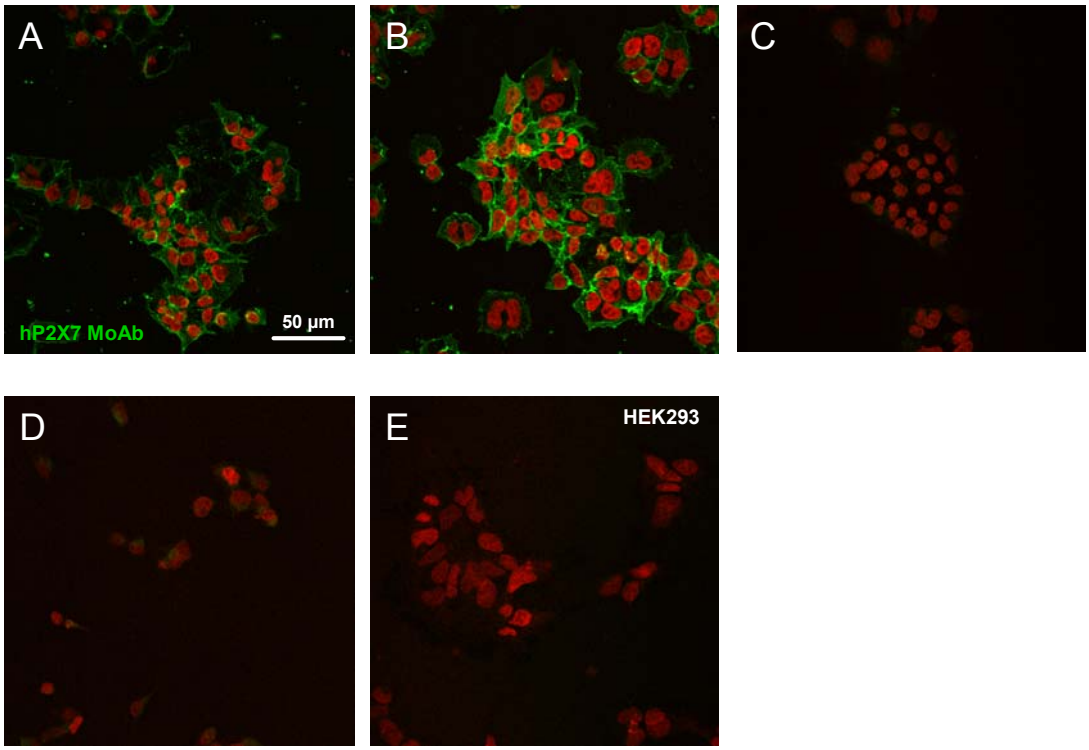

Figure 5.5 Human P2X7 monoclonal antibody labels human P2X7 receptors stably expressed in HEK293 cells.
A,B: Images showing cells labelled with the mouse monoclonal antibody to human P2X7 in green (A, 1:1000; B 1:500 dilution). To-Pro-3 (red) was used (1:1000) as a nuclear label.
C: Example image showing the selectivity of the secondary antibody, Donkey anti-mouse, Alexa-Fluor 488. Nuclei are labelled with To-Pro-3.
D: Example image showing the absence of autofluorescence of the primary antibody, mouse anti-human P2X7 (1:500). Nuclei are labelled with To-Pro-3.
E: Example image showing HEK293 non-transfected cells and the absence of fluorescence with the mouse anti-human P2X7 (1:500) and Alex Fluor 488 (1:200). Nuclei are labelled with To-Pro-3.

5.3.3.1.1 Human and Rat P2X7 Receptors stably expressed in HEK293 cells.

Mouse monoclonal anti-human P2X7 antibody (MoAb) labelled human P2X7 receptors stably expressed in HEK293 cells at a dilution factor or 1:1000 and 1:500 (Figure 5.5A and 5.5B). Rat P2X7 receptors stably expressed in HEK293 cells were also labelled by this antibody, at slightly more concentrated levels of 1:500 and 1:250 dilutions (Figure 5.6A and 5.6B). There was no background fluorescence seen with the primary or the secondary antibody in either cell type (Figures 5.5C, 5.5D, and 5.6C). To confirm the specificity of the fluorescence in these cells to the P2X7 protein, rather than non-specific binding, wild-type, non-transfected HEK293 cells were also tested at 1:500 dilution and showed no immunofluorescence (Figure 5.5E).

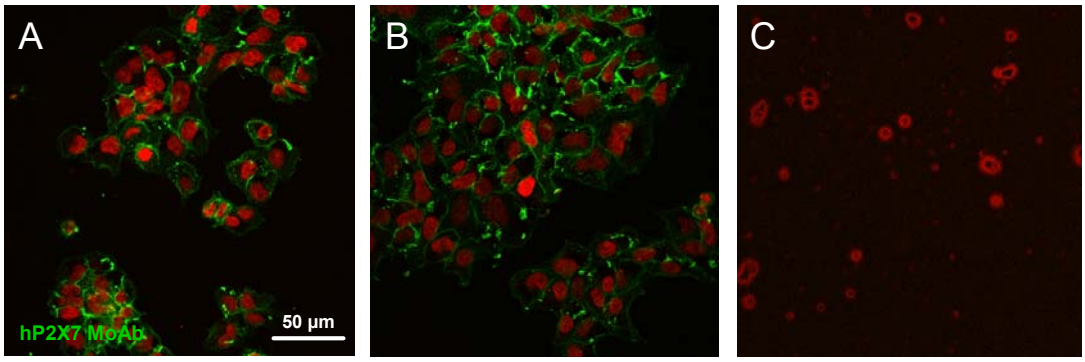

Figure 5.6 Human P2X7 monoclonal antibody labels rat P2X7 receptors stably expressed in HEK293 cells.
A,B: Images showing cells labelled with the mouse monoclonal antibody to human P2X7 in green (A, 1:500; B 1:250 dilution). To-Pro-3 (red) was used (1:1000) as a nuclear label.
C: Example image showing the selectivity of the secondary antibody, Donkey anti-mouse, Alexa-Fluor 488. Nuclei are labelled with To-Pro-3.

5.3.3.1.2 Other P2X receptors

The sequence homology between P2X7 and other P2X receptors ranges from 40-50%, with P2X4 sharing the most similarity. Due to the overlapping nature of P2X4 and P2X7 expression it was considered important to assess the potential interaction of the antibody with P2X4. Other P2X receptors of interest are the P2X3, P2X2 and P2X2/3 heteromer, as these are found both on non-neuronal and neuronal cells. As neurones are also present in these cultures a cross-reactivity of P2X2, P2X3 and P2X2/3 was considered.

HEK293 cells stably expressing human P2X4 or rat P2X4 were incubated with the anti-human P2X7 antibody (1:250 dilution) and then the secondary antibody (Alex Fluor 488) (Figure 5.7Ai,Bi) with no specific labelling visible. This was further confirmed with the control experiment in Figure 5.7 Aii and Bii, where only the secondary antibody was applied.

CHO cells stably expressing human P2X2 and human P2X3 were incubated with the anti-human P2X7 antibody (1:250 dilution) and then the secondary antibody (Alex Fluor 488) (Figure 5.7Ci). As can be seen from the control, only secondary incubated, (Figure 5.7Cii), the green labelling is non-specific and quite different in morphology to the positive immunofluorescence, thought to be P2X7 protein, seen in Figures 5.5 and 5.6.

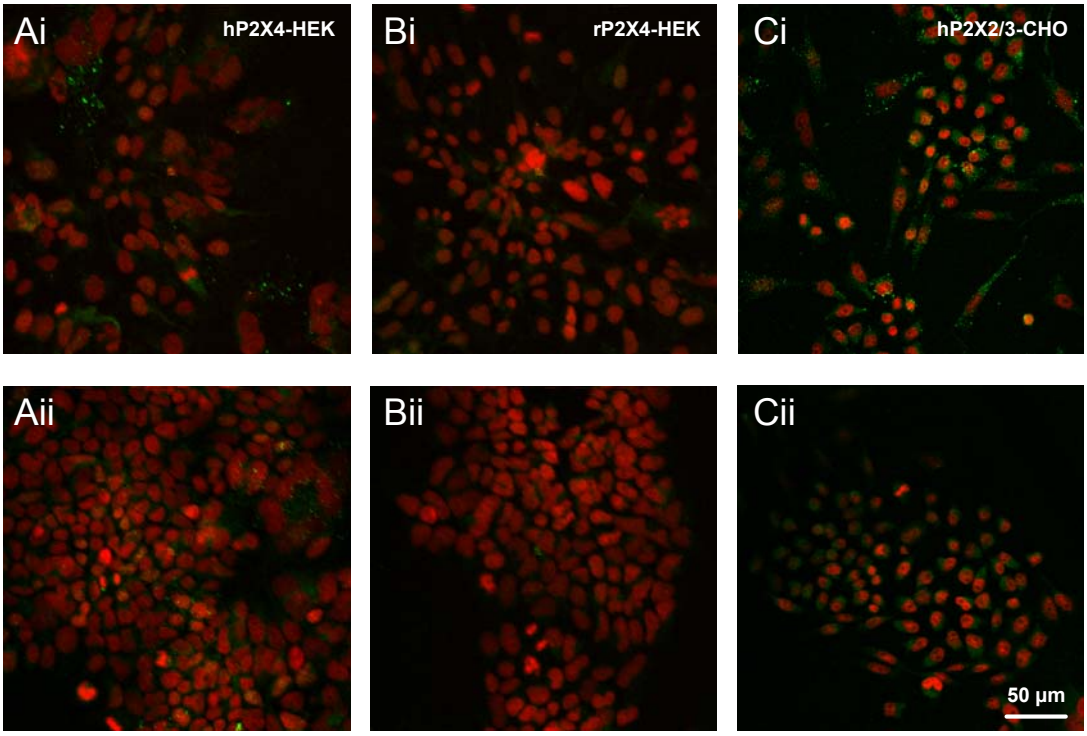

Figure 5.7 Selectivity of hP2X7 monoclonal antibody over other P2X receptors
A,B: HEK293 cells stably expressing Human P2X4 receptors (A) or Rat P2X4 receptors (B), incubated with hP2X7 monoclonal antibody (1:250, Ai, Bi) and Donkey anti-mouse conjugated to Alexa Fluor 488 (green) , or only secondary antibody incubation (Aii, Bii). Nuclei are labelled with To-Pro-3 (red).
C: CHO-K1 cells stably expressing Human P2X2 and Human P2X3 receptors, incubated with hP2X7 monoclonal antibody (1:250, Ci) and Donkey anti-mouse conjugated to Alexa Fluor 488 (green), or only secondary antibody incubation (Cii).

5.3.3.2 P2X7 labelling in rat DRG cultures

The anti-human P2X7 antibody was then use to label P2X7 subunits present in the rat DRG cultures that had been used for the electrophysiological experiments previously detailed in this chapter. The spindle-shaped cells in these rat DRG cultures had positive immunofluorescence at 1:500 (Figure 5.8B) and more clearly at 1:250 (Figure 5.8C) dilution of the antibody. This was well above any non-specific background fluorescence seen following incubation with either only the secondary antibody (Figure 5.8D), or only the primary antibody (Figure 5.8E). However, as can be seen in Figure 5.8C, there is also distinct labelling of round structures that are around 15-20µm in diameter and look more neuronal in morphology (labelled with * on this figure). This is also highlighted in Figure 5.8F where a number of more neuronal-like cells have been labelled (*).

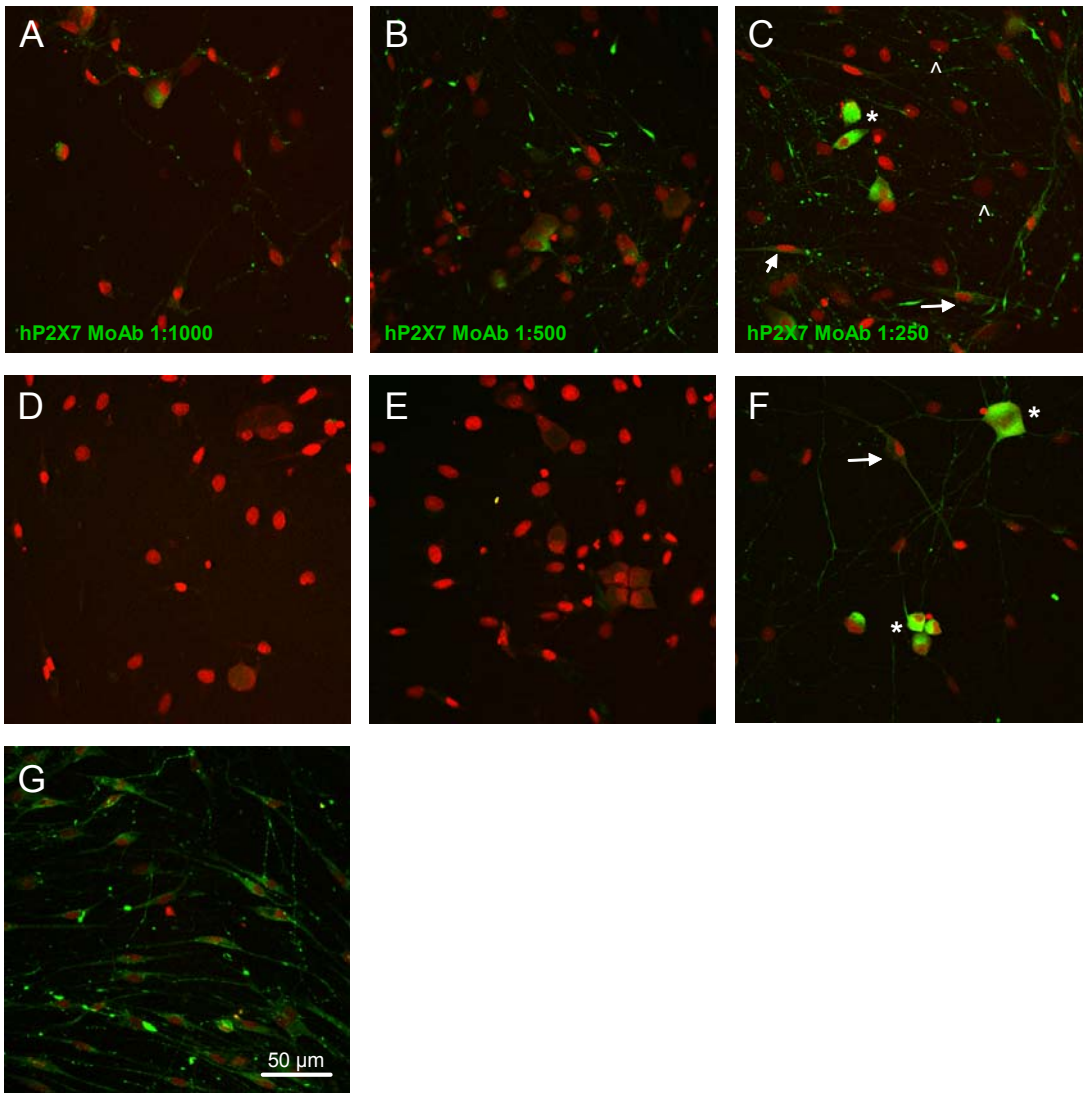

Figure 5.8 P2X7 localization in rat DRG cultures
A,B,C,G: rat DRG cultures with P2X7 receptor labelling using hP2X7 monoclonal antibody (Dilutions factors of A,1:1000, B,1:500, C, G, 1:250) and Donkey anti-mouse conjugated to Alexa Fluor 488. Examples of non-neuronal cell labelling are marked with →. Unlabelled cells are marked with >.
D: Example image showing the selectivity of the secondary antibody, Donkey anti-mouse, Alexa-Fluor 488.
E: Example image showing the absence of autofluorescence of the primary antibody, mouse anti-human P2X7 (1:250). Nuclei are labelled with To-Pro-3.
F: Rat DRG cultures with P2X7 receptor labelling using hP2X7 monoclonal antibody (1:250) and Donkey anti-mouse conjugated to Alexa Fluor 488. Note the labelling of cells with apparent neuronal morphology in these cultures (*).

5.3.3.3 Identification of P2X7 positive cell types

5.3.3.3.1 P2X7 labelling on neuronal cells

In order to confirm that the larger, round cells that had been positive for P2X7 immunofluorescence were indeed neurones, an antibody to β3-tubulin was used. The antibody was characterised using the rat DRG cultures and showed neuronal labelling only in the mixed cell population (Figure 5.9). Co-labelling studies were performed on rat DRG cultures to define the cell population that is brightly labelled by the hP2X7 monoclonal antibody (see Figure 5.8F). P2X7 labelling was co-localised with β3-tubulin on cells with round morphology rather than cells with a spindle shaped structure. There was also evidence of co-labelling of processes but it was unclear as to their origin. The labelling was specific as determined by the lack of non-specific background fluorescence recorded following incubation with only secondary or primary antibodies (Figure 5.10).

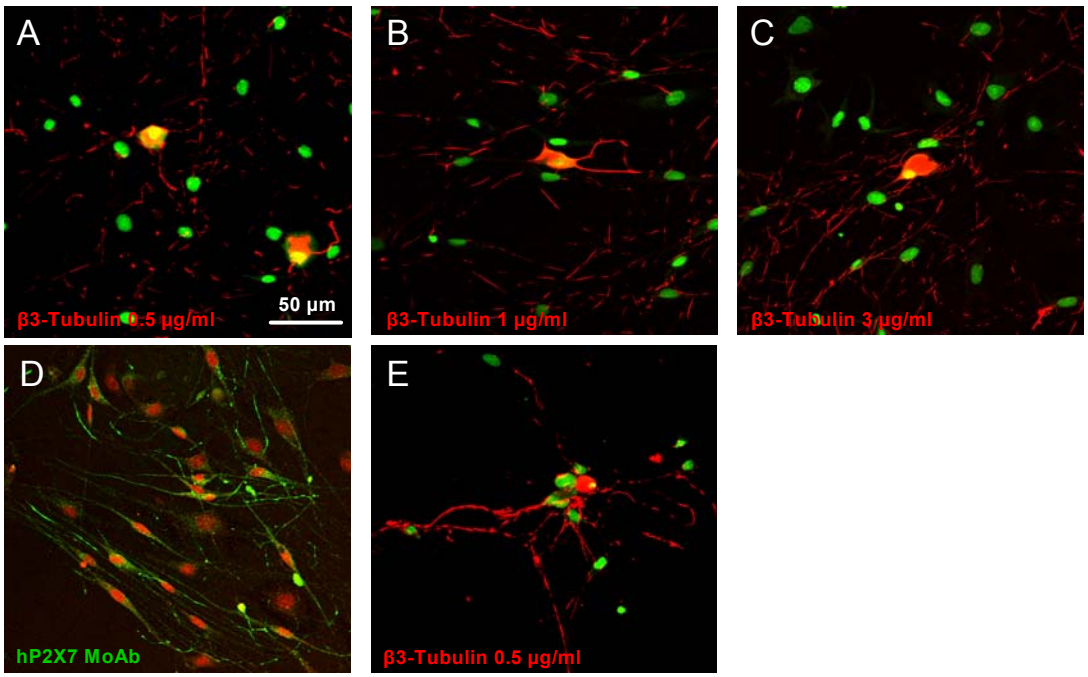

Figure 5.9 β3-Tubulin antibody labels neurones in rDRG cultures
A,B,C: Rat DRG cultures labelling using β3tubulin polyclonal antibody (Dilutions of A: 0.5 µg/ml. B: 1µg/ml. C:3 µg/ml) and Donkey anti-mouse conjugated to Alexa Fluor 647 (Red). Nuclei are labelled with Sytox Green (1:5000, Green). Note the labelling of neuronal cell bodies and processes.
D: Rat DRG cultures with P2X7 receptor labelling using hP2X7 monoclonal antibody (1:250; Green) and Donkey anti-mouse conjugated to Alexa Fluor 488. Nuclei are labelled with To-Pro-3 (1:1000, red).
E: Maximum view of labelled Rat DRG cultures using β3tubulin polyclonal antibody (0.5 µg/ml) and Donkey anti-mouse conjugated to Alexa Fluor 647 (Red). Nuclei are labelled with Sytox Green (1:5000, Green).

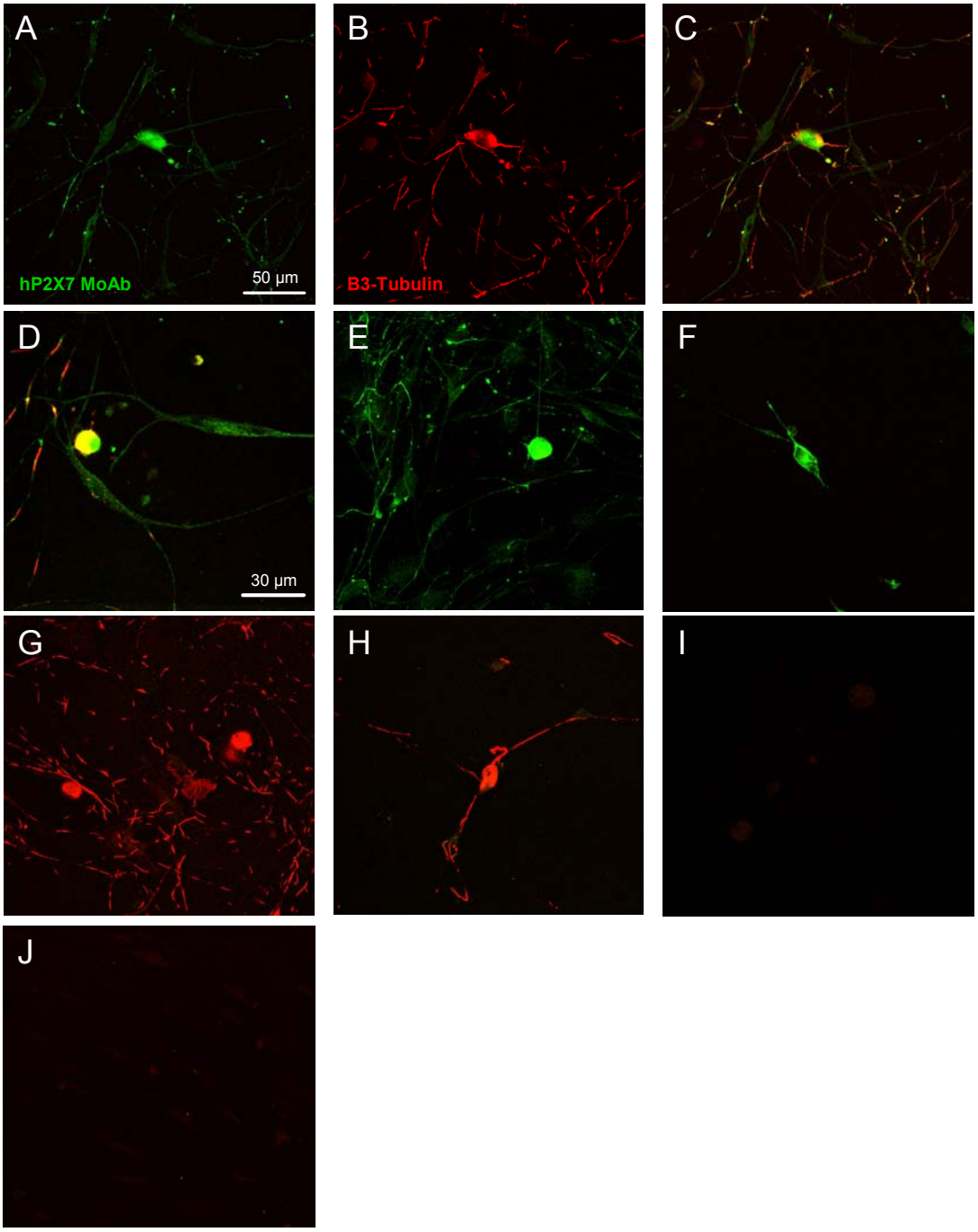
A
hP2X7 MoAb
50 µm
B
B3-Tubulin
C
D
30 µm
E
F
G
H
I
J

Figure 5.10 β3-Tubulin antibody co-localised with P2X7 labelling
AB: Example image showing rat DRG cultured cells with (A) P2X7 receptor labelling using hP2X7 monoclonal antibody (1:250) and Donkey anti-mouse conjugated to Alexa Fluor 488 (green). (B) β3tubulin labelling using β3tubulin rabbit polyclonal antibody (0.5 μg/ml) and Donkey anti-rabbit conjugated to Alexa Fluor 647 (red).
C: Merged image of (A) and (B) showing double immunofluorescence with a hP2X7 positive cell also labelled with β3tubulin, indicating neuronal cell type.
D: Example image of rat DRG cultured cells showing double immunofluoresecent labelling of P2X7 receptors using hP2X7 monoclonal antibody (1:250) and Donkey anti-mouse conjugated to Alexa Fluor 488 (green) and β3tubulin using β3tubulin rabbit polyclonal antibody (0.5 μg/ml) and Donkey anti-rabbit conjugated to Alexa Fluor 647 (red). This is using the 63x water immersion lens. Note the overlapping labelling on the neurone and not on the non-neuronal cells.
E: Example image showing the absence of fluorescence of the primary antibody to β3tubulin, when applied to P2X7 labelled cells (1:250).
F: Example image showing the absence of fluorescence of the secondary antibody used to label β3tubulin (Alexa Fluor 647), when applied to P2X7 labelled cells (1:250).
G: Example image showing the absence of fluorescence of the primary antibody to hP2X7, when applied to β3tubulin labelled cells (0.5 μg/ml).
H: Example image showing the absence of fluorescence of the secondary antibody used to label hP2X7 (Alexa Fluor 488), when applied to β3tubulin labelled cells (0.5 μg/ml).
I: Example image showing the selectivity of the primary antibodies, hP2X7 β3tubulin.
J: Example image showing the selectivity of the secondary antibodies, Donkey anti-mouse, Alexa-Fluor 488, and Donkey anti-rabbit Alexa Fluor 647.

5.3.3.3.2 P2X7 co-localisation with astrocytic markers

P2X7 expression was identified on cells of non-neuronal origin but the exact nature of these cells is not known, therefore co-localisation studies were done to try to define the cell type.

S100beta (S100β) is a member of the S100 family of proteins containing 2 EF-hand calcium binding motifs, localised to the cytoplasm and/or nucleus of a wide range of neurones and non-neuronal cells (Zimmer and Van Eldik 1987; Sugimura et al. 1989; Vega et al. 1991). The proteins are involved in the regulation of a number of cellular processes such as cell cycle progression and differentiation (Zimmer et al. 1995). In these cultures of DRG, S100β labels two types of non-neuronal cells, the elongated spindle-shaped cells most clearly (→), but also more diffuse labelling is seen in cells marked with (⊣) (Figure 5.11A-C). This is highlighted at higher magnification in Figure 5.11E. No labelling was seen in any cells following incubation with the secondary antibody only (Figure 5.11D). DRG cultures were then incubated with anti-S100β antibody and anti-

hP2X7 antibodies and co-immunofluorescence was seen in many cells (Figure 5.12A-C). Relevant controls were performed to show the lack of an effect of the co-addition of the S100β to hP2X7 labelling and vice versa (Figures 5.12D-F), and no non-specific labelling was observed.

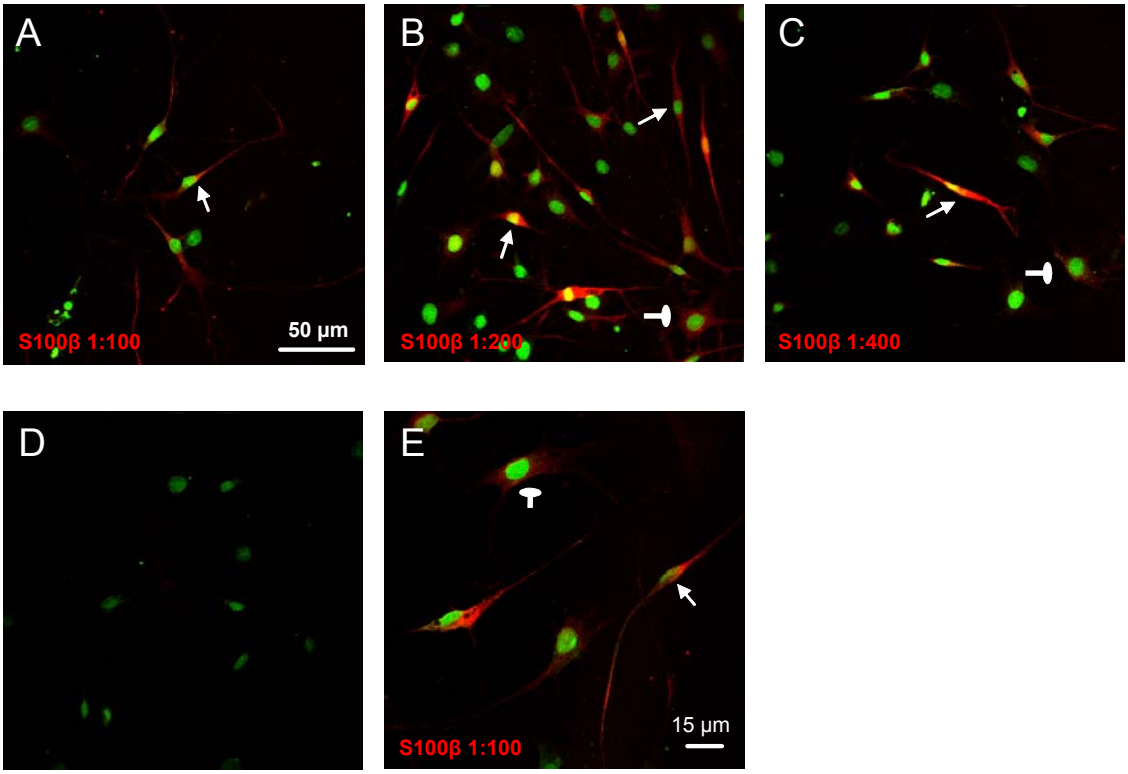

Figure 5.11 S100β labels a subset of non-neuronal cells in DRG cultures
A,B,C: rat DRG cultures labelled with anti-S100beta (Dilutions factors of A,1:100, B,1:200, C,1:400) and Donkey anti-rabbit conjugated to Alexa Fluor 647 in red. Nuclei are labelled with Sytox Green.D: Example image showing the selectivity of the secondary antibody, Donkey anti-rabbit, Alexa-Fluor 647.E: Example image showing the S100beta labelling (1:100 dilution) using a water immersion 63x lens. Nuclei are labelled with Sytox Green.Note the 2 different cells types labelled by S100beta. Spindle shaped cells marked with →, and more diffusely labelled cells marked with ⊣.

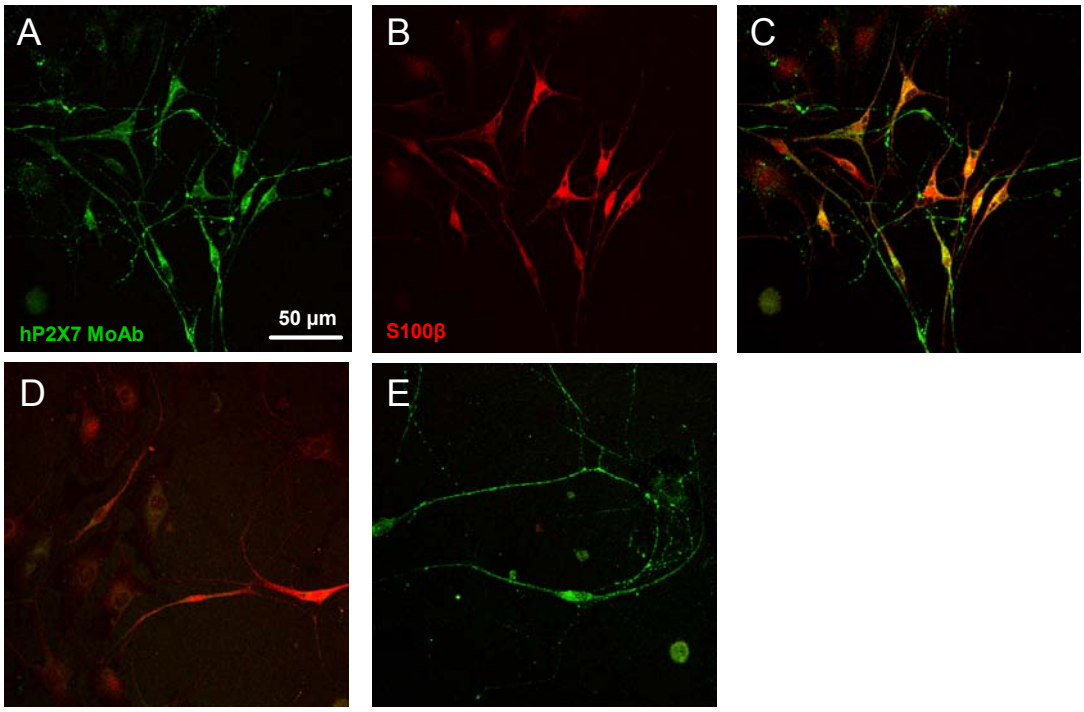

Figure 5.12 S100β co-localised with P2X7 in DRG cultures
A,B: Example image showing rat DRG cultured cells with (A) P2X7 receptor labelling using hP2X7 monoclonal antibody (1:250) and Donkey anti-mouse conjugated to Alexa Fluor 488 in green. (B) S100beta labelling using S100beta rabbit monoclonal antibody (1:400) in red and Donkey anti-rabbit conjugated to Alexa Fluor 647 in red.
C: Merged image of (A) and (B) showing double immunofluorescence with many S100beta positive cells also showing P2X7 labelling.
D: Example image showing rat DRG cultured cells labelled with S100beta rabbit monoclonal antibody (1:400) and both donkey anti-rabbit conjugated to Alexa Fluor 647, and donkey anti-mouse conjugated to Alexa Fluor 488.
E: Example image showing rat DRG cultured cells labelled with hP2X7 mouse monoclonal antibody (1:250) and both donkey anti-rabbit conjugated to Alexa Fluor 647, and donkey anti-mouse conjugated to Alexa Fluor 488.

The antibody to Glutamine Synthetase labelled most of the cells in the DRG cultures (Figure 5.13A,B), with no labelling was observed in any cells following incubation with the secondary antibody only (Figure 5.13C). Cell were then incubated with Anti-glutamine synthetase antibody and anti-hP2X7 antibodies and co-immunofluorescence was seen in all spindle-shaped cells (Figure 5.13D-G). Relevant controls were performed to show the lack of an effect of the co-addition of the glutamine synthetase to hP2X7 labelling and vice versa (Figures 5.13H), and no non-specific fluorescence was observed.

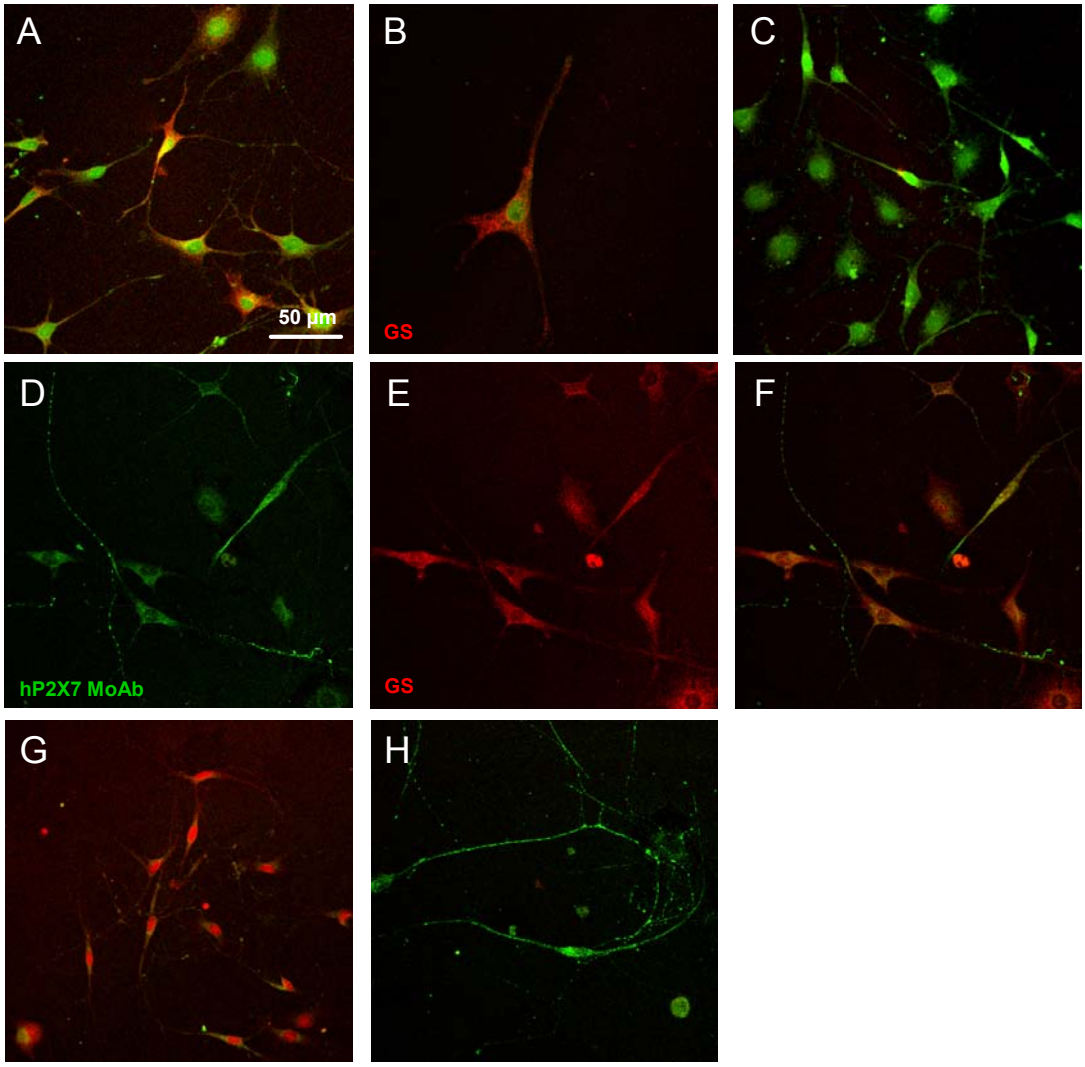

Figure 5.13 Glutamine Synthetase is co-localised with P2X7 in DRG cultures
A: Example image showing rat DRG cultured cells labelled with Glutamine snythetase polyclonal antibody 1:2000) in red and Donkey anti-rabbit conjugated to Alexa Fluor 647. Nuclei are labelled with Sytox green. B: Example image showing the Glutamine Synthetase labelling (1:2000 dilution) using a water immersion 63x lens.
C: Example image showing the selectivity of the secondary antibody, Donkey anti-rabbit, Alexa-Fluor 647. Nuclei are labelled with Sytox Green.
D,E: Example image showing rat DRG cultured cells with (D) P2X7 receptor labelling using hP2X7 monoclonal antibody (1:250) and Donkey anti-mouse conjugated to Alexa Fluor 488 in green. (E) Glutamine Synthetase labelling using Glutamine synthetase rabbit polyclonal antibody (1:2000) and Donkey anti-rabbit conjugated to Alexa Fluor 647 in red.
F: Merged image of (D) and (E) showing double immunofluorescence with Glutamine synthetase positive cells also showing P2X7 labelling.
G: Example image showing rat DRG cultured cells labelled with Glutamine synthetase rabbit polyclonal antibody (1:2000) and both donkey anti-rabbit conjugated to Alexa Fluor 647, and donkey anti-mouse conjugated to Alexa Fluor 488.
H: Example image showing rat DRG cultured cells labelled with hP2X7 mouse monoclonal antibody (1:250) and both donkey anti-rabbit conjugated to Alexa Fluor 647, and donkey anti-mouse conjugated to Alexa Fluor 488.

5.4 Discussion

In this study the satellite and Schwann cells present in DRG primary cultures were shown to express functional P2X7 receptors by pharmacological, biophysical and immunofluorescence techniques. Native P2X7 receptor expressed on DRG non-neuronal cells were shown to have many of the properties of recombinant P2X7 receptors that have been detailed in Chapter 3, in regards to the response to agonist activation and pharmacology. However a number of the characteristics present in the recombinant receptor may be a consequence of the expression system as they are absent from native cells expressing P2X7.

5.4.1 Defining P2X7 receptor expression on non-neuronal cells in DRG cultures

The data reported here show that the non-neuronal cells from DRG cultures possess functional P2X7 receptors. However a number of measures were needed in order to confirm this, due to the co-localisation and overlapping pharmacology and biophysical profiles of P2X7 receptors with P2Y receptors (Lyons et al. 1994; Kobayashi et al. 2006), and other P2X receptors, including P2X2 (Vulchanova et al. 1997), P2X4 (Irnich et al. 2001) and P2X6 possibly as heteromeric receptors with P2X2 and P2X4 (Kobayashi et al. 2005).

Firstly, all of the non-neuronal cells that were recorded responded to BzATP (100 μM), an agonist at P2X2, P2X4 receptors, as well as at P2X7 receptors (Bianchi et al. 1999), with inward currents. These currents activated quickly and showed little desensitisation in the presence of the agonist, exhibiting many of the hallmarks of P2X receptor activation (North 2002). The currents produced following BzATP addition were greater, in amplitude, compared to those produced by same concentration of ATP (Figure 5.1A,B), and it is this difference in potency that is one of the key features of P2X7 receptor activation (North and Surprenant 2000). It was also important to make this comparison with ATP due to the activity of BzATP at other P2X receptor subtypes (Bianchi et al. 1999). Secondly, the linear current-voltage relationship recorded for both BzATP and ATP activated currents is as expected for P2X7 (Surprenant et al. 1996), and P2X4

receptors (Jones et al. 2000), but rules out any involvement of P2X2 receptors as these channels usually show strong inward rectification (Brake et al. 1994; Evans et al. 1996).

The potency of BzATP and ATP at the receptors in these cells was determined and for BzATP produced values (EC_{50} = 10 μM) in line with previously reported data from recombinantly expressed rat P2X7 receptors (6-10 μM; Surprenant et al. 1996; Hibell et al. 2000), and also from DRG non-neuronal cells (26 μM; Zhang et al. 2005b). It was difficult to determine the maximum current response to ATP, possibly due to a change in affinity at the receptor (discussed in Chapter 3) or due to the activation of other P2X receptors. The EC_{50} value of 534 μM for the effect of ATP was a little higher than that recorded in other studies on the recombinant rat P2X7 receptor (EC50=100μM; Surprenant et al. 1996; EC50=407μM; Hibell et al. 2000). However, it is unlikely that P2X4 receptors were being activated as the proposed EC_{50} values for the effect of ATP at rat P2X4 receptors has been reported as 7-20 μM (Seguela et al. 1996; Soto et al. 1996) so a much greater current response would have been expected at the lower concentrations applied.

The biophysical properties of the currents activated in non-neuronal cells exhibit many of the properties associated with P2X receptors and in particular P2X7 receptors. As mentioned above, they activate rapidly and have little desensitisation throughout the agonist application. They deactivate slowly, and there is some evidence for a slowing of deactivation in some cells (Figure 5.2B), a property of P2X7 receptors that has been extensively detailed in previous studies (Surprenant et al. 1996; Hibell et al. 2001a), and here in Chapter 3.

Finally, pharmacological evaluation of these BzATP-activated currents was conducted. BzATP-activated currents in these cells were blocked by the novel P2X7 antagonist, GSK314181A (Figure 5.3B), and by Zn^{2+} ions (Figure 5.4). GSK314181A is a potent antagonist of BzATP- and ATP-activated recombinant P2X7 receptors (Chapter 4; Figure 4.2C and 4.4C). Although GSK314181A inhibited BzATP-activated currents in the non-neuronal cells, it was around 20-fold less potent compared to its activity at recombinant

rat P2X7 receptors (IC_{50} value of 23 ± 2 nM compared to 1 ± 0.2 nM; see Figure 4.2C). It was unlikely that GSK314181A was acting through inhibition of other P2X receptors, specifically, P2X4 and P2X2/3 receptors (See Chapter 4, Figure 4.6 and 4.7), as it is around 200-400 fold less potent at these subtypes, with IC_{50} >10 μM and = 5μM, respectively. One other difference between the native and recombinant groups was in the Hill slope reported for inhibition with the compound, which were 2 for native cells and nearer to 1 for rP2X7 recombinant cells. The difference in the slope can be seen in Figure 5.3B, and may be indicative of a change in the number of ATP molecules that are needed to be bound the receptor in the recombinant system (lack of positive cooperativity), or could imply that the native cells express a heteromeric receptor that requires the binding of GSK314181A to multiple subunits for inhibition to occur.

Modulation of P2X7 responses have been extensively studied with many ions, including Ca^{2+}, Mg^{2+}, Cu^{2+}, H^{+} and Zn^{2+} ions, all of which inhibit P2X7 currents (Virginio et al. 1997; Acuna-Castillo et al. 2007; Jiang 2008). Zn^{2+} is particularly useful, as it differentiates between P2X receptors, potentiating current through P2X2 and P2X4 receptors with EC_{50} values of 20 μM and 2 μM respectively (Wildman et al. 1998; Wildman et al. 1999). The inhibition of BzATP-activated currents by Zn^{2+} ions in these cells (IC_{50} = 1.4μM), provides further evidence for P2X7 mediated currents, and is also very similar to values reported here for Zn^{2+} inhibition of rat P2X7 recombinant receptors of 1.9 μM (see Chapter 4, Figure 4.1).

Another possible complication of studying P2X7 receptors is the possible existence of P2X4/P2X7 heteromeric receptors in these cells. Although initially P2X7 receptors were believed to only be homo-oligomeric receptors (Torres et al. 1998b), more recent data from Guo and colleagues provided both biochemical and electrophysiological evidence for a P2X4/P2X7 heteromeric receptor (Guo et al. 2007). P2X7 and P2X4 receptors are located on the same chromosome and have the greatest sequence homology of all the P2X subunits (North 2002). Although they have an overlapping distribution in immune cells, epithelial and microglia (Brandle et al. 1998a; Bowler et al. 2003; Ma et al. 2006), their expression on astrocytes is not conclusive. Initial localisation data from juvenile

hippocampus (Kukley et al. 2001) was not backed up by more recent studies only identified P2X4 receptors on microglia in spinal dorsal horn (Tsuda et al. 2003; Zhang et al. 2008). Previous work has highlighted the changes in pharmacology that can occur with heteromerisation of P2X receptors. P2X2/3 heteromeric receptors are a perfect example of this. Pharmacologically they are activated by αβme-ATP and inhibited by TNP-ATP, properties from P2X3 receptor; but potentiated by low pH and show little desensitisation, properties from P2X2 (Evans et al. 1996; Virginio et al. 1998).

The agonist potency data and biophysical and pharmacological data provide solid functional evidence for P2X7 receptors present on the non-neuronal cells in DRG cultures.

Due to the overlapping biophysical properties and pharmacology of P2X receptors, the expression of P2X7 receptors in DRG culture was investigated. A monoclonal antibody to the extracellular loop of the human P2X7 receptor (Buell et al. 1998a), was used. It labelled the hP2X7 stably expressed in HEK293 cells, as also shown in Buell et al, (1998a), with no background labelling in HEK293 wild-type cells, and no non-specific binding following the incubation of the primary antibody or secondary antibody alone (Figures 5.5). The rP2X7 expressing HEK293 cells were also labelled following incubation with the hP2X7 monoclonal antibody at slightly more concentrated antibody levels (1:500; 2µg/ml and 1:250; 4µg/ml; Figure 5.6). This is at odds with a lack of a functional effect on rat and mouse P2X7 currents reported for this antibody at 1 µg/ml (Buell et al. 1998a). One explanation for this discrepancy in the data may be that although the hP2X7 monoclonal antibody binds to the rat P2X7 receptor as shown here, this binding does not affect the receptors ability to function as a non-selective cation channel. As the exact epitope of the antibody is unknown it is difficult to determine where on the extracellular domain of the P2X7 receptor protein it is binding. The binding site for the antibody on the human P2X7 protein may be more involved in the functioning of the channel either through a direct occlusion of the pore or through a conformational change following binding, compared to the other P2X7 orthologues. The extracellular domain of the P2X7 receptor is around 226-280 amino acids (Surprenant et al. 1996; Rassendren et

al. 1997) and so chimera and site-directed mutagenesis work would be required in order to try and ascertain the extracellular amino acids that constitute the epitope for the hP2X7 antibody before further conclusions can be made.

As previously mentioned, there is some evidence for P2X2 and P2X4 expression in these cells and so the selectivity of the hP2X7 monoclonal antibody was tested at these P2X subtypes when they are stably expressed in HEK cells (rat and human P2X4) and CHO cells (P2X2 and P2X3 homomeric and P2X2/3 heteromers). There was some non-specific immunofluoresence recorded for the P2X2/3 expressing cells defined as such from the pattern of green fluorescence that was seen following incubation of the secondary antibody (Alex-Fluor 488) only (Figure 5.7Cii), in the absence of the primary antibody. No specific immunofluoresence was observed in rat or human P2X4 expressing HEK cells, confirming data from Buell et al (Buell et al. 1998a).

P2X7 immunofluoresence was detected in DRG cultured cells in a subset of cells (Figures 5.9C, 5.9F, 5.9G and 5.10D) in all cultures tested at concentrations of antibody of 4μg/ml and above. The labelling was specific as no fluorescence was observed when only primary or secondary antibodies were applied. Previously, P2X7 protein has been detected in non-neuronal cells from rat DRG cultures (Zhang et al. 2005b), and was present in satellite cells surrounding neurones in sections from human DRGs (Chessell et al. 2005). The immunofluoresence recorded in these cultures was variable depending upon the number of non-neuronal cells present following the initial ganglia dissociation and although cultures were fixed within 3 days following dissociation, the fixation and immunocytochemical methods can lead to the loss of cells that have not stuck to the coverslip sufficiently. See Figures 5.9F and 5.10D for comparison. Surprisingly, there was more intense immunofluoresence seen in cells that had the morphology of neurones in these cultures (Figure 5.8F) and this is discussed later.

5.4.2 Differences between recombinant and native P2X7 receptors

There are some studies detailing the electrophysiological characteristics of P2X7 receptors in native cells, although often in the context of defining P2X receptor subtype

expression (Brandle et al. 1998a; Grubb and Evans 1999; Kukley et al. 2001; North 2002; Kobayashi et al. 2005), rather than as a comparison as to their functioning when expressed recombinantly. The P2X7 receptor stably expressed in HEK293 cells has some interesting properties, such as a non-static response to agonist activation recorded as changes in current amplitude and deactivation rates, little of which has been commented on in native cells, and some of which could have important consequences for physiology. Therefore it is interesting to determine whether these effects are inherent to the receptor function or if they are a property of the different expression systems for native and recombinant cells.

The currents recorded in response to BzATP were similar in their kinetics to those recorded from recombinant cells. However there is very little change in the peak current amplitude in response to multiple agonist additions (112 ± 13% of control at the 6^{th} application; Figure 5.2A). A much greater and consistent increase in the current amplitude was recorded in all rP2X7-HEK cells in response to BzATP (335 ± 49% of control at the 6^{th} application; Figure 3.3B). The current growth associated with multiple applications of agonist was initially proposed to be due to pore dilation of the P2X7 channel (Chessell et al. 1997). Therefore, the lack of current growth in these cells may represent an absence of pore formation, as proposed for these cells in Zhang et al, where pore formation was measured using an extracellular NMDG-containing solution (Zhang et al. 2005b). However, a failure to detect current growth with supramaximal agonist applications, and a change in agonist potency following pre-exposure to ATP (Hibell et al. 2000), suggests that a change in agonist affinity may be occurring instead. More recent data suggested that current growth recorded in P2X7 expressing HEK293 cells was thought to underlie a secondary, dilated state of the P2X7 receptor (Yan et al. 2008) through which large organic ions, such as NMDG, may permeate, but which is distinct from entry pathways for YOPRO (Jiang et al. 2005; Yan et al. 2008). Therefore the lack of current growth may also be due to a change in the functioning of the receptor in these cells, where no change to the agonist affinity occurs following multiple P2X7 activation. It has been shown previously that the pathway for YOPRO uptake, Pannexins proteins, are present in glial cells (Lai et al. 2007; Liu et al. 2008a), although the expression in

these cultured cells is currently unknown. Further work in these cells using NMDG containing solutions and measuring ethidium bromide uptake, make prove useful to determine whether these cells form large diameter pores, and whether they are through P2X7 receptor dilation or via activation of Pannexin proteins.

The deactivation of BzATP-activated currents in the non-neuronal cells in these cultures was very similar to that recorded for the rP2X7 receptors stably expressed in HEK293 cells. Deactivation of currents slowed with multiple applications of agonist (6^{th} application of BzATP was significantly different from the deactivation time of the first application; $p=0.002$), and was voltage-dependent. However, there was a difference between these 2 groups as the 95-50% deactivation time of the first agonist application is significantly different to that recorded in the rP2X7-HEK recombinant cells. This difference was unexpected, and may represent a real change in the activation time of the receptor, but is probably of little importance as the deactivation time did slow with each subsequent agonist application in line with data from the recombinantly expressed P2X7 receptor.

There are many possible reasons why differences would be seen between native receptors and those expressed in a recombinant system. Previously differences between expression systems, in both pharmacology and biophysics, have been described previously, for example, $GABA_A$ receptors (Sapp and Yeh 1998) and voltage-gated proton channels (Musset et al. 2008). The most likely reasons for disparity are differences in the receptor expression levels, the interactions with auxiliary subunits and post-translational modification, in the form of phosphorylation, dephosphorylation and glycosylation, all of which occur at P2X7 receptors (Kim et al. 2001a; North 2002; Feng et al. 2005). There were significantly lower receptor expression levels in the native cells than recorded for the recombinant cells, an assumption made from the lower current density measurements, although changes in single channel conductance would also manifest itself in this way. Noise analysis or single channel analysis would be needed to rule this out.

There is much evidence for the requirement for auxiliary subunits for the modification of voltage-gated channels (Arikkath and Campbell 2003; Jerng et al. 2005; Chahine et al. 2005), but this has not been reported for P2X7 receptors. P2X7 does interact with a number of proteins such as those involved in the cytoskeleton of cells, e.g. β-actin, heat shock proteins, phosphatidylinositol 4-kinase and receptor protein tyrosine phosphatase-β (RPTPβ) (Kim et al. 2001a), and is thought to exist in a multimeric complex (Kim et al. 2001b), but this work was completed in HEK293 cells stably expressing rat P2X7 receptors and so may not account for any of the biophysical differences reported here.

5.4.3 Neuronal labelling using anti-hP2X7 antibody

As mentioned above, P2X7 monoclonal antibody also labelled cells with a neuronal morphology in these cultures and to a much greater intensity compared with the non-neuronal cells (Figure 5.8F). The cell type was confirmed as neuronal by co-expression of P2X7 and β3-tubulin (Figure 5.10C) in all neurones viewed in these cultures. β3-tubulin is a protein that, in combination with α-tubulin, forms microtubules. These are hollow tubes involved in cellular movement and in the maintenance and changing of cell morphology (Wade 2007). β3-tubulin is considered a neuron-specific marker, and is found throughout the peripheral and central nervous system (Katsetos et al. 2003), and the lack of non-neuronal distribution of this protein is further highlighted at a higher magnification (63x water immersion lens, Figure 5.10D). The neuronal expression of P2X7 receptors is still subject to some debate (review in Introduction and Chapter 4 discussion). However, in these cells the expression of P2X7 receptors on DRG neurones was particularly unexpected as work using the same antibody on sections of human DRG gave no neuronal labelling (Chessell et al. 2005). Further validation of the antibody would usually be required, with preincubation of it with the epitope, often called exhaustion of the antibody. However as the exact sequence of the epitope is unknown, it is not possible to perform such an experiment. The previous work done using commercially available P2X7 antibodies have highlighted an apparent ‘P2X7-like’ protein that is present in rat brain and astrocytes from 2 different P2X7 knock-out mice, but not in peripheral tissues or microglia (Sim et al. 2004). The epitopes recognised by the antibody are identical to the genuine P2X7 receptor but differ in the sequence that has

been disrupted by genetic manipulation in the Pfizer knockout mouse (Sanchez-Nogueiro et al. 2005). Functional studies in cerebellar granule neurons taken from the Pfizer knockout mouse showed a similar, but not identical, Ca^{2+} uptake response following agonist application (Sanchez-Nogueiro et al. 2005). Unfortunately, the work using the hP2X7 monoclonal antibody detailed here cannot be replicated using cells from WT and knockout mice as the antibody does not label the mouse P2X7 orthologue. These experiments are often used to determine the specificity of antibodies, and would also be of use to determine any other off-target interactions the antibody may have. It remains to be investigated whether this protein is an alternative splicing product of P2X7 or a novel 'P2X7-like' protein, and whether it is also expressed in genetically intact animals. Further work to investigate the neuronal P2X7 expression could focus on whether other neuronal cultures, such as cortical, hippocampal or spinal dorsal horn primary cultures express neuronal P2X7 receptors. Extension of this work could involve assessment of the phenotype of positively labelled DRG neurones with dual staining experiments assessing the expression of chemicals known to be present in subsets of DRG neurones, e.g. the NGF receptor trkA, IB4 binding, Substance P or CGRP.

5.4.4 Non-neuronal cell type expressing P2X7 receptors

Robust labelling of non-neuronal cells was detected in these cultures and matched the morphological identification of cells chosen for electrophysiological experiments. However the culture of cells from DRG will contain a mixture of non-neuronal cells, including Schwann cells, satellite glial cells and fibroblasts, macrophages and endothelial cells (Olsson 1990; Nascimento et al. 2008), and so the exact cell type expressing P2X7 receptors needed to be determined.

S100β is a member of the S100 family of proteins that participate in the regulation of intracellular Ca^{2+} homeostasis (Baimbridge et al. 1992; Barger and Van Eldik 1992). S100β was located in the spindle shaped cells in these cultures and was fully co-localised with P2X7 protein (Figure 5.12C) as previously reported in hippocampal astrocytes (Kukley et al. 2001). From previous data it is known that S100β labels satellite glial cells and Schwann cells (Albuerne et al. 1998; Gonzalez-Martinez et al. 2003), in the

periphery, indicating that the cells co-labelled here are likely to be a mixture of both these cell types. Although S100β proteins have also been found in a few large and intermediate sized neurons (Vega et al. 1991), no neuronal labelling was observed here, possibly due to the pre-plating step (See Methods), that removes many of the large DRG neurones. In an effort to remove the possible contamination of neuronal labelling and to confirm the results, antibodies to glutamine synthetase were also tested in these cultures. Glutamine synthetase is an enzyme that converts ammonia and glutamate to glutamine. Therefore it has an important role in the regulation of the neurotransmitter glutamate. Glutamine synthetase was co-localised with P2X7 in all of the spindle shaped non-neuronal cells and so allowed the identification of satellite glial cells and Schwann cells as those that are expressing P2X7 receptors in these cultures. Previously it is been localised to astrocytes (Norenberg and Martinez-Hernandez 1979) and oligodendrocytes (D'Amelio et al. 1990) in the central nervous system, and in satellite glial cells and Schwann cells in peripheral ganglia (Miller et al. 2002), but importantly not in neurones and so is an ideal tool with which to identify these cells in mixed cell populations such as this DRG preparation.

These two immunocytochemical studies define the expression of P2X7 receptors as localised to satellite and Schwann cells, but do not allow differentiation between these 2 cell types. It is known that in cultures more than 1 day old, satellite cells tend to migrate away from the neurones, and so distinguishing them from Schwann cells is problematic (Hanani 2005). Also, morphologically Schwann cells and satellite cells are very similar when dissociated from DRG ganglia. They have a bipolar, spindle shape morphology and over time will proliferate and begin to align in parallel, forming tracks (Li et al. 1996; Wilkinson et al. 1999) (Figure 5.8G and 5.9D). The overlapping molecular characteristics of these 2 cell types also make the use of markers to distinguish between them difficult (Hanani 2005). In Wilkinson et al, the close anatomical association of satellite cells with primary neurones was utilised in order to get a pure satellite cell primary culture (Wilkinson et al. 1999). This technique could be a way to determine the expression and function of P2X7 receptors in this cell type alone. Another possible way to clarify the expression profile would be to prepare sections from DRG in order to confirm the satellite cell labelling, and also use either an established rat schwann cell line or primary

cultures from sciatic nerve (Brockes et al. 1979) in order to confirm Schwann cell labelling.

5.4.5 Possible roles for P2X7 receptors in these cells

As functional P2X7 receptor expression has been demonstrated in the non-neuronal cells in DRG cultures, and is likely to be on satellite glial cells and possibly Schwann cells, the role of the receptors on these cell types must be investigated further. It is known that satellite cells can influence neuronal activity through the uptake or release of neurotransmitters, cytokines and growth factors (Hanani 2005 for review; Zhang et al. 2007). The activation of P2X7 receptors on satellite cells, from neuronal ATP release, can lead to the release of TNF-α, which can in turn increase the excitability of neurones, through potentiation of P2X3 responses (Zhang et al. 2007). Information from the same group confirmed this interaction between P2X7 and P2X3 receptors, showing that a reduction in P2X7 expression or activity resulted in an upregulation of P2X3 expression., and produced abnormal nociceptive behaviours *in vivo* (Chen et al. 2008). This suggests that neuronal somata have a significant role in inter-cell signalling and satellite cells can influence neuronal activity. It would have been interesting to have assessed the release of cytokines, especially, IL-1β, IL-6 and TNF-α, from the non-neuronal cells in these cultures, following priming and P2X7 receptor activation. The pharmacology of this response could also have been assessed to determine whether it was specific to P2X7 receptors. It would also be interesting to further the work done previously and establish neuronal-glial co-cultures to investigate if activating or inhibiting P2X7 receptors could affect neuronal function. As would further investigation of the full repertoire of P2X7 receptors, including the relevance of slowing of deactivation of P2X7 receptors, pore formation and cytokine release, when expressed in native cells. This could provide an insight into the relevance of these results to the physiological, or more likely, pathophysiological role of P2X7 receptors when expressed in DRG.

Chapter 6: Lamotrigine antagonism of P2X7 – A possible role in pain and epilepsy

6.1. Introduction

Lamotrigine (Lamictal™, Figure 6.1A) is approved for use as an anticonvulsant and is primarily known as an effective broad-spectrum anti-epileptic agent with efficacy in absence seizures and Lennox-Gastaut syndrome (Matsuo 1999; McCabe 2000). The proposed mechanisms of action of Lamotrigine are use-dependent inhibition of voltage-gated sodium channels (Xie et al. 1995), inhibition of calcium channels (Stefani et al. 1996; Wang et al. 1996; Hainsworth et al. 2003) leading to inhibition of pre-synaptic glutamate release (Leach et al. 1986), but whether or not other pharmacological activities contribute to its overall mechanism of action has not been determined unequivocally. Sipatrigine (Figure 6.1B), an effective neuroprotective agent (Leach et al. 1993; Graham et al. 1994; Smith et al. 1997) and chemical analogue of Lamotrigine is known to have a similar pharmacological profile to Lamotrigine; inhibiting voltage-gated Na^+ channels (Xie and Garthwaite 1996; Stefani et al. 1998) and Ca^{2+} channels (McNaughton et al. 1997; McNaughton et al. 2000; Hainsworth et al. 2003).

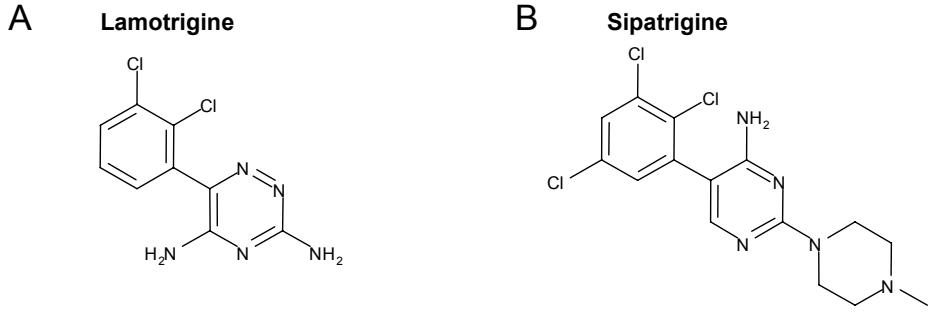

Figure 6.1: Chemical Structure of Lamotrigine and Sipatrigine

Neuropathic pain results from chronic injury to, or disease of, neurons, and often responds poorly to commonly used analgesics and to standard doses of opioid analgesics (Tremont-Lukats et al. 2000). Antiepileptic drugs, including Lamotrigine, are often used "off label" to treat a wide range of neuropathic pain disorders (Zaremba et al. 2006 for

review). The efficacy of a number of antiepileptic drugs in the treatment of pain syndromes suggests common features of their respective pathophysiology.

Given the target validation data implicating IL-1β in neuropathic pain (see Introduction), I investigated whether the upstream trigger for IL-1β release, P2X7 receptor activation, represents a potential target for the action of Lamotrigine. It was also interesting to investigate whether this is an effect specific to Lamotrigine, or a compound class effect that can be recorded across chemical analogues, and specifically for the Lamotrigine analogue and neuroprotective agent Sipatrigine.

6.2. Methods Summary

6.2.1 Whole Cell patch Clamp

Experiments were performed using whole-cell patch-clamp electrophysiology. The following cells were used in this study; P2X7 and P2X4 receptors stably expressed in HEK293 cells, satellite cells from DRG culture expressing P2X7 receptors and P2X2/3 receptors stably expressed in CHO cells. Detailed methods can be found in Chapter 2.

6.2.2 Hippocampal Slice Recordings

Hippocampal slices were prepared as detailed in the Material and Methods section (Chapter 2), and extracellular recordings were obtained following modification of the perfusing solution by either the combined addition of the $GABA_A$ and $GABA_B$ receptor antagonists Bicuculline (10 μM) and CGP55845 (10 μM), or by the removal of extracellular magnesium ions from the perfusing medium.

6.3. Results

6.3.1 Lamotrigine inhibits rat and human P2X7 currents

In this study, the effect of Lamotrigine on P2X7 receptors was evaluated using whole-cell patch clamp technique on HEK293 cells stably transfected with rat or human P2X7 receptors. Lamotrigine was preincubated and co-applied with BzATP and the peak

current response recorded. Lamotrigine (300 μM) inhibited BzATP-activated rP2X7 currents by 82 ± 3% (n=6) and was fully reversible within 2 minutes (see Figure 6.2A). Additional concentrations were tested from 30 μM to 100 μM allowing the production of a concentration-response curve, which yielded an IC_{50} value of 100 ± 9 μM, (Hill slope 1.4 ± 0.2, n=3-6) (Figure 6.2C).

Given the many examples of differences in the potency of ligands acting at rat and human P2X7 receptors (North and Surprenant 2000), the inhibitory effects of Lamotrigine were examined at the human P2X7 receptor stably expressed in HEK293 cells. Lamotrigine (10 μM) inhibited BzATP-activated hP2X7 currents by 57 ± 4% (n=4) and was fully reversible within 2 minutes (see Figure 6.2B). In the example traces, Figure 6.2B, the currents did not fully deactivate over the time scale shown (see the lack of return to baseline), although they did return to the pre-activated level over the 2 minutes between BzATP applications. This has been reported for these currents previously (Klapperstuck et al. 2000a). Additional concentrations were tested from 1 μM to 300 μM allowing the production of a concentration-response curve, which yielded an IC_{50} value of 6.4 ± 0.7 μM, (Hill slope 0.9 ± 0.1, n=4-5) (Figure 6.2C).

Although BzATP is an analogue of ATP, it was thought prudent to confirm that Lamotrigine could inhibit human P2X7 receptors activated by the endogenous ligand, ATP. Human P2X7 receptors were activated by ATP (5mM) and a range of concentrations of Lamotrigine were applied allowing the production of a concentration-response curve which yielded an IC_{50} value of 8 ± 1 μM, (Hill slope of 0.9 ± 0.1, n=4; Figure 6.2D), indicating a similar potency to Lamotrigine's inhibition of BzATP-activated hP2X7 receptors.

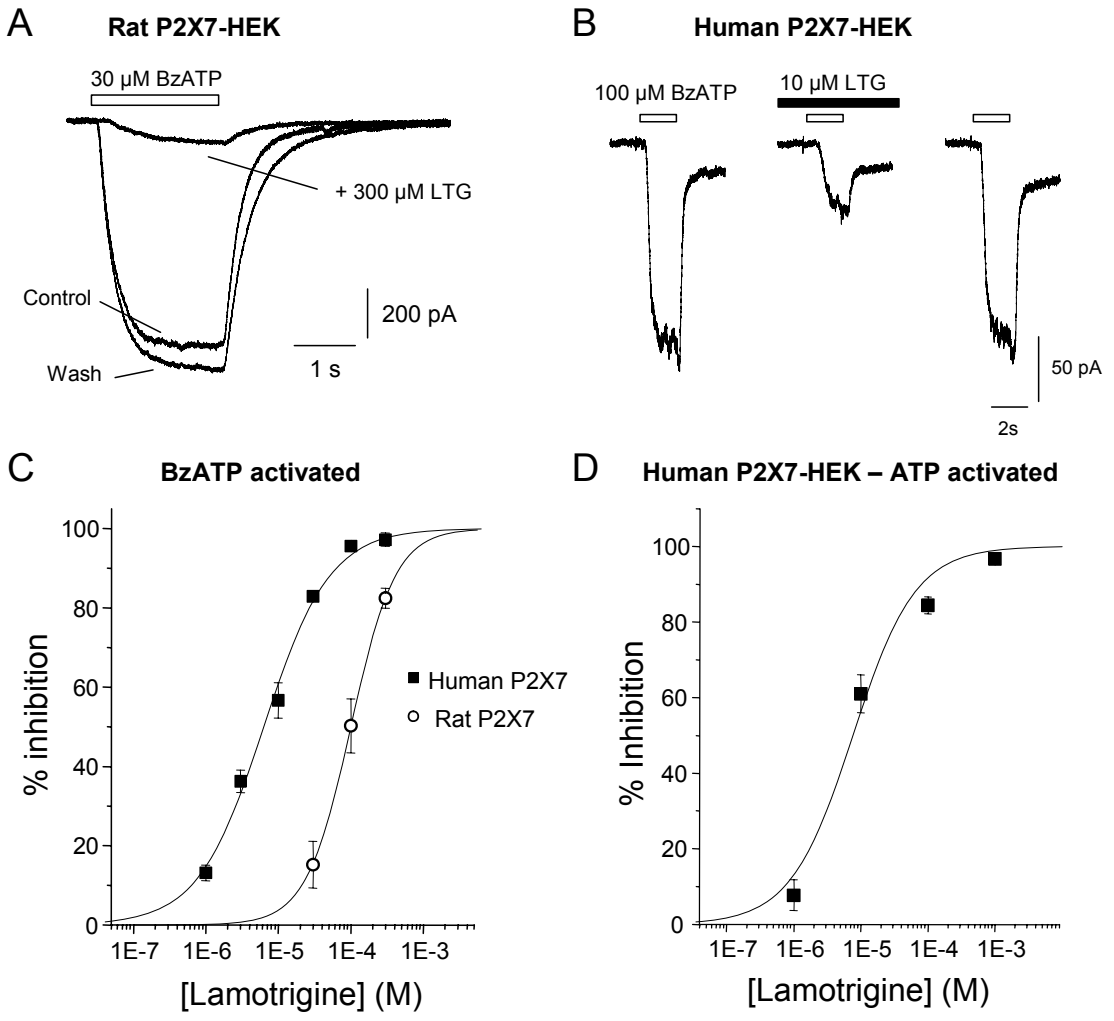

Figure 6.2: Lamotrigine inhibits rat and human P2X7 currents
A. Example recording showing Lamotrigine (LTG, 300 µM) reversibly inhibiting 30 µM BzATP-activated rP2X7 current by 82 ± 3% and the recovery to pre-addition levels in 2 min.
B. Lamotrigine 10 µM inhibits 100 µM BzATP-activated hP2X7 current by 57 ± 4 %, n=4. Inhibition with Lamotrigine peaked within 2 minutes and currents recovered to baseline levels within 4 min.
C. Concentration-response curves for Lamotrigine at rP2X7 and hP2X7 activated by 30 µM BzATP or 100 µM BzATP respectively. Curves were fit to raw data and yielded IC_{50} value of 100 ± 9 µM, Hill slope of (1.4 ± 0.2, n=3-6) for rat P2X7 receptors and IC_{50} value of 6.4 ± 0.7 µM (Hill slope 0.9 ± 0.1, n=4-5) for human P2X7 receptors.
D. Concentration-response curves for LTG at hP2X7 activated by 5 mM ATP. Curve was fit to raw data and yielded IC_{50} value of 8 ± 1 µM, (Hill slope of 0.9 ± 0.1, n=4).

The effect of holding cells at positive potentials on the inhibition with Lamotrigine was assessed at hP2X7 receptors. Lamotrigine inhibited BzATP-activated currents by 59 ± 2% (n=4) when cells were voltage-clamped at +60mV, a value that is not significant different to that recorded at a holding potential of -60mV (57 ± 5 % inhibition, n=4, p=0.64, Figure 6.3A).

In addition, the ability of Lamotrigine to inhibit BzATP-activated hP2X7 current when applied intracellularly was investigated (Figure 6.3B). A high concentration of Lamotrigine (100 μM) was included in the standard whole-cell intracellular solution. In all recordings a robust BzATP-activated current was observed following the first application of BzATP (183 ± 38 pA, n=5). Subsequent applications of BzATP resulted in the normal increase in the current amplitude and no abnormal changes in the kinetics of the responses were observed. In all 4 cells a subsequent extracellular application of 100 μM Lamotrigine produced its signature inhibition of currents to 9 ± 3 % of control, n=5, which was reversible on washout of the drug (Figure 6.3B).

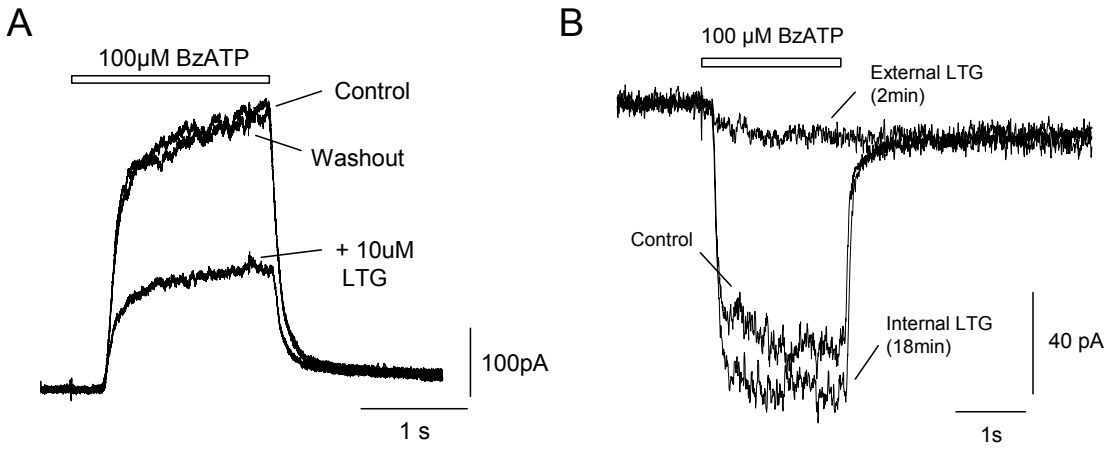

Figure 6.3: Lamotrigine inhibits hP2X7 currents at +60mV and but does not inhibit currents when applied intracellularly.

A. Example traces for the effect of Lamotrigine (10 μM) on BzATP-activated hP2X7 currents while cells were voltage-clamped at +60mV. Lamotrigine was preincubated for 2 minutes before being co-applied with 100μM BzATP and reversibly inhibited peak hP2X7 currents by 59 ± 2% (n=4).

B. Example traces showing the first current response to BzATP (100 μM) recorded with 100 μM Lamotrigine within the recording electrode and then after 18 minutes. The other trace shows the inhibition of the response to 100 μM BzATP in the presence of extracellular application of Lamotrigine (100 μM).

6.3.2 Lamotrigine inhibits native rat P2X7 currents

Confirmation of the inhibitory activity of Lamotrigine was sought at native P2X7 receptors. The satellite cells that surround DRG neurones have been shown to express functional P2X7 receptors and robust currents can be recorded following the addition of BzATP (100μM) (see Chapter 5, Figure 5.1). We confirmed that Lamotrigine could inhibit the native rat P2X7 receptor in non-neuronal dorsal root ganglia cells, with 100 μM Lamotrigine producing 35 ± 6 % (n=6) inhibition of the peak current (Figure 6.4A). Additional concentrations of Lamotrigine were applied allowing the production of a concentration-response curves which yielded an IC_{50} value of 262 ± 50 μM, (Hill slope 0.7 ± 0.1, n=3-6, Figure 6.4B).

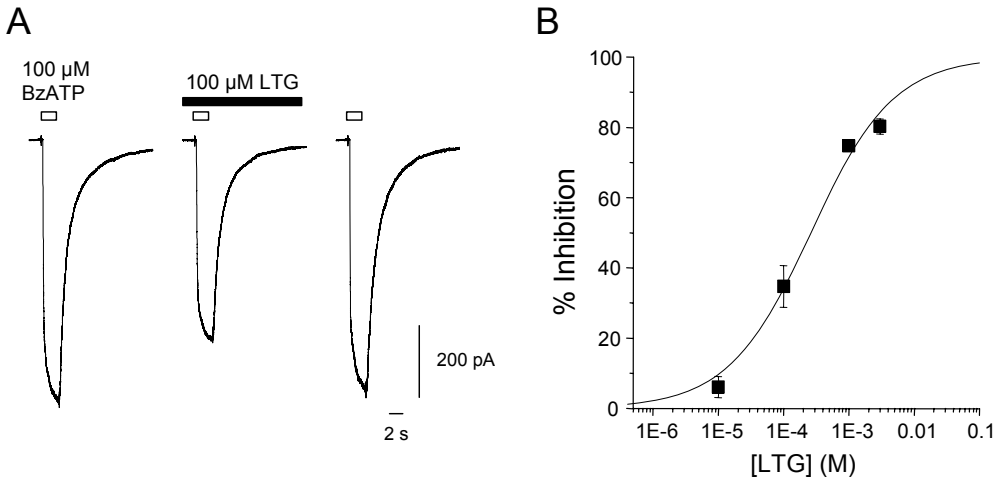

Figure 6.4: Lamotrigine inhibits native rat P2X7 currents
A. Example traces for the effect of Lamotrigine (100 μM) on 100 μM BzATP-activated rat P2X7 current in DRG non-neuronal cells. Lamotrigine (100μM) was preincubated for 2 minutes before being co-applied with 100μM BzATP (Black bar) and reversibly inhibited peak currents by 35 ± 6 % (n=6).
B. Concentration-response curves for Lamotrigine at native rP2X7 activated by 100 μM BzATP. The curve was fit to raw data and yielded IC_{50} value of 262 ± 50 μM, (Hill slope 0.7 ± 0.1, n=3-6).

6.3.3 Investigation of Lamotrigine's activity at closely related P2X receptors

Given the activity of Lamotrigine at P2X7 receptors, it is interesting to assess it's selectivity for P2X7 over the other P2X receptor subtypes. P2X4 receptors are located on the same chromosome as P2X7 and share the most homology out of all P2X receptor subtypes (North 2002; for review). As Lamotrigine was most potent at human P2X7 receptors, recombinant cell lines of stably transfected human P2X4 receptors were used for these selectivity studies. P2X4 receptors were activated by ATP (10μM). Lamotrigine (100 μM) was preincubated for 4 minutes and co-applied and had no significant effect on currents at 100 μM (0.03 ± 1.92 % block, n=4; Figure 6.5A). TNP-ATP (30 μM) was used as a positive control and inhibited currents by 98 ± 1 %, (n=4) (Virginio et al. 1998).

P2X3 and P2X2/3 receptors have been implicated in mediating ATP-related nociception (See Introduction; Burnstock 2006). An inhibitory effect of Lamotrigine on these receptors was considered important to investigate when considering other mechanisms that would account for its analgesic action. Due the previously reported high positive correlation between ligand binding at heteromeric P2X2/3 and homomeric P2X3 receptors (Jarvis et al. 2004), only the effect of Lamotrigine at P2X2/3 receptors was investigated here. Following multiple applications of αβmeATP, the peak current decreased and so the peak current values were baseline gradient adjusted to enable the effects of the compounds to be more accurately analysed (see Chapter 2 - 2.3.4.4 and 2.3.4.6). Using this protocol for analysis, Lamotrigine (100 μM) reversibly inhibited P2X2/3 mediated currents by 14 ± 3 %, n=7 (Figure 6.5B). A greater degree of inhibition of P2X2/3 receptors was confirmed by the use of Compound X, which reversibly inhibited P2X2/3 currents by 84 ± 1% (n=3), (Figure 6.5B).

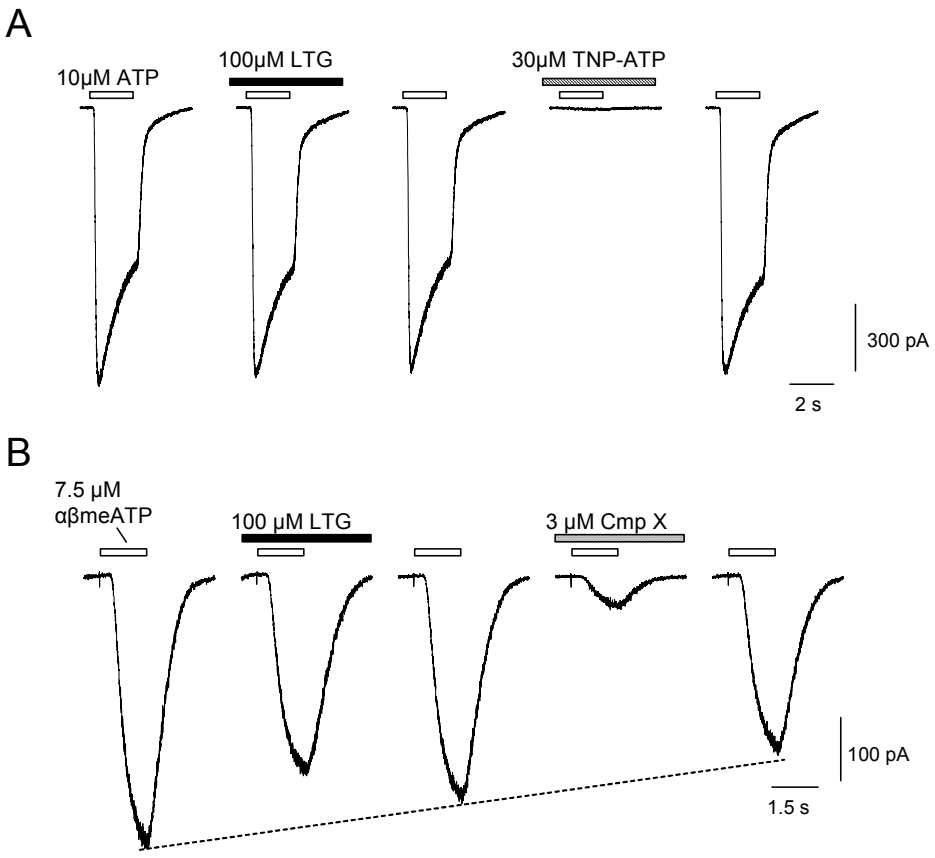

Figure 6.5: Effect of Lamotrigine at P2X4 and P2X2/3 receptors
A. Example traces for the effect of Lamotrigine (100 μM) on 10 μM ATP-activated rat P2X4 currents. Lamotrigine (100μM) had no effect on ATP-activated hP2X4 currents (0.0 ± 1.9% inhibition, n=4), where as TNP-ATP (30 μM) reversibly inhibited currents by 98 ± 1 %, (n=4). B. Example recording showing Lamotrigine (100 μM) inhibits 7.5 μM αβ-meATP-activated hP2X2/3 current by 14 ± 3% (n=7). Clear bars show 7.5 μM αβmeATP application alone and the black bars show the application of 7.5 μM αβmeATP in the presence of Lamotrigine. Compound X (3 μM), a GSK P2X2/3 antagonist, reversibly inhibited currents by 84 ± 1 %, (n=3).

6.3.4 Lamotrigine analogues are P2X7 inhibitors

Although we have shown that Lamotrigine is a potent inhibitor of human P2X7 receptors, it is interesting to establish if an analogue of the compound also has inhibitory actions at P2X7 receptors. Sipatrigine (GV230822) is a chemical derivative of Lamotrigine (Figure 6.1B). Sipatrigine (10 μM) reversibly inhibited BzATP-activated currents in human

P2X7-HEK293, reaching a maximum inhibition of 77 ± 5% (n=4) within 4 minutes (Figure 6.6A). To enable an estimate of the IC_{50} concentration for inhibition of BzATP-activation of hP2X7 by Sipatrigine, additional experiments were conducted from 10 nM to 100 µM. Raw data were fit and yielding an IC_{50} value of 2.6 ± 0.7 µM (Hill slope 0.6 ± 0.1, n=3-6; Figure 6.6B). Also included in Figure 6.6B is the concentration-response curve for Lamotrigine at hP2X7 receptors, due to the closeness of the IC_{50} values for the inhibition of hP2X7 receptors by both of these compounds.

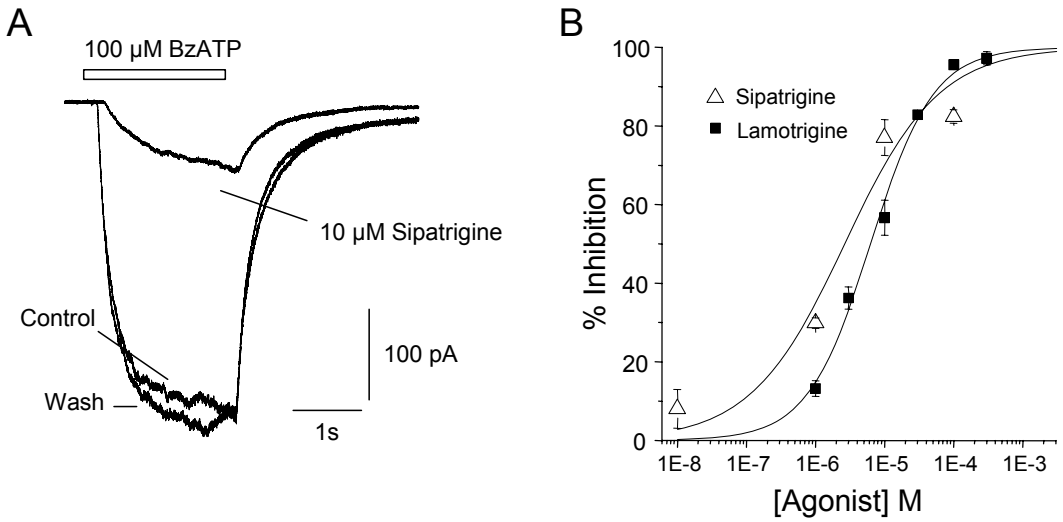

Figure 6.6: Lamotrigine analogue, Sipatrigine, is a P2X7 antagonist
A. Example traces for the effect of Sipatrigine (10 µM) on 100 µM BzATP-activated hP2X7 currents. Sipatrigine (10µM) was preincubated for 2 minutes before being co-applied with 100µM BzATP and reversibly inhibited peak currents by 77 ± 5 % (n=4).
B. Concentration-response curves for Sipatrigine at hP2X7 activated by 100 µM BzATP. Curves were fit to raw data and yielded IC_{50} value of 2.6 ± 0.7 µM (Hill slope 0.6 ± 0.1, n=3-6). Lamotrigine concentration-response curve is also included for comparison.

6.3.5 Role of P2X7 receptors in epileptiform activity

P2X7 receptors have been implicated in epileptogenesis based around their expression and function in astrocytes (Ballerini et al. 1996; Kukley et al. 2001). Therefore, it is interesting to speculate on whether any of Lamotrigine's antiepileptic effects could be via inhibition of P2X7 receptors. To try to establish what effect, if any, P2X7 inhibition

would have on epilepsy, *in vitro* hippocampal slice models of epileptiform activity were used.

6.3.5.1 Compound A inhibits rat P2X7 currents

Compound A was identified from high throughput screening as an inhibitor of P2X7 receptors. It was used instead of GSK314181A to investigate the function of P2X7 receptors in hippocampal epileptiform activity models due to its more attractive *in vivo* pharmacokinetic profile. This would enable the work detailed here to be extended to assess the activity of the compound in animal models of epilepsy.

Confirmation of the potency of compound A at rat P2X7 receptors was sought using whole-cell patch-clamp techniques. Compound A (3 μM) inhibited BzATP-activated rP2X7 currents by 75 ± 6 % (n=3) and was fully reversible within 2 minutes (see Figure 6.7A). Additional concentrations were tested from 100nM to 20 μM allowing the production of a concentration-response curve, which yielded an IC_{50} value of 1.4 ± 0.2 μM, (Hill slope 0.7, n=3-7) (Figure 6.7B).

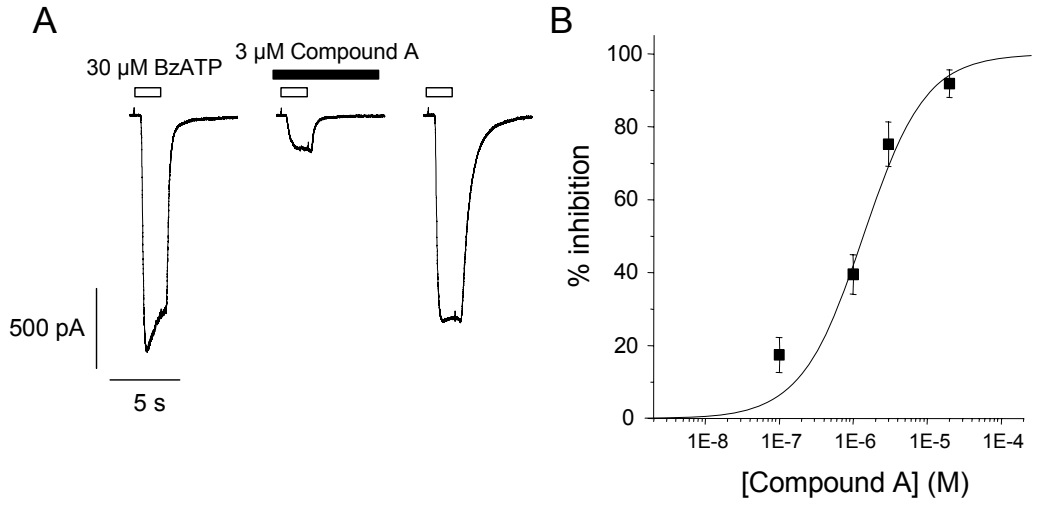

Figure 6.7: Compound A inhibits rat P2X7 currents
A. Example recording showing Compound A (3 μM) reversibly inhibiting 30 μM BzATP-activated rP2X7 current by 75 ± 6% (n=3), and the recovery to pre-addition levels in 2 min.
B. Concentration-response curves for Compound A at rP2X7 activated by 30 μM BzATP. Curves were fit to raw data and yielded IC_{50} values of 1.4 ± 0.2 μM (Hill slope 0.7, n=3-7).

6.3.5.2 Low Mg^{2+} model of epileptiform activity

In this model, the epileptiform activity was induced by modulating the ionic composition of the extracellular artificial cerebrospinal fluid (aCSF). The removal of extracellular Mg^{2+} from the aCSF is an established brain slice model of epileptiform bursting, which produces synchronous, stable frequency, bursting activity in the CA3 cell body region of the hippocampal slice. The model was chosen because astrocytic glutamate release produced prolonged neuronal depolarization which contributed to the epileptiform activity (Tian et al. 2005).

Extracellular recordings were made in stratum pyramidale of area CA3, and within 30 minutes of removal of Mg^{2+} from the aCSF, inter-ictal bursts, comprising of 1-2 population spikes were recorded. The epileptiform bursting occurred at a mean frequency of 0.18 ± 0.11 Hz (range 0.06 – 0.50 Hz) and with a mean burst duration of 750 ± 61 ms, (varying between 622 ms to 896 ms; n=4; see figure 6.8). Bath application of Compound A (10-100μM) had no significant effect on the frequency or duration of bursts (Figure 6.8B, 6.8C). Lamotrigine was tested in all slices and reduced the frequency of epileptiform bursting by 38 ±5 % (n=4, p=0.006), and caused a small but non-significant increase in the duration of bursts (128 ± 12 %; n=4).

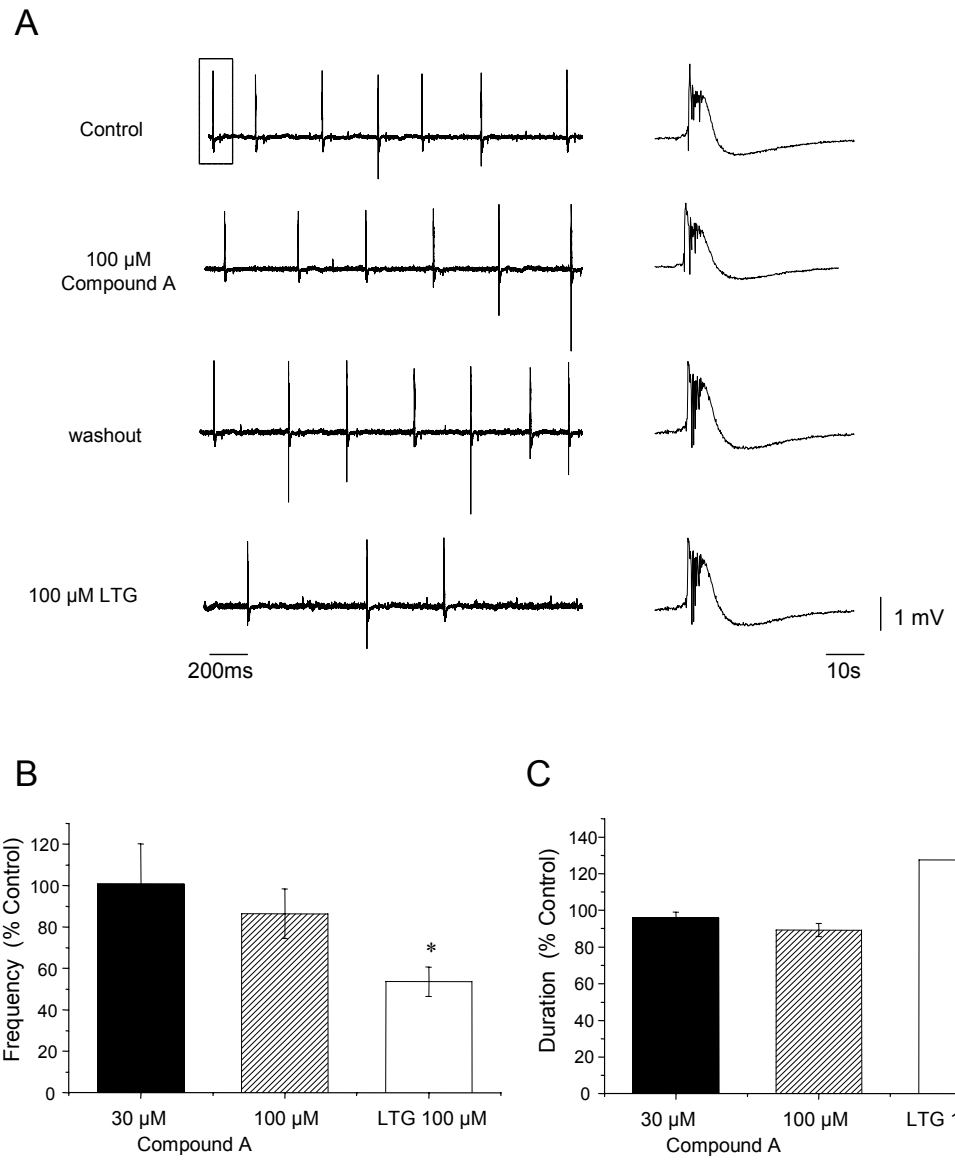

Figure 6.8: Compound A has no effect on low Mg^{2+} induced spontaneous epileptiform activity.

A. The traces from top to bottom are excerpts of raw data showing spontaneous burst firing recorded extracellularly over a 2 minute period in control conditions (low Mg^{2+} aCSF), in the presence of 100 µM Compound A, washout, and in the presence of 100 µM LTG. To the right of each excerpt is an expanded example of the first burst recorded under each experimental condition.

B. The bar graph shows the effect of 30 µM and 100 µM Compound A, and 100 µM LTG on the frequency of events in the low Mg^{2+} model.

C. The bar graph shows the effect of 30 µM and 100 µM Compound A, and 100 µM LTG on the bursting event duration in the low Mg^{2+} model.

6.3.5.3 Disinhibition Model of epileptiform activity

Having established that Compound A had no significant effect on epileptiform activity induced by removal of extracellular Mg^{2+} ions, the effect of Compound A on epileptiform activity induced by changing the balance of inhibitory to excitatory synaptic transmission using antagonists of GABA-mediated synaptic transmission was assessed. Again, there is evidence for an involvement of glutamate released from astrocytes in this model (Tian et al. 2005).

Here the combined application of the $GABA_A$ and $GABA_B$ receptor antagonists, Bicuculline (10 μM) and CGP55845 (10 μM), respectively, in the bathing solution consistently induced synchronous interictal-like, burst discharges in CA3 pyramidal neurones. Under these conditions bursting events occurred at a mean frequency of 0.25 ± 0.03 Hz (range 0.12 – 0.33 Hz), and were comprised of a primary burst, sometimes comprising multiple population spikes. Overall the mean individual burst duration was 1333 ± 290 ms, ranging from 862 to 2356 ms (Figure 6.9A); values consistent with activity reported previously (Empson and Jefferys 2001). Bath application of Compound A (10 μM - 200 μM) had no significant effect on the frequency of spontaneous synchronous bursting (75 ± 14% of control in 200 μM, p=0.1) or the duration of individual bursts (112 ± 21% of control in 200 μM) (Figure 6.9B and 6.9C). Lamotrigine (100 μM) significantly reduced epileptiform bursting frequency in 3 out of 4 slices to 38 ± 17% (n=4, p=0.01), but this was not accompanied by a change in the duration of the events that were left (112 ± 9 % of control, n=4; Figure 6.9C).

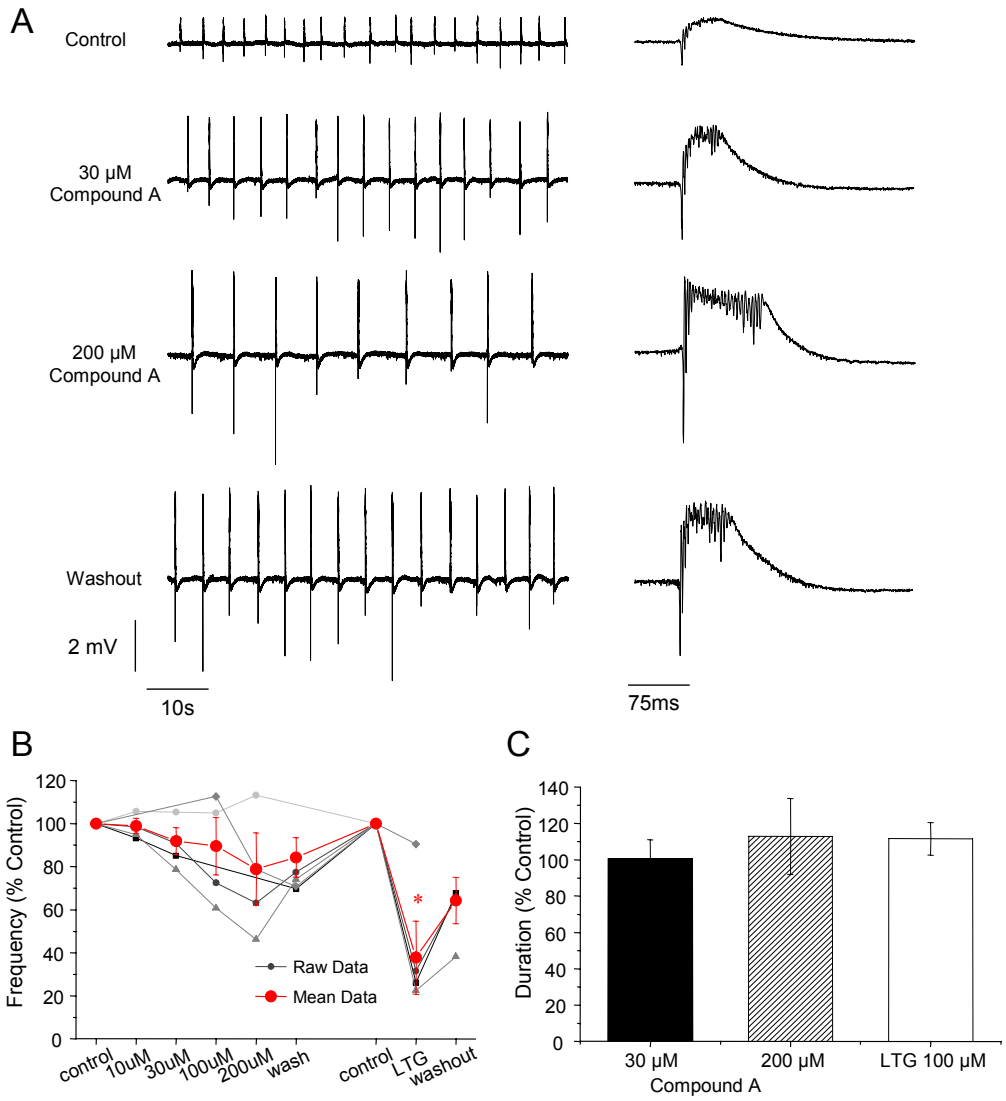

Figure 6.9: Compound A has no effect on the disinhibition model of spontaneous epileptiform activity.

A. The traces from top to bottom are excerpts of raw data showing spontaneous burst firing recorded extracellularly over a 1 minute period in control conditions (10µM Bicuculline and 10µM CGP55845), in the presence of 100 µM Compound A, washout, and in the presence of 100 µM LTG. To the right of each excerpt is an expanded example of the first burst recorded under each experimental condition.

B. The graph shows the effect of 10µM -200µM Compound A, and 100µM LTG on the frequency of bursting events in the disinhibition model. 4 separate cells are shown illustrating the variability of the effect of the compound, and the mean data (red dots). LTG (100µM) inhibited the frequency of events in 3 out 4 recordings.

C. The bar graph shows the effect of 30µM and 100µM Compound A, and 100µM LTG on the bursting event duration in the disinhibition model.

6.4. Discussion

In this study we investigated whether the marketed anti-epileptic, Lamotrigine, (Lamictal™), and the neuroprotective agent and chemical analogue, Sipatrigine were antagonists at P2X7 receptors. Lamotrigine inhibited both rat P2X7 receptors which were stably expressed in HEK293 cells and native P2X7 receptors expressed on the non-neuronal cells in DRG cultures. It had a much higher potency at the human P2X7 receptor, inhibiting BzATP-activated currents with an IC_{50} value of 6μM, one of the most potent actions of Lamotrigine reported to date. This effect at human P2X7 was also evident with Sipatrigine and produced an IC_{50} value of 3μM. Following on from this work the effect of a novel P2X7 antagonist, Compound A, was assessed in two models of epileptiform activity. No significant effect on the duration or frequency of epileptiform bursting activity was produced by Compound A in either model.

6.4.1 Rationale for the assessment of Lamotrigine's activity at P2X7 receptors

P2X7 receptors were considered as a possible target for Lamotrigine for a number of reasons. Firstly, although Lamotrigine is marketed as an anticonvulsant and as a treatment for bipolar disorder, it has demonstrated efficacy in a number of animal neuropathic pain studies (Nakamura-Craig and Follenfant 1995; Hunter et al. 1997; Erichsen et al. 2003; Fox et al. 2003; Joshi et al. 2006), and has also been under clinical evaluation for neuropathic pain. Efficacy has been demonstrated in some of these clinical studies, including in diabetic neuropathy (Eisenberg et al. 1998), and trigeminal neuralgia patients (Canavero and Bonicalzi 1997; Zakrzewska et al. 1997; McCleane 2000).

Secondly, although the pathophysiology of neuropathic pain is complex and dependent upon the aetiology, there is accumulating evidence of the role of P2X7 receptors in mediating this disorder (See Chapter 1, Introduction, section 1.4.6.1). The rationale highlights the key role of glial cells in spinal cord in the pathogenesis of pain (Watkins et al. 2001; DeLeo and Yezierski 2001), with both microglia and astrocyte activation observed in the spinal cord of rodents in models of chronic pain (Colburn et al. 1999; Sweitzer et al. 2001; Raghavendra et al. 2002; Milligan et al. 2003). Activation of P2X7

receptors located on microglia and astrocytes cause the release of cytokines including tumor necrosis factor-α (TNF-α) (Hide et al. 2000), interleukin-6 (IL-6) (Shigemoto-Mogami et al. 2001), and interleukin-1β (IL-1β) (Ferrari et al. 1996; Sanz and Di Virgilio 2000), providing further evidence for an important role for these receptors in this disease. IL-1β may be of further importance as its release, after P2X7 activation, caused an increase in the expression levels of P2X7 receptors in astrocytes (Narcisse et al. 2005). This is also mimicked in satellite cells in nerve and DRG sections from patients suffering with persistent neuropathic pain conditions (Chessell et al. 2005).

Finally, there is also precedence for a wide-ranging pharmacological profile of Lamotrigine. The proposed mechanisms of action of Lamotrigine are use-dependent inhibition of voltage-gated sodium channels (Xie et al. 1995), inhibition of calcium channels (Stefani et al. 1996; Wang et al. 1996; Hainsworth et al. 2003) and inhibition of pre-synaptic glutamate release (Leach et al. 1986). However a number of other actions of Lamotrigine have been reported, including inhibition of hERG currents, (IC50 = 229 μM; Danielsson et al. 2005), A-type potassium currents (I_A) (IC50=160μM Huang et al. 2004), and nicotinic acetylcholine receptors (nAChR) (Valles et al. 2007), and positive modulation of transient potassium currents (100 μM increased I_D in hippocampal neurones) (Grunze et al. 1998a; Grunze et al. 1998b); (EC50=226μM; Zona et al. 2002), with the latter two considered as possible contributors to Lamotrigine's efficacy.

6.4.2 Inhibition of P2X7 receptors by Lamotrigine

The majority of the data for the receptors and channels that Lamotrigine has been found to interact with are recorded from recombinantly expressed channels or from native (rodent) tissue/cells. When comparing the potency of Lamotrigine to inhibit rat P2X7 receptors (rP2X7-HEK IC_{50} = 100μM, Figure 6.2C; rDRG IC_{50} = 262 μM, Figure 6.4B) reported here, it is within this range of concentrations previously considered as candidates for underlying Lamotrigine's efficacy *in vivo*.

The activity at human P2X7 receptors (IC_{50} = 6μM) is one of the most potent effects of Lamotrigine reported to date, and higher than many of the reported potencies for

Lamotrigine at voltage-gated sodium (IC_{50} = 100 μM at Vh of -60mV; (Xie et al. 1995) and calcium channels (IC_{50} = 12.3 μM, (Stefani et al. 1996); the proposed primary sites of its action. Unlike Lamotrigine's effect on hP2X7 receptors, where an equal degree of inhibition was recorded at a holding voltage of -60mV or +60mV (Figure 6.3A), the action of Lamotrigine on sodium channels has been shown to be enhanced at depolarised potentials, consistent with use-dependent inhibition (Xie et al. 1995). Therefore the holding voltage must be taken into account when comparing its potency at different channels. A measurement of the affinity of Lamotrigine for the inactivated state of sodium channels is a more useful and possibly a more accurate value to use when considering its activity to reduce action potential firing. Ki values of 9 μM, (Vh of -70mV) in rat hippocampal neurones (Kuo and Lu 1997), and 38 μM (Vh of -70mV) for TTX-sensitive sodium currents in rat DRGs (Ilyin et al. 2006) have been previously reported, highlighting a more potent activity of Lamotrigine at key targets that are likely to mediate it's efficacy *in vivo*.

Intracellular application of Lamotrigine produced no inhibition of BzATP-activated currents in hP2X7 expressing cells, strongly suggesting an extracellular binding site of the molecule and no requirement for intracellular access to produce inhibition. However, as this was also the case for Lamotrigine's inhibition of sodium channels (Kuo 1998), even though binding occurs within transmembrane regions (Liu et al. 2003), definitive conclusions on the site of binding cannot be deduced from this study.

6.4.3 Sipatrigine and P2X7 receptor inhibition

There have been a few chemical analogues of Lamotrigine reported in the literature but by far the most widely investigated has been Sipatrigine (BW619C89). It is known to have a similar pharmacological profile to Lamotrigine; inhibiting voltage-gated Na^+ channels (Xie and Garthwaite 1996; Stefani et al. 1998) and Ca^{2+} channels (McNaughton et al. 1997; McNaughton et al. 2000; Hainsworth et al. 2003). However it has a much weaker *in vivo* anticonvulsant activity in seizure models (Meldrum 1994; Reddy et al. 1998) compared to Lamotrigine, and instead is a more effective neuroprotective agent in models of stroke (Graham et al. 1994; Smith et al. 1997). There is also rationale for a role

for P2X7 receptors in neurodegenerative processes that underlie brain trauma such as stroke. Prolonged activation of P2X7 receptors can be cytotoxic and releases cytokines such as IL-1β (Di Virgilio 1995; Le Feuvre et al. 2002b). Blockade of P2X7 receptors using Oxidised ATP increased neuronal survival in LPS-injected brain (Choi et al. 2007) and improved functional recovery following spinal cord injury (Wang et al. 2004a). However studies using P2X7 KO mice saw no change in neuronal death in various middle cerebral artery occlusion (MCAO) models, and no effect of P2X7 antagonists on ischemic or excitotoxic cell death (Le Feuvre et al. 2003), suggesting that P2X7 receptors are not primary mediators of experimentally induced neuronal death. Conflicting data was also reported using ischemia models to show that activation of P2X7 receptors may be beneficial when treating ischemic brain damage (Yanagisawa et al. 2008). Therefore although Sipatrigine is an equipotent antagonist of P2X7 receptors as Lamotrigine (IC_{50} = 3 μM), this may just represent an interesting addition to the list of its pharmacological activities and further work must be done to establish whether it is of relevance as a mechanism involved in neurodegeneration (Le Feuvre et al. 2002a).

6.4.4 The role of P2X7 receptor inhibition by Lamotrigine in pain

The inhibition of P2X7 receptors by Lamotrigine represents a potent activity when put in context with existing data for the effects of Lamotrigine at other ion channels. However, to link the effect of Lamotrigine to inhibit P2X7 receptors and its efficacy in neuropathic pain, the therapeutic concentrations required for efficacy must be considered. As mentioned above, there have been many positive animal neuropathic pain studies (Nakamura-Craig and Follenfant 1995; Hunter et al. 1997; Erichsen et al. 2003; Fox et al. 2003; Joshi et al. 2006), but the pharmacokinetic data relating the therapeutic effects to the plasma or brain concentrations are not included. Therefore patient data must be considered to assess the relationship between the pharmacokinetic and pharmacodynamic effects of Lamotrigine. Lamotrigine was assessed in a number of neuropathic pain patient groups, initially showing efficacy in trigeminal neuralgia open label trials (Lunardi et al. 1997), and then in larger randomised controlled trials across a number of different patient populations (Eisenberg et al. 2005; Eisenberg et al. 2007). The reported therapeutic total concentrations for the effect of Lamotrigine in neuropathic pain are 3-7 μg/ml according

to 2 open-label trials (Peck 1991), corresponding to 12-30 μM approximately. A similar value (4.5 μg/ml, or 15 μM) was recorded in healthy volunteers, and in both trials and volunteer studies these correlated well to pain scores (Webb and Kamali 1998). In the work reported here, a corresponding concentration of Lamotrigine (10 μM) produced a large inhibition (61 ± 5 % block) of ATP-activated hP2X7 currents.

When considering the impact of these findings it was interesting to know if this activity of Lamotrigine represents a specific action at P2X7 receptors as opposed to a more non-specific purinergic receptor activity. We focused on P2X receptors that are known to be involved in pain processing so their activity could be excluded as a mechanism by which Lamotrigine is analgesic. The role of P2X2/3 receptors in mediating ATP-related nociception (Burnstock 2006), and P2X4 receptors in chronic pain (Inoue et al. 2004) are well established (see Chapter 1, Introduction section 1.4.6). Lamotrigine had no effect at human P2X4 receptors at a concentration that gives full inhibition of human P2X7 receptors (100 μM, Figure 6.5A). The inhibition of human P2X2/3 receptors, (14% inhibition at 100 μM, Figure 6.5B) is around 16 fold higher than the IC_{50} value for Lamotrigine's activity at human P2X7 receptors, and so very little inhibition of P2X2/3 receptors would be expected at the circulating concentrations detailed above.

Therefore, although one can hypothesise as to the effect this degree of hP2X7 receptor inhibition may have *in vivo*, it is difficult to relate these data presented here to an endogenous activation of the receptor. As mentioned in Chapter 4 discussion, the pharmacokinetic values only provide a measure of the circulating drug concentrations and do not represent the concentration of the drug at the site of action. Lamotrigine has been reported to be around 50% bound to plasma proteins (Morris et al. 1998), which can also affect the availability of active drug concentrations, and would imply that the total Lamotrigine concentrations reported in the studies by Peck, and Webb and Kamali, would be reduced by half. Despite these caveats, the potency with which Lamotrigine inhibits P2X7 receptors and the rationale that inhibition of P2X7 receptors is analgesic means that this activity must be considered as a contributing factor to the efficacy seen in these trials.

6.4.5 The role of P2X7 receptor inhibition by Lamotrigine in epilepsy

Lamotrigine's inhibition of P2X7 receptors led to an assessment of the potential of P2X7 receptor antagonists in epileptiform activity. There is evidence for a role of P2X7 receptors in mediating epileptic discharges *in vivo* through a variety of mechanisms. These are detailed in the Introduction in Chapter 1, and include increases in presynaptic neurotransmitter release (Deuchars et al. 2001; Sperlagh et al. 2002), changes in the responsiveness or expression of P2X7 receptors in epilepsy (Vianna et al. 2002), a role for IL-1β in epileptogenesis (Vezzani and Baram 2007; for review) and P2X7-mediated astrocytic glutamate release leading to neuronal synchronisation (Angulo et al. 2004; Fellin et al. 2004). However, the novel P2X7 antagonist, Compound A, had no significant effect in two *in vitro* models of epileptiform activity (Figure 6.8 and 6.9) at concentrations up to 100 μM. In both models Lamotrigine inhibited the frequency of epileptiform bursting (Figure 6.8 and 6.9). It is unlikely that Compound A was ineffective due to inadequate exposure as the concentrations used were 10-100 times the IC_{50} value at rat P2X7 receptors (IC_{50} = 1.4 ± 0.2 μM, Figure 6.7C). The epileptiform models used here were chosen as they may incorporate some of the possible mechanisms of P2X7 activity including; astrocytic glutamate release, IL-1β release and an upregulation of P2X7 receptors in hippocampus. However, as for any *in vitro* model, there are limitations when comparing to an *in vivo* situation. Glutamate released from astrocytes occurs via a number of mechanisms (Parpura et al. 2004), not all P2X7 mediated, and although it contributes to the epileptiform activity 'strength', it may not be required to produce bursting *in vitro* (Fellin et al. 2006). The upregulation and the release of IL-1β following seizures has been detailed in whole animal studies (Vezzani et al. 1999; Vezzani et al. 2004) but not as yet in the various *in vitro* models used to study epileptiform activity. Therefore it is possible that the mechanisms used to induce synchronous bursting activity, or the duration of the models used here, is not sufficient to produce an increase in cytokine production. Further work could be done to investigate the role of astrocytes and IL-1β in these models in order to more directly assess a contribution of P2X7 receptors. The recording of paroxysmal depolarising shifts (PDS) in the presence TTX, may also

allow a more specific assessment of the effect of P2X7 antagonists on astrocytic glutamate release in an *in vitro* epilepsy model (Tian et al. 2005).

The fact that Lamotrigine was effective in reducing epileptiform activity in the two *in vitro* models used would suggest that the main mechanism of its action is not via inhibition of P2X7 receptors. When considering the clinical situation, it is clear that the potency of Lamotrigine inhibition of human P2X7 receptors (IC_{50} = 6μM) is within the proposed range of therapeutic circulating Lamotrigine concentrations that are anticonvulsant (1-4 μg/ml, (Brodie et al. 1995); 3-14 μg/ml, (Morris et al. 1998), and the measured therapeutic threshold plasma concentrations of 4-42 μM for Lamotrigine (Sondergaard et al. 2008). However, although this is true for patients, the data for the effect of Lamotrigine at the rat receptors fits less well into therapeutic range of concentrations reported the maximal electroshock test (MEST), a model used to test the anticonvulsant profile of compounds. The circulating plasma concentrations from MEST studies of 4-5 μg/ml (~19 μM) (Castel-Branco et al. 2003), would only inhibit native rat P2X7 or rP2X7-HEK923 receptors by around 6-15% (based on 6% inhibition with 10 μM Lamotrigine at native rP2X7 and 15% inhibition with 30 μM Lamotrigine at rP2X7 receptors expressed in HEK293 cells; See Figure 6.2C and 6.4)

6.4.6 Conclusions

In conclusion, the data presented here is the first defined activity of Lamotrigine at P2X receptors, and demonstrates Lamotrigine to be an effective inhibitor of rat and human P2X7 receptors stably expressed in a recombinant system and native P2X7 receptors expressed in DRG non-neuronal cells. The inhibition of human P2X7 is a potent effect of Lamotrigine and fits in well with the measured effective plasma concentrations of this compound in pain studies. These findings are supportive of another new pharmacological action of Lamotrigine and one that must be considered when investigating mechanisms of action of the analgesic actions of this drug in a number of diseases but in particular neuropathic pain.

Chapter 7: General Discussion

7.1 Discussion

The therapeutic potential of P2X7 receptor antagonists in pain has been suggested since the work by Dell'Antonio and colleagues using oxidised ATP, (initially thought of as a selective P2X7 antagonist), in pain models (Dell'Antonio et al. 2002a; Dell'Antonio et al. 2002b). In the work detailed in Chapter 4, GSK314181A represents one of the most potent P2X7 antagonists reported to date, showing little species differences often associated with P2X7 antagonists. The data showing its selectivity over closely related P2X receptors adds weight to the interpretation that the reduction in the hypersensitivity induced in the *in vivo* FCA model are mediated through P2X7 receptor antagonism. This adds to the wealth of novel compound data published over the last 2 years by a number of different pharmaceutical companies (Donnelly-Roberts and Jarvis 2007; Romagnoli et al. 2008), many of which display improvements in potency, selectivity and have less species dependence than older tool antagonists (Honore et al. 2006; Nelson et al. 2008). The data produced with GSK314181A is also important when considering its use as a selective *in vitro* tool with which to study P2X7 receptors expressed in native tissue. The study of native P2X7 receptors can often by beset by caveats over specificity of the effects recorded due to the often overlapping pharmacological profile of P2X receptor antagonists (North and Surprenant 2000). Tool P2X7 antagonists validated at recombinant and native P2X7 receptors, such as GSK314181A, are very useful compounds with which to dissect out P2X7 receptor function in cells containing such heterogeneity of P2X receptors.

The proposed mechanism of action of P2X7 receptor antagonists in reversing hypersensitivity is thought to centre around the inhibition of IL-1β release from immune cells and CNS glial cells, such as astrocytes and microglia (Ferrari et al. 1997a; Ferrari et al. 1997b), and suggests a key role for these receptors in neuro-glial interactions. The role of glial cells in pain pathophysiology has become more apparent through work from a number of different groups (For reviews; Watkins and Maier 2003; Scholz and Woolf

2007). Although there is strong evidence for a role of immune cells and CNS glia in pain (Watkins and Maier 2003; Tsuda et al. 2005), the role of peripheral glial cells in sensory ganglia has, as yet, had little interest, even though their activation following peripheral nerve injury has been described and they have many of the hallmarks associated with CNS glial activation (Dublin and Hanani 2007). The expression of P2X7 receptors on non-neuronal cells in DRG cultures was confirmed here in Chapter 5 using a P2X7 monoclonal antibody. This work was expanded to define the specific cell types expressing P2X7 receptors as satellite glial cells and Schwann cells using dual labelling. As DRG are outside the blood-brain and blood-nerve barrier (Wadhwani and Rapoport 1994), the cells contained in the ganglia are easily accessible to systemic administration of drugs, but are often ignored as a potential site of action. The localisation of P2X7 receptors on these cells highlights a possible previously under investigated site of action for P2X7 antagonists or other compounds that influence neuro-glial interactions, and hence neuronal excitability.

The role of P2X7 receptor localisation on satellite cells in DRG is yet to be fully established. There is evidence that P2X7 receptors are important in bi-directional communication between neurones and satellite cells in the DRG (Zhang et al. 2007), and also can influence expression levels of neuronal P2X3 receptors (Chen et al. 2008). There is also evidence for ectopic discharge of neuronal cells of DRG, an effect that is exacerbated following injury (Devor and Seltzer 1999), indicating that neuronal stimulation of ATP release from DRG neurones is likely. However, the physiological relevance of the interaction between neurones and satellite cells in DRG and the potential influence it may have on neuronal excitability needs further exploration, as does the specific function of P2X7 receptors in this region. The likelihood of P2X7 receptor activation under physiological conditions has always been debated due to the high concentration of agonist required to activate them (> 100 μM). Although concentrations around this level may be released during normal conditions, the enzymatic degradation of ATP by ectonucleotidases will limit the time for P2X receptor activation. However, the relevance of ATP activation of P2X7 may be higher if inflammatory cells are exposed repeatedly to pulses of ATP released from damaged cells under inflammatory conditions

(Hibell et al. 2000). P2X7 receptors may also be “primed” from an initial ATP activation to respond to ADP and AMP, which are both products of ectonucleotidase degradation of ATP (Chakfe et al. 2002). The slowing of deactivation seen for recombinant and native cells, as recorded here in Chapter 3 and 5, may also mean that even short ATP applications would produce much longer channel opening times with subsequent P2X7 receptor activation. There is also evidence for higher extracellular ATP concentrations under inflammatory conditions (Bodin and Burnstock 1998), suggesting that P2X7 receptors may act as a ‘danger sensor’ where activation would mainly occur under pathophysiological conditions.

A number of pharmaceutical companies have recognised the therapeutic potential of P2X7 antagonists across a range of disorders. The key role P2X7 receptors are known to play in regulating inflammatory processes has made them targets for diseases which have inflammation underlying their aetiology, including epilepsy (Rappold et al. 2006) and inflammatory and neuropathic pain (Donnelly-Roberts and Jarvis 2007), as discussed in this thesis. Following on from evidence from preclinical inflammatory and neuropathic pain models, a number of pharmaceutical companies are conducting clinical studies. These are in rheumatoid arthritis (RA) and pain, and have reported positive data in Phase II for Astrazeneca with AZD-9056, and Pfizer with CE-224535. When considering the clinical value of P2X7 antagonists, it is also worth noting some of potential problems that must be addressed. Many single-nucleotide polymorphisms (SNP) in the P2X7 receptor genes have been described, and some of which are found in up to 20% of the population (Glu496 to Ala; Gu et al. 2001). These have implicated P2X7 receptors in psychiatric illness, especially mood disorders (Reviewed in Bennett 2007), and in Crohn's disease (Haas et al. 2007), and have also raised the possibility that low P2X7 receptor function may be a genetic susceptibility factor in a range of infections such as tuberculosis and Chlamydia (Gu et al. 2004). These associations also highlight risks that must be discharged for small molecule P2X7 receptor antagonists during more extensive clinical trials.

Lamotrigine's antagonism of P2X7 receptors was an interesting finding when considering the clinical use of Lamotrigine as an anticonvulsant and also the investigation of its efficacy in neuropathic pain. The lack of an effect of a P2X7 antagonist on epileptiform activity may suggest that the inhibition of P2X7 may represent an additional pharmacological action of Lamotrigine rather than a mechanism through which it produces its anticonvulsant effects. However, the increasing evidence of a crucial role of inflammatory processes in epilepsy (Vezzani et al. 2004), specifically around IL-1β release (Vezzani and Baram 2007) and the possible limitations of the *in vitro* models used here mean that a role of P2X7 receptors in this mechanism must be considered. Although there are many antiepileptic drugs currently available, it is estimated that for around 30% of epileptic patients, pharmacoresistance is a significant issue. Many of the most widely used therapies act primarily at voltage-gated ion channels (Wuttke and Lerche 2006), and even though newer molecules have provided an increase in efficacy and a reduction in side effects, an unmet need persists in this subpopulation. Therefore, further investigation into new mechanisms, such as P2X7 receptor antagonism, would be extremely beneficial to try to extend the range of therapies available.

7.2 Future Work

The work in this thesis presents a number of different directions for future study:

Novel P2X7 Antagonists

- It would be interesting to determine the mechanism of action of the tool compound, GSK314181A, and also its specific binding site in order to provide information on how this compound and others that are chemically similar interact with the P2X7 receptor, information that may be useful in selectivity studies or in comparisons of activity across orthologues. Further work would be needed using site-directed mutagenesis techniques to gain binding site information and detailed pharmacological analysis is required to ascertain whether GSK314181A has a competitive or non-competitive mechanism of action. These studies can only be done by looking at shifts in the agonist concentration-response curves and may be

better performed using plate-based assay formats such as FLIPR-Ca and ethidium bromide uptake experiments.

Neuronal Localisation of P2X7

- Confirmation of the neuronal localisation of P2X7 receptors in DRGs recorded in Chapter 5. This could be looked into through functional electrophysiology recordings using the selective pharmacological tools available such as GSK314181A, or using immunocytochemical or immunohistochemical techniques. This could also be extended to other CNS regions and also importantly to human tissues or cells.
- Investigation into the epitope of the monoclonal antibody used in Chapter 5 would be needed in order to further work using this reagent. Chimeric experiments, followed by site-directed mutagenesis may be used to try to ascertain the epitope. This may then enable validation of the labelling with this antibody e.g. epitope preincubation (antibody exhaustion).
- Investigation of the phenotype of the neuronal P2X7 expressing cells using dual labelling experiments, e.g. with calcitonin gene-related peptide (CGRP) or isolectin B4 (IB4), may determine if a subset of neurones were expressing P2X7.

Role of P2X7 receptors on satellite cells

- Further investigation of the function of P2X7 on the satellite cells in DRG is required. Specifically focusing on the two other consequences of P2X7 receptor activation; pore formation and cytokine release. Whether pore formation is occurring via P2X7 receptor dilation or via activation of Pannexin protein would investigated. The pharmacology of these responses could also be assessed to determine specific P2X7 receptor activity, and also to define if pore formation and cytokine release were reversible with small molecule antagonists in these cells. These data would give more information as to the role, if any, these cells may have in mediating the antihyperalgesic effects of P2X7 antagonists (as the rationale is focused on blocking the release of IL-1β), but also add to the data

presented in Chapter 5 as to whether these native receptors function in the same way as the recombinantly expressed receptor.

- Neuronal-glial co-cultures, or intact or slices of DRG, could be used to investigate if activating or inhibiting P2X7 receptors affects neuronal function. As would further investigation of the full repertoire of P2X7 receptors, including the relevance of slowing of deactivation of P2X7 receptors, pore formation and cytokine release, when expressed in native cells. This could provide an insight into the relevance of these results to the physiological, or more likely, pathophysiological role of P2X7 receptors when expressed in DRG.
- Following the results in Chapter 4 it would be interesting to assess the role satellite cells in DRG have in mediating the efficacy seen in the inflammatory pain model. The experiments detailed above could be replicated in tissues/cells taken from animals that have undergone an inflammatory insult to see look for significant changes in the various measures of P2X7 function.

Inhibition of P2X7 receptors by Lamotrigine

- Further work to address whether Lamotrigine can inhibit other consequences of P2X7 receptors activation such as YOPRO uptake and IL-1β release.
- Investigation into whether the activity of Lamotrigine at P2X7 receptors has any therapeutic relevance. Due to the analgesic effects of P2X7 receptor inhibition and sodium channel inhibition it is difficult to assess the role of P2X7 inhibition in the efficacious effects of Lamotrigine *in vivo*. Therefore an indirect effect of P2X7 receptor activation, such as measurement of IL-1β levels in blood following FCA-induced hypersensitivity, would have to be assessed. These levels could be measured following Lamotrigine or a sodium channel blocker with no P2X7 activity and compared to vehicle and P2X7 antagonist dosing groups.
- Further investigation into the role of P2X7 receptors in epilepsy. The effect of P2X7 receptor inhibition on the induction and maintenance of epileptiform events could be assessed in a range of *in vitro* models, as could the effect of P2X7 antagonists in *in vivo* convulsant models such as MEST or Pentylenetetrazole.

Chapter 8: References

Reference List

Abbott NJ, Ronnback L, Hansson E. Astrocyte-endothelial interactions at the blood-brain barrier. Nat Rev Neurosci 2006;7:41-53.

Abbracchio MP, Burnstock G, Boeynaems JM, Barnard EA, Boyer JL, Kennedy C, Knight GE, Fumagalli M, Gachet C, Jacobson KA, Weisman GA. International Union of Pharmacology LVIII: update on the P2Y G protein-coupled nucleotide receptors: from molecular mechanisms and pathophysiology to therapy. Pharmacol Rev 2006;58:281-341.

Acuna-Castillo C, Coddou C, Bull P, Brito J, Huidobro-Toro JP. Differential role of extracellular histidines in copper, zinc, magnesium and proton modulation of the P2X7 purinergic receptor. J Neurochem 2007;101:17-26.

Albuerne M, Mammola CL, Naves FJ, Levanti B, Germana G, Vega JA. Immunohistochemical localization of S100 proteins in dorsal root, sympathetic and enteric ganglia of several mammalian species, including man. J Peripher Nerv Syst 1998;3:243-253.

Alcaraz L, Baxter A, Bent J, Bowers K, Braddock M, Cladingboel D, Donald D, Fagura M, Furber M, Laurent C, Lawson M, Mortimore M, McCormick M, Roberts N, Robertson M. Novel P2X7 receptor antagonists. Bioorg Med Chem Lett 2003;13:4043-4046.

Alcaraz L, Furber M, Mortimore M. Adamantane Derivatives. (WO2000061569A1). 2000.
Ref Type: Patent

Allgaier C, Reinhardt R, Schadlich H, Rubini P, Bauer S, Reichenbach A, Illes P. Somatic and axonal effects of ATP via P2X2 but not P2X7 receptors in rat thoracolumbar sympathetic neurones. J Neurochem 2004;90:359-367.

Amaya F, Oh-hashi K, Naruse Y, Iijima N, Ueda M, Shimosato G, Tominaga M, Tanaka Y, Tanaka M. Local inflammation increases vanilloid receptor 1 expression within distinct subgroups of DRG neurons. Brain Res 2003;963:190-196.

Anderson BJ. Paracetamol (Acetaminophen): mechanisms of action. Paediatr Anaesth 2008;18:915-921.

Andrei C, Dazzi C, Lotti L, Torrisi MR, Chimini G, Rubartelli A. The secretory route of the leaderless protein interleukin 1beta involves exocytosis of endolysosome-related vesicles. Mol Biol Cell 1999;10:1463-1475.

Angulo MC, Kozlov AS, Charpak S, Audinat E. Glutamate released from glial cells synchronizes neuronal activity in the hippocampus. J Neurosci 2004;24:6920-6927.

Araque A, Parpura V, Sanzgiri RP, Haydon PG. Tripartite synapses: glia, the unacknowledged partner. Trends Neurosci 1999;22:208-215.

Arikkath J, Campbell KP. Auxiliary subunits: essential components of the voltage-gated calcium channel complex. Curr Opin Neurobiol 2003;13:298-307.

Armstrong JN, Brust TB, Lewis RG, MacVicar BA. Activation of presynaptic P2X7-like receptors depresses mossy fiber-CA3 synaptic transmission through p38 mitogen-activated protein kinase. J Neurosci 2002;22:5938-5945.

Aschrafi A, Sadtler S, Niculescu C, Rettinger J, Schmalzing G. Trimeric architecture of homomeric P2X2 and heteromeric P2X1+2 receptor subtypes. J Mol Biol 2004;342:333-343.

Ashburn MA, Staats PS. Management of chronic pain. Lancet 1999;353:1865-1869.

Atkinson L, Batten TF, Moores TS, Varoqui H, Erickson JD, Deuchars J. Differential co-localisation of the P2X7 receptor subunit with vesicular glutamate transporters VGLUT1 and VGLUT2 in rat CNS. Neuroscience 2004;123:761-768.

Auerbach A, Sigurdson W, Chen J, Akk G. Voltage dependence of mouse acetylcholine receptor gating: different charge movements in di-, mono- and unliganded receptors. J Physiol. 494, 155-170. 1996.
Ref Type: Abstract

Baimbridge KG, Celio MR, Rogers JH. Calcium-binding proteins in the nervous system. Trends Neurosci 1992;15:303-308.

Ballerini P, Rathbone MP, Di IP, Renzetti A, Giuliani P, D'Alimonte I, Trubiani O, Caciagli F, Ciccarelli R. Rat astroglial P2Z (P2X7) receptors regulate intracellular calcium and purine release. Neuroreport 1996;7:2533-2537.

Barbe MT, Monyer H, Bruzzone R. Cell-cell communication beyond connexins: the pannexin channels. Physiology (Bethesda) 2006;21:103-114.

Barger SW, Van Eldik LJ. S100 beta stimulates calcium fluxes in glial and neuronal cells. J Biol Chem 1992;267:9689-9694.

Beck PW, Handwerker HO, Zimmermann M. Nervous outflow from the cat's foot during noxious radiant heat stimulation. Brain Res 1974;67:373-386.

Bennett MR. Synaptic P2X7 receptor regenerative-loop hypothesis for depression. Aust N Z J Psychiatry 2007;41:563-571.

Bernard JF, Bester H, Besson JM. Involvement of the spino-parabrachio -amygdaloid and -hypothalamic pathways in the autonomic and affective emotional aspects of pain. Prog Brain Res 1996;107:243-255.

Bessou P, Perl ER. Response of cutaneous sensory units with unmyelinated fibers to noxious stimuli. J Neurophysiol 1969;32:1025-1043.

Bezzi P, Carmignoto G, Pasti L, Vesce S, Rossi D, Rizzini BL, Pozzan T, Volterra A. Prostaglandins stimulate calcium-dependent glutamate release in astrocytes. Nature 1998;391:281-285.

Bianchi BR, Lynch KJ, Touma E, Niforatos W, Burgard EC, Alexander KM, Park HS, Yu H, Metzger R, Kowaluk E, Jarvis MF, van BT. Pharmacological characterization of recombinant human and rat P2X receptor subtypes. Eur J Pharmacol 1999;376:127-138.

Bianchi M, Dib B, Panerai AE. Interleukin-1 and nociception in the rat. J Neurosci Res 1998;53:645-650.

Blomstrand F, Aberg ND, Eriksson PS, Hansson E, Ronnback L. Extent of intercellular calcium wave propagation is related to gap junction permeability and level of connexin-43 expression in astrocytes in primary cultures from four brain regions. Neuroscience 1999;92:255-265.

Bo X, Jiang LH, Wilson HL, Kim M, Burnstock G, Surprenant A, North RA. Pharmacological and biophysical properties of the human P2X5 receptor. Mol Pharmacol 2003;63:1407-1416.

Bo X, Zhang Y, Nassar M, Burnstock G, Schoepfer R. A P2X purinoceptor cDNA conferring a novel pharmacological profile. FEBS Lett 1995;375:129-133.

Bodin P, Burnstock G. Increased release of ATP from endothelial cells during acute inflammation. Inflamm Res 1998;47:351-354.

Boue-Grabot E, Archambault V, Seguela P. A protein kinase C site highly conserved in P2X subunits controls the desensitization kinetics of P2X(2) ATP-gated channels. J Biol Chem 2000;275:10190-10195.

Bowler JW, Bailey RJ, North RA, Surprenant A. P2X4, P2Y1 and P2Y2 receptors on rat alveolar macrophages. Br J Pharmacol 2003;140:567-575.

Brake AJ, Wagenbach MJ, Julius D. New structural motif for ligand-gated ion channels defined by an ionotropic ATP receptor. Nature 1994;371:519-523.

Brandle U, Guenther E, Irrle C, Wheeler-Schilling TH. Gene expression of the P2X receptors in the rat retina. Brain Res Mol Brain Res 1998a;59:269-272.

Brandle U, Kohler K, Wheeler-Schilling TH. Expression of the P2X7-receptor subunit in neurons of the rat retina. Brain Res Mol Brain Res 1998b;62:106-109.

Braun N, Sevigny J, Robson SC, Hammer K, Hanani M, Zimmermann H. Association of the ecto-ATPase NTPDase2 with glial cells of the peripheral nervous system. Glia 2004;45:124-132.

Brockes JP, Fields KL, Raff MC. Studies on cultured rat Schwann cells. I. Establishment of purified populations from cultures of peripheral nerve. Brain Res 1979;165:105-118.

Brodie MJ, Richens A, Yuen AW. Double-blind comparison of lamotrigine and carbamazepine in newly diagnosed epilepsy. UK Lamotrigine/Carbamazepine Monotherapy Trial Group. Lancet 1995;345:476-479.

Broom DC, Matson DJ, Bradshaw E, Buck ME, Meade R, Coombs S, Matchett M, Ford KK, Yu W, Yuan J, Sun SH, Ochoa R, Krause JE, Wustrow DJ, Cortright DN. Characterization of N-(adamantan-1-ylmethyl)-5-[(3R-amino-pyrrolidin-1-yl)methyl]-2-chloro-ben zamide, a P2X7 antagonist in animal models of pain and inflammation. J Pharmacol Exp Ther 2008;327:620-633.

Brown SG, Townsend-Nicholson A, Jacobson KA, Burnstock G, King BF. Heteromultimeric P2X(1/2) receptors show a novel sensitivity to extracellular pH. J Pharmacol Exp Ther 2002;300:673-680.

Buell G, Chessell IP, Michel AD, Collo G, Salazzo M, Herren S, Gretener D, Grahames C, Kaur R, Kosco-Vilbois MH, Humphrey PP. Blockade of human P2X7 receptor function with a monoclonal antibody. Blood 1998a;92:3521-3528.

Buell G, Lewis C, Collo G, North RA, Surprenant A. An antagonist-insensitive P2X receptor expressed in epithelia and brain. EMBO J 1996;15:55-62.

Buell GN, Talabot F, Gos A, Lorenz J, Lai E, Morris MA, Antonarakis SE. Gene structure and chromosomal localization of the human P2X7 receptor. Receptors Channels 1998b;5:347-354.

Buisman HP, Steinberg TH, Fischbarg J, Silverstein SC, Vogelzang SA, Ince C, Ypey DL, Leijh PC. Extracellular ATP induces a large nonselective conductance in macrophage plasma membranes. Proc Natl Acad Sci U S A 1988;85:7988-7992.

Burnstock G. Purinergic nerves. Pharmacol Rev 1972;24:509-581.

Burnstock G. A basis for distinguishing two types of purinergic receptor. Cell Membrane Receptors for Drugs and Hormones: A Multidisciplinary Approach. New York: Raven Press, 1978. pp. 107-118.

Burnstock G. Purine-mediated signalling in pain and visceral perception. Trends Pharmacol Sci 2001;22:182-188.

Burnstock G. Purinergic P2 receptors as targets for novel analgesics. Pharmacol Ther 2006;110:433-454.

Burnstock G. Purinergic signalling and disorders of the central nervous system. Nat Rev Drug Discov 2008;7:575-590.

Burnstock G, Campbell G, Satchell D, Smythe A. Evidence that adenosine triphosphate or a related nucleotide is the transmitter substance released by non-adrenergic inhibitory nerves in the gut. Br J Pharmacol 1970;40:668-688.

Bushong EA, Martone ME, Jones YZ, Ellisman MH. Protoplasmic astrocytes in CA1 stratum radiatum occupy separate anatomical domains. J Neurosci 2002;22:183-192.

Calvert JA, Evans RJ. Heterogeneity of P2X receptors in sympathetic neurons: contribution of neuronal P2X1 receptors revealed using knockout mice. Mol Pharmacol 2004;65:139-148.

Canavero S, Bonicalzi V. Lamotrigine control of trigeminal neuralgia: an expanded study. J Neurol 1997;244:527.

Carroll WA, Kalvin DM, Perez MA, Florjancic AS, Wang Y, Donnelly-Roberts DL, Namovic MT, Grayson G, Honore P, Jarvis MF. Novel and potent 3-(2,3-dichlorophenyl)-4-(benzyl)-4H-1,2,4-triazole P2X7 antagonists. Bioorg Med Chem Lett 2007;17:4044-4048.

Castel-Branco M, Lebre V, Falcao A, Figueiredo I, Caramona M. Relationship between plasma and brain levels and the anticonvulsant effect of lamotrigine in rats. Eur J Pharmacol 2003;482:163-168.

Chahine M, Ziane R, Vijayaragavan K, Okamura Y. Regulation of Nav channels in sensory neurons. Trends Pharmacol Sci 2005;26:496-502.

Chakfe Y, Seguin R, Antel JP, Morissette C, Malo D, Henderson D, Seguela P. ADP and AMP induce interleukin-1beta release from microglial cells through activation of ATP-primed P2X7 receptor channels. J Neurosci 2002;22:3061-3069.

Chen CC, Akopian AN, Sivilotti L, Colquhoun D, Burnstock G, Wood JN. A P2X purinoceptor expressed by a subset of sensory neurons. Nature 1995;377:428-431.

Chen Y, Zhang X, Wang C, Li G, Gu Y, Huang LY. Activation of P2X7 receptors in glial satellite cells reduces pain through downregulation of P2X3 receptors in nociceptive neurons. Proc Natl Acad Sci U S A 2008;105:16773-16778.

Chessell IP, Grahames C, Michel AD, Humphrey PP. Dynamics of P2X7 Receptor Pore Dilation:Pharmacological and Functional Consequences. Drug Development Research 2001;53:60-65.

Chessell IP, Hatcher JP, Bountra C, Michel AD, Hughes JP, Green P, Egerton J, Murfin M, Richardson J, Peck WL, Grahames CB, Casula MA, Yiangou Y, Birch R, Anand P, Buell GN. Disruption of the P2X7 purinoceptor gene abolishes chronic inflammatory and neuropathic pain. Pain 2005;114:386-396.

Chessell IP, Michel AD, Humphrey PP. Properties of the pore-forming P2X7 purinoceptor in mouse NTW8 microglial cells. Br J Pharmacol 1997;121:1429-1437.

Chessell IP, Michel AD, Humphrey PP. Effects of antagonists at the human recombinant P2X7 receptor. Br J Pharmacol 1998a;124:1314-1320.

Chessell IP, Simon J, Hibell AD, Michel AD, Barnard EA, Humphrey PP. Cloning and functional characterisation of the mouse P2X7 receptor. FEBS Lett 1998b;439:26-30.

Chizh BA, Illes P. P2X receptors and nociception. Pharmacol Rev 2001;53:553-568.

Choi HB, Ryu JK, Kim SU, McLarnon JG. Modulation of the purinergic P2X7 receptor attenuates lipopolysaccharide-mediated microglial activation and neuronal damage in inflamed brain. J Neurosci 2007;27:4957-4968.

Clayton NM, Oakley I, Thompson S, Wheeldon A, Sargent B, Bountra C. Validation of the dual channel weight averager as an instrument for the measurement of inflammatory pain. Br J Pharmacol Proc Supplement (75). 1997.
Ref Type: Abstract

Cockayne DA, Dunn PM, Zhong Y, Rong W, Hamilton SG, Knight GE, Ruan HZ, Ma B, Yip P, Nunn P, McMahon SB, Burnstock G, Ford AP. P2X2 knockout mice and P2X2/P2X3 double knockout mice reveal a role for the P2X2 receptor subunit in mediating multiple sensory effects of ATP. J Physiol 2005;567:621-639.

Cockayne DA, Hamilton SG, Zhu QM, Dunn PM, Zhong Y, Novakovic S, Malmberg AB, Cain G, Berson A, Kassotakis L, Hedley L, Lachnit WG, Burnstock G, McMahon SB, Ford AP. Urinary bladder hyporeflexia and reduced pain-related behaviour in P2X3-deficient mice. Nature 2000;407:1011-1015.

Colburn RW, DeLeo JA. The effect of perineural colchicine on nerve injury-induced spinal glial activation and neuropathic pain behavior. Brain Res Bull 1999;49:419-427.

Colburn RW, DeLeo JA, Rickman AJ, Yeager MP, Kwon P, Hickey WF. Dissociation of microglial activation and neuropathic pain behaviors following peripheral nerve injury in the rat. J Neuroimmunol 1997;79:163-175.

Colburn RW, Rickman AJ, DeLeo JA. The effect of site and type of nerve injury on spinal glial activation and neuropathic pain behavior. Exp Neurol 1999;157:289-304.

Collo G, Neidhart S, Kawashima E, Kosco-Vilbois M, North RA, Buell G. Tissue distribution of the P2X7 receptor. Neuropharmacology 1997;36:1277-1283.

Collo G, North RA, Kawashima E, Merlo-Pich E, Neidhart S, Surprenant A, Buell G. Cloning OF P2X5 and P2X6 receptors and the distribution and properties of an extended family of ATP-gated ion channels. J Neurosci 1996;16:2495-2507.

Colomar A, Amedee T. ATP stimulation of P2X(7) receptors activates three different ionic conductances on cultured mouse Schwann cells. Eur J Neurosci 2001;14:927-936.

Coutinho-Silva R, Persechini PM. P2Z purinoceptor-associated pores induced by extracellular ATP in macrophages and J774 cells. Am J Physiol 1997;273:C1793-C1800.

Cummins TR, Waxman SG. Downregulation of tetrodotoxin-resistant sodium currents and upregulation of a rapidly repriming tetrodotoxin-sensitive sodium current in small spinal sensory neurons after nerve injury. J Neurosci 1997;17:3503-3514.

D'Amelio F, Eng LF, Gibbs MA. Glutamine synthetase immunoreactivity is present in oligodendroglia of various regions of the central nervous system. Glia 1990;3:335-341.

Dahlquist R, Diamant B. Interaction of ATP and calcium on the rat mast cell: effect on histamine release. Acta Pharmacol Toxicol (Copenh) 1974;34:368-384.

Danielsson BR, Lansdell K, Patmore L, Tomson T. Effects of the antiepileptic drugs lamotrigine, topiramate and gabapentin on hERG potassium currents. Epilepsy Res 2005;63:17-25.

Dayer JM, de RB, Burrus B, Demczuk S, Dinarello CA. Human recombinant interleukin 1 stimulates collagenase and prostaglandin E2 production by human synovial cells. J Clin Invest 1986;77:645-648.

De Alba J, Clayton NM, Collins SD, Colthup P, Chessell I, Knowles RG. GW274150, a novel and highly selective inhibitor of the inducible isoform of nitric oxide synthase (iNOS), shows analgesic effects in rat models of inflammatory and neuropathic pain. Pain 2006;120:170-181.

DeLeo JA, Yezierski RP. The role of neuroinflammation and neuroimmune activation in persistent pain. Pain 2001;90:1-6.

Dell'Antonio G, Quattrini A, Cin ED, Fulgenzi A, Ferrero ME. Relief of inflammatory pain in rats by local use of the selective P2X7 ATP receptor inhibitor, oxidized ATP. Arthritis Rheum 2002a;46:3378-3385.

Dell'Antonio G, Quattrini A, Dal CE, Fulgenzi A, Ferrero ME. Antinociceptive effect of a new P(2Z)/P2X7 antagonist, oxidized ATP, in arthritic rats. Neurosci Lett 2002b;327:87-90.

Denlinger LC, Fisette PL, Sommer JA, Watters JJ, Prabhu U, Dubyak GR, Proctor RA, Bertics PJ. Cutting edge: the nucleotide receptor P2X7 contains multiple protein- and lipid-interaction motifs including a potential binding site for bacterial lipopolysaccharide. J Immunol 2001;167:1871-1876.

Deuchars SA, Atkinson L, Brooke RE, Musa H, Milligan CJ, Batten TF, Buckley NJ, Parson SH, Deuchars J. Neuronal P2X7 receptors are targeted to presynaptic terminals in the central and peripheral nervous systems. J Neurosci 2001;21:7143-7152.

Devor M, Seltzer Z. Pathophysiology of damaged nerves in relation to chronic pain. In: Wall PD, Melzack R, editors. Textbook of Pain. Edinburgh, UK: Churchill Livingston, 1999. pp. 138-139.

Di Virgilio F. The P2Z purinoceptor: an intriguing role in immunity, inflammation and cell death. Immunol Today 1995;16:524-528.

Ding S, Sachs F. Single channel properties of P2X2 purinoceptors. J Gen Physiol 1999;113:695-720.

Donnelly-Roberts DL, Jarvis MF. Discovery of P2X7 receptor-selective antagonists offers new insights into P2X7 receptor function and indicates a role in chronic pain states. Br J Pharmacol 2007;151:571-579.

Donnelly-Roberts DL, Namovic MT, Faltynek CR, Jarvis MF. Mitogen-activated protein kinase and caspase signaling pathways are required for P2X7 receptor (P2X7R)-induced pore formation in human THP-1 cells. J Pharmacol Exp Ther 2004;308:1053-1061.

Donnelly-Roberts DL, Namovic MT, Surber B, Vaidyanathan SX, Perez-Medrano A, Wang Y, Carroll WA, Jarvis MF. [(3)H]A-804598 ([(3)H]2-cyano-1-[(1S)-1-phenylethyl]-3-quinolin-5-ylguanidine) is a novel, potent, and selective antagonist radioligand for P2X7 receptors. Neuropharmacology 2008.

Duan S, Anderson CM, Keung EC, Chen Y, Chen Y, Swanson RA. P2X7 receptor-mediated release of excitatory amino acids from astrocytes. J Neurosci 2003;23:1320-1328.

Dublin P, Hanani M. Satellite glial cells in sensory ganglia: their possible contribution to inflammatory pain. Brain Behav Immun 2007;21:592-598.

Dubner R. Neurophysiology of pain. Dent Clin North Am 1978;22:11-30.

Duce IR, Keen P. Selective uptake of [3H]glutamine and [3H]glutamate into neurons and satellite cells of dorsal root ganglia in vitro. Neuroscience 1983;8:861-866.

Eisenberg E, Alon N, Ishay A, Daoud D, Yarnitsky D. Lamotrigine in the treatment of painful diabetic neuropathy. Eur J Neurol 1998;5:167-173.

Eisenberg E, River Y, Shifrin A, Krivoy N. Antiepileptic drugs in the treatment of neuropathic pain. Drugs 2007;67:1265-1289.

Eisenberg E, Shifrin A, Krivoy N. Lamotrigine for neuropathic pain. Expert Rev Neurother 2005;5:729-735.

Empson RM, Jefferys JG. Ca(2+) entry through L-type Ca(2+) channels helps terminate epileptiform activity by activation of a Ca(2+) dependent afterhyperpolarisation in hippocampal CA3. Neuroscience 2001;102:297-306.

Ennion S, Hagan S, Evans RJ. The role of positively charged amino acids in ATP recognition by human P2X1 receptors. J Biol Chem 2000;275:35656.

Ennion SJ, Evans RJ. Conserved cysteine residues in the extracellular loop of the human P2X(1) receptor form disulfide bonds and are involved in receptor trafficking to the cell surface. Mol Pharmacol 2002;61:303-311.

Erichsen HK, Hao JX, Xu XJ, Blackburn-Munro G. A comparison of the antinociceptive effects of voltage-activated Na+ channel blockers in two rat models of neuropathic pain. Eur J Pharmacol 2003;458:275-282.

Eriksson NP, Persson JK, Svensson M, Arvidsson J, Molander C, Aldskogius H. A quantitative analysis of the microglial cell reaction in central primary sensory projection territories following peripheral nerve injury in the adult rat. Exp Brain Res 1993;96:19-27.

Evans RJ, Lewis C, Buell G, Valera S, North RA, Surprenant A. Pharmacological characterization of heterologously expressed ATP-gated cation channels (P2x purinoceptors). Mol Pharmacol 1995;48:178-183.

Evans RJ, Lewis C, Virginio C, Lundstrom K, Buell G, Surprenant A, North RA. Ionic permeability of, and divalent cation effects on, two ATP-gated cation channels (P2X receptors) expressed in mammalian cells. J Physiol 1996;497 (Pt 2):413-422.

Faria RX, Defarias FP, Alves LA. Are second messengers crucial for opening the pore associated with P2X7 receptor? Am J Physiol Cell Physiol 2005;288:C260-C271.

Fellin T, Gomez-Gonzalo M, Gobbo S, Carmignoto G, Haydon PG. Astrocytic glutamate is not necessary for the generation of epileptiform neuronal activity in hippocampal slices. J Neurosci 2006;26:9312-9322.

Fellin T, Pascual O, Gobbo S, Pozzan T, Haydon PG, Carmignoto G. Neuronal synchrony mediated by astrocytic glutamate through activation of extrasynaptic NMDA receptors. Neuron 2004;43:729-743.

Feng YH, Wang L, Wang Q, Li X, Zeng R, Gorodeski GI. ATP stimulates GRK-3 phosphorylation and beta-arrestin-2-dependent internalization of P2X7 receptor. Am J Physiol Cell Physiol 2005;288:C1342-C1356.

Ferrari D, Chiozzi P, Falzoni S, Dal SM, Melchiorri L, Baricordi OR, Di VF. Extracellular ATP triggers IL-1 beta release by activating the purinergic P2Z receptor of human macrophages. J Immunol 1997a;159:1451-1458.

Ferrari D, Chiozzi P, Falzoni S, Hanau S, Di VF. Purinergic modulation of interleukin-1 beta release from microglial cells stimulated with bacterial endotoxin. J Exp Med 1997b;185:579-582.

Ferrari D, Los M, Bauer MK, Vandenabeele P, Wesselborg S, Schulze-Osthoff K. P2Z purinoreceptor ligation induces activation of caspases with distinct roles in apoptotic and necrotic alterations of cell death. FEBS Lett 1999;447:71-75.

Ferrari D, Pizzirani C, Adinolfi E, Lemoli RM, Curti A, Idzko M, Panther E, Di VF. The P2X7 receptor: a key player in IL-1 processing and release. J Immunol 2006;176:3877-3883.

Ferrari D, Villalba M, Chiozzi P, Falzoni S, Ricciardi-Castagnoli P, Di VF. Mouse microglial cells express a plasma membrane pore gated by extracellular ATP. J Immunol 1996;156:1531-1539.

Fonfria E, Chambers LJ, Demont EH, Roman SA, Skaper SD, Michel AD. Species- and temperature-dependent effects of a novel P2X7 receptor antagonist on recombinant and native P2X7 receptors. Society for Neuroscience Annual Meeting Washington, D.C.(958.1.). 2005.
Ref Type: Abstract

Fonnum F, Johnsen A, Hassel B. Use of fluorocitrate and fluoroacetate in the study of brain metabolism. Glia 1997;21:106-113.

Fox A, Gentry C, Patel S, Kesingland A, Bevan S. Comparative activity of the anti-convulsants oxcarbazepine, carbamazepine, lamotrigine and gabapentin in a model of neuropathic pain in the rat and guinea-pig. Pain 2003;105:355-362.

Freist W, Verhey JF, Stuhmer W, Gauss DH. ATP binding site of P2X channel proteins: structural similarities with class II aminoacyl-tRNA synthetases. FEBS Lett 1998;434:61-65.

Gallis B, Prickett KS, Jackson J, Slack J, Schooley K, Sims JE, Dower SK. IL-1 induces rapid phosphorylation of the IL-1 receptor. J Immunol 1989;143:3235-3240.

Garcia-Guzman M, Soto F, Gomez-Hernandez JM, Lund PE, Stuhmer W. Characterization of recombinant human P2X4 receptor reveals pharmacological differences to the rat homologue. Mol Pharmacol 1997;51:109-118.

Garcia-Guzman M, Soto F, Laube B, Stuhmer W. Molecular cloning and functional expression of a novel rat heart P2X purinoceptor. FEBS Lett 1996;388:123-127.

Gargett CE, Wiley JS. The isoquinoline derivative KN-62 a potent antagonist of the P2Z-receptor of human lymphocytes. Br J Pharmacol 1997;120:1483-1490.

Garrison CJ, Dougherty PM, Kajander KC, Carlton SM. Staining of glial fibrillary acidic protein (GFAP) in lumbar spinal cord increases following a sciatic nerve constriction injury. Brain Res 1991;565:1-7.

Gauriau C, Bernard JF. A comparative reappraisal of projections from the superficial laminae of the dorsal horn in the rat: the forebrain. J Comp Neurol 2004;468:24-56.

Gonzalez-Martinez T, Perez-Pinera P, az-Esnal B, Vega JA. S-100 proteins in the human peripheral nervous system. Microsc Res Tech 2003;60:633-638.

Goodwin JS. Toxicity of nonsteroidal anti-inflammatory drugs. Arch Intern Med 1987;147:34-35.

Gordon GR, Baimoukhametova DV, Hewitt SA, Rajapaksha WR, Fisher TE, Bains JS. Norepinephrine triggers release of glial ATP to increase postsynaptic efficacy. Nat Neurosci 2005;8:1078-1086.

Gordon JL. Extracellular ATP: effects, sources and fate. Biochem J 1986;233:309-319.

Graham SH, Chen J, Lan J, Leach MJ, Simon RP. Neuroprotective effects of a use-dependent blocker of voltage-dependent sodium channels, BW619C89, in rat middle cerebral artery occlusion. J Pharmacol Exp Ther 1994;269:854-859.

Greig AV, Linge C, Terenghi G, McGrouther DA, Burnstock G. Purinergic receptors are part of a functional signaling system for proliferation and differentiation of human epidermal keratinocytes. J Invest Dermatol 2003;120:1007-1015.

Grubb BD, Evans RJ. Characterization of cultured dorsal root ganglion neuron P2X receptors. Eur J Neurosci 1999;11:149-154.

Grunze H, Greene RW, Moller HJ, Meyer T, Walden J. Lamotrigine may limit pathological excitation in the hippocampus by modulating a transient potassium outward current. Brain Res 1998a;791:330-334.

Grunze H, Von WJ, Greene RW, Walden J. Modulation of calcium and potassium currents by lamotrigine. Neuropsychobiology 1998b;38:131-138.

Gu BJ, Sluyter R, Skarratt KK, Shemon AN, Dao-Ung LP, Fuller SJ, Barden JA, Clarke AL, Petrou S, Wiley JS. An Arg307 to Gln polymorphism within the ATP-binding site causes loss of function of the human P2X7 receptor. J Biol Chem 2004;279:31287-31295.

Gu BJ, Zhang W, Worthington RA, Sluyter R, Dao-Ung P, Petrou S, Barden JA, Wiley JS. A Glu-496 to Ala polymorphism leads to loss of function of the human P2X7 receptor. J Biol Chem 2001;276:11135-11142.

Gu JG, MacDermott AB. Activation of ATP P2X receptors elicits glutamate release from sensory neuron synapses. Nature 1997;389:749-753.

Guo C, Masin M, Qureshi OS, Murrell-Lagnado RD. Evidence for functional P2X4/P2X7 heteromeric receptors. Mol Pharmacol 2007;72:1447-1456.

Guo LH, Trautmann K, Schluesener HJ. Expression of P2X4 receptor by lesional activated microglia during formalin-induced inflammatory pain. J Neuroimmunol 2005;163:120-127.

Gureje O, Von KM, Simon GE, Gater R. Persistent pain and well-being: a World Health Organization Study in Primary Care. JAMA 1998;280:147-151.

Guthrie PB, Knappenberger J, Segal M, Bennett MV, Charles AC, Kater SB. ATP released from astrocytes mediates glial calcium waves. J Neurosci 1999;19:520-528.

Haas SL, Ruether A, Singer MV, Schreiber S, Bocker U. Functional P2X7 receptor polymorphisms (His155Tyr, Arg307Gln, Glu496Ala) in patients with Crohn's disease. Scand J Immunol 2007;65:166-170.

Hagmann J, Burger MM, Dagan D. Regulation of plasma membrane blebbing by the cytoskeleton. J Cell Biochem 1999;73:488-499.

Hainsworth AH, McNaughton NC, Pereverzev A, Schneider T, Randall AD. Actions of sipatrigine, 202W92 and lamotrigine on R-type and T-type Ca2+ channel currents. Eur J Pharmacol 2003;467:77-80.

Hajos F, Csillik B, Knyihar-Csillik E. Alterations in glial fibrillary acidic protein immunoreactivity in the upper dorsal horn of the rat spinal cord in the course of transganglionic degenerative atrophy and regenerative proliferation. Neurosci Lett 1990;117:8-13.

Hall LL, Borke RC, Anders JJ. Transection or electrical stimulation of the hypoglossal nerve increases glial fibrillary acidic protein immunoreactivity in the hypoglossal nucleus. Brain Res 1989;490:157-161.

Hamon Y, Luciani MF, Becq F, Verrier B, Rubartelli A, Chimini G. Interleukin-1beta secretion is impaired by inhibitors of the ATP binding cassette transporter, ABC1. Blood 1997;90:2911-2915.

Hanani M. Satellite glial cells in sensory ganglia: from form to function. Brain Res Brain Res Rev 2005;48:457-476.

Hanani M, Huang TY, Cherkas PS, Ledda M, Pannese E. Glial cell plasticity in sensory ganglia induced by nerve damage. Neuroscience 2002;114:279-283.

Handwerker HO, Kobal G. Psychophysiology of experimentally induced pain. Physiol Rev 1993;73:639-671.

Hanisch UK, Kettenmann H. Microglia: active sensor and versatile effector cells in the normal and pathologic brain. Nat Neurosci 2007;10:1387-1394.

Haydon PG. GLIA: listening and talking to the synapse. Nat Rev Neurosci 2001;2:185-193.

Hayes GM, Woodroofe MN, Cuzner ML. Microglia are the major cell type expressing MHC class II in human white matter. J Neurol Sci 1987;80:25-37.

Hechler B, Lenain N, Marchese P, Vial C, Heim V, Freund M, Cazenave JP, Cattaneo M, Ruggeri ZM, Evans R, Gachet C. A role of the fast ATP-gated P2X1 cation channel in thrombosis of small arteries in vivo. J Exp Med 2003;198:661-667.

Hervas C, Perez-Sen R, Miras-Portugal MT. Presence of diverse functional P2X receptors in rat cerebellar synaptic terminals. Biochem Pharmacol 2005;70:770-785.

Hibell AD, Kidd EJ, Chessell IP, Humphrey PP, Michel AD. Apparent species differences in the kinetic properties of P2X(7) receptors. Br J Pharmacol 2000;130:167-173.

Hibell AD, Thompson KM, Simon J, Xing M, Humphrey PP, Michel AD. Species- and agonist-dependent differences in the deactivation-kinetics of P2X7 receptors. Naunyn Schmiedebergs Arch Pharmacol 2001a;363:639-648.

Hibell AD, Thompson KM, Xing M, Humphrey PP, Michel AD. Complexities of measuring antagonist potency at P2X(7) receptor orthologs. J Pharmacol Exp Ther 2001b;296:947-957.

Hide I, Tanaka M, Inoue A, Nakajima K, Kohsaka S, Inoue K, Nakata Y. Extracellular ATP triggers tumor necrosis factor-alpha release from rat microglia. J Neurochem 2000;75:965-972.

Hogquist KA, Nett MA, Unanue ER, Chaplin DD. Interleukin 1 is processed and released during apoptosis. Proc Natl Acad Sci U S A 1991;88:8485-8489.

Honore P, Donnelly-Roberts D, Namovic MT, Hsieh G, Zhu CZ, Mikusa JP, Hernandez G, Zhong C, Gauvin DM, Chandran P, Harris R, Medrano AP, Carroll W, Marsh K, Sullivan JP, Faltynek CR, Jarvis MF. A-740003 [N-(1-{[(cyanoimino)(5-quinolinylamino) methyl]amino}-2,2-dimethylpropyl)-2-(3,4-dimethoxyphenyl)acetamide], a novel and selective P2X7 receptor antagonist, dose-dependently reduces neuropathic pain in the rat. J Pharmacol Exp Ther 2006;319:1376-1385.

Huang CW, Huang CC, Liu YC, Wu SN. Inhibitory effect of lamotrigine on A-type potassium current in hippocampal neuron-derived H19-7 cells. Epilepsia 2004;45:729-736.

Humphreys BD, Virginio C, Surprenant A, Rice J, Dubyak GR. Isoquinolines as antagonists of the P2X7 nucleotide receptor: high selectivity for the human versus rat receptor homologues. Mol Pharmacol 1998;54:22-32.

Hunter JC, Gogas KR, Hedley LR, Jacobson LO, Kassotakis L, Thompson J, Fontana DJ. The effect of novel anti-epileptic drugs in rat experimental models of acute and chronic pain. Eur J Pharmacol 1997;324:153-160.

Illes P, Alexandre RJ. Molecular physiology of P2 receptors in the central nervous system. Eur J Pharmacol 2004;483:5-17.

Ilyin VI, Pomonis JD, Whiteside GT, Harrison JE, Pearson MS, Mark L, Turchin PI, Gottshall S, Carter RB, Nguyen P, Hogenkamp DJ, Olanrewaju S, Benjamin E, Woodward RM. Pharmacology of 2-[4-(4-chloro-2-fluorophenoxy)phenyl]-pyrimidine-4-carboxamide: a potent, broad-spectrum state-dependent sodium channel blocker for treating pain states. J Pharmacol Exp Ther 2006;318:1083-1093.

Inoue K, Tsuda M, Koizumi S. ATP- and adenosine-mediated signaling in the central nervous system: chronic pain and microglia: involvement of the ATP receptor P2X4. J Pharmacol Sci 2004;94:112-114.

Ireland MF, Noakes PG, Bellingham MC. P2X7-like receptor subunits enhance excitatory synaptic transmission at central synapses by presynaptic mechanisms. Neuroscience 2004;128:269-280.

Irnich D, Burgstahler R, Bostock H, Grafe P. ATP affects both axons and Schwann cells of unmyelinated C fibres. Pain 2001;92:343-350.

Ishii K, Kaneda M, Li H, Rockland KS, Hashikawa T. Neuron-specific distribution of P2X7 purinergic receptors in the monkey retina. J Comp Neurol 2003;459:267-277.

Jahr CE, Jessell TM. ATP excites a subpopulation of rat dorsal horn neurones. Nature 1983;304:730-733.

Janeway CA, Travers P, Walport M, Shlomchik M. Immunobiology. New York: Garland Publishing, 2001.

Jarvis MF. Contributions of P2X3 homomeric and heteromeric channels to acute and chronic pain. Expert Opin Ther Targets 2003;7:513-522.

Jarvis MF, Bianchi B, Uchic JT, Cartmell J, Lee CH, Williams M, Faltynek C. [3H]A-317491, a novel high-affinity non-nucleotide antagonist that specifically labels human P2X2/3 and P2X3 receptors. J Pharmacol Exp Ther 2004;310:407-416.

Jarvis MF, Burgard EC, McGaraughty S, Honore P, Lynch K, Brennan TJ, Subieta A, van BT, Cartmell J, Bianchi B, Niforatos W, Kage K, Yu H, Mikusa J, Wismer CT, Zhu CZ, Chu K, Lee CH, Stewart AO, Polakowski J, Cox BF, Kowaluk E, Williams M, Sullivan J, Faltynek C. A-317491, a novel potent and selective non-nucleotide antagonist of P2X3 and P2X2/3 receptors, reduces chronic inflammatory and neuropathic pain in the rat. Proc Natl Acad Sci U S A 2002;99:17179-17184.

Jerng HH, Kunjilwar K, Pfaffinger PJ. Multiprotein assembly of Kv4.2, KChIP3 and DPP10 produces ternary channel complexes with ISA-like properties. J Physiol 2005;568:767-788.

Jiang LH. Inhibition of P2X(7) receptors by divalent cations: old action and new insight. Eur Biophys J 2008.

Jiang LH, Mackenzie AB, North RA, Surprenant A. Brilliant blue G selectively blocks ATP-gated rat P2X(7) receptors. Mol Pharmacol 2000a;58:82-88.

Jiang LH, Rassendren F, Mackenzie A, Zhang YH, Surprenant A, North RA. N-methyl-D-glucamine and propidium dyes utilize different permeation pathways at rat P2X(7) receptors. Am J Physiol Cell Physiol 2005;289:C1295-C1302.

Jiang LH, Rassendren F, Surprenant A, North RA. Identification of amino acid residues contributing to the ATP-binding site of a purinergic P2X receptor. J Biol Chem 2000b;275:34190-34196.

Jo YH, Schlichter R. Synaptic corelease of ATP and GABA in cultured spinal neurons. Nat Neurosci 1999;2:241-245.

John GR, Simpson JE, Woodroofe MN, Lee SC, Brosnan CF. Extracellular nucleotides differentially regulate interleukin-1beta signaling in primary human astrocytes: implications for inflammatory gene expression. J Neurosci 2001;21:4134-4142.

Jonakait GM, Schotland S, Hart RP. Interleukin-1 specifically increases substance P in injured sympathetic ganglia. Ann N Y Acad Sci 1990;594:222-230.

Jones CA, Chessell IP, Simon J, Barnard EA, Miller KJ, Michel AD, Humphrey PP. Functional characterization of the P2X(4) receptor orthologues. Br J Pharmacol 2000;129:388-394.

Joshi SK, Hernandez G, Mikusa JP, Zhu CZ, Zhong C, Salyers A, Wismer CT, Chandran P, Decker MW, Honore P. Comparison of antinociceptive actions of standard analgesics in attenuating capsaicin and nerve-injury-induced mechanical hypersensitivity. Neuroscience 2006;143:587-596.

Kahlenberg JM, Dubyak GR. Mechanisms of caspase-1 activation by P2X7 receptor-mediated K+ release. Am J Physiol Cell Physiol 2004;286:C1100-C1108.

Kai-Kai MA, Howe R. Glutamate-immunoreactivity in the trigeminal and dorsal root ganglia, and intraspinal neurons and fibres in the dorsal horn of the rat. Histochem J 1991;23:171-179.

Kang TC, Park SK, Hwang IK, An SJ, Won MH. GABA(B) receptor-mediated regulation of P2X7 receptor expression in the gerbil hippocampus. Brain Res Mol Brain Res 2004;121:12-18.

Katsetos CD, Herman MM, Mork SJ. Class III beta-tubulin in human development and cancer. Cell Motil Cytoskeleton 2003;55:77-96.

Kawai S. Cyclooxygenase selectivity and the risk of gastro-intestinal complications of various non-steroidal anti-inflammatory drugs: a clinical consideration. Inflamm Res 1998;47 Suppl 2:S102-S106.

Keast JR, Stephensen TM. Glutamate and aspartate immunoreactivity in dorsal root ganglion cells supplying visceral and somatic targets and evidence for peripheral axonal transport. J Comp Neurol 2000;424:577-587.

Kettenmann H, Schachner M. Pharmacological properties of gamma-aminobutyric acid-, glutamate-, and aspartate-induced depolarizations in cultured astrocytes. J Neurosci 1985;5:3295-3301.

Khakh BS, Bao XR, Labarca C, Lester HA. Neuronal P2X transmitter-gated cation channels change their ion selectivity in seconds. Nat Neurosci 1999a;2:322-330.

Khakh BS, Proctor WR, Dunwiddie TV, Labarca C, Lester HA. Allosteric control of gating and kinetics at P2X(4) receptor channels. J Neurosci 1999b;19:7289-7299.

Kidd EJ, Grahames CB, Simon J, Michel AD, Barnard EA, Humphrey PP. Localization of P2X purinoceptor transcripts in the rat nervous system. Mol Pharmacol 1995;48:569-573.

Kim M, Jiang LH, Wilson HL, North RA, Surprenant A. Proteomic and functional evidence for a P2X7 receptor signalling complex. EMBO J 2001a;20:6347-6358.

Kim M, Spelta V, Sim J, North RA, Surprenant A. Differential assembly of rat purinergic P2X7 receptor in immune cells of the brain and periphery. J Biol Chem 2001b;276:23262-23267.

King BF, Townsend-Nicholson A, Wildman SS, Thomas T, Spyer KM, Burnstock G. Coexpression of rat P2X2 and P2X6 subunits in Xenopus oocytes. J Neurosci 2000;20:4871-4877.

King BF, Wildman SS, Ziganshina LE, Pintor J, Burnstock G. Effects of extracellular pH on agonism and antagonism at a recombinant P2X2 receptor. Br J Pharmacol 1997;121:1445-1453.

Klapperstuck M, Buttner C, Bohm T, Schmalzing G, Markwardt F. Characteristics of P2X7 receptors from human B lymphocytes expressed in Xenopus oocytes. Biochim Biophys Acta 2000a;1467:444-456.

Klapperstuck M, Buttner C, Nickel P, Schmalzing G, Lambrecht G, Markwardt F. Antagonism by the suramin analogue NF279 on human P2X(1) and P2X(7) receptors. Eur J Pharmacol 2000b;387:245-252.

Klapperstuck M, Buttner C, Schmalzing G, Markwardt F. Functional evidence of distinct ATP activation sites at the human P2X(7) receptor. J Physiol 2001;534:25-35.

Kobayashi K, Fukuoka T, Yamanaka H, Dai Y, Obata K, Tokunaga A, Noguchi K. Differential expression patterns of mRNAs for P2X receptor subunits in neurochemically characterized dorsal root ganglion neurons in the rat. J Comp Neurol 2005;481:377-390.

Kobayashi K, Fukuoka T, Yamanaka H, Dai Y, Obata K, Tokunaga A, Noguchi K. Neurons and glial cells differentially express P2Y receptor mRNAs in the rat dorsal root ganglion and spinal cord. J Comp Neurol 2006;498:443-454.

Koles L, Furst S, Illes P. P2X and P2Y receptors as possible targets of therapeutic manipulations in CNS illnesses. Drug News Perspect 2005;18:85-101.

Kostura MJ, Tocci MJ, Limjuco G, Chin J, Cameron P, Hillman AG, Chartrain NA, Schmidt JA. Identification of a monocyte specific pre-interleukin 1 beta convertase activity. Proc Natl Acad Sci U S A 1989;86:5227-5231.

Kress M, Reeh PW. In: Belmont C, Cervero F, editors. Neurobiology of Nociceptors. New York: Oxford University Press., 1996. pp. 370-389.

Kreutzberg GW. Microglia: a sensor for pathological events in the CNS. Trends Neurosci 1996;19:312-318.

Krishtal OA, Marchenko SM, Pidoplichko VI. Receptor for ATP in the membrane of mammalian sensory neurones. Neurosci Lett 1983;35:41-45.

Kukley M, Barden JA, Steinhauser C, Jabs R. Distribution of P2X receptors on astrocytes in juvenile rat hippocampus. Glia 2001;36:11-21.

Kukley M, Stausberg P, Adelmann G, Chessell IP, Dietrich D. Ecto-nucleotidases and nucleoside transporters mediate activation of adenosine receptors on hippocampal mossy fibers by P2X7 receptor agonist 2'-3'-O-(4-benzoylbenzoyl)-ATP. J Neurosci 2004;24:7128-7139.

Kumagai M, Saino T. Effects of ATP on intracellular calcium dynamics of neurons and satellite cells in rat superior cervical ganglia. Histochem Cell Biol 2001;115:285-292.

Kuo CC. A common anticonvulsant binding site for phenytoin, carbamazepine, and lamotrigine in neuronal Na+ channels. Mol Pharmacol 1998;54:712-721.

Kuo CC, Lu L. Characterization of lamotrigine inhibition of Na+ channels in rat hippocampal neurones. Br J Pharmacol 1997;121:1231-1238.

Labasi JM, Petrushova N, Donovan C, McCurdy S, Lira P, Payette MM, Brissette W, Wicks JR, Audoly L, Gabel CA. Absence of the P2X7 receptor alters leukocyte function and attenuates an inflammatory response. J Immunol 2002;168:6436-6445.

Lai CP, Bechberger JF, Thompson RJ, MacVicar BA, Bruzzone R, Naus CC. Tumor-suppressive effects of pannexin 1 in C6 glioma cells. Cancer Res 2007;67:1545-1554.

Lappin SC, Winyard L, Clayton N, Chambers LJ, Demont EH, Chessell IP, Richardson JC, Gunthorpe MJ. Reversal of mechanical hyperalgesia in a rat model of inflammatory pain by a potent and selective P2X7 antagonist. Society for Neuroscience Washington(,

L.J., Demont, E.H., Chessell, I.P., Richardson, J.C. & Gunthorpe, M.J.). 2005.
Ref Type: Abstract

Le Feuvre R, Brough D, Rothwell N. Extracellular ATP and P2X7 receptors in neurodegeneration. Eur J Pharmacol 2002a;447:261-269.

Le Feuvre RA, Brough D, Iwakura Y, Takeda K, Rothwell NJ. Priming of macrophages with lipopolysaccharide potentiates P2X7-mediated cell death via a caspase-1-dependent mechanism, independently of cytokine production. J Biol Chem 2002b;277:3210-3218.

Le Feuvre RA, Brough D, Touzani O, Rothwell NJ. Role of P2X7 receptors in ischemic and excitotoxic brain injury in vivo. J Cereb Blood Flow Metab 2003;23:381-384.

Le KT, Babinski K, Seguela P. Central P2X4 and P2X6 channel subunits coassemble into a novel heteromeric ATP receptor. J Neurosci 1998;18:7152-7159.

Leach MJ, Marden CM, Miller AA. Pharmacological studies on lamotrigine, a novel potential antiepileptic drug: II. Neurochemical studies on the mechanism of action. Epilepsia 1986;27:490-497.

Leach MJ, Swan JH, Eisenthal D, Dopson M, Nobbs M. BW619C89, a glutamate release inhibitor, protects against focal cerebral ischemic damage. Stroke 1993;24:1063-1067.

Ledeboer A, Sloane EM, Milligan ED, Frank MG, Mahony JH, Maier SF, Watkins LR. Minocycline attenuates mechanical allodynia and proinflammatory cytokine expression in rat models of pain facilitation. Pain 2005;115:71-83.

Lewis C, Neidhart S, Holy C, North RA, Buell G, Surprenant A. Coexpression of P2X2 and P2X3 receptor subunits can account for ATP-gated currents in sensory neurons. Nature 1995;377:432-435.

Li RH, Sliwkowski MX, Lo J, Mather JP. Establishment of Schwann cell lines from normal adult and embryonic rat dorsal root ganglia. J Neurosci Methods 1996;67:57-69.

Lifschitz MD. Renal effects of nonsteroidal anti-inflammatory agents. J Lab Clin Med 1983;102:313-323.

Lindblom U, Merskey H, Mumford J.M, Nathan P.W, Noordenbos W., Sunderland S. Pain terms a current list with definitions and notes on usage. Pain 1986;24:S215-S221.

Lindsay RM. Nerve growth factors (NGF, BDNF) enhance axonal regeneration but are not required for survival of adult sensory neurons. J Neurosci 1988;8:2394-2405.

Lister MF, Sharkey J, Sawatzky DA, Hodgkiss JP, Davidson DJ, Rossi AG, Finlayson K. The role of the purinergic P2X7 receptor in inflammation. J Inflamm (Lond) 2007;4:5.

Liu G, Yarov-Yarovoy V, Nobbs M, Clare JJ, Scheuer T, Catterall WA. Differential interactions of lamotrigine and related drugs with transmembrane segment IVS6 of voltage-gated sodium channels. Neuropharmacology 2003;44:413-422.

Liu HT, Toychiev AH, Takahashi N, Sabirov RZ, Okada Y. Maxi-anion channel as a candidate pathway for osmosensitive ATP release from mouse astrocytes in primary culture. Cell Res 2008a;18:558-565.

Liu X, Surprenant A, Mao HJ, Roger S, Xia R, Bradley H, Jiang LH. Identification of key residues coordinating functional inhibition of P2X7 receptors by zinc and copper. Mol Pharmacol 2008b;73:252-259.

Locovei S, Scemes E, Qiu F, Spray DC, Dahl G. Pannexin1 is part of the pore forming unit of the P2X(7) receptor death complex. FEBS Lett 2007;581:483-488.

Lu X, Richardson PM. Inflammation near the nerve cell body enhances axonal regeneration. J Neurosci 1991;11:972-978.

Lunardi G, Leandri M, Albano C, Cultrera S, Fracassi M, Rubino V, Favale E. Clinical effectiveness of lamotrigine and plasma levels in essential and symptomatic trigeminal neuralgia. Neurology 1997;48:1714-1717.

Lundy PM, Nelson P, Mi L, Frew R, Minaker S, Vair C, Sawyer TW. Pharmacological differentiation of the P2X7 receptor and the maitotoxin-activated cationic channel. Eur J Pharmacol 2004;487:17-28.

Lynn B. Neurogenic inflammation caused by cutaneous polymodal receptors. Prog Brain Res 1996;113:361-368.

Lyons SA, Morell P, McCarthy KD. Schwann cells exhibit P2Y purinergic receptors that regulate intracellular calcium and are up-regulated by cyclic AMP analogues. J Neurochem 1994;63:552-560.

Ma W, Korngreen A, Weil S, Cohen EB, Priel A, Kuzin L, Silberberg SD. Pore properties and pharmacological features of the P2X receptor channel in airway ciliated cells. J Physiol 2006;571:503-517.

Mackenzie A, Wilson HL, Kiss-Toth E, Dower SK, North RA, Surprenant A. Rapid secretion of interleukin-1beta by microvesicle shedding. Immunity 2001;15:825-835.

Martinez-Francois JR, Morales-Tlalpan V, Vaca L. Characterization of the maitotoxin-activated cationic current from human skin fibroblasts. J Physiol 2002;538:79-86.

Martinon F, Tschopp J. Inflammatory caspases: linking an intracellular innate immune system to autoinflammatory diseases. Cell 2004;117:561-574.

Matsuo F. Lamotrigine. Epilepsia 1999;40 Suppl 5:S30-S36.

McCabe PH. New anti-epileptic drugs for the 21st century. Expert Opin Pharmacother 2000;1:633-674.

McCleane GJ. Lamotrigine in the management of neuropathic pain: a review of the literature. Clin J Pain 2000;16:321-326.

McGaraughty S, Jarvis MF. Antinociceptive properties of a non-nucleotide P2X3/P2X2/3 receptor antagonist. Drug News Perspect 2005;18:501-507.

McGaraughty S, Wismer CT, Zhu CZ, Mikusa J, Honore P, Chu KL, Lee CH, Faltynek CR, Jarvis MF. Effects of A-317491, a novel and selective P2X3/P2X2/3 receptor antagonist, on neuropathic, inflammatory and chemogenic nociception following intrathecal and intraplantar administration. Br J Pharmacol 2003;140:1381-1388.

McNaughton NC, Hainsworth AH, Green PJ, Randall AD. Inhibition of recombinant low-voltage-activated Ca(2+) channels by the neuroprotective agent BW619C89 (Sipatrigine). Neuropharmacology 2000;39:1247-1253.

McNaughton NC, Leach MJ, Hainsworth AH, Randall AD. Inhibition of human N-type voltage-gated Ca2+ channels by the neuroprotective agent BW619C89. Neuropharmacology 1997;36:1795-1798.

Meldrum BS. The role of glutamate in epilepsy and other CNS disorders. Neurology 1994;44:S14-S23.

Meller ST, Dykstra C, Grzybycki D, Murphy S, Gebhart GF. The possible role of glia in nociceptive processing and hyperalgesia in the spinal cord of the rat. Neuropharmacology 1994;33:1471-1478.

Mellor JR, Randall AD. Voltage-dependent deactivation and desensitization of GABA responses in cultured murine cerebellar granule cells. J Physiol. 15(506), 377-390. 1998. Ref Type: Abstract

Michel AD, Chessell IP, Humphrey PP. Ionic effects on human recombinant P2X7 receptor function. Naunyn Schmiedebergs Arch Pharmacol 1999;359:102-109.

Michel AD, Kaur R, Chessell IP, Humphrey PP. Antagonist effects on human P2X(7) receptor-mediated cellular accumulation of YO-PRO-1. Br J Pharmacol 2000;130:513-520.

Mico JA, Ardid D, Berrocoso E, Eschalier A. Antidepressants and pain. Trends Pharmacol Sci 2006;27:348-354.

Migita K, Haines WR, Voigt MM, Egan TM. Polar residues of the second transmembrane domain influence cation permeability of the ATP-gated P2X(2) receptor. J Biol Chem 2001;276:30934-30941.

Millan MJ. The induction of pain: an integrative review. Prog Neurobiol 1999;57:1-164.

Miller KE, Richards BA, Kriebel RM. Glutamine-, glutamine synthetase-, glutamate dehydrogenase- and pyruvate carboxylase-immunoreactivities in the rat dorsal root ganglion and peripheral nerve. Brain Res 2002;945:202-211.

Milligan ED, Mehmert KK, Hinde JL, Harvey LO, Martin D, Tracey KJ, Maier SF, Watkins LR. Thermal hyperalgesia and mechanical allodynia produced by intrathecal administration of the human immunodeficiency virus-1 (HIV-1) envelope glycoprotein, gp120. Brain Res 2000;861:105-116.

Milligan ED, O'Connor KA, Nguyen KT, Armstrong CB, Twining C, Gaykema RP, Holguin A, Martin D, Maier SF, Watkins LR. Intrathecal HIV-1 envelope glycoprotein gp120 induces enhanced pain states mediated by spinal cord proinflammatory cytokines. J Neurosci 2001;21:2808-2819.

Milligan ED, Twining C, Chacur M, Biedenkapp J, O'Connor K, Poole S, Tracey K, Martin D, Maier SF, Watkins LR. Spinal glia and proinflammatory cytokines mediate mirror-image neuropathic pain in rats. J Neurosci 2003;23:1026-1040.

Mollace V, Colasanti M, Muscoli C, Lauro GM, Iannone M, Rotiroti D, Nistico G. The effect of nitric oxide on cytokine-induced release of PGE2 by human cultured astroglial cells. Br J Pharmacol 1998;124:742-746.

Morgan E, Mikhail MS, Murray MJ. Pain Management. Clinical Anesthesiology McGraw-Hill, 2005.

Morris RG, Black AB, Harris AL, Batty AB, Sallustio BC. Lamotrigine and therapeutic drug monitoring: retrospective survey following the introduction of a routine service. Br J Clin Pharmacol 1998;46:547-551.

Mulryan K, Gitterman DP, Lewis CJ, Vial C, Leckie BJ, Cobb AL, Brown JE, Conley EC, Buell G, Pritchard CA, Evans RJ. Reduced vas deferens contraction and male infertility in mice lacking P2X1 receptors. Nature 2000;403:86-89.

Musset B, Cherny VV, Morgan D, Okamura Y, Ramsey IS, Clapham DE, DeCoursey TE. Detailed comparison of expressed and native voltage-gated proton channel currents. J Physiol 2008;586:2477-2486.

Nakamura-Craig M, Follenfant RL. Effect of lamotrigine in the acute and chronic hyperalgesia induced by PGE2 and in the chronic hyperalgesia in rats with streptozotocin-induced diabetes. Pain 1995;63:33-37.

Narcisse L, Scemes E, Zhao Y, Lee SC, Brosnan CF. The cytokine IL-1beta transiently enhances P2X7 receptor expression and function in human astrocytes. Glia 2005;49:245-258.

Nascimento RS, Santiago MF, Marques SA, Allodi S, Martinez AM. Diversity among satellite glial cells in dorsal root ganglia of the rat. Braz J Med Biol Res 2008.

Neary JT, van BC, Forster E, Norenberg LO, Norenberg MD. ATP stimulates calcium influx in primary astrocyte cultures. Biochem Biophys Res Commun 1988;157:1410-1416.

Nelson DW, Sarris K, Kalvin DM, Namovic MT, Grayson G, Donnelly-Roberts DL, Harris R, Honore P, Jarvis MF, Faltynek CR, Carroll WA. Structure-activity relationship studies on N'-aryl carbohydrazide P2X7 antagonists. J Med Chem 2008;51:3030-3034.

Newbolt A, Stoop R, Virginio C, Surprenant A, North RA, Buell G, Rassendren F. Membrane topology of an ATP-gated ion channel (P2X receptor). J Biol Chem 1998;273:15177-15182.

Nicke A, Baumert HG, Rettinger J, Eichele A, Lambrecht G, Mutschler E, Schmalzing G. P2X1 and P2X3 receptors form stable trimers: a novel structural motif of ligand-gated ion channels. EMBO J 1998;17:3016-3028.

Nicke A, Kerschensteiner D, Soto F. Biochemical and functional evidence for heteromeric assembly of P2X1 and P2X4 subunits. J Neurochem 2005;92:925-933.

Nimmerjahn A, Kirchhoff F, Helmchen F. Resting microglial cells are highly dynamic surveillants of brain parenchyma in vivo. Science 2005;308:1314-1318.

Norenberg MD, Martinez-Hernandez A. Fine structural localization of glutamine synthetase in astrocytes of rat brain. Brain Res 1979;161:303-310.

North RA. P2X receptors: a third major class of ligand-gated ion channels. Ciba Found Symp 1996;198:91-105.

North RA. Molecular physiology of P2X receptors. Physiol Rev 2002;82:1013-1067.

North RA, Surprenant A. Pharmacology of cloned P2X receptors. Annu Rev Pharmacol Toxicol 2000;40:563-580.

Novakovic SD, Kassotakis LC, Oglesby IB, Smith JA, Eglen RM, Ford AP, Hunter JC. Immunocytochemical localization of P2X3 purinoceptors in sensory neurons in naive rats and following neuropathic injury. Pain 1999;80:273-282.

Olsson Y. Microenvironment of the peripheral nervous system under normal and pathological conditions. Crit Rev Neurobiol 1990;5:265-311.

Panchin Y, Kelmanson I, Matz M, Lukyanov K, Usman N, Lukyanov S. A ubiquitous family of putative gap junction molecules. Curr Biol 2000;10:R473-R474.

Panchin YV. Evolution of gap junction proteins--the pannexin alternative. J Exp Biol 2005;208:1415-1419.

Panenka W, Jijon H, Herx LM, Armstrong JN, Feighan D, Wei T, Yong VW, Ransohoff RM, MacVicar BA. P2X7-like receptor activation in astrocytes increases chemokine

monocyte chemoattractant protein-1 expression via mitogen-activated protein kinase. J Neurosci 2001;21:7135-7142.

Pannese E. The satellite cells of the sensory ganglia. Adv Anat Embryol Cell Biol 1981;65:1-111.

Papp L, Vizi ES, Sperlagh B. Lack of ATP-evoked GABA and glutamate release in the hippocampus of P2X7 receptor-/- mice. Neuroreport 2004;15:2387-2391.

Parpura V, Scemes E, Spray DC. Mechanisms of glutamate release from astrocytes: gap junction "hemichannels", purinergic receptors and exocytotic release. Neurochem Int 2004;45:259-264.

Parvathenani LK, Tertyshnikova S, Greco CR, Roberts SB, Robertson B, Posmantur R. P2X7 mediates superoxide production in primary microglia and is up-regulated in a transgenic mouse model of Alzheimer's disease. J Biol Chem 2003;278:13309-13317.

Paukert M, Osteroth R, Geisler HS, Brandle U, Glowatzki E, Ruppersberg JP, Grunder S. Inflammatory mediators potentiate ATP-gated channels through the P2X(3) subunit. J Biol Chem 2001;276:21077-21082.

Paulsen RE, Contestabile A, Villani L, Fonnum F. An in vivo model for studying function of brain tissue temporarily devoid of glial cell metabolism: the use of fluorocitrate. J Neurochem 1987;48:1377-1385.

Peck AW. Clinical pharmacology of lamotrigine. Epilepsia 1991;32 Suppl 2:S9-12.

Pelegrin P, Surprenant A. Pannexin-1 mediates large pore formation and interleukin-1beta release by the ATP-gated P2X7 receptor. EMBO J 2006;25:5071-5082.

Pelegrin P, Surprenant A. Pannexin-1 couples to maitotoxin- and nigericin-induced interleukin-1beta release through a dye uptake-independent pathway. J Biol Chem 2007;282:2386-2394.

Perregaux D, Gabel CA. Interleukin-1 beta maturation and release in response to ATP and nigericin. Evidence that potassium depletion mediated by these agents is a necessary and common feature of their activity. J Biol Chem 1994;269:15195-15203.

Peters A. Observation on the connexions between myelin sheaths and glial cells in the optic nerves of young rats. J Anat 1964;98:125-134.

Peters A, Palay SL, Webster Hd. The fine structure of the nervous system. J Anat 1964;98:125-134.

Petrou S, Ugur M, Drummond RM, Singer JJ, Walsh JV, Jr. P2X7 purinoceptor expression in Xenopus oocytes is not sufficient to produce a pore-forming P2Z-like phenotype. FEBS Lett 1997;411:339-345.

Petruska JC, Cooper BY, Gu JG, Rau KK, Johnson RD. Distribution of P2X1, P2X2, and P2X3 receptor subunits in rat primary afferents: relation to population markers and specific cell types. J Chem Neuroanat 2000;20:141-162.

Pfeiffer ZA, Aga M, Prabhu U, Watters JJ, Hall DJ, Bertics PJ. The nucleotide receptor P2X7 mediates actin reorganization and membrane blebbing in RAW 264.7 macrophages via p38 MAP kinase and Rho. J Leukoc Biol 2004;75:1173-1182.

Pitkanen A, Sutula TP. Is epilepsy a progressive disorder? Prospects for new therapeutic approaches in temporal-lobe epilepsy. Lancet Neurol 2002;1:173-181.

Prince DA. Neurophysiology of epilepsy. Annu.Rev.Neurosci. 1, 395-415. 1978.
Ref Type: Abstract

Radford KM, Virginio C, Surprenant A, North RA, Kawashima E. Baculovirus expression provides direct evidence for heteromeric assembly of P2X2 and P2X3 receptors. J Neurosci 1997;17:6529-6533.

Raghavendra V, Rutkowski MD, DeLeo JA. The role of spinal neuroimmune activation in morphine tolerance/hyperalgesia in neuropathic and sham-operated rats. J Neurosci 2002;22:9980-9989.

Raghavendra V, Tanga F, DeLeo JA. Inhibition of microglial activation attenuates the development but not existing hypersensitivity in a rat model of neuropathy. J Pharmacol Exp Ther 2003;306:624-630.

Raghavendra V, Tanga FY, DeLeo JA. Attenuation of morphine tolerance, withdrawal-induced hyperalgesia, and associated spinal inflammatory immune responses by propentofylline in rats. Neuropsychopharmacology 2004a;29:327-334.

Raghavendra V, Tanga FY, DeLeo JA. Complete Freunds adjuvant-induced peripheral inflammation evokes glial activation and proinflammatory cytokine expression in the CNS. Eur J Neurosci 2004b;20:467-473.

Ralevic V, Burnstock G. Receptors for purines and pyrimidines. Pharmacol Rev 1998;50:413-492.

Ramer MS, Kawaja MD, Henderson JT, Roder JC, Bisby MA. Glial overexpression of NGF enhances neuropathic pain and adrenergic sprouting into DRG following chronic sciatic constriction in mice. Neurosci Lett 1998;251:53-56.

Ramer MS, Thompson SW, McMahon SB. Causes and consequences of sympathetic basket formation in dorsal root ganglia. Pain 1999;Suppl 6:S111-S120.

Ramirez AN, Kunze DL. P2X purinergic receptor channel expression and function in bovine aortic endothelium. Am J Physiol Heart Circ Physiol 2002;282:H2106-H2116.

Rappold PM, Lynd-Balta E, Joseph SA. P2X7 receptor immunoreactive profile confined to resting and activated microglia in the epileptic brain. Brain Res 2006;1089:171-178.

Rassendren F, Buell GN, Virginio C, Collo G, North RA, Surprenant A. The permeabilizing ATP receptor, P2X7. Cloning and expression of a human cDNA. J Biol Chem 1997;272:5482-5486.

Ravizza T, Gagliardi B, Noe F, Boer K, Aronica E, Vezzani A. Innate and adaptive immunity during epileptogenesis and spontaneous seizures: evidence from experimental models and human temporal lobe epilepsy. Neurobiol Dis 2008;29:142-160.

Reddy NL, Fan W, Magar SS, Perlman ME, Yost E, Zhang L, Berlove D, Fischer JB, Burke-Howie K, Wolcott T, Durant GJ. Synthesis and pharmacological evaluation of N,N'-diarylguanidines as potent sodium channel blockers and anticonvulsant agents. J Med Chem 1998;41:3298-3302.

Ren J, Bian X, DeVries M, Schnegelsberg B, Cockayne DA, Ford AP, Galligan JJ. P2X2 subunits contribute to fast synaptic excitation in myenteric neurons of the mouse small intestine. J Physiol 2003;552:809-821.

Rettinger J, Aschrafi A, Schmalzing G. Roles of individual N-glycans for ATP potency and expression of the rat P2X1 receptor. J Biol Chem 2000;275:33542-33547.

Rettinger J, Braun K, Hochmann H, Kassack MU, Ullmann H, Nickel P, Schmalzing G, Lambrecht G. Profiling at recombinant homomeric and heteromeric rat P2X receptors identifies the suramin analogue NF449 as a highly potent P2X1 receptor antagonist. Neuropharmacology 2005;48:461-468.

Rhee JS, Wang ZM, Nabekura J, Inoue K, Akaike N. ATP facilitates spontaneous glycinergic IPSC frequency at dissociated rat dorsal horn interneuron synapses. J Physiol 2000;524 Pt 2:471-483.

Rizzo MA, Kocsis JD, Waxman SG. Selective loss of slow and enhancement of fast Na+ currents in cutaneous afferent dorsal root ganglion neurones following axotomy. Neurobiol Dis 1995;2:87-96.

Roberts JA, Evans RJ. ATP binding at human P2X1 receptors. Contribution of aromatic and basic amino acids revealed using mutagenesis and partial agonists. J Biol Chem 2004;279:9043-9055.

Roberts JA, Vial C, Digby HR, Agboh KC, Wen H, tterbury-Thomas A, Evans RJ. Molecular properties of P2X receptors. Pflugers Arch 2006;452:486-500.

Romagnoli R, Baraldi PG, Cruz-Lopez O, Lopez-Cara C, Preti D, Borea PA, Gessi S. The P2X7 receptor as a therapeutic target. Expert Opin Ther Targets 2008;12:647-661.

Romagnoli R, Baraldi PG, Di Virgilio F. Recent progress in the discovery of antagonists acting at P2X7 receptor. Expert Opin Ther Patents 2005; 15:271-287.

Ruggieri MR, Sr. Mechanisms of disease: role of purinergic signaling in the pathophysiology of bladder dysfunction. Nat Clin Pract Urol 2006;3:206-215.

Samad TA, Moore KA, Sapirstein A, Billet S, Allchorne A, Poole S, Bonventre JV, Woolf CJ. Interleukin-1beta-mediated induction of Cox-2 in the CNS contributes to inflammatory pain hypersensitivity. Nature 2001;410:471-475.

Samways DS, Li Z, Egan TM. Binding, gating, and conduction of ATP-gated ion channels. In: Arias H, editor. Biophysical Aspects of Ligand-Gated Ion Channel Receptor Superfamilies. Kerala: Research Signpost, Kerala, 2006. pp. 419-443.

Sanchez-Nogueiro J, Marin-Garcia P, Miras-Portugal MT. Characterization of a functional P2X(7)-like receptor in cerebellar granule neurons from P2X(7) knockout mice. FEBS Lett 2005;579:3783-3788.

Sanz JM, Di Virgilio F. Kinetics and mechanism of ATP-dependent IL-1 beta release from microglial cells. J Immunol 2000;164:4893-4898.

Sapp DW, Yeh HH. Ethanol-GABAA receptor interactions: a comparison between cell lines and cerebellar Purkinje cells. J Pharmacol Exp Ther 1998;284:768-776.

Sawynok J, Downie JW, Reid AR, Cahill CM, White TD. ATP release from dorsal spinal cord synaptosomes: characterization and neuronal origin. Brain Res 1993;610:32-38.

Schilling WP, Sinkins WG, Estacion M. Maitotoxin activates a nonselective cation channel and a P2Z/P2X(7)-like cytolytic pore in human skin fibroblasts. Am J Physiol 1999a;277:C755-C765.

Schilling WP, Wasylyna T, Dubyak GR, Humphreys BD, Sinkins WG. Maitotoxin and P2Z/P2X(7) purinergic receptor stimulation activate a common cytolytic pore. Am J Physiol 1999b;277:C766-C776.

Scholz J, Woolf CJ. The neuropathic pain triad: neurons, immune cells and glia. Nat Neurosci 2007;10:1361-1368.

Schwei MJ, Honore P, Rogers SD, Salak-Johnson JL, Finke MP, Ramnaraine ML, Clohisy DR, Mantyh PW. Neurochemical and cellular reorganization of the spinal cord in a murine model of bone cancer pain. J Neurosci 1999;19:10886-10897.

Seguela P, Haghighi A, Soghomonian JJ, Cooper E. A novel neuronal P2x ATP receptor ion channel with widespread distribution in the brain. J Neurosci 1996;16:448-455.

Shigemoto-Mogami Y, Koizumi S, Tsuda M, Ohsawa K, Kohsaka S, Inoue K. Mechanisms underlying extracellular ATP-evoked interleukin-6 release in mouse microglial cell line, MG-5. J Neurochem 2001;78:1339-1349.

Silberberg SD, Chang TH, Swartz KJ. Secondary structure and gating rearrangements of transmembrane segments in rat P2X4 receptor channels. J Gen Physiol 2005;125:347-359.

Sim JA, Chaumont S, Jo J, Ulmann L, Young MT, Cho K, Buell G, North RA, Rassendren F. Altered hippocampal synaptic potentiation in P2X4 knock-out mice. J Neurosci 2006;26:9006-9009.

Sim JA, Young MT, Sung HY, North RA, Surprenant A. Reanalysis of P2X7 receptor expression in rodent brain. J Neurosci 2004;24:6307-6314.

Simon J, Kidd EJ, Smith FM, Chessell IP, Murrell-Lagnado R, Humphrey PP, Barnard EA. Localization and functional expression of splice variants of the P2X2 receptor. Mol Pharmacol 1997;52:237-248.

Sjostrand J. Neuroglial proliferation in the hypoglossal nucleus after nerve injury. Exp Neurol 1971;30:178-189.

Smart ML, Gu B, Panchal RG, Wiley J, Cromer B, Williams DA, Petrou S. P2X7 receptor cell surface expression and cytolytic pore formation are regulated by a distal C-terminal region. J Biol Chem 2003;278:8853-8860.

Smith FM, Humphrey PP, Murrell-Lagnado RD. Identification of amino acids within the P2X2 receptor C-terminus that regulate desensitization. J Physiol 1999;520 Pt 1:91-99.

Smith SE, Hodges H, Sowinski P, Man CM, Leach MJ, Sinden JD, Gray JA, Meldrum BS. Long-term beneficial effects of BW619C89 on neurological deficit, cognitive deficit and brain damage after middle cerebral artery occlusion in the rat. Neuroscience 1997;77:1123-1135.

Solle M, Labasi J, Perregaux DG, Stam E, Petrushova N, Koller BH, Griffiths RJ, Gabel CA. Altered cytokine production in mice lacking P2X(7) receptors. J Biol Chem 2001;276:125-132.

Sommer C, Petrausch S, Lindenlaub T, Toyka KV. Neutralizing antibodies to interleukin 1-receptor reduce pain associated behavior in mice with experimental neuropathy. Neurosci Lett 1999;270:25-28.

Sondergaard KM, Nielsen KA, Dahl M, Wolf P. Lamotrigine therapeutic thresholds. Seizure 2008;17:391-395.

Song P, Zhao ZQ. The involvement of glial cells in the development of morphine tolerance. Neurosci Res 2001;39:281-286.

Soto F, Garcia-Guzman M, Gomez-Hernandez JM, Hollmann M, Karschin C, Stuhmer W. P2X4: an ATP-activated ionotropic receptor cloned from rat brain. Proc Natl Acad Sci U S A 1996;93:3684-3688.

Soto F, Lambrecht G, Nickel P, Stuhmer W, Busch AE. Antagonistic properties of the suramin analogue NF023 at heterologously expressed P2X receptors. Neuropharmacology 1999;38:141-149.

Spataro LE, Sloane EM, Milligan ED, Wieseler-Frank J, Schoeniger D, Jekich BM, Barrientos RM, Maier SF, Watkins LR. Spinal gap junctions: potential involvement in pain facilitation. J Pain 2004;5:392-405.

Spencer HJ, Gribkoff VK, Cotman CW, Lynch GS. GDEE antagonism of iontophoretic amino acid excitations in the intact hippocampus and in the hippocampal slice preparation. Brain Res 1976;105:471-481.

Sperlagh B, Kofalvi A, Deuchars J, Atkinson L, Milligan CJ, Buckley NJ, Vizi ES. Involvement of P2X7 receptors in the regulation of neurotransmitter release in the rat hippocampus. J Neurochem 2002;81:1196-1211.

Sperlagh B, Vizi ES, Wirkner K, Illes P. P2X7 receptors in the nervous system. Prog Neurobiol 2006;78:327-346.

Stefani A, Hainsworth AH, Spadoni F, Bernardi G. On the inhibition of voltage activated calcium currents in rat cortical neurones by the neuroprotective agent 619C89. Br J Pharmacol 1998;125:1058-1064.

Stefani A, Spadoni F, Siniscalchi A, Bernardi G. Lamotrigine inhibits Ca2+ currents in cortical neurons: functional implications. Eur J Pharmacol 1996;307:113-116.

Steinberg TH, Newman AS, Swanson JA, Silverstein SC. ATP4- Permeabilizes the Plasma Membrane of Mouse Macrophages to Fluorescent Dyes. J Biol Chem 1987;262:8884-8888.

Steinhauser C, Seifert G. Glial membrane channels and receptors in epilepsy: impact for generation and spread of seizure activity. Eur J Pharmacol 2002;447:227-237.

Stokes L, Jiang LH, Alcaraz L, Bent J, Bowers K, Fagura M, Furber M, Mortimore M, Lawson M, Theaker J, Laurent C, Braddock M, Surprenant A. Characterization of a selective and potent antagonist of human P2X(7) receptors, AZ11645373. Br J Pharmacol 2006;149:880-887.

Stoll G, Jander S. The role of microglia and macrophages in the pathophysiology of the CNS. Prog Neurobiol 1999;58:233-247.

Suadicani SO, Brosnan CF, Scemes E. P2X7 receptors mediate ATP release and amplification of astrocytic intercellular Ca2+ signaling. J Neurosci 2006;26:1378-1385.

Sugimura K, Haimoto H, Nagura H, Kato K, Takahashi A. Immunohistochemical differential distribution of S-100 alpha and S-100 beta in the peripheral nervous system of the rat. Muscle Nerve 1989;12:929-935.

Suh BC, Kim JS, Namgung U, Ha H, Kim KT. P2X7 nucleotide receptor mediation of membrane pore formation and superoxide generation in human promyelocytes and neutrophils. J Immunol 2001;166:6754-6763.

Surprenant A, Rassendren F, Kawashima E, North RA, Buell G. The cytolytic P2Z receptor for extracellular ATP identified as a P2X receptor (P2X7). Science 1996;272:735-738.

Sweitzer SM, Colburn RW, Rutkowski M, DeLeo JA. Acute peripheral inflammation induces moderate glial activation and spinal IL-1beta expression that correlates with pain behavior in the rat. Brain Res 1999;829:209-221.

Sweitzer SM, Schubert P, DeLeo JA. Propentofylline, a glial modulating agent, exhibits antiallodynic properties in a rat model of neuropathic pain. J Pharmacol Exp Ther 2001;297:1210-1217.

Tatham PE, Lindau M. ATP-induced pore formation in the plasma membrane of rat peritoneal mast cells. J Gen Physiol 1990;95:459-476.

Thornberry NA, Bull HG, Calaycay JR, Chapman KT, Howard AD, Kostura MJ, Miller DK, Molineaux SM, Weidner JR, Aunins J, . A novel heterodimeric cysteine protease is required for interleukin-1 beta processing in monocytes. Nature 1992;356:768-774.

Tian GF, Azmi H, Takano T, Xu Q, Peng W, Lin J, Oberheim N, Lou N, Wang X, Zielke HR, Kang J, Nedergaard M. An astrocytic basis of epilepsy. Nat Med 2005;11:973-981.

Tikka T, Fiebich BL, Goldsteins G, Keinanen R, Koistinaho J. Minocycline, a tetracycline derivative, is neuroprotective against excitotoxicity by inhibiting activation and proliferation of microglia. J Neurosci 2001;21:2580-2588.

Torres GE, Egan TM, Voigt MM. N-Linked glycosylation is essential for the functional expression of the recombinant P2X2 receptor. Biochemistry 1998a;37:14845-14851.

Torres GE, Egan TM, Voigt MM. Hetero-oligomeric assembly of P2X receptor subunits. Specificities exist with regard to possible partners. J Biol Chem 1999;274:6653-6659.

Torres GE, Haines WR, Egan TM, Voigt MM. Co-expression of P2X1 and P2X5 receptor subunits reveals a novel ATP-gated ion channel. Mol Pharmacol 1998b;54:989-993.

Tremont-Lukats IW, Megeff C, Backonja MM. Anticonvulsants for neuropathic pain syndromes: mechanisms of action and place in therapy. Drugs 2000;60:1029-1052.

Tsuda M, Inoue K, Salter MW. Neuropathic pain and spinal microglia: a big problem from molecules in "small" glia. Trends Neurosci 2005;28:101-107.

Tsuda M, Shigemoto-Mogami Y, Koizumi S, Mizokoshi A, Kohsaka S, Salter MW, Inoue K. P2X4 receptors induced in spinal microglia gate tactile allodynia after nerve injury. Nature 2003;424:778-783.

Valera S, Hussy N, Evans RJ, Adami N, North RA, Surprenant A, Buell G. A new class of ligand-gated ion channel defined by P2x receptor for extracellular ATP. Nature 1994;371:516-519.

Valera S, Talabot F, Evans RJ, Gos A, Antonarakis SE, Morris MA, Buell GN. Characterization and chromosomal localization of a human P2X receptor from the urinary bladder. Receptors Channels 1995;3:283-289.

Valles AS, Garbus I, Barrantes FJ. Lamotrigine is an open-channel blocker of the nicotinic acetylcholine receptor. Neuroreport 2007;18:45-50.

Van HJ, Gybels J. C nociceptor activity in human nerve during painful and non painful skin stimulation. J Neurol Neurosurg Psychiatry 1981;44:600-607.

Vane JR. Inhibition of prostaglandin synthesis as a mechanism of action for aspirin-like drugs. Nat New Biol 1971;231:232-235.

Vega JA, del Valle-Soto ME, Calzada B, varez-Mendez JC. Immunohistochemical localization of S-100 protein subunits (alpha and beta) in dorsal root ganglia of the rat. Cell Mol Biol 1991;37:173-181.

Vezzani A, Baram TZ. New roles for interleukin-1 Beta in the mechanisms of epilepsy. Epilepsy Curr 2007;7:45-50.

Vezzani A, Conti M, De LA, Ravizza T, Moneta D, Marchesi F, De Simoni MG. Interleukin-1beta immunoreactivity and microglia are enhanced in the rat hippocampus by focal kainate application: functional evidence for enhancement of electrographic seizures. J Neurosci 1999;19:5054-5065.

Vezzani A, Granata T. Brain inflammation in epilepsy: experimental and clinical evidence. Epilepsia 2005;46:1724-1743.

Vezzani A, Moneta D, Richichi C, Perego C, De Simoni MG. Functional role of proinflammatory and anti-inflammatory cytokines in seizures. Adv Exp Med Biol 2004;548:123-133.

Vial C, Evans RJ. P2X receptor expression in mouse urinary bladder and the requirement of P2X(1) receptors for functional P2X receptor responses in the mouse urinary bladder smooth muscle. Br J Pharmacol 2000;131:1489-1495.

Vial C, Roberts JA, Evans RJ. Molecular properties of ATP-gated P2X receptor ion channels. Trends Pharmacol Sci 2004a;25:487-493.

Vial C, Tobin AB, Evans R. G-protein-coupled receptor regulation of P2X(1) receptors does not involve direct channel phosphorylation. Biochem J 382, 101-110. 2004b.
Ref Type: Abstract

Vianna EP, Ferreira AT, Naffah-Mazzacoratti MG, Sanabria ER, Funke M, Cavalheiro EA, Fernandes MJ. Evidence that ATP participates in the pathophysiology of pilocarpine-induced temporal lobe epilepsy: fluorimetric, immunohistochemical, and Western blot studies. Epilepsia 2002;43 Suppl 5:227-229.

Virginio C, Church D, North RA, Surprenant A. Effects of divalent cations, protons and calmidazolium at the rat P2X7 receptor. Neuropharmacology 1997;36:1285-1294.

Virginio C, Mackenzie A, North RA, Surprenant A. Kinetics of cell lysis, dye uptake and permeability changes in cells expressing the rat P2X7 receptor. J Physiol 1999a;519 Pt 2:335-346.

Virginio C, Mackenzie A, Rassendren FA, North RA, Surprenant A. Pore dilation of neuronal P2X receptor channels. Nat Neurosci 1999b;2:315-321.

Virginio C, Robertson G, Surprenant A, North RA. Trinitrophenyl-substituted nucleotides are potent antagonists selective for P2X1, P2X3, and heteromeric P2X2/3 receptors. Mol Pharmacol 1998;53:969-973.

Vulchanova L, Riedl MS, Shuster SJ, Buell G, Surprenant A, North RA, Elde R. Immunohistochemical study of the P2X2 and P2X3 receptor subunits in rat and monkey sensory neurons and their central terminals. Neuropharmacology 1997;36:1229-1242.

Wade RH. Microtubules: an overview. Methods Mol Med 2007;137:1-16.

Wadhwani KC, Rapoport SI. Transport properties of vertebrate blood-nerve barrier: comparison with blood-brain barrier. Prog Neurobiol 1994;43:235-279.

Waksman JC, Brody A, Phillips SD. Nonselective nonsteroidal antiinflammatory drugs and cardiovascular risk: are they safe? Ann Pharmacother 2007;41:1163-1173.

Wang CM, Chang YY, Kuo JS, Sun SH. Activation of P2X(7) receptors induced [(3)H]GABA release from the RBA-2 type-2 astrocyte cell line through a Cl(-)/HCO(3)(-)-dependent mechanism. Glia 2002;37:8-18.

Wang Q, Wang L, Feng YH, Li X, Zeng R, Gorodeski GI. P2X7 receptor-mediated apoptosis of human cervical epithelial cells. Am J Physiol Cell Physiol 2004a;287:C1349-C1358.

Wang SJ, Huang CC, Hsu KS, Tsai JJ, Gean PW. Inhibition of N-type calcium currents by lamotrigine in rat amygdalar neurones. Neuroreport 1996;7:3037-3040.

Wang X, Arcuino G, Takano T, Lin J, Peng WG, Wan P, Li P, Xu Q, Liu QS, Goldman SA, Nedergaard M. P2X7 receptor inhibition improves recovery after spinal cord injury. Nat Med 2004b;10:821-827.

Watanabe N, Kawaguchi M, Kobayashi Y. Activation of interleukin-1beta-converting enzyme by nigericin is independent of apoptosis. Cytokine 1998;10:645-653.

Watano T, Calvert JA, Vial C, Forsythe ID, Evans RJ. P2X receptor subtype-specific modulation of excitatory and inhibitory synaptic inputs in the rat brainstem. J Physiol 2004;558:745-757.

Watano T, Matsuoka I, Kimura J. Characteristics of ATP-induced current through P2X7 receptor in NG108-15 cells: unique antagonist sensitivity and lack of pore formation. Jpn J Pharmacol 2002;88:428-435.

Watkins LR, Maier SF. Beyond neurons: evidence that immune and glial cells contribute to pathological pain states. Physiol Rev 2002;82:981-1011.

Watkins LR, Maier SF. Glia: a novel drug discovery target for clinical pain. Nat Rev Drug Discov 2003;2:973-985.

Watkins LR, Maier SF, Goehler LE. Immune activation: the role of pro-inflammatory cytokines in inflammation, illness responses and pathological pain states. Pain 1995;63:289-302.

Watkins LR, Martin D, Ulrich P, Tracey KJ, Maier SF. Evidence for the involvement of spinal cord glia in subcutaneous formalin induced hyperalgesia in the rat. Pain 1997;71:225-235.

Watkins LR, Milligan ED, Maier SF. Glial activation: a driving force for pathological pain. Trends Neurosci 2001;24:450-455.

Webb J, Kamali F. Analgesic effects of lamotrigine and phenytoin on cold-induced pain: a crossover placebo-controlled study in healthy volunteers. Pain 1998;76:357-363.

Werner P, Seward EP, Buell GN, North RA. Domains of P2X receptors involved in desensitization. Proc Natl Acad Sci U S A 1996;93:15485-15490.

Wienrich M, Kettenmann H. Activation of substance P receptors leads to membrane potential responses in cultured astrocytes. Glia 1989;2:155-160.

Wildman SS, King BF, Burnstock G. Zn2+ modulation of ATP-responses at recombinant P2X2 receptors and its dependence on extracellular pH. Br J Pharmacol 1998;123:1214-1220.

Wildman SS, King BF, Burnstock G. Modulation of ATP-responses at recombinant rP2X4 receptors by extracellular pH and zinc. Br J Pharmacol 1999;126:762-768.

Wiley JS, Chen R, Jamieson GP. The ATP4- receptor-operated channel (P2Z class) of human lymphocytes allows Ba2+ and ethidium+ uptake: inhibition of fluxes by suramin. Arch Biochem Biophys 1993;305:54-60.

Wiley JS, Dao-Ung LP, Li C, Shemon AN, Gu BJ, Smart ML, Fuller SJ, Barden JA, Petrou S, Sluyter R. An Ile-568 to Asn polymorphism prevents normal trafficking and function of the human P2X7 receptor. J Biol Chem 2003;278:17108-17113.

Wiley JS, Gargett CE, Zhang W, Snook MB, Jamieson GP. Partial agonists and antagonists reveal a second permeability state of human lymphocyte P2Z/P2X7 channel. Am J Physiol 1998;275:C1224-C1231.

Wilkinson R, Leaver C, Simmons A, Pereira RA. Restricted replication of herpes simplex virus in satellite glial cell cultures clonally derived from adult mice. J Neurovirol 1999;5:384-391.

Willis WD, Coggeshall RE. Sensory mechanisms of the spinal cord. New York: Plenum Press., 1991.

Willis WD, Westlund KN. Neuroanatomy of the pain system and of the pathways that modulate pain. J Clin Neurophysiol 1997;14:2-31.

Wilson KP, Black JA, Thomson JA, Kim EE, Griffith JP, Navia MA, Murcko MA, Chambers SP, Aldape RA, Raybuck SA, . Structure and mechanism of interleukin-1 beta converting enzyme. Nature 1994;370:270-275.

Woodham P, Anderson PN, Nadim W, Turmaine M. Satellite cells surrounding axotomised rat dorsal root ganglion cells increase expression of a GFAP-like protein. Neurosci Lett 1989;98:8-12.

Woolf CJ. Evidence for a central component of post-injury pain hypersensitivity. Nature 1983;306:686-688.

Woolf CJ. Generation of acute pain: central mechanisms. Br Med Bull 1991;47:523-533.

Woolf CJ, Allchorne A, Safieh-Garabedian B, Poole S. Cytokines, nerve growth factor and inflammatory hyperalgesia: the contribution of tumour necrosis factor alpha. Br J Pharmacol 1997;121:417-424.

Woolf CJ, Salter MW. Neuronal plasticity: increasing the gain in pain. Science 2000;288:1765-1769.

Woolf CJ, Thompson SW. The induction and maintenance of central sensitization is dependent on N-methyl-D-aspartic acid receptor activation; implications for the treatment of post-injury pain hypersensitivity states. Pain 1991;44:293-299.

Woolf CJ, Walters ET. Common patterns of plasticity contributing to nociceptive sensitization in mammals and Aplysia. Trends Neurosci 1991;14:74-78.

Worthington RA, Smart ML, Gu BJ, Williams DA, Petrou S, Wiley JS, Barden JA. Point mutations confer loss of ATP-induced human P2X(7) receptor function. FEBS Lett 2002;512:43-46.

Wuttke TV, Lerche H. Novel anticonvulsant drugs targeting voltage-dependent ion channels. Expert Opin Investig Drugs 2006;15:1167-1177.

Xie X, Lancaster B, Peakman T, Garthwaite J. Interaction of the antiepileptic drug lamotrigine with recombinant rat brain type IIA Na+ channels and with native Na+ channels in rat hippocampal neurones. Pflugers Arch 1995;430:437-446.

Xie XM, Garthwaite J. State-dependent inhibition of Na+ currents by the neuroprotective agent 619C89 in rat hippocampal neurons and in a mammalian cell line expressing rat brain type IIA Na+ channels. Neuroscience 1996;73:951-962.

Yan Z, Li S, Liang Z, Tomic M, Stojilkovic SS. The P2X7 receptor channel pore dilates under physiological ion conditions. J Gen Physiol 2008;132:563-573.

Yanagisawa D, Kitamura Y, Takata K, Hide I, Nakata Y, Taniguchi T. Possible involvement of P2X7 receptor activation in microglial neuroprotection against focal cerebral ischemia in rats. Biol Pharm Bull 2008;31:1121-1130.

Yiangou Y, Facer P, Durrenberger P, Chessell IP, Naylor A, Bountra C, Banati RR, Anand P. COX-2, CB2 and P2X7-immunoreactivities are increased in activated microglial cells/macrophages of multiple sclerosis and amyotrophic lateral sclerosis spinal cord. BMC Neurol 2006;6:12.

Yoshida K, Gage FH. Cooperative regulation of nerve growth factor synthesis and secretion in fibroblasts and astrocytes by fibroblast growth factor and other cytokines. Brain Res 1992;569:14-25.

Young MT, Pelegrin P, Surprenant A. Amino acid residues in the P2X7 receptor that mediate differential sensitivity to ATP and BzATP. Mol Pharmacol 2007;71:92-100.

Zakrzewska JM, Chaudhry Z, Nurmikko TJ, Patton DW, Mullens EL. Lamotrigine (lamictal) in refractory trigeminal neuralgia: results from a double-blind placebo controlled crossover trial. Pain 1997;73:223-230.

Zanovello P, Bronte V, Rosato A, Pizzo P, Di Virgilio F. Responses of mouse lymphocytes to extracellular ATP. II. Extracellular ATP causes cell type-dependent lysis and DNA fragmentation. J Immunol 1990;145:1545-1550.

Zaremba PD, Bialek M, Blaszczyk B, Cioczek P, Czuczwar SJ. Non-epilepsy uses of antiepilepsy drugs. Pharmacol Rep 2006;58:1-12.

Zhang RX, Liu B, Wang L, Ren K, Qiao JT, Berman BM, Lao L. Spinal glial activation in a new rat model of bone cancer pain produced by prostate cancer cell inoculation of the tibia. Pain 2005a;118:125-136.

Zhang X, Chen Y, Wang C, Huang LY. Neuronal somatic ATP release triggers neuron-satellite glial cell communication in dorsal root ganglia. Proc Natl Acad Sci U S A 2007;104:9864-9869.

Zhang XF, Han P, Faltynek CR, Jarvis MF, Shieh CC. Functional expression of P2X7 receptors in non-neuronal cells of rat dorsal root ganglia. Brain Res 2005b;1052:63-70.

Zhang Z, Zhang ZY, Fauser U, Schluesener HJ. Mechanical allodynia and spinal up-regulation of P2X4 receptor in experimental autoimmune neuritis rats. Neuroscience 2008;152:495-501.

Zheng LM, Zychlinsky A, Liu CC, Ojcius DM, Young JD. Extracellular ATP as a trigger for apoptosis or programmed cell death. J Cell Biol 1991;112:279-288.

Zhou XF, Deng YS, Chie E, Xue Q, Zhong JH, McLachlan EM, Rush RA, Xian CJ. Satellite-cell-derived nerve growth factor and neurotrophin-3 are involved in noradrenergic sprouting in the dorsal root ganglia following peripheral nerve injury in the rat. Eur J Neurosci 1999;11:1711-1722.

Zimmer DB, Cornwall EH, Landar A, Song W. The S100 protein family: history, function, and expression. Brain Res Bull 1995;37:417-429.

Zimmer DB, Van Eldik LJ. Tissue distribution of rat S100 alpha and S100 beta and S100-binding proteins. Am J Physiol 1987;252:C285-C289.

Zona C, Tancredi V, Longone P, D'Arcangelo G, D'Antuono M, Manfredi M, Avoli M. Neocortical potassium currents are enhanced by the antiepileptic drug lamotrigine. Epilepsia 2002;43:685-690.

Appendix A

1 *In Vivo* Inflammatory Pain study

1.1 Animals

Male Random-Hooded rats (weight, 180–200 g; B & K Universal, Hull, UK) were used in weight-bearing studies. Animals were housed in groups of 5 in a temperature-controlled environment (20°C ± 1°C) maintained on a 12-hour light/dark cycle with access to food and water. All experiments were performed in accordance with the Animals (Scientific Procedures) Act 1896 under the authority of a Home Office Project License and complied with local GlaxoSmithKline (GSK) regulations regarding the care of experimental animals.

1.2 Behavioural Readouts -Assessment of Weight-Bearing Capacity

The distribution of weight between the 2 hind paws was measured using a dual channel weight averager (Bioengineering, GlaxoSmithkline; (Clayton et al. 1997)). Normal rats distribute their body weight equally between the 2 hind paws, but when a hind paw is inflamed and/or painful, the weight is redistributed so that less weight is put on the affected paw. Assessment of this change using the dual channel weight averager is a sensitive method for measuring the development of hypersensitivity. The 2 hind paws were placed on separate sensors, and the drug-induced percent reversal of FCA-induced weight-bearing deficit was calculated over a period of 4 seconds (De Alba et al. 2006).

1.3 Established Inflammation-Induced Hyperalgesia

FCA (100 µl of 1 mg/ml *M. tuberculosis* (1 mg/ml)) was injected intraplantar into the left hind paw (n = 7 per group). GSK314181A (3-30 mg/kg s.c.), and Celecoxib (10 mg/kg p.o.) were administered 24 hours post-FCA. The effect on weight bearing of the inflamed paw was determined at 0.5, 1, 3, 6 and 24 hours post-dosing.

1.4 Data Analysis and Statistics

Hypersensitivity to pain was measured as % of decrease in weight bearing on the inflamed left hind paw. Weight-bearing ability was recorded in grams and expressed as

the difference between the FCA-injected paw and the contralateral paw. The percentage reversal was calculated for each animal using the formula: (testΔ - mean vehicleΔ/base-lineΔ - mean vehicleΔ) x 100, expressed as mean ± S.E.M., and an ED_{50} (with confidence limits). Drug-treated groups were compared with vehicle using Fisher's test.